Research Technical Completion Report

THERMAL GROUND WATER FLOW SYSTEMS IN THE THRUST ZONE IN SOUTHEASTERN IDAHO

By

Dr. Dale R. Ralston
Department of Geology

Alan L. Mayo

Department of Geology

John L. Arrigo
Joseph V. Baglio, Jr.
Leonard M. Coleman
Joel M. Hubbell
Karl Souder

Graduate Assistants

Idaho Water and Energy Resources Research Institute
University of Idaho
Moscow, Idaho 83843

May, 1983

Research Technical Competion Report

THERMAL GROUND WATER FLOW SYSTEMS IN THE THRUST ZONE IN SOUTHEASTERN IDAHO

By

Dr. Dale R. Ralston
Department of Geology

John L. Arrigo
Joseph V. Baglio, Jr.
Leonard M. Coleman
Joel M. Hubbell
Karl Souder

Graduate Assistants

Alan L. Mayo
Department of Geology

Submitted to:

Idaho Department of Water Resources

Idaho Water and Energy Research Institute
University of Idaho
Moscow, Idaho 83843

May, 1983

ABSTRACT

This report presents the results of a regional study of thermal and non-thermal ground water flow systems in the thrust zone of southern Idaho and western Wyoming. The study involved hydrogeologic and hydrochemical data collection and interpretation. Particular emphasis was placed on analyzing the role that thrust zones play in controlling the movement of thermal and non-thermal fluids.

The geology of the area is complex; thrust faulting, normal faulting and tear faulting are all important in controlling water movement through the thick sequence of mostly sedimentary strata. The thrust faults are not believed to create zones of either significantly higher or lower hydraulic conductivity. The most important hydrologic impact of thrust faulting is probably the alteration of the normal stratigraphic sequence of formations. Thrust zones are identified in deep drilling logs primarily by a repeat of section.

The total discharge of thermal waters within the study area is quite small. Discharge of 30°C or more amount to approximately 500 l/s. Most thermal and non-thermal discharges are controlled by structural features with secondary control by stratigraphy. Graben bounding faults are most important in controlling thermal flow systems.

Graphic and statistical analyses of the major-ion data enabled the delineation of several statistical distinct water types which are associated with geographically distinct areas. These are: (a) sodium chloride waters of the Swan Valley to Star Valley graben, (b) calcium bicarbonate waters of the Meade Peak thrust block and adjacent areas, (c) sodium chloride waters of the Maple Grove area, (d) high sodium chloride waters of the Basin and Range province, and (e) low TDS waters from various locales throughout the study area.

Deuterium and oxygen-18 results indicate that, with the exception of sites S-13 and S-14, aquifer temperatures are not significantly above 80°C in the study area; also, that differences in recharge elevation are not apparent.

Carbon isotope analyses indicate that the thermal waters of the study area which were analyzed for ^{14}C have undergone contact times in excess of 25,000 years B.P. for those springs whose temperatures are greater than 25°C. The extremely low concentrations of modern carbon in the thermal waters above 25°C indicate that essentially no mixing of waters younger than several thousand years has occurred.

TABLE OF CONTENTS

	Page
ABSTRACT	i
LIST OF TABLES	vii
LIST OF FIGURES	x
INTRODUCTION	1
Statement of the Problem	1
Purpose and Objectives	1
Method of Study	3
Previous Investigations	5
HYDROGEOLOGY OF THE THRUST ZONE	8
Introduction	8
Geologic History	8
Characteristics of the Meade Thrust	11
Introduction	11
General Stratigraphy	13
Petrology of Thrust Features	13
Fault Breccia	13
Fault Gouge	17
Interbedded Gouge	17
Porosity and Permeability	17
Interpretation of Results	18
Regional Hydrostratigraphy	19
Introduction	19
Method of Study	20
Presentation and Analysis of Data	24
Stream Gain-loss Data	24
Spring Inventory	37
Interpretation of Results	42
HYDROGEOLOGIC RECONNAISSANCE OF THE NORTHERN SUBAREA	47
Introduction	47
Method of Study	47
Geographic Setting	52
Hydrogeology of the Study Area	54
Physical and Chemical Settings of Springs and Wells	62
Introduction	62
Thermal Springs with High Specific Conductivities	62
Heise Hot Springs	62
Fall Creek Mineral Springs	73

Page

Alpine Hot Springs 74
Auburn Hot Springs and Johnson Springs 76
Unnamed Springs at 1N 40E 4abcS 77
Brockman Hot Springs 78
Thermal Springs with Low Specific Conductivities 78
Elkhorn and Hawley Warm Springs 79
Unnamed Springs at 3N 41E 32bbdS 79
Dyer and Anderson Wells 80
Warm Spring 81
Nonthermal Springs 81
Analysis of Data 82
Analysis of Springs and Wells Utilizing Physical Data 82
Introduction 82
Structural Controls on Springs and Wells 82
Geologic Formations Associated with Spring and Well Sites 85
Discharge of Springs 85
Elevation of Discharge 87
Analysis of Springs and Wells Utilizing Chemical Data 88
Evolution of Major Ions in Ground Water Flow Systems. 88
Total Dissolved Solids as an Indicator of Flow Path Length 93
Classification of Springs and Wells Using WATEQF 93
Correlation of Springs and Wells Utilizing Stiff Diagrams 98
Statistical Analysis of Chemical Data 101
Introduction 101
UNIVARIATE Analysis 102
Stepwise MANOVA Analysis 107
Discussion of the Results 108
Ground Water Flow Patterns 109

HYDROGEOLOGIC RECONNAISSANCE OF THE MEADE THRUST SUBAREA 113

Introduction 113
Geologic Setting 116
Stratigraphy of the Allochthon and Adjacent Areas 116
Structure of the Allochthon 118
Physical and Chemical Characteristics of Springs and Wells 125
Overview 125
Description of Springs and Wells 127
Periphery Extension Fault Groups 127
Corral Creek (1) 127
Western Frontal Fault Group (2-9) 134
Henry Group (10-15) 144
Chubb Spring Group (16 and 17) 149

Page

Periphery Thrust Fault Splay Groups 150
Georgetown Canyon Group (18-20) 150
Eastern Thrust Zone Group (21-29) 152
Interior Groups (30-41) 154
Analysis of Chemical Data 155
Graphical Analysis and Hydrochemical Facies 155
Ca/Mg Ratios 160
Mineral Equilibrium 166
Ca-Mg-HCO_3 Concentrations 171
Deuterium-Oxygen Analysis 172
Radiocarbon Chronometry 179
Origin of Carbon-14 179
Principles of Radiocarbon Chronometry 181
Mechanisms Controlling the Initial ^{14}C Activity in Ground water 182
Isotopic Fractionation 184
Ground Water Ages from the Meade Thrust Allochthon . 186
Aquifer Temperatures 192
Flow Patterns Suggested by Chemical and Physical Data ... 197
Periphery Extension Aquifers 198
Periphery Thrust and Interior Aquifers 200
Proposed Three Tier Ground Water Flow Model 203

HYDROGEOLOGIC RECONNAISSANCE OF THE SOUTHERN SUBAREA 211

Introduction 211
Geologic Setting 213
Physical and Chemical Characteristics of Springs and Wells ... 221
Analysis of Physical Data 221
Introduction 221
Associated Geologic Features 231
Discharge of Springs 235
Analysis of Chemical Data 235
Introduction 235
Multivariate Methods 237
Factor Analysis 237
Cluster Analysis 240
Multiple Discriminant Analysis 243
Discussion of Results 245
Ground Water Flow Patterns 248
Non-Thermal Systems 248
Soda Springs Group 249
Gem Valley Group 251
Isolated Thermal Discharges 252

HYDROCHEMISTRY OF THERMAL FLOW SYSTEMS 253

Introduction 253
Regional Hydrogeologic Setting 255

Page

Presentation of Chemical and Physical Data 257
Introduction 257
Water Quality Data 259
Physical Characteristics of Thermal Discharge Sites 259
Comparability of Water Quality Data 274
Deuterium and Oxygen-18 Data 277
Carbon Isotope Analysis 277
Thermal Water Groups Delineated by Major Ion Data and Site Geology 279
Introduction 279
Graphic Analysis Techniques 279
Statistical Analysis of Major Ion Groups 281
WATEQF Analysis of Chemical Equilibria and Speciation 282
Ground Water Geochemical Environments in the Study Area 284
Introduction 284
Thermal Waters of the Swan Valley to Star Valley Graben and Adjacent Areas (Group 3) 284
Thermal Waters of the Meade Peak Thrust Block (Group 1) .. 285
Thermal Waters of the Areas Adjacent to the Meade Peak Block (Group 2) 286
Thermal Waters of the Maple Grove Area 288
Thermal Waters of the Basin and Range Province 290

GEOTHERMAL ANALYSIS FROM REGIONAL DEEP DRILLING 294

Objectives and Method of Study 294
Deep Drilling Data 295
Introduction 295
Geologic Data 295
Temperature Data from Deep Drilling 301
Geothermal Gradient 316

CONCLUSIONS 322

REFERENCES 326

LIST OF TABLES

Table		Page
II-1	Generalized stratigraphy of southeast Idaho	14
II-2	The name, location, date measured, exposed formation, number of measurements and type of access for stream gain-loss sites in southeast Idaho	27
II-3	Stream gain-loss data for Horse Creek	31
II-4	Summary of stream gain-loss data for stream sections measured in southeastern Idaho	36
II-5	Summary of spring inventory data from southeastern Idaho .	41
II-6	Estimation of relative hydraulic conductivity and factors controlling hydraulic conductivity for the formations in southeast Idaho, based on stream gain-loss and spring inventory data	43
III-1	Physical settings of springs and wells in the vicinity of the Caribou Range, southeastern Idaho and western Wyoming	64
III-2	Hydrochemistry of springs and wells in the vicinity of the Caribou Range, southeastern Idaho and western Wyoming	68
III-3	Geologic formation associated with springs and wells in the vicinity of the Caribou Range, southeastern Idaho and western Wyoming	86
III-4	Results of analyses to determine relative length of flow paths by dominant anions and total dissolved solids and groups formed by cluster analysis in the vicinity of the Caribou Range, southeastern Idaho and western Wyoming	91
III-5	Saturation index of selected minerals for springs and well in the vicinity of the Caribou Range, southeastern Idaho and western Wyoming	95
III-6	Results of stepwise MANOVA analysis for springs and wells in Caribou Range study area, southeastern Idaho and western Wyoming	108
IV-1	Chemical analysis of springs and well waters collected in the Meade thrust area, southeastern Idaho	128
IV-2	Physical settings of springs and wells in the Meade thrust area, southeastern Idaho	131

Table		Page
IV-3	SI, Ca/Mg ratios, and PCO_2 of water samples collected in the Meade thrust area, southeastern Idaho	161
IV-4	Deuterium and oxygen-18 analyses of spring and well waters in the Meade thrust areas, southeastern Idaho	177
IV-5	Ground water ages and dating input parameters of nine springs and one flowing well in the Meade thrust area, southeastern Idaho	190
IV-6	Results of discharge temperature t tests	195
IV-7	Summary of the chemical and physical characteristics of discharges from springs and wells in the Meade thrust area, southeastern Idaho	199
V-1	Stratigraphic column for Bear River Range and surrounding areas, southeastern Idaho.................................	214
V-2	Inventory of and hydrogeologic data from springs and wells sampled in southeastern Idaho	223
V-3	Hydrochemical data from springs and wells sampled in southeastern Idaho	227
V-4	Geologic formation associated with springs and wells in the vicinity of the Bear River Range, southeastern Idaho ..	232
V-5	Correlation coefficient matrix for the hydrochemical parameters: temperature, total dissolved solids (TDS), pH, calcium, magnesium, sodium, potassium, chloride, fluoride, bicarbonate, sulfate, and silica	239
V-6	Comparison of geologic formations and structures with statistically derived hydrochemical groups	244
V-7	Summary of physical and chemical characteristics of springs and wells in southeastern Idaho	246
VI-1	Sources of water quality data used in this report	258
VI-2	Hydrochemical data for thermal springs and wells of the study area	260
VI-3	Physical characteristics of thermal spring and well sites in the study area	267
VI-4	Comparison of IDWR and Thrust Geothermal project chemical analysis (1980 samples)	276

Table		Page
VI-5	Comparison of Thrust Geothermal project (1980 samples) and University of Idaho Agricultural Science Analytical Laboratory chemical analysis (1981 samples)	276
VI-6	Isotopic and geochemical characteristics, and estimated ages of selected thermal and non-thermal waters in southeastern Idaho	278
VII-1	Inventory of oil and gas wells drilled in southeastern Idaho	297
VII-2	Examples of geologic logs from four wells drilled in southeastern Idaho showing faults penetrated	300
VII-3	Temperature data obtained on wells drilled in southeastern Idaho	302

LIST OF FIGURES

Figure		Page
I-1	Data sources and subareas	2
II-1	Generalized structural map of the overthrust belt in southeastern Idaho, western Wyoming and northern Utah	9
II-2	Typical diagrammatic east-west cross section of the overthrust belt	12
II-3	Fault breccia sites examined in southeastern Idaho	15
II-4	Examples of gaining and losing streams from Winter (1979)	22
II-5	Location of stream sections for gain-loss measurements from Arrigo (1982)	25
II-6	Geology of Horse Creek area	28
II-7	Cross-section of Horse Creek area	29
II-8	Area covered by spring inventory	38
III-1	Boundary and geographic subdivisions of Caribou Range study area, southeastern Idaho and western Wyoming	48
III-2	Geologic map of Caribou Range study area in southeastern Idaho and western Wyoming	55
III-3	Cross section A-A' in the Caribou Range study area in southeastern Idaho and western Wyoming	56
III-4	Location and temperature of springs and wells in the vicinity of the Caribou Range, southeastern Idaho and western Wyoming	63
III-5	Stiff diagrams of water chemistries of selected springs and wells in the vicinity of the Caribou Range, southeastern Idaho and western Wyoming	99
III-6	UNIVARIATE data summary of the variable temperature for springs and wells in the vicinity of the Caribou Range, southeastern Idaho and western Wyoming	103
III-7	Twelve variable cluster diagram for springs and wells in Caribou Range study area, southeastern Idaho and western Wyoming	106

Figure		Page
IV-1	Generalized structural map of the overthrust belt in southeastern Idaho and western Wyoming	114
IV-2	Map of physiographic regions of the Meade thrust area, southeastern Idaho	115
IV-3	Generalized geologic map of the Meade thrust area showing the location of structure sections described in the text	119
IV-4	Generalized east-west structure section through the overthrust belt of southeastern idaho and western Wyoming	120
IV-5	Generalized east-west structure section through the Meade thrust area, southeastern Idaho	121
IV-6	Location of water quality sampling sites in the Meade thrust area, southeastern Idaho	126
IV-7	North-south structure section through the Corral Creek area, southeastern Idaho	135
IV-8a	North-south structure section through Sinkhole spring (2) area	138
IV-8b	East-west structure section through Woodall spring (3) area	138
IV-9	East-west structure section through Formation spring (5), Aspen Range, and Bear River graben, southeastern Idaho ...	141
IV-10	North-south structure section through Lone Tree (10), Pelican Ridge #1 (39) and North Pelican (41) springs, southeastern Idaho	146
IV-11	East-west structure section through Sage Valley (22) area, southeastern Idaho	153
IV-12	Classification diagram for anion and cation facies in terms of major-ion percentages	156
IV-13	Trilinear diagram of chemical analyses of discharge waters from 3 wells and 38 springs in the Meade thrust area, southeastern Idaho	157
IV-14	Stiff diagrams of chemical analyses of waters from 3 wells and 38 springs in the Meade thrust area, southeastern Idaho	159

Figure		Page
IV-15	Comulative frequency distribution of calcium-magnesium molar ratios in ground water samples collected from springs and wells in the Meade thrust area, southeastern Idaho	163
IV-16	Saturation of water samples with respect to calcite and fluorite for 41 sites in the Meade thrust area, southeastern Idaho	168
IV-17	δD and $\delta^{18}O$ values from spring and well waters in the Meade thrust area, southeastern Idaho	178
IV-18	Radiocarbon ground water ages of nine springs and one flowing well in the Meade thrust area, southeastern Idaho	191
IV-19	Cumulative frequence distribution of discharge temperature grouped by discharge groups	194
IV-20	Postulated three tier ground water flow model in the Meade thrust area, southeastern Idaho	204
IV-21	Postulated ground water flow directions in tier two	207
V-1	Location map of study area in southeastern Idaho	212
V-2	Geologic map of the study area in southeastern Idaho	217
V-3	Map of well and spring sampling location in southeastern Idaho	222
V-4	Dendrogram of hydrochemical groups resulting from a cluster analysis using the variables: temperature, sodium, chloride, calcium, magnesium, and bicarbonate	242
V-5	Map of areal distribution of statistically derived hydrochemical groups in southeastern Idaho	247
VI-1	Data sources and subareas	254
VI-2	Major geologic structures in southeastern Idaho, northern Utah, and western Wyoming	256
VI-3	Regional hydrochemistry of thermal occurrences in southeastern Idaho, western Wyoming, and northern Utah	pocket

Figure		Page
VII-1	Location of oil and gas wells in southeastern Idaho	296
VII-2	High resolution temperature log for King 2-1	304
VII-3a	High resolution temperature log for Gentile Valley #1-9: Run #1	305
VII-3b	High resolution temperature log for Gentile Valley #1-9: Run #2	306
VII-3c	High resolution termerature log for Gentile Valley #1-9: Run #3	307
VII-4a	High resolution temperature log for Stoor A#1: Run #1	308
VII-4b	High resolution temperature log for Stoor A#1: Run #2	309
VII-4c	High resolution temperature log for Stoor A#1: Run #3	310
VII-5	High resolution temperature log for Federal 1-8 Elk Valley	311
VII-6	High resolution temperature log for Federal Elk Valley #1 .	312
VII-7	High resolution temperature log for Jensen #22-1	313
VII-8	High resolution temperature log for North Rabbit Creek Federal 6-21	314
VII-9	High resolution temperature log for Grace Federal 10-1	315
VII-10	Calculated geothermal gradient of selected oil and gas wells in southeastern Idaho	318
VII-11	Bottom hole temperatures versus total depth and surface elevation in comparison to suggested geothermal gradients .	319
VII-12	Geologic log and temperature log of well King 2-1	321

CHAPTER I

INTRODUCTION

Statement of the Problem

The thrust zone of southeastern Idaho and western Wyoming has potential for geothermal development to compliment oil and gas and phosphate resources. Evidence of the geothermal resource includes warm springs, warm water from shallow wells and reports of hot water at depth in oil and gas test holes. The geology of the area is complex; thrust faulting, normal faulting and tear faulting are important in controlling water movement through the thick sequence of mostly sedimentary strata. This report presents the results of a regional study of geothermal systems in the thrust zone of Idaho and Wyoming (Figure I-1). The study involved analysis of thermal and non-thermal ground water flow systems based upon hydrogeologic and hydrochemical data collection and interpretation. Particular emphasis was placed on analyzing the role that the thrust zones play in controlling the movement of thermal and non-thermal fluids.

Purpose and Objectives

The purpose of this research is to utilize the sciences of hydrogeology, hydrochemistry and structural geology to evaluate the geothermal system believed present in the thrust belt of southeastern Idaho. The general objective of

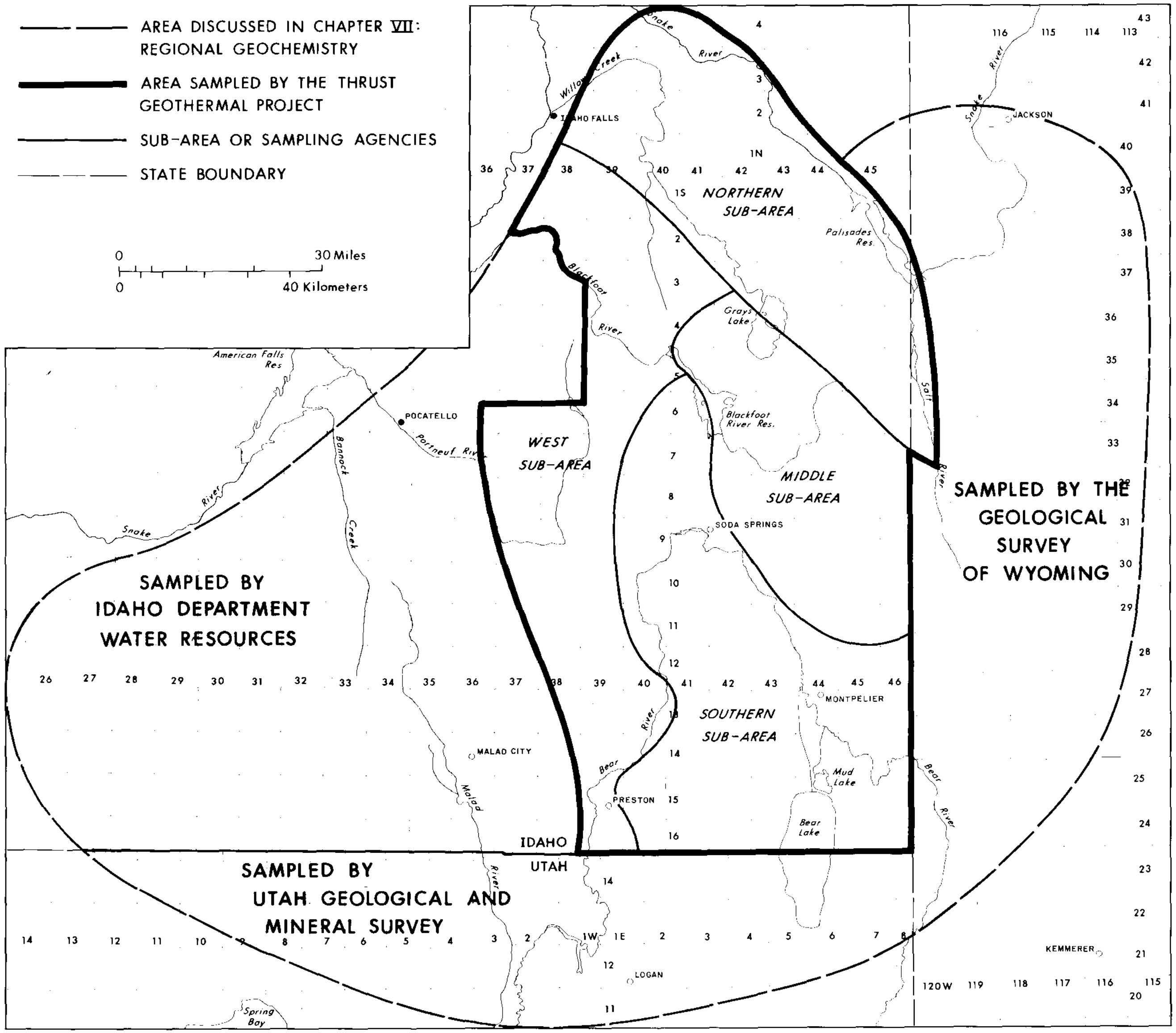

Figure I-1. Data sources and subareas.

this project is to provide a reconnaissance evaluation of the hydrogeologic controls for the occurrence and movement of thermal ground water in the thrust belt of southeastern Idaho.

The specific objectives are given below:

1. Identify the structural framework of the thrust belt and the physical characteristics of the thrust zones.
2. Inventory and analyze the thermal and non-thermal ground water discharges controlled by thrust related structural features.
3. Analyze the available thermal and lithologic data from deep test holes drilled in the thrust belt in southeastern Idaho and western Wyoming.
4. Combine the above results into a reconnaissance evaluation of the hydrogeologic controls for the geothermal system underlying the general thrust zone.

Method of Study

This research project was undertaken by the College of Mines and Earth Resources at the University of Idaho in connection with the graduate program in hydrology. The project was divided into subprojects forming the Master's research topics for four M. S. students in hydrology. In addition, one Ph. D. student in geology worked partially on this project and partially on a project funded through the Idaho Mining and Minerals Resources Research Institute. All of the students were under the direct supervision of Dr. Dale Ralston, Professor of Hydrogeology at the University of Idaho. A summary of the results of the individual subprojects are presented as chapters within this report.

Three of the subprojects involved regional reconnaissance studies of thermal and non-thermal flow systems within three portions of the thrust area in Idaho and Wyoming (Figure I-1). Field work for these subprojects involved location, measurement, and sampling of ground water discharges that appeared to be controlled by structural features. Particular emphasis was placed on structural features associated with the thrust zones. Water samples were collected following EPA procedures and analyzed for selected chemical constituents. Summaries of the results from these investigations are reported in chapters III, IV, and V for the northern, Meade Thrust and southern subareas. The theses are by Hubbell (1981), Mayo (1982), and Baglio (1983). A student in geology investigated the physical characteristics of the thrust zones associated with the Meade thrust block. Emphasis was placed on analysis of the degree and form of fracturing associated with the thrusting activity. The results of this investigation are included in chapter II. One M. S. student examined the chemistry of geothermal flow systems on a regional basis roughly bounded by Raft River on the east, northern Utah on the south, western Wyoming on the east and the Island Park KGRA on the north. His analysis included data collected by the other field investigators plus additional sites not covered as part of their studies. A summary of results of this investigation are presented in chapter VI. The thesis is by Souder (1983). The last M. S. student evaluated the regional hydrostratigraphy of the thrust zone. A summary of these results are presented in chapter II. The thesis is by Arrigo (1982). Data from deep drill holes including geological, geophysical, and temperature information were also evaluated. Analysis of these data provides important insights on deep geothermal flow systems. This information is presented in chapter VII.

Previous Investigations

Previous investigations of importance to this research effort are found in three different fields: geology, hydrology and geothermal. The geology of the thrust belt has been investigated by a number of individuals. Mansfield (1927) prepared an extensive report on the geology of the overthrust zone. Specific 7.5 and 15 minute quad areas were mapped in the 1950-1970 period by various USGS geologists (Cressman, 1964; Armstrong, 1969; Gulbrandsen and others, 1956; and others). Papers by Armstrong and Cressman (1963), Eardly (1967), Rubey (1955) and Royse, Warner and Reese

(1975) presented structural interpretations of the thrust zone. Mabey and Oriel (1970) conducted regional geophysical surveys of the southeast Idaho portion of the thrust area.

The ground water hydrology of the thrust zone has been the subject of major researh efforts at the University of Idaho. Ralston and others (1977) and Ralston and others (1980) reported on the investigation of ground water-surface water systems near existing or proposed phosphate mines. These two research reports summarize the findings from two Ph. D. dissertations and six Master's theses. Dion (1969, 1974) investigated the ground water hydrology in the Bear River and Blackfoot Reservoir areas as part of a cooperative State of Idaho-U. S. Geological Survey effort. An Environmental Impact Statement on Phosphate Mining (USDI, 1976) presented a general overview of the hydrology of the western phosphate field.

Four geothermal reports have been prepared that are concerned, at least in part, with the thrust area. Three of these reports were published by the Idaho Department of Water Resources as part of their series on the geothermal potential within the State. The study areas were the Cache Valley area, the Blackfoot Reservoir area, and as part of a state-wide study (Mitchell, 1976a; Mitchell, 1976b; Mitchell and others, 1980). The preliminary results from the present study were presented by Ralston and others (1981).

Information from all of the above reports plus additional information on ground water flow systems, chemistry of geothermal and non-geothermal systems and structural geology were analyzed as part of the investigation of the geothermal potential of the thrust area.

CHAPTER II

HYDROGEOLOGY OF THE THRUST ZONE

Introduction

The purpose of this chapter is to present a) a brief summary of the geologic history of the thrust belt in Idaho, Wyoming and Utah, b) the results of the geologic investigation of the Meade thrust zone, and c) the results of the investigation of regional hydrostratigraphy.

Geologic History

The name "overthrust belt" has been applied by geologists, and more recently the general public, to that part of the Cordilleran Mountain system which lies in western Wyoming, southeastern Idaho and northern Utah (Figure II-1). This is part of a major system that may be traced from Mexico to Canada. The overthrust belt extends in an arcuate pattern from the Snake River Plain in the vicinity of Idaho Falls, Idaho, to the vicinity of Salt Lake City, Utah, a distance of some 320 kilometers. The east-west extent of the overthrust belt is less readily defined. The eastern margin is the Darby-Hogsback fault trace on the western edge of the Green River Basin in Wyoming. The western boundary lies well to the west of the trace of the Paris-Willard fault system and west of outcrops of Precambrian age rocks near Pocatello,

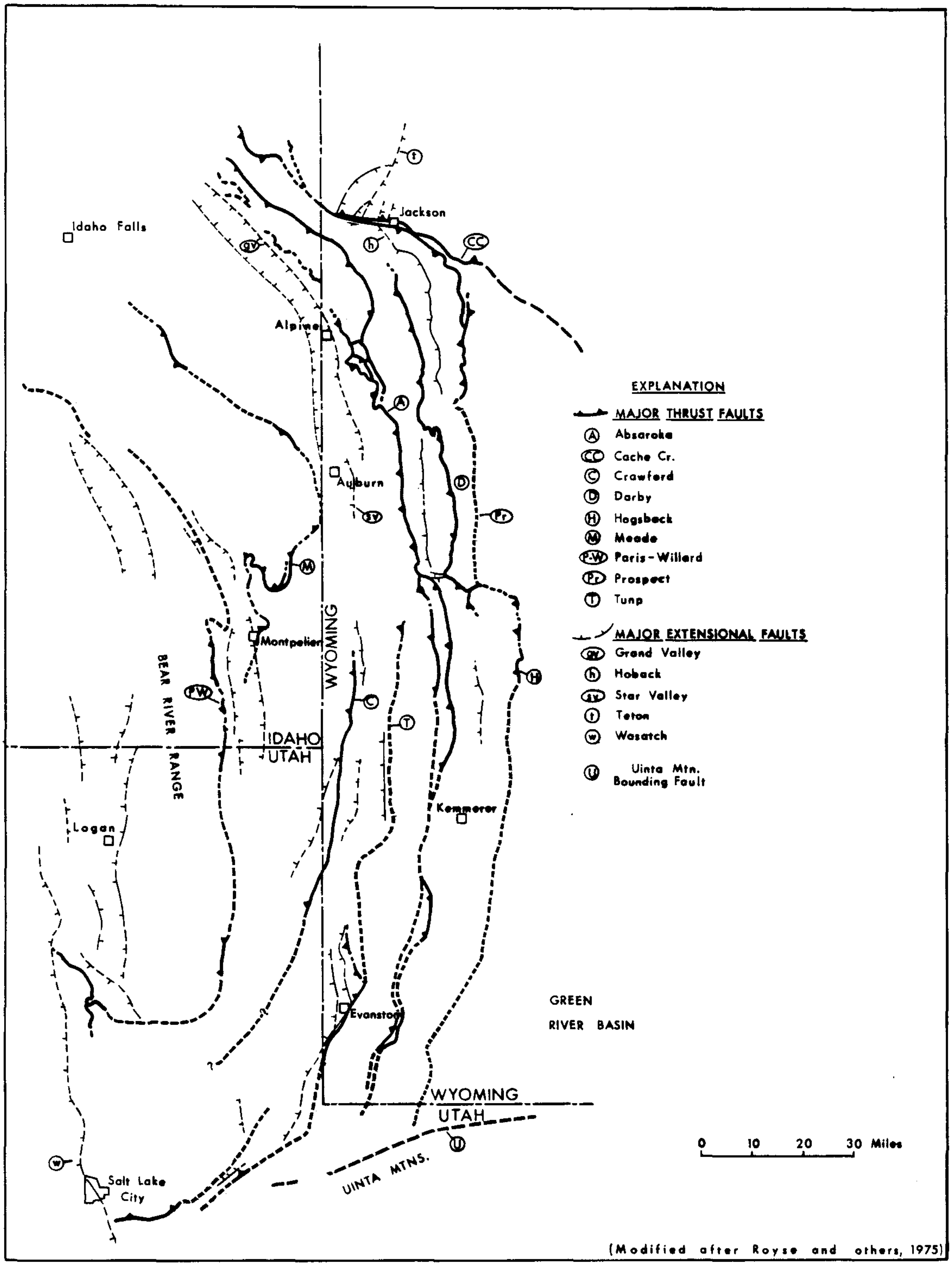

Figure II-1. Generalized structural map of the overthrust belt in southeastern Idaho, western Wyoming and northern Utah.

Idaho. At present the western edge or root zone is poorly understood (Blackstone, 1977).

Geologic development of the overthrust belt has occurred in three major stages: 1) deposition in a miogeosyncline, 2) development of northward-trending folds and thrusts faults, and 3) development of block faults that produce horst ranges and graben valleys. An excellent description of these stages is given by Armstrong and Oriel (1965). To maintain consistency in this report, their measurements are converted to metric units.

> During Paleozoic time about 20 km (kilometers) of marine sediments, mostly limestone and dolomite, were deposited in a miogeosyncline and about 2 km of mixed marine sediments were deposited on the shelf to the east... Starting in Mississippian time, the belt between shelf and miogeosyncline, where thicknesses increase markedly, shifted progressively eastward. During Mesozoic time about 11 km of marine and continental sediments were deposited in the western part of the region and about 4.5 km in the eastern part,... In late Triassic a belt on the west rose and the miogeosyncline started to break up. (Armstrong and Oriel, 1965, p. 1847).

The break up or destruction of the miogeosyncline began the second stage in the geologic development of the overthrust belt. The major faults in the overthrust belt are shown on Figure II-1.

> The second stage, which overlapped the first, produced folds overturned toward the east and thrust faults dipping gently west in a zone, convex to the east, 322 km long and 96 km wide. Stratigraphic throw on many larger faults is about 7 km; horizontal displacement is at least 16 to 24 km. Lack of metamorphism and mylonite along the

> faults is striking. From west to east, the thrust faults cut progressively younger beds,... Thrusting started in the west in latest Jurassic and ended in the east perhaps as late as early Eocene time;... (Armstrong and Oriel, 1965, p. 1847).

Block faulting is the third stage in the development of the overthrust belt. The easing of compressional forces resulted in the formation of major normal faults in the area. Faulting started in Eocene time and has continued to the Recent (Armstrong and Oriel, 1965). Block faulting produced major horst ranges and graben valleys forming the present topography. The major normal faults in the area are shown on Figure II-1.

The above is a simplified description of the complex geologic history of the overthrust belt. A typical diagrammatic cross-section of the overthrust belt is presented in Figure II-2. This diagram illustrates the complex structure of the overthrust belt.

Characteristics of the Meade Thrust

Introduction

The Meade thrust lies within the Aspen and Preuss ranges of southeastern Idaho (Figure II-1). The elevation of the area ranges between 1870 meters (m) and 3030m.

The general objective of this portion of the research was to determine how the thrust zones control flow systems. The objective was met by studying the petrologic

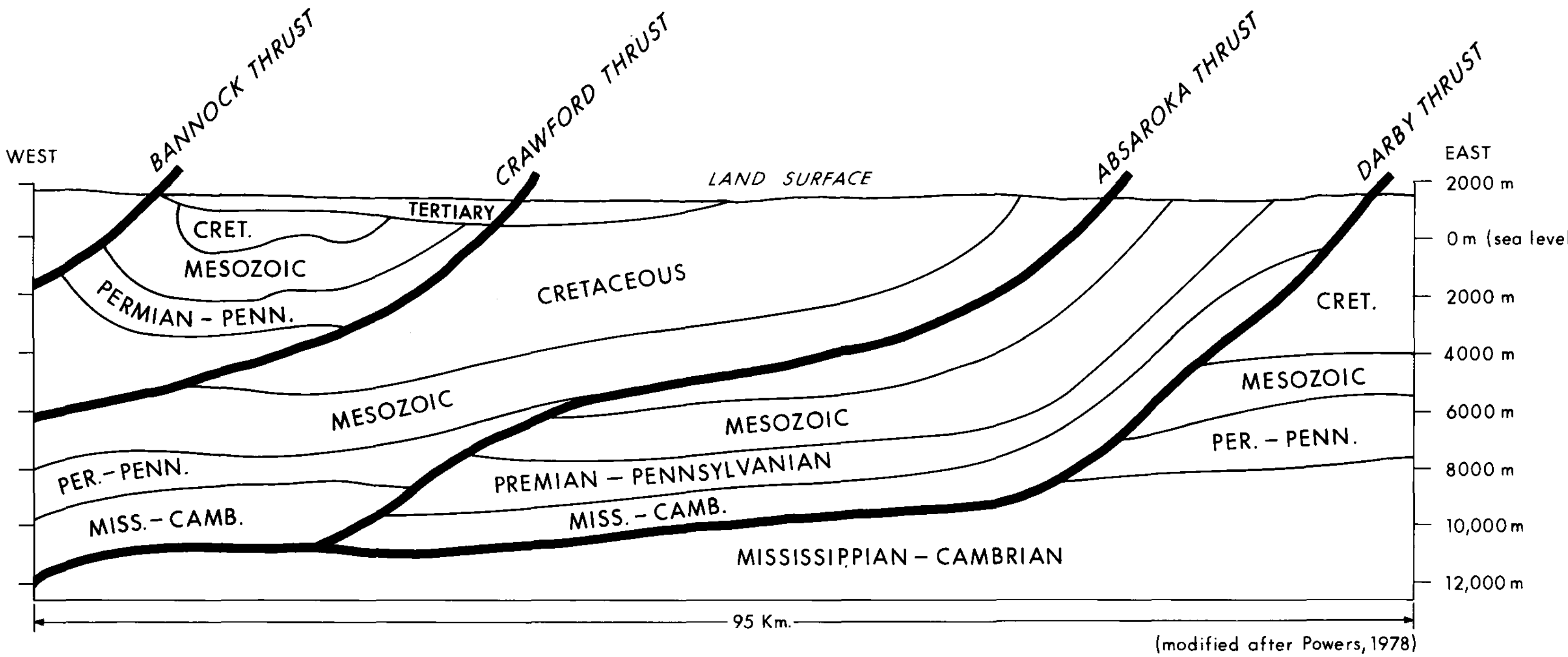

Figure II-2. Typical diagrammatic east-west cross section of the overthrust belt.

characteristics of the thrust features, such as fault gouge, fault breccias and interbedded gouge. Field work was carried out during a 60-day period in the summer and fall of 1980.

General Stratigraphy

The rocks within the Meade thrust plate range in age from Mississippian to Recent (Table II-1). Sediments of Mississippian to Jurassic age are predominately limestone, dolomite, shale and quartz sandstone. The sequence of lithologies from Mississippian to Cretaceous is conformable and is approximately 7300 m thick. Tertiary rocks are fluvial and lacustrine in nature and are found with varying thicknesses in the region. Small patches of Tertiary basalt can be found at several sites. No lithologies older than Mississippian can be found in the area. The Meade thrust has been dated by Cressman (1964) as Early Cretaceous to Eocene.

Petrology of Thrust Features

Fault Breccia. As noted by Cressman (1964), the trace of the thrust fault is marked by a breccia zone wherever Mississippian rocks are found in the upper plate. This breccia zone is seen in Georgetown Canyon near Church Hollow (Figure II-3). It is also found to the east of the Left Fork of Twin Creek and in Big Canyon, north of Georgetown and along the Star Valley thrust near Freedom, Wyoming. The breccia is yellow-red to gray in color, and variable in

Table II-1. Generalized stratigraphy of southeast Idaho (after Cressman, 1964 and Armstrong, 1953).

System	Series	Group, Formation	Thickness (m)
Tertiary	Pliocene	Salt Lake Formation	920+
	Eocene	Wasatch Formation	not known
Cretaceous		Gannett Group	1500
Jurassic	Upper Jurassic	Stump Sandstone	100-150
		Preuss Sandstone	525±
	Middle Jurassic	Twin Creek Limestone	734-1410+
		Nugget Sandstone	275-520
Triassic		Ankareh Formation	60-120 +
	Lower Triassic	Thaynes Formation	325-1125
		Dinwoody Formation	425-550
Permian		Phosphoria Formation	170
Pennsylvanian		Wells Formation	425-580
Mississippian		Mission Canyon Limestone	450-600
		Lodgepole Limestone	200-300
Devonian	Upper Devonian	Three Forks Limestone	55±
	Middle Devonian	Jefferson Dolomite	285±
Silurian	Middle Silurian	Laketown Dolomite	390
Ordovician	Upper Ordovician	Fish Haven Dolomite	150
	Lower Ordovician	Swan Peak Quartzite	180±
		Garden City Limestone	420±
Cambrian	Upper Cambrian	St. Charles Limestone	290±
	Middle Cambrian	Nounan Dolomite	335±
		Bloomington Formation	215±
		Blacksmith Formation	320±
		Ute Limestone	215±
		Langston Formation	100±
	Lower Cambrian	Brigham Quartzite	1200±

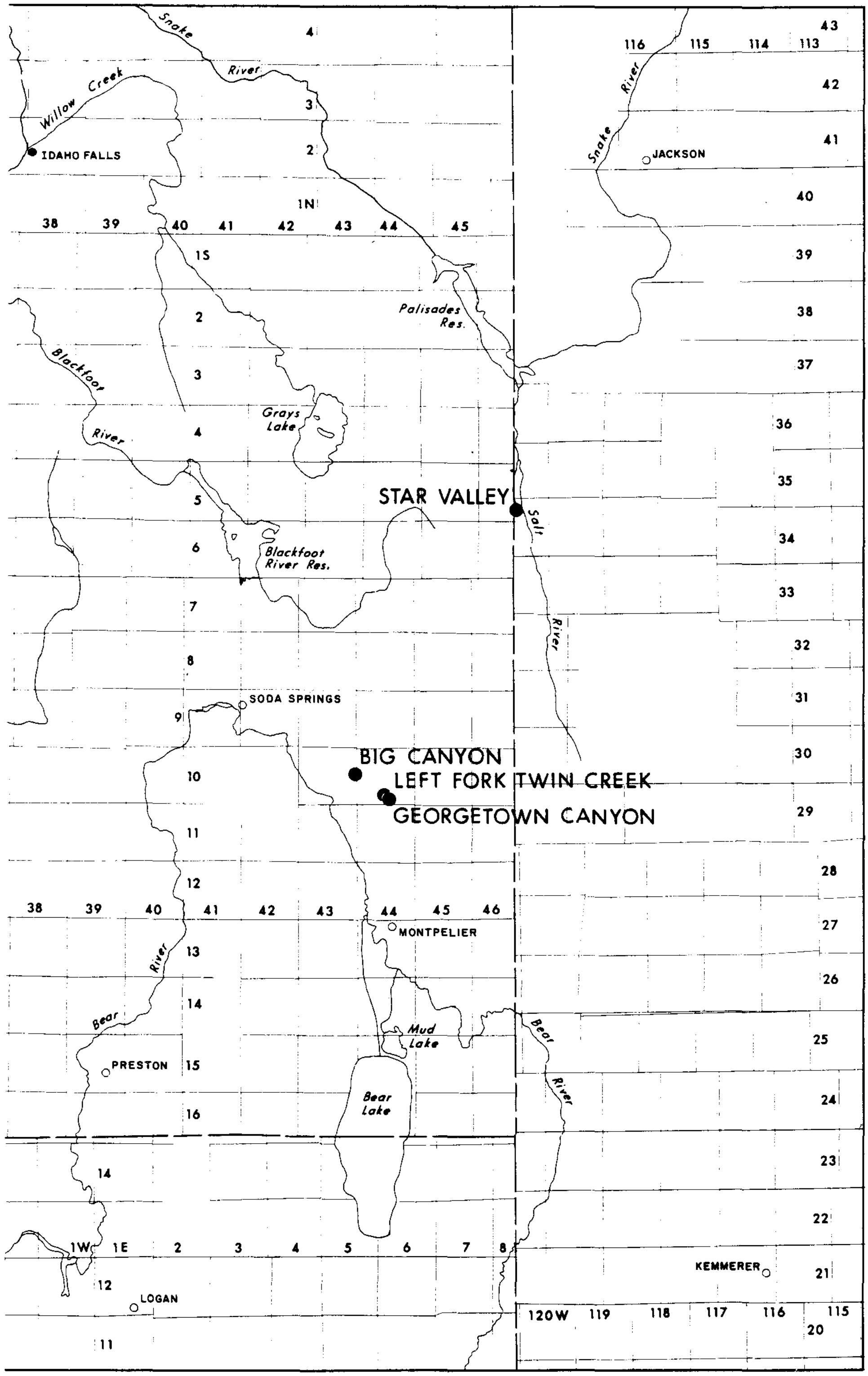

Figure II-3. Fault breccia sites examined in southeastern Idaho.

thickness, possibly up to 10 m thick. The breccia is vuggy and contains boxworks in places.

Cressman (1964) considers the breccia to be one unit, totally comprised of fault breccia. Petrographic examination of the breccia from the Meade block shows that it can be divided into three types: 1) a carbonate (limestone) unit, 2) a carbonate-clastic unit, and 3) a clastic unit. The carbonate unit (Type 1) can be described as a gray, non-permeable breccia. The clasts in this unit are angular to sub-rounded. Cathodoluminesence shows that the cement in this type is of one generation. The carbonate-clastic unit (Type 2) is comprised of two types of clasts. One is a grayish limestone and the other is a green to yellow clastic/carbonate. Cathodoluminesence shows that the cement in the carbonate portion is of one generation. The cement in the clastic/carbonate section is multi-generation.The clasts of both types are rounded. Type 3 is composed almost entirely of clastic grains that are rounded and have multi-generational cement.

Note that in the above discussion of breccias, the carbonate unit involved is predominately the Lodgepole Limestone and this is almost exclusively limestone. While using the term clastic to describe one type of clasts, it should be pointed out that the "Clastic" units involved are the Twin Creek Limestone and the Wells Formation, which may have calcareous beds. These units are described as clastic because of the high amount of detrital quartz visible under cathodoluminesence.

Fault Gouge. Fault gouge is found only in one section in Georgetown Canyon (Figure II-3). The gouge is found within the Wells Formation, above the chert layer. The gouge ranges in thickness from a few centimeters to a maximum of one meter. The gouge is black in color and is very friable. In thin section, the gouge is 99 percent chert.

Interbeded Gouge. Interbedded gouge occurs in limited areas, predominately in the Twin Creek Limestone along Crow Creek. It is difficult to recognize in the field. The gouge is characterized by micro-fractures along bedding planes in an otherwise massively bedded unit.

Porosity and Permeability. The laboratory measurements of porosity and permeability do not take into account the amount of fracturing present in the lithology. Type 1 (carbonate) breccias generally have low porosity (1-5%) and low permeabilities (1-50 millidarcies) (md). Type 2 breccias have intermediate porosities (2-10%) and intermediate permeabilities (10-500 md). Type 3 breccias (clastic) have the highest porosities (5-17%) and the highest permeabilities (500-17,000 md).

All of the various lithologies have extremely low primary porosities (0-3%) and permeabilities (0-10 md). However, formations such as the Wells or Dinwoody may be highly jointed and fractured and thus may transmit a considerable amount of water.

It was not possible to measure the porosity of the gouge due to the nature of the material. In the field it appeared to be highly porous.

Interpretation of Results

Cressman (1964) states that the Meade thrust started as a bedding plane thrust within or at the base of the Madison (Lodgepole) Limestone. The thrust followed this horizon for 27 km before cutting up diagonally through Mississippian to Jurassic sediments before settling in as a bedding plane thrust again, now in the Jurassic Twin Creek Formation. Gretener (1979) notes that thrust faults tend to linger in incompetent strata and step through competent strata at relatively steep angles. The Meade thrust fault seems to be no different in this respect.

The thrust deformation features were formed in the brittle field under lower pore pressure. All the thrust features occurred when the thrust was stepping up. Because brittle deformation tends to create a rock with high permeability and porosity, the fault breccias have the highest porosity and permeability of the samples measured. Ductile deformation tends to leave a dense rock. It is likely that this is the condition that existed for much of the time thrusting occurred.

In conclusion, because of the limited extent of thrust related features and because of their relatively high porosities and permeabilities, it is not likely that the thrusting within the Meade plate has created a barrier to any flow systems. The thrust may, however, be regarded as a secondary control in preferentially positioning lithologies with high permeability against less permeable lithologies.

Regional Hydrostratigraphy

Introduction

The relationship between structural and stratigraphic features in southeastern Idaho is very complex. Thermal and non-thermal springs in the area indicate the presence of equally complex ground water flow systems. Previous investigators have documented that the flow systems are controlled by both the complex structural setting of the area and the variations in hydraulic conductivity between individual stratigraphic units in the sedimentary rock sequence. Winter (1979) found that the hydraulic conductivity values within several stratigraphic units were areally consistent and provided a key to understanding ground water flow systems in a portion of southeast Idaho.

This study was directed toward understanding the variations in the water bearing characteristics of selected stratigraphic units in southeast Idaho, expanding upon the data base provided by Winter (1979). The usual classification of the geologic formations based on their age, lithologic and paleontological characteristics, may not be an accurate criterion for judging their hydrologic properties. Therefore, in ground water studies, a different classification is used based on the capacity of the rock to yield water from storage (storativity) and on its capacity to transmit water (hydraulic conductivity). The resulting rock units of this classification are called hydrostratigraphic units (Mohammad, 1976, p. 35). The boundaries of these units may or may not coincide with the boundaries of the geological formations.

The purpose of this portion of the study is to provide a better understanding of the hydrostratigraphic controls for ground water flow in southeast Idaho. The general objective is to utilize stream flow measurements, a spring inventory, and knowledge of geology and hydrology to define hydrostratigraphic controls for ground water flow in units of the geologic column in southeast Idaho.

Method of Study

Data from stream flow measurements and a spring inventory were utilized to describe the hydrostratigraphic controls on ground water flow in southeast Idaho. The results of these analyses were used to test the hypothesis that the hydrostratigraphic controls on ground water flow are areally consistent.

Stream flow measurements and a spring inventory were used to locate and catagorize the hydrogeologic characteristics of units which support ground water flow systems. Ground water flow systems are indicated on the surface by the presence of recharge and discharge areas. Spring discharges are clearly indications of ground water flow systems. Gain or loss in stream flow are also indications of the presence of a ground water flow system. If a stream flows over a recharge area, water from the stream will enter the ground water system and the stream will lose flow. Conversely a stream will gain flow in a ground water discharge area. A lack of change in stream flow across a unit does not necessarily indicate the unit has low hydraulic conductivity. Stream flow may not change across a unit with high hydraulic conductivity if the unit is structurally isolated from a flow system. The characteristics of gaining, losing and no gain or loss sections of a stream are illustrated in Figure II-4.

Stream flow measurements were taken during August, 1980, and September, 1981. The late summer time frame was chosen so that stream flow could be measured at or near baseflow levels.

Initially, stream flow measurement sites were selected in the office prior to the field season. Geologic maps were examined to find the streams which flowed over formations of

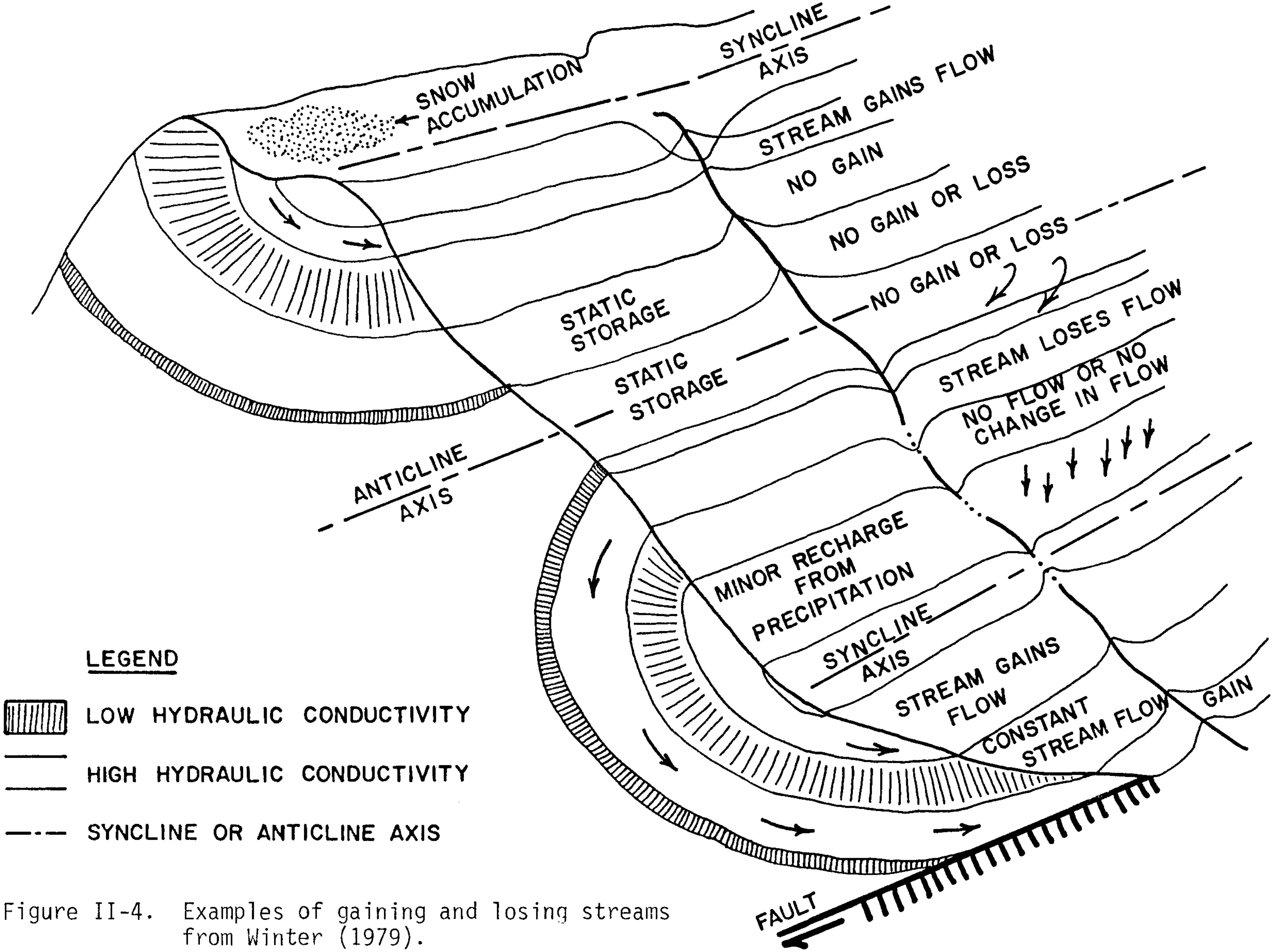

Figure II-4. Examples of gaining and losing streams from Winter (1979).

interest to this study. In the field, it was realized that the hydrostratigraphy of various formations could not be analyzed because of the limited availability of suitable stream flow measurement sites. As a result, data were only collected for streams which flowed over selected Jurassic, Mississipppian, Ordovician and Cambrian formations.

Once a suitable flowing stream was located, the actual measurement sites were selected based upon several criteria: a) there be flow across a formation of interest, b) the stream channel be underlain by a minimum of valley fill material, and c) the measurement sites have some means of reasonable access, either by vehicle or on foot. Measurement sites were generally located at or near the point where the stream flowed over a formation contact. This was done to obtain a measured flow across the exposed formation. Formation contacts were located originally by examining geologic maps and, where possible, were verified in the field by examining rock outcrops.

Stream flow was measured by one of two methods: a) a pygmy current meter and a topsetting rod and b) a sixty-degree, V-notch flume constructed of fiberglass with a sidewall and headscale. The flume was capable of measuring discharge over a range of 0.003 to 2.33 liter/sec. The flume was used where stream flow was too low to use the current meter. The accuracy of the two measurement techniques was assumed to be plus or minus 10 percent.

The spring inventory was conducted in the office during October and November, 1981. Spring sites were initially located by examining U.S. Geological Survey 7.5 and 15 minute topographic quadrangles. Topographic maps of this scale identify where springs are located. Spring sites identified from the topographic maps were then located on geologic maps of the same area. The local geology at each spring site was evaluated to determine from what formation the spring discharged. The presence of structural features near the spring site, such as faults or folds, was recorded.

Presentation and Analysis of Data

Stream Gain-Loss Data. Stream flow data have been collected for ten stream sections in southeast Idaho. The location of the measured sections within the study area are shown on Figure II-5. Stream gain-loss characteristics are discussed according to three different groups of streams based upon the age of the formations exposed in the stream channel. The first group includes four streams that flow over the Jurassic Nugget or Twin Creek Formations. Two streams which cross over the Mississippian Mission Canyon Formation make up the second group. The third group is comprised of four streams that flow over formations ranging in age from the Ordovician Swan Peak Formation to the Lower Cambrian Brigham Formation. General data for streams, such as name, location and measurement data are listed on Table

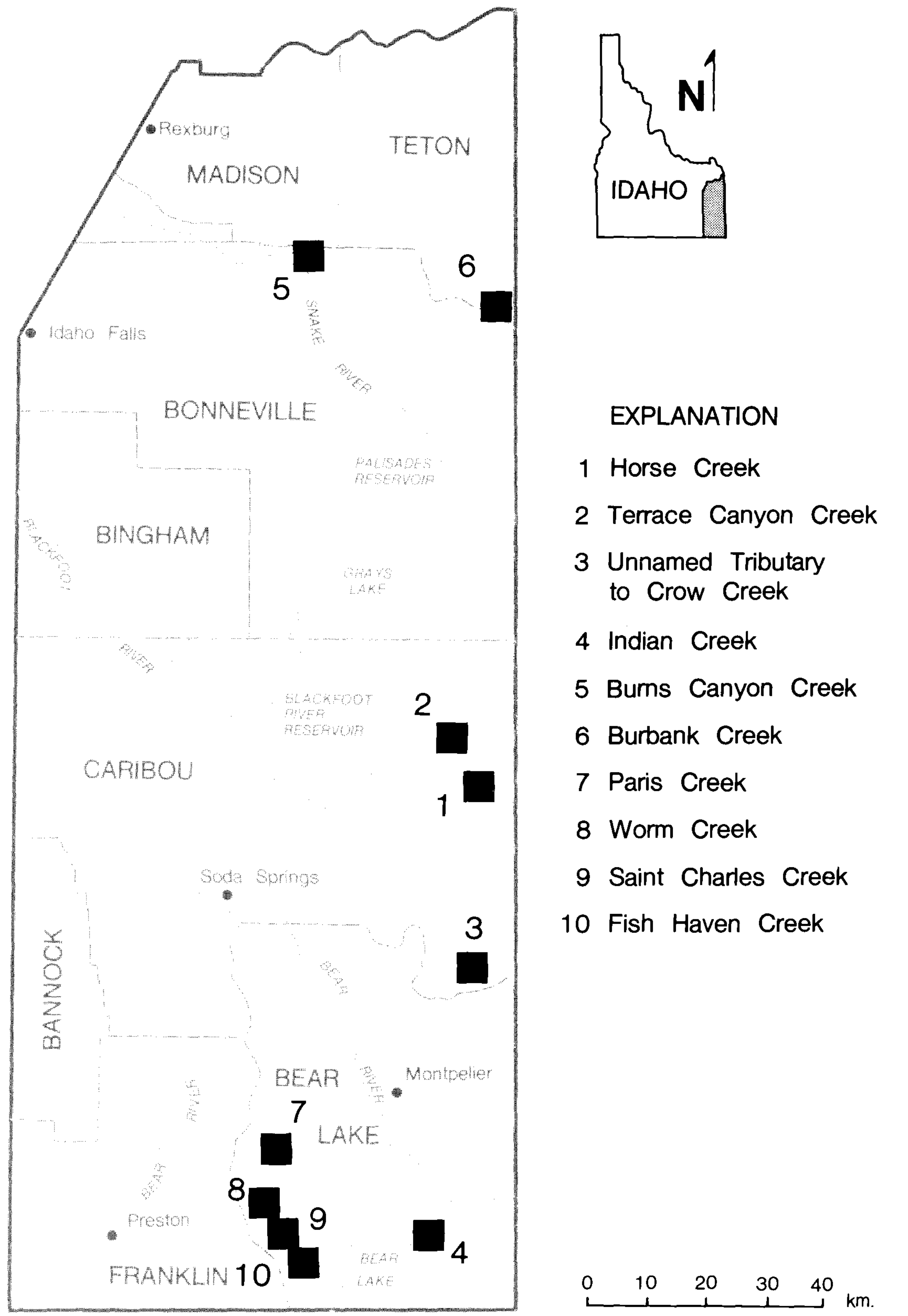

Figure II-5. Location of stream sections for gain - loss measurements from Arrigo (1982).

II-2. Additional details on stream flow measurements are given in Arrigo (1982).

A classification system was developed to analyze stream flow data. The system is based upon the percent of change in stream discharge between measurement sites. The percent of change in the discharge between measurement sites is used to quantify whether the data show no indication or a moderate or strong indication of high hydraulic conductivity. An 11 to 20 percent change in flow is considered a moderate indication of high hydraulic conductivity. A flow change greater than 20 percent is considered a strong indication of high hydraulic conductivity.

The four study streams that flow over the Jurassic formations are Horse Creek, Terrace Canyon Creek, unnamed tributary to Crow Creek and Indian Creek (Figure II-5). The investigation of the Horse Creek section is presented in detail in the following paragraph as an example of the descriptions given in Arrigo (1982).

The section of Horse Creek that was measured flows over the Twin Creek and Nugget Formations. The geology of the Horse Creek area and the location of stream flow measurement sites are shown on Figure II-6. A geologic cross-section through the Horse Creek area, along the line X-X' shown on Figure II-6, is presented on Figure II-7. Triassic, Jurassic and Tertiary Formations are exposed in the area shown on

Table II-2. The name, location, date measured, exposed formation, number of measurements and type of access for stream gain-loss sites in southeast Idaho.

Site	Date Measured	Exposed Formation	Number of Measurements	Access
Horse Creek 7S 46E 20	9-21-81	Jt, Jn	3	Hike
Terrace Canyon Creek 6S 45E 28 & 27	9-22-81	Jt, Jn	3	Hike
Unnamed Tributary to Crow Creek 10S 46E 35	9-22-81	Jp, Jt	2	Pickup
Indian Creek 15S 46E 19, 20 & 30	9-23-81	Jn, Jt	4	Pickup
Burns Canyon Creek 3N 43E 6 & 12	9-20-81	Mm	2	Hike
Burbank Creek 2N 46E 9	9-9-81	Mm	2	Hike
Paris Creek 14S 42E 13 14S 43E 18	7-14-80 7-15-80	Ꞓbo, Ꞓbl Ꞓu, Ꞓl, Ꞓq	7	Pickup
Worm Creek 15S 43E 6 & 5	7-16-80	Ꞓs, Ꞓn, Ꞓbo, Ꞓbl	5	Pickup and Hike
Saint Charles Creek 15S 42E 26 & 24	7-17-80	Os, Og	3	Pickup
Fish Haven Creek	9-24-81	Og, Ꞓs, Ꞓn	5	Pickup

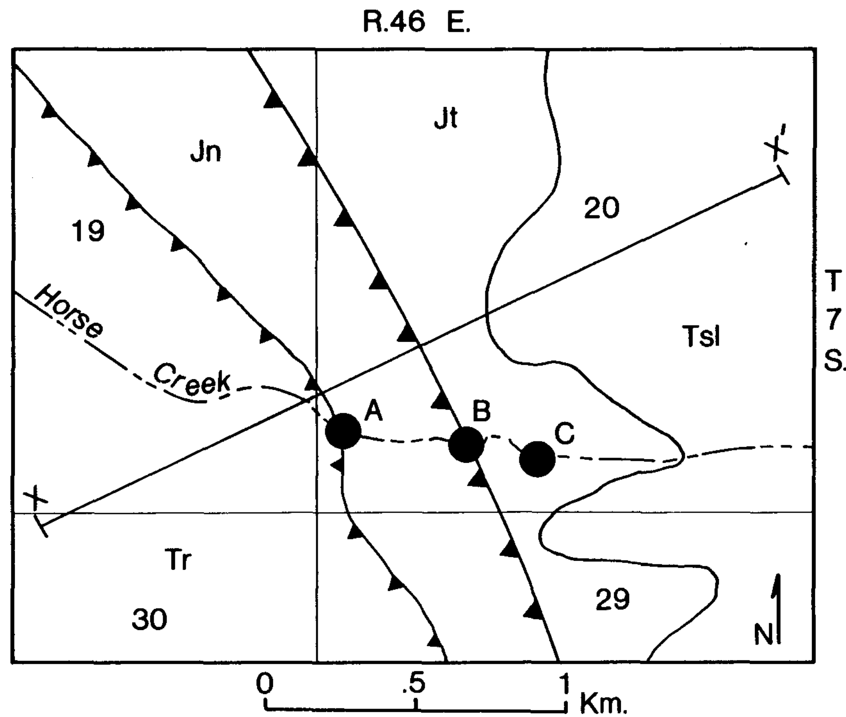

Site	Discharge
A	24 l/s
B	19 l/s
C	40 l/s

Figure II-6. Geology of Horse Creek area from Arrigo (1982).

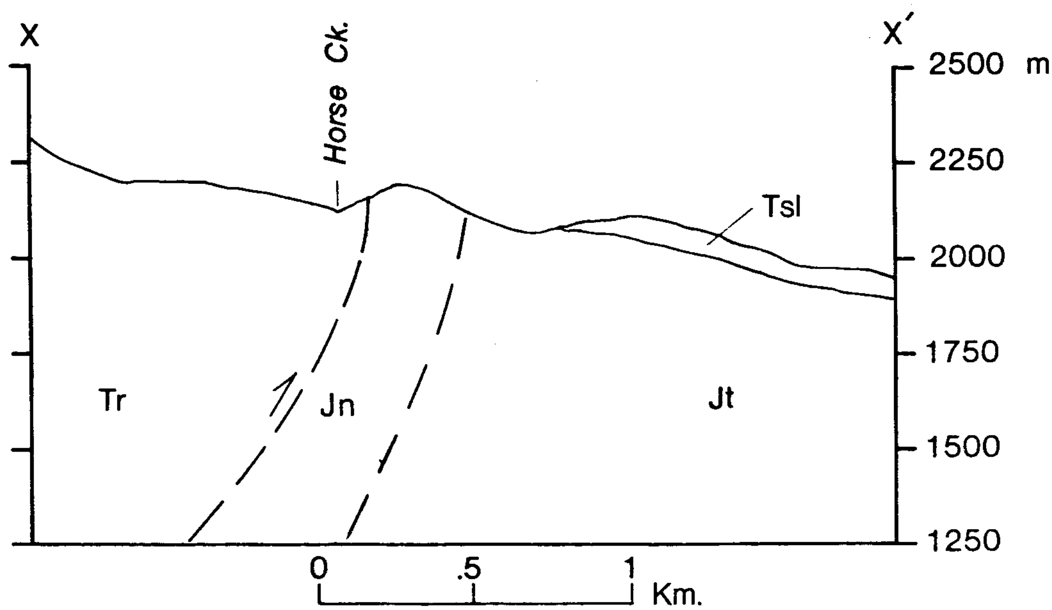

Figure II-7. Cross-section of Horse Creek area from Arrigo (1982).

Figure II-6. Directly west of this area lies the axis of a north-south-trending anticline. Thus, formations in the area generally dip to the east. The main structural features in the area are two branches of a northwest-trending thrust fault. The thrust fault dips to the west. The western thrust fault places undifferentiated Tertiary formations unconformably over the Nugget Formation and the eastern thrust fault places the older Nugget Formation on top of the younger Twin Creek Formation (see Figure II-7). On the eastern side of Figure II-6, terrace deposits lap against the Twin Creek Formation. These poorly-consolidated sediments are part of the Tertiary Salt Lake Formation.

Three stream flow measurements were taken on Horse Creek. The objective of measuring flow at Horse Creek was to obtain measured flow across the Nugget and Twin Creek Formations. The first measurement site was located where the creek starts to flow over the Nugget Formation. The second site was placed downstream, at approximately the Nugget-Twin Creek contact. This contact is the trace of the thrust fault. The third measurement station was located downstream of the second site where the Twin Creek Formation is exposed in the channel. Stream gain-loss data for Horse Creek are listed on Table II-3.

Stream flow data from Horse Creek show a strong indication that both the Nugget and the Twin Creek Formations have zones of high hydraulic conductivity. Stream flow

Table II-3. Stream gain-loss data for Horse Creek

Site	Discharge (l/s)	Difference (l/s)	Change (%)	Indication of High K	Exposed Formation
A	24				
		-5	-21	strong	Jn
B	19				
		+21	+110	strong	Jt
C	40				

decreased considerably between sites A and B because of water entering the Nugget Formation. A large amount of ground water discharged into the stream from the Twin Creek Formation between sites B and C. It is possible that the thrust fault in the area creates a zone of high hydraulic conductivity due to fracturing. Distinct discharge or recharge points were not identifiable along the section of Horse Creek that was measured.

Stream flow data from Terrace Canyon Creek show a moderate indication of high hydraulic conductivity for the Nugget Formation. The data also show a strong indication of high hydraulic conductivity for the Twin Creek Formation. Stream flow increased between measurement sites over both units; ground water discharged from the Nugget and Twin Creek Formations into the stream. It is possible that a thrust fault in the area is a significant control for ground water flow. The occurrence of a spring near the thrust fault indicates that the fault has created a zone of high hydraulic conductivity through which ground water discharges.

The section of the unnamed tributary to Crow Creek that was measured flows over the Twin Creek Formation. Stream flow was estimated to be approximately equal at each of the two measurement sites. Data do not show any indication of high hydraulic conductivity for the Twin Creek Formation at this site.

Four stream flow measurements were taken on Indian Creek. The objective of the measurement placement was to obtain a measured flow across the Twin Creek and Nugget Formations. Stream flow across the Twin Creek Formation slightly increased but does not indicate high hydraulic conductivity. The small gain in stream flow measured across the Nugget Formation may be the result of water discharging from a zone of high hydraulic conductivity along a thrust fault. It appears that structural features are the primary factors which control the distribution of hydraulic conductivity at the Indian Creek site.

The two study streams that flow over the Mississippian Mission Canyon Formation are Burns Canyon Creek and Burbank Creek (Figure II-5). The stream flow data from the two measurement sites on Burns Canyon Creek do not show any indication of high hydraulic conductivity for the Mission Canyon Formation. Stream flow data from the two measurement sites on Burbank Creek show a strong indication of high hydraulic conductivity for the Mission Canyon Formation. Stream flow increased considerably across the Mission Canyon Formation.

The four study streams that flow over Ordovician and Cambrian Formations are Paris Creek, Worm Creek, St. Charles Creek and Fish Haven Creek (Figure II-5). Seven stream flow measurements were taken at Paris Creek. The objective of the measurement placement was to obtain a measured flow across the Blacksmith, Ute, Langston and Brigham Formations. Stream flow data for Paris Creek show no indication of high hydraulic conductivity for the Blacksmith and Brigham Formations. Also, the data show a strong indication of high hyraulic conductivity for the Ute Formation and a moderate indication for the Langston Formation. Stream flow increased across the Ute Formation and decreased across the Langston Formation. Stream flow remained unchanged across the Blacksmith and Brigham Formations. These data indicate that the Ute and Langston Formations have zones of high hydraulic conductivity in the Paris Creek area. The spring at the head of Paris Canyon discharges from the Bloomington Formation. The presence of this spring indicates that the Bloomington Formation contains a zone of high hydraulic conductivity.

Five stream flow measurements were taken on Worm Creek. The objective of the measurement placement was to obtain a measured flow across the Saint Charles, Nounan, Bloomington and Blacksmith Formations. Indication of high hydraulic conductivity for stream gain-loss data at Worm Ceek are as follows: moderate for the Saint Charles Formation, strong for the Nounan Formation, none for the Bloomington Formation and moderate for the Blacksmith Formation. Stream flow increased across the Saint Charles Formation, decreased significantly across the Nounan Formation, remained unchanged across the Bloomington Formation and decreased slightly across the Blacksmith Formation.

Three stream flow measurements were taken on Saint Charles Creek. The objective of the measurement placement was to obtain a measured flow across the Swan Peak and Garden City Formation. Stream flow data show a moderate indication of high hydraulic conductivity for the Swan Peak and Garden City Formations. A measurement could not be obtained near the Swan Peak-Garden City contact; the formation across which flow was lost thus cannot be determined. A large spring discharges from the Garden City Formation indicating that this formation contains a zone of high hydraulic conductivity. With the incomplete stream flow data, only the presence of the spring discharging from the Garden City Formation can be used as an indication of high hydraulic conductivity in the area.

Five stream flow measurements were taken on Fish Haven Creek. The objective of the measurement placement was to obtain a measured flow across the Garden City, Saint Charles, Nounan and Bloomington Formations. Stream gain-loss data show a strong indication of high hydraulic conductivity for the Saint Charles and Nounan Formations. Stream flow increased significantly across both of these formations. Stream flow data do not show any indication of high hydraulic conductivity for the Garden City Formation. However, the presence of a spring discharging from the Garden City Formation indicates the presence of a high hydraulic conductivity zone within this formation.

Gain-loss data from the stream sections measured in southeastern Idaho are summarized on Table II-4. The analysis of stream gain-loss data shows strong indications of high hydraulic conductivity for the Twin Creek (Jt) and Nounan (Cn) Formations at two locations. A strong indication of high hydraulic conductivity was also measured for the Nugget (Jn), Mission Canyon (Mm), Ute (Cu) and Swan Peak (Os) Formations. Moderate indications of high hydraulic conductivity were observed for the Nugget (Jn) and Garden City (Og) Formations at two locations and for the Twin Creek (Jt), Swan Peak (Os), Saint Charles (Cs), Bloomington (Cbo), Blacksmith (Cbl) and Langston (Cl) Formations at single locations.

Given the complex geologic setting of southeastern Idaho, it is difficult to determine whether the indications

Table II-4. Summary of stream gain-loss data for stream sections measured in southeastern Idaho.

Stream Name	Exposed Formation	Indication of High Hydraulic Conductivity*	Other Indication of High Hydraulic Conductivity	Structural Feature Affecting Hydraulic Conductivity
Horse Creek	Nugget (Jn)	strong	-	fault
	Twin Creek (Jt)	strong	-	fault
Terrace Canyon Creek	Nugget (Jn)	moderate	-	fault
	Twin Creek (Jt)	strong	moderate (spring discharge)	fault
Unnamed Tributary to Crow Creek	Twin Creek (Jt)	none		fault
Indian Creek	Twin Creek (Jt)	none	moderate (spring discharges)	syncline/fault
	Nugget (Jn)	moderate		fault
Burns Canyon Creek	Mission Canyon (Mm)	none	-	fault
Burbank Creek	Mission Canyon (Mm)	strong	moderate (spring discharge)	none identifiable
Paris Creek	Bloomington (Єbo)	none	moderate (spring discharge)	syncline
	Blacksmith (Єbl)	none	-	syncline
	Ute (Єu)	strong	-	syncline
	Langston (Єl)	moderate	-	syncline
	Brigham (Єq)	none	-	syncline
Worm Creek	Saint Charles (Єs)	moderate	-	syncline
	Nounan (Єn)	strong	-	syncline
	Bloomington (Єbo)	none	-	syncline
	Blacksmith (Єbl)	moderate	-	syncline
Saint Charles Creek	Swan Peak (Os)	moderate	-	syncline
	Garden City (Og)	moderate	moderate (spring discharge)	syncline
Fish Haven Creek	Garden City (Og)	none	moderate (spring discharge)	syncline
	Saint Charles (Єs)	strong	-	syncline
	Nounan (Єn)	strong	-	syncline

* Indication of high hydraulic conductivity
0-10 percent gain or loss equals no indication
11-20 percent gain or loss equals moderate indication
>20 percent gain or loss equals strong indication

of high hydraulic conductivity within a formation represent a regional pattern of primary and secondary hydraulic conductivity or localized zones created by faulting and folding. Structural features affecting hydraulic conductivity were identified at practically all of the measured stream sections. This suggests that structural features are important factors which control hydraulic conductivity in southeastern Idaho.

Spring Inventory. The location, elevation and geology of 281 spring sites were recorded for the spring inventory. A detailed list of spring inventory data is presented in Arrigo (1982). A total of forty 7.5 minute and six 15 minute topographic quadrangles were examined for the spring inventory. The portion of the study area covered by the spring inventory is shown on Figure II-8. Many quadrangles in the study area could not be inspected for spring discharges because of the lack of corresponding geologic maps. Thus, the inventory is biased toward the formations on the quadrangles examined. To adjust for the bias, spring data from formations that are exposed in a limited area were not included in the inventory. Springs which discharge from alluvium, basalt or the Tertiary Salt Lake Formation were also excluded from the spring inventory. The water-bearing characteristics of these formations are known from previous studies (Dion, 1969, 1974) and are only locally important in the hydrostratigraphic framework of southeastern Idaho.

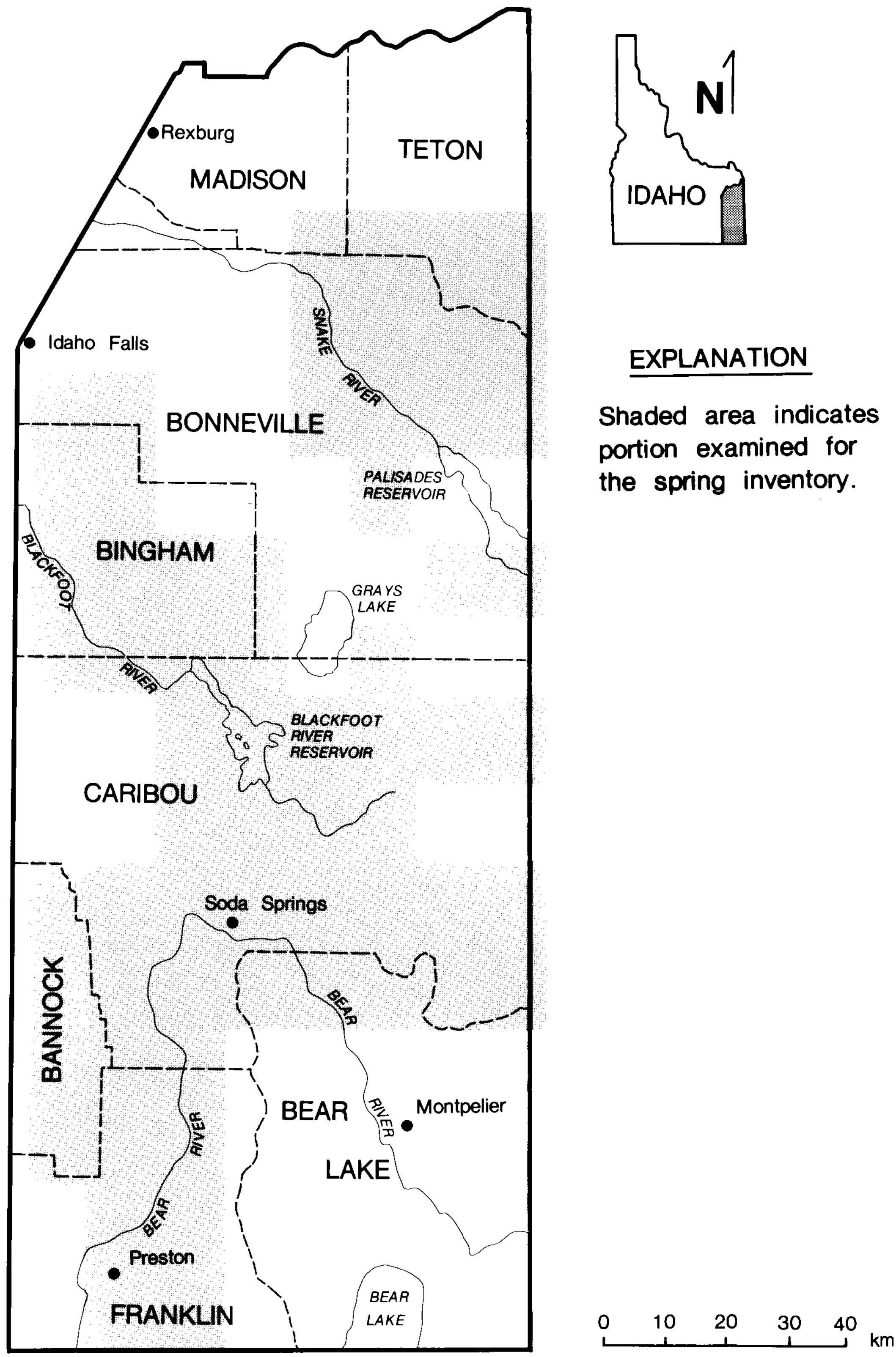

Figure II-8. Area covered by spring inventory from Arrigo (1982).

The location of a spring discharge is dependent upon stratigraphy and structure. The lithology and thickness of a unit, and the position of a permeable unit relative to an impermeable unit are stratigraphic features which influence the location of spring discharges. Faults and folds are structural features that affect the location of spring discharges. Many springs are situated along zones of high hydraulic conductivity caused by faults or folds. The presence of structural features at or near a spring site was recorded for the spring inventory to aid in describing the factors which control hydraulic conductivity.

A classification system was developed for this study to aid the analysis of spring inventory data. The classification system is based on the total number of springs determined to be discharging from each formation. The number of springs discharging from a formation was used to quantify whether inventory data show a weak, moderate or strong indication of high hydraulic conductivity. Five or less springs discharging from a formation represents a weak indication of high hydraulic conductivity. A total of six to ten springs discharging from an individual formation is considered a moderate indication of high hydraulic conductivity. Greater than ten springs discharging from a formation represents a strong indication of high hydraulic conductivity.

A summary of spring inventory data is presented on Table II-5. This table lists each formation and the number of springs found discharging from each formation. Indications of high hydraulic conductivity are also shown on Table II-5. A strong indication of high hydraulic conductivity was calculated for the following formations: Kirkham Hollow (Tk), Frontier (Kf), Gannett (Kg), Thaynes (Trt), Dinwoody (Trd), Wells (PPw), Bloomington (Cbl) and Brigham (Cq). For the following formations, the spring inventory showed a moderate indication of high hydraulic conductivity: Wayan (Kw), Bear River (Kb), Twin Creek (Jt), Phosphoria (Pp), Mission Canyon (Mm), Gallatin (Cq), and Nounan (Cn). The spring inventory showed a weak indication or no indication of high hydraulic conductivity for the remaining formations on Table II-5.

The number and percent of springs associated with structural features are also shown on Table II-5. Of the 281 springs recorded for the spring inventory, 162 or 58 percent were located at or near structural features.Given the high degree of faulting and folding in southeastern Idaho, it is probable that the majority of springs in the study area are associated with structural features. Minor faults and folds are too numerous to be shown on geologic maps; thus, it was not possible to record the presence of small faults or folds that may be affecting some spring sites. The large number of

Table II-5. Summary of spring inventory data from southeastern Idaho.

Formation Name	Number of Springs	Indication of High Hydraulic Conductivity*	Springs Associated with Structural Features Number	%
Kirkham Hollow (Tk)	20	strong	0	0
Wasatch (Tw)	0	-	0	0
Wayan (Kw)	9	moderate	4	44
Frontier (Kf)	18	strong	10	55
Aspen (Ka)	3	weak	1	33
Bear River (Kb)	9	moderate	2	22
Gannett (Kg)	16	strong	11	69
Stump (Js)	2	weak	1	50
Preuss (Jp)	4	weak	4	100
Twin Creek (Jt)	9	moderate	6	66
Nugget (Jn)	2	weak	1	50
Ankareh (Tra)	5	weak	3	60
Thaynes (Trt)	29	strong	22	76
Woodside (Trw)	1	weak	0	0
Dinwoody (Trd)	34	strong	23	68
Phosphoria (Pp)	8	moderate	5	63
Wells (PPw)	31	strong	23	74
Tensleep (PPt)	5	weak	4	80
Amsden (PPa)	1	weak	0	0
Mission Canyon (Mm)	10	moderate	7	70
Lodgepole (Ml)	5	weak	3	60
Darby (Dd)	2	weak	0	0
Beirdneau (Db)	0	-	0	0
Hyrum (Dh)	0	-	0	0
Laketown (Sl)	0	-	0	0
Bighorn (Ob)	0	-	0	0
Fish Haven (Of)	0	-	0	0
Swan Peak (Os)	4	weak	2	50
Garden City (Og)	5	weak	1	20
Gallatin (Ꞓg)	7	moderate	7	100
Saint Charles (Ꞓs)	2	weak	1	50
Nounan (Ꞓn)	6	moderate	3	50
Gros Ventre (Ꞓgv)	1	weak	0	0
Bloomington (Ꞓbo)	12	strong	9	75
Blacksmith (Ꞓbl)	2	weak	1	50
Ute (Ꞓu)	0	-	0	0
Langston (Ꞓl)	2	weak	1	50
Brigham (Ꞓq)	17	strong	7	41
Total	281		162	58

* Indication of high hydraulic conductivity
0-5 springs equal weak indication
6-10 springs equal moderate indication
>10 springs equal strong indication

springs situated at or near structural features suggests structural features are important factors which control the location of springs in southeastern Idaho.

Interpretation of Results

Estimates of the hydraulic conductivity of individual formations in southeastern Idaho based on stream gain-loss data and spring inventory data, are presented on Table II-6. This table lists the indications of high hydraulic conductivity that were determined from stream gain-loss measurements and the spring inventory. Arrigo (1982) presents details concerning the formulation of Table II-6. The factors controlling hydraulic conductivity, if identifiable, are shown for each formation in Table II-6. This classification is based upon the percentage of springs inventoried associated with structural features.

The hydrostratigraphic controls which influence the movement of groundwater in southeast Idaho were identified by estimating the relative hydraulic conductivity of individual formations and the controls on hydraulic conductivity. The consistency of and the controls on hydraulic conductivty were evaluated using streamflow data to test the hypothesis that the hydrostratigraphic controls on groundwater flow are areally consistent. Stream flow was measured across the Twin Creek Formation at four sites, the Nugget Formation at three sites, and twice across the Garden

Table II-6. Estimation of relative hydraulic conductivity and factors controlling hydraulic conductivity for the formations in southeast Idaho, based on stream gain-loss and spring inventory data.

	Stream Gain-Loss Data		Spring Inventory Data			
Formation Name	Indication of High Hydraulic Conductivity	Structural Feature Affecting Hydraulic Conductivity	Indication of High Hydraulic Conductivity	Percent Springs Associated with Structural Features	Estimate of Relative Hydraulic Conductivity	Factor Controlling Hydraulic Conductivity
Kirkham Hollow (Tk)	-	-	strong	0	high	stratigraphy
Wasatch (Tw)	-	-	-	-	not estimated	none identifiable
Wayan (Kw)	-	-	moderate	44	medium	stratigraphy/structure
Frontier (Kf)	-	-	strong	55	high	structure/stratigraphy
Aspen (Ka)	-	-	weak	33	low	stratigraphy/structure
Bear River (Kb)	-	-	moderate	22	medium	stratigraphy
Gannett (Kg)	-	-	strong	69	high	structure/stratigraphy
Stump (Js)	-	-	weak	50	low	structure/stratigraphy
Preuss (Jp)	-	-	weak	100	low	structure
Twin Creek (Jt)	strong	fault	moderate	66	medium to high	structure/stratigraphy
"	strong	fault				
"	none	fault				
"	moderate	syncline/fault				
Nugget (Jn)	strong	fault	weak	50	low to high	structure/stratigraphy
"	moderate	fault				
"	moderate	fault				
Ankareh (Tra)	-	-	weak	60	low	structure/stratigraphy
Thaynes (Trt)	-	-	strong	76	high	structure
Woodside (Trw)	-	-	weak	0	low	stratigraphy
Dinwoody (Trd)	-	-	strong	68	high	structure/stratigraphy
Phosphoria (Pp)	-	-	moderate	63	medium	structure/stratigraphy
Wells (PPw)	-	-	strong	74	high	structure/stratigraphy
Tensleep (PPt)	-	-	weak	80	low	structure
Amsden (PPa)	-	-	weak	-	low	stratigraphy
Mission Canyon (Mm)	none	fault	moderate	70	medium to high	structure/stratigraphy
"	strong	none identifiable				
Lodgepole (Ml)	-	-	weak	60	low	structure/stratigraphy
Darby (Dd)	-	-	weak	0	low	stratigraphy
Beirdneau (Db)	-	-	-	-	not estimated	none identifiable
Hyrum (Dh)	-	-	-	-	not estimated	none identifiable
Laketown (Sl)	-	-	-	-	not estimated	none identifiable
Bighorn (Ob)	-	-	-	-	not estimated	none identifiable
Fish Haven (Of)	-	-	-	-	not estimated	none identifiable
Swan Peak (Os)	moderate	syncline	weak	50	low to medium	structure/stratigraphy

Table II-6. Continued.

Formation Name	Stream Gain-Loss Data: Indication of High Hydraulic Conductivity	Stream Gain-Loss Data: Structural Feature Affecting Hydraulic Conductivity	Spring Inventory Data: Indication of High Hydraulic Conductivity	Spring Inventory Data: Percent Springs Associated with Structural Features	Estimate of Relative Hydraulic Conductivity	Factor Controlling Hydraulic Conductivity
Garden City (Og)	moderate	syncline	weak	20	low to medium	stratigraphy
"	moderate	syncline				
Gallatin (Єg)	-	-	moderate	100	medium	structure
Saint Charles (Єs)	moderate	syncline	weak	50	low to high	structure/stratigraphy
"	strong	syncline				
Nounan (Єn)	strong	syncline	moderate	50	medium to high	structure/stratigraphy
"	strong	syncline				
Gros Ventre (Єgv)	-	-	weak	0	low	stratigraphy
Bloomington (Єbo)	moderate	syncline	strong	75	medium to high	structure
"	none	syncline				
Blacksmith (Єbl)	none	syncline	weak	50	low to medium	structure/stratigraphy
"	moderate	syncline				
Ute (Єu)	strong	syncline	-	-	high	stratigraphy
Langston (Єl)	moderate	syncline	strong	50	medium to high	structure/stratigraphy
Brigham (Єq)	none	syncline	strong	41	high	stratigraphy/structure

City, Saint Charles, Nounan, Bloomington and Blacksmith Formations. The data suggest that the hydraulic conductivity of most of the formations is not areally consistent.

The areal consistency of hydraulic conductivity was also evaluated by examining the estimates of hydraulic conductivity. The formations in Table II-6 estimated to have high hydrualic conductivity are composed of either sandstone or limestone, with the exception of the Kirkham Hollow and Brigham Formations, which are composed of rhyolite and quartzite, respectively. The formations in Table II-6 estimated to have low hydraulic conductivity are composed of either shale, siltstone, sandstone interbedded with siltstone or limestone interbedded with siltstone. Formations estimated to have low hydraulic conductivity that have different lithologies are the Tensleep Formation which is composed of quartzite, and the Lodgepole Formation which consists of limestone and dolomite. This information indicates that lithology is a control on hydraulic conductivity in southeast Idaho.

The strongest indication of areal consistency is obtained from an examination of lithology. In southeast Idaho, the formations that are composed of either sandstone or limestone generally have relatively high hydrualic conductivity. Formations that are composed of either shale, siltstone, sandstone interbedded with siltstone or limestone interbedded with siltstone generally have relatively low hydraulic conductivity.

CHAPTER III

HYDROGEOLOGIC RECONNAISSANCE OF THE NORTHERN SUBAREA

Introduction

This portion of the study is a hydrogeologic reconnaissance of thermal and non-thermal ground water flow systems in the northern portion of the project area (Figures I-1 and III-1). The northern subarea includes approximately 3800 square kilometers and is located predominantly in Bonneville County, with smaller portions in Caribou, Jefferson and Madison Counties, Idaho and Lincoln County, Wyoming.

Method of Study

The method of study described in this section was followed for all of the subarea studies. Springs were initially identified by examining USGS topographic maps, Forest Service maps, or by word of mouth by people in the area. The springs were then visited in the field. All springs or wells warmer than 15.5 degrees Centigrade were sampled. In addition, perennial springs associated with major faults were also sampled.

The surrounding geology was studied at each site. The water temperature, pH, field bicarbonate concentration and specific conductivity of each spring was measured in the field. The spring discharges were either estimated or

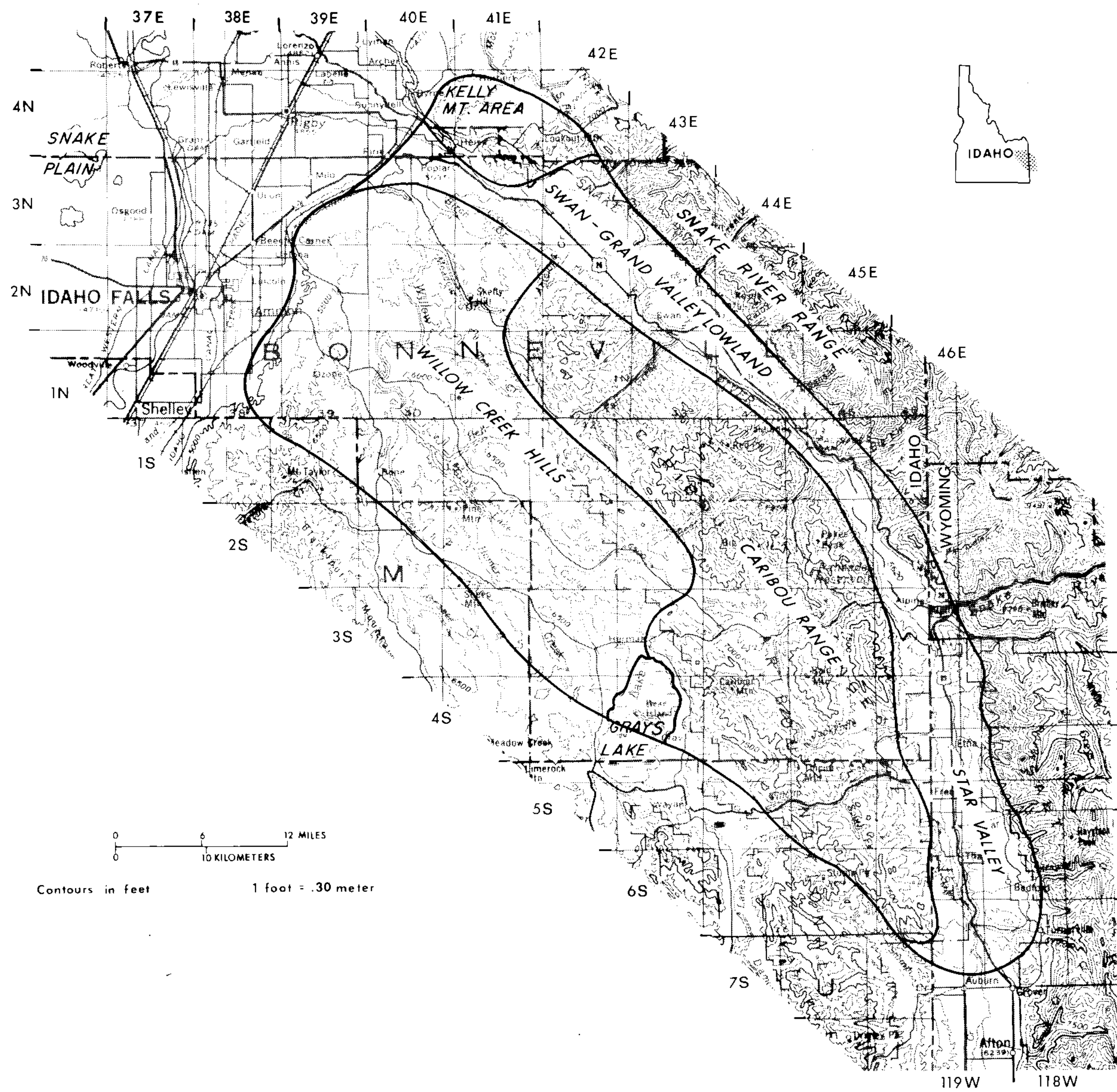

Figure III-1. Boundary and geographic subdivisions of Caribou Range study area, southeastern Idaho and western Wyoming.

measured. Temperature was measured with a Taylor thermometer accurate to 2°F in the 1980 field season and with a VWR thermometer accurate to 0.2°C for the 1981 field season. The pH measurement was done with either: 1) a VWR Digital Mini pH meter model 45 with 0.01 pH resolution and 0.05 pH reproducibility, or 2) a Corning model 3D portable pH meter with 0.01 pH resolution and 0.02 pH reproducibility. Samples for the pH determination were placed in a beaker to still the water before taking a reading. The pH meters were calibrated with pH 4 and pH 7 buffered test solutions before each determination. Specific electrical conductance was determined with a Hach model 16300 meter with an accuracy of plus or minus one percent of full scale. This meter was calibrated daily with a Hach standard solution. At several spring sites it was necessary to dilute the sample 1:2 with deionized water to obtain an on-scale reading. Bicarbonate (HCO_3^-) concentration was determined by hydrochloric acid (HCl) titration using a Hach digital titrator. The titrant was either: 1) prepared by University of Idaho personnel, or 2) was from Hach pre-packaged cartridges. Bicarbonate titrations were done until two analyses agreed within five mg/l. The HCO_3^- samples were analysed within five minutes after they were collected and care was taken to prevent undue aeration of the sample during collection.

Duplicate water samples were collected for laboratory analysis. During the 1980 field season, samples were collected in the following manner:

1. Two 250 ml samples, filtered and acidified to a pH of less than two were collected for atomic absorption spectrometric analysis and for the sulfate determination.
2. Two 60 ml filtered samples were collected for fluoride and chloride analysis.
3. At selected sites, water samples were collected in two four ounce amber glass bottles for deuterium/oxygen-18 (D/O-18) analysis. These were filled nearly to the top, left to cool, and then sealed with parafin to prevent any atmospheric exchange with the sample.

Water samples from the 1981 field season were treated in the same manner except that it was found to be sufficient to collect only one set of 250 ml samples in addition to the D/O-18 samples.

Carbon-isotope samples were obtained at selected sites. These samples were gathered in the following manner:

1. Two 50 liter carboys were filled with spring water, filtered when necessary to remove organic materials.
2. Sodium hydroxide was added to a minimum pH of 12 to convert all bicarbonate to carbonate.
3. An excess of barium chloride was added to precipitate out all carbonate.
4. Samples were allowed to sit overnight while the precipitate settled to the bottom.

5. The supernate was then decanted and the precipitate transferred to one liter Nalgene containers. Samples of carbonate rock material were sent for ^{13}C analysis to aid in the interpretation of the ^{14}C ages.

The deuterium and oxygen 18 samples and the carbonate rock samples were all analysed at the Isotope Geochemistry Laboratory at the University of Arizona.

Laboratory water quality analyses were conducted by the field investigators utilizing equipment at the University of Idaho. Recommended Environmental Protection Agency practices were used for laboratory tests (U.S.E.P.A., 1974). The Mohr volumetric method was used for chloride, a gravimetric method was used for sulphate, specific ion probe for fluoride; concentrations of sodium, potassium, magnesium, calcium and silicia were determined by atomic absorption spectroscopy.

Duplicate samples were analysed for each study site, and the concentrations averaged when they were close. Samples were reanalysed when large differences between the duplicates were noted. Methods for Chemical Analysis of Water and Wastes (U.S.E.P.A., 1979) reports deviations of 1 to 5% from the known values by single laboratories analysizing multiple known cation samples.

The net accuracy of the analyses was checked by computing the cation-ion balance by:

$$\% \text{ Error} = \frac{\Sigma \text{ meg/l Cations} - \Sigma \text{ meg/l Anions}}{\Sigma \text{ meg/l Cations} + \Sigma \text{ meg/l Anions}} \times 100$$

Error in this balance may be caused by analytical error or by the effect of ion species which were not determined. Minor constituent analyses done previously by IDWR indicate that the error contribution from undetermined species is small (Mitchell, Johnson, and Anderson, 1980).

Geographic Setting

The Grand Valley fault forms the northern and eastern boundary of the northern subarea (Figure II-1). This fault is located along the north side of the Swan and Grand Valleys and the eastern side of Star Valley. The location of the Meade thrust fault forms the southern boundary and the western boundary is the Snake Plain.

The study area can be divided into several general areas (Figure III-1). The Swan-Grand Valley lowland is a northwest trending basin and range structure that extends from the Kelly Mountain area at the north to Alpine, Wyoming in the southeast. There it curves to the south and blends into Star Valley. These valleys slope toward the northwest with an average gradient of 3.6 m per km. The width varies from 7 km in Swan Valley to 0.3 km at Calamity Point, the site of Palisades dam. The waters backed up by this dam fill the entire length of Grand Valley. The elevation varies from 1850 m at Auburn, Wyoming, to 1550 m south of Lookout Mountain. The Kelly Mountain area is located northwest of the Swan-Grand Valley lowland. The highest elevation of this area is approximately 2000 m.

The Caribou Range is a rugged, mountainous area south of the Swan-Grand Valley lowland. It parallels the lowland for more than 80 km. The maximum elevation of this area is 2988 m at Caribou Mountain. Seven other peaks in this area have elevations over 2500 m. The streams in this area have cut deep canyons into this mountain range.

The Willow Creek hills form a western and southwestern portion of the study area. This is a hilly region with local relief of 100 to 150 m. The highest elevation is 1980 m near Herman with a general slope toward the northwest to the City of Ammon where the elevation is 1520 m.

Grays Lake is in the southern portion of this area. This marshy area was once flooded with water but at present has only a few open patches of water. The elevation of Grays Lake is 1950 m.

All streams in the study area are tributary to the Snake River. The Snake River enters the study area near Alpine, Wyoming, follows the Swan-Grand Valley lowland northwest to the Snake Plain where it changes its course to flow toward the southeast. The important streams that drain the study area are Tincup and Salt Rivers, McCoy, Bear, Fall, and Willow Creeks and Grays Lake Outlet.

Mean annual precipitation varies from less than 25 cm in the northwestern portion of the study area near Ammon to more than 89 cm on several of the higher mountains such as Big Elk Mountain or Caribou Mountain (U.S.D.I., 1976). The precipitation generally increases toward the southeast. More than half of the precipitation falls from October to March, with most of this as snow. The average annual temperatures as recorded at Idaho Falls, Irwin, and Afton are 5.3, 5.5, and 2.9 degrees Celsius (U.S.D.C., 1964).

Hydrogeology of the Study Area

The rocks within the study area range in age from Cambrian to Recent. The Paleozoic rocks are mostly marine limestones, with some sandstone and minor shales. Mesozoic rocks consist of alternating limestones, sandstone, and shales. Cenozoic strata consist of conglomerates, volcanic ash, sandstone, alluvium, and colluvium. Igneous rocks of Tertiary and Quaternary age consist of rhyolite tuffs and basalts. A hydrogeologic classification of the formations is shown on Table II-6 based upon the regional study of hydrostratigraphy.

The geology of the area is extremely complex (Figures III-2 and III-3). The area has been intricately folded and faulted during periods of thrusting. The movement was toward the northeast with displacement in the order of 16 to 24 km

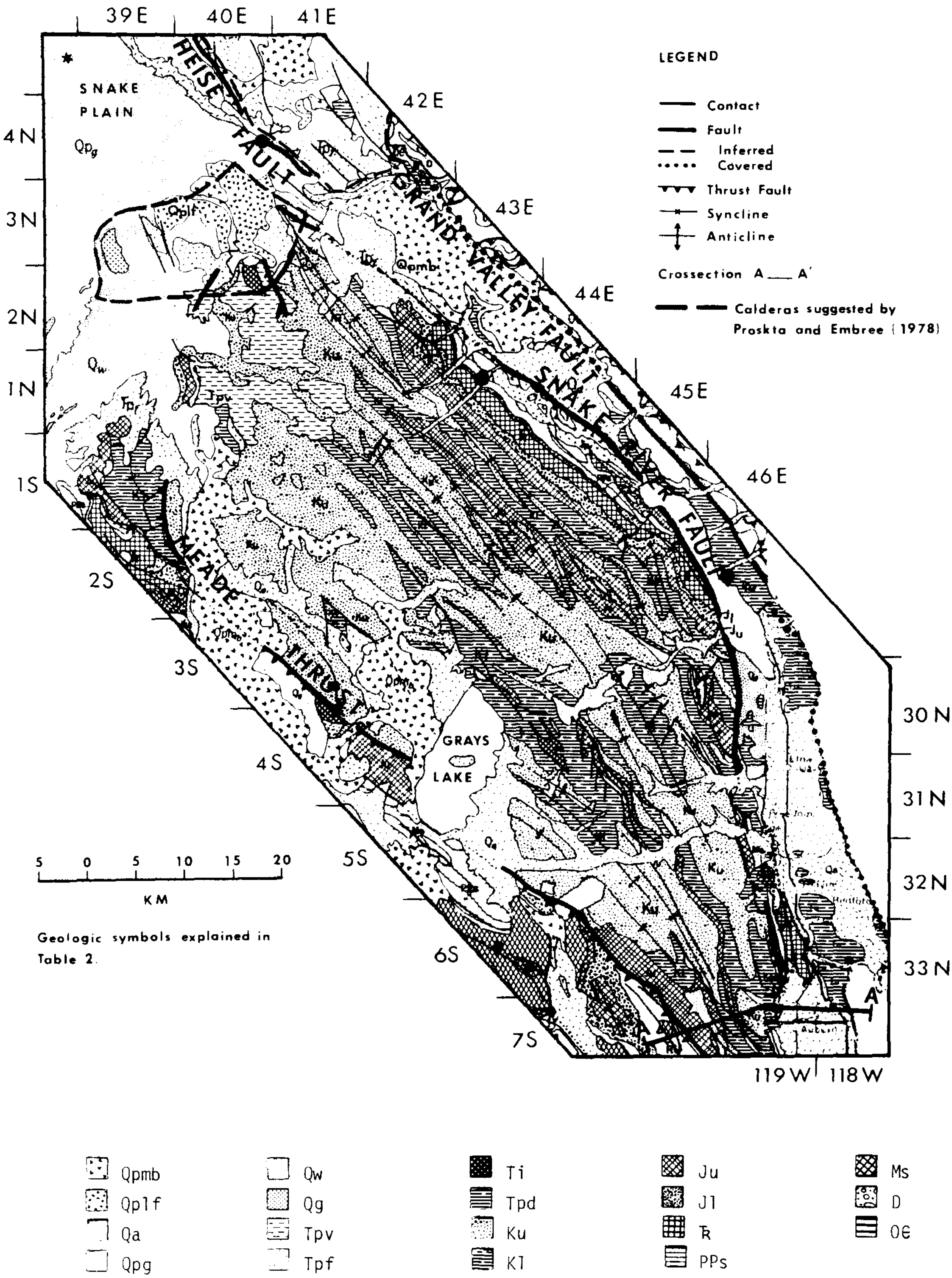

Figure III-2. Geologic map of Caribou Range study area in southeastern Idaho and western Wyoming.

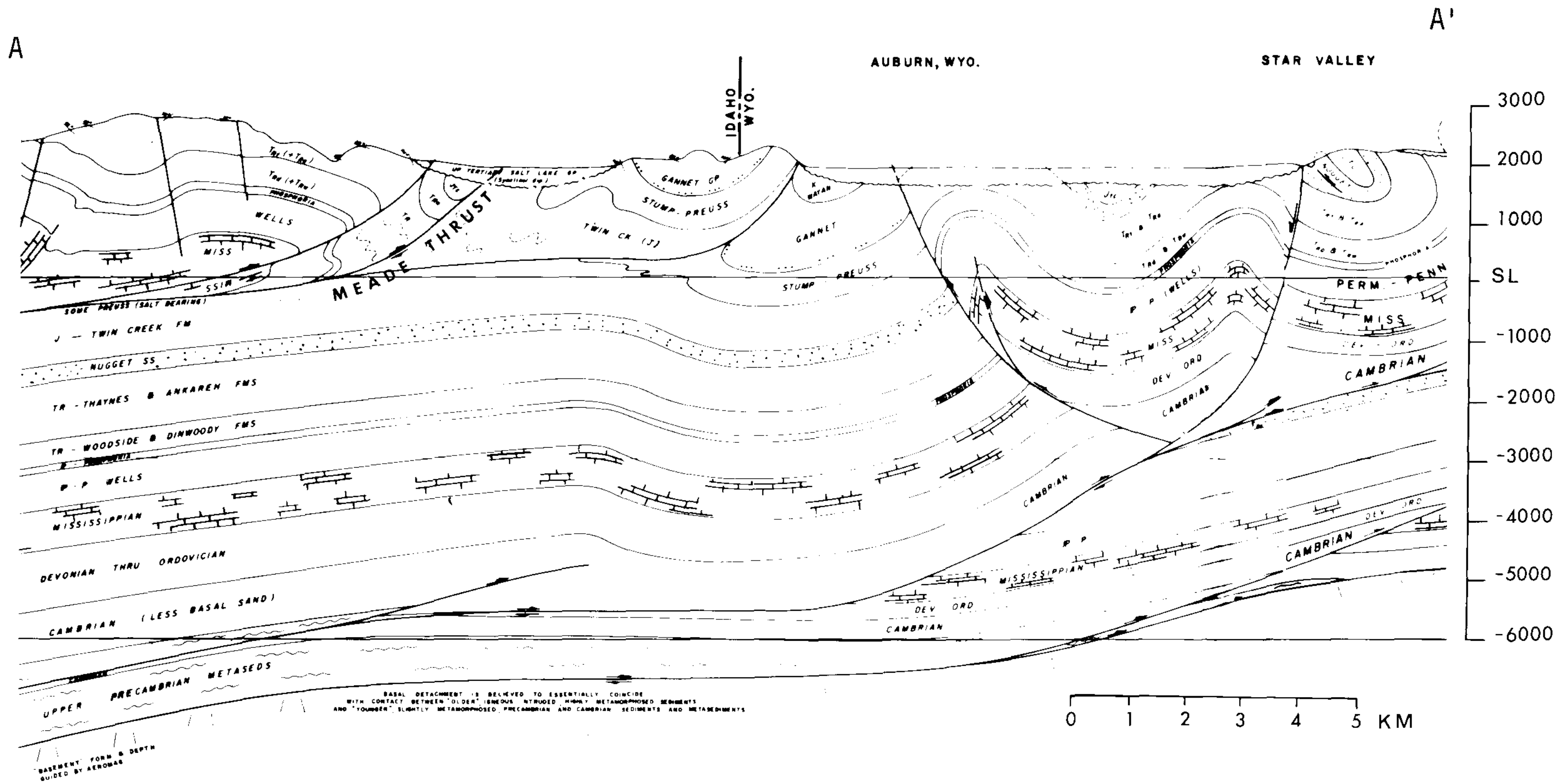

Figure III-3. Cross section A-A' in the Caribou Range study area in southeastern Idaho and western Wyoming.

(Armstrong and Oriel, 1965). The easing of the compressive forces associated with thrusting resulted in the formation of normal faults along the Swan-Grand Valley lowland. Igneous rocks complicate the geology in the northwestern portion of the study area. Proskta and Embree (1978) suggest that several calderas may be present in this region.

The distribution of hydraulic conductivity throughout the study area is highly variable. Overall, this area probably has a relatively high hydraulic conductivity at the surface which decreases with depth resulting from closing of fractures and increasing cementation and compaction.

The Swan-Grand Valley lowland is a graben with at least 300 m of displacement. It has been filled to its present level with an undetermined thickness of alluvium, colluvium, and in the northern portion, volcanics (Figure III-2). Rocks of Paleozoic, Mesozoic, and Cenozoic age lie beneath these valley-filling materials. Two major faults border this lowland. The northeastern fault associated with this graben is the Grand Valley fault. This high angle normal or reverse fault extends the full length of Swan, Grand, and Star valleys. The trace of this fault is hidden most of its length by rocks of the late Tertiary and Quaternary age. The southeastern boundary of this graben is the Snake River fault. It extends from the Snake Plain in the northwest to the Star Valley in the southeast, where it joins the fault along the west side of Star Valley. The trace of this fault is also hidden most of its length by rocks of late Tertiary and Quaternary age. This fault is a high angle normal fault that dips to the northeast. The Snake River and Grand Valley faults may combine to join with the Absaroka thrust (Figure III-3). The downthrown block bounded by these faults is interpreted to be rotated to dip northeastward toward the Grand Valley fault. Both the Grand Valley and the Snake River faults are considered active. Witkind (1975) dates the last activity of the Grand Valley fault as having displaced beds of Holocene age (5000 years). The Swan Valley fault has been active in the last 20 million years and presently shows a lot of seismic activity.

The unconsolidated sediments in the lowland probably have higher hydraulic conductivities than the older formations located below and to either side of them. The faults on either side of the valley probably act as a zone of higher hydraulic conductivity caused by fracturing. This is suggested by springs located on the trace of these faults.

Drill logs from wells in Swan Valley indicate the potential surface is very near land surface and reflects the elevation of the Snake River. Gain-loss studies from Alpine to Heise by Stearns and others (1937) show that the river gains water during low flow and loses water during high flow indicating that bank storage is a factor in this hydrologic system. Most of the ground water flow in this lowland probably occurs in the shallow unconsolidated alluvial sediments following the course of the valley toward the northwest. The relatively low elevation of this area relative to the mountain ranges to the north and south, suggests that this is a regional ground water discharge area. Discharge from regional flow systems should occur along Snake River and Grand Valley faults, not in the interior of the lowland.

The Kelly Mountain area is on the northeastern boundary of the Swan-Grand Valley lowland. This area is made up of Pliocene rhyolites and welded tuffs that overlie undifferentiated Paleozoic and Mesozoic rocks. It has been mapped as a caldera by Proskta and Embree (1978). The Grand Valley fault continues through the Kelly Mountain area; several major faults, including the Heise fault, parallel its trend. The Heise fault acts in the same manner as the Grand Valley fault, down dropping rocks on its southern border. The caldera structure forms a closed basin bordered by faults. The primary hydraulic conductivity of the units filling the caldera is very low but zones with high hydraulic conductivity are formed by faulting, paleosoils, and interflow zones. There are many small springs in this area associated with the zones of high hydraulic conductivity, some of which are warm. There are no large springs in this area.

The Caribou Range is a mountainous area composed of Paleozoic and Mesozoic rocks intricately twisted in tight parallel folds and broken by faults. These sediments, which tend to get younger to the north, are made up predominantly of limestones, sandstones, and shales. The folding of these sedimentary rocks has affected the distribution of hydraulic conductivity in two ways. Folding changes the relative positions of aquifers and aquitards and the primary hydraulic conductivity is altered by the fracturing associated with folding.

Figure III-3 shows tilted and deformed rocks on the surface with attenuation of folding as the depth increases. It is believed that the bedding planes are approximately horizontal at depth. The thrusts are also thought to be nearly horizontal under the study area. The entire study area, excepting possible caldera structures in the northern portions, has been overthrust with movement toward the northeast. The depth to the gliding plane of the thrust is unknown.

The Caribou Range is a regional high with a high rate of precipitation and probably is a recharge area for numerous local and intermediate flow systems. The large amount of relief and complex geologic structure probably limit the possibility of regional flow. The flow systems formed here are mainly controlled by the stratigraphic units and the geologic structures produced by folding and faulting. Numerous small springs and seeps occur in the mountains but most of these dry up in the late fall. There are only a few large springs in this area.

Grays Lake is a swampy lowland located southwest of the Caribou Range. This area has lacusterine sediments overlying sedimentary rocks of Jurassic and Cretaceous age. The lake is formed by the accumulation of runoff from the surrounding mountains; it may be a ground water discharge area.

The Willow Creek Hills are located west and are topographically lower than the Caribou Range. The southern portion of this area is made up of intensely folded and faulted sedimentary rocks of Cretaceous age which have been overlain in areas by canyon-filling basalts. The northern portion of this area has Jurassic and Cretaceous sedimentary rocks overlain by silicic welded tuffs, air fall volcanics, and loess. Proskta and Embree (1978) suggest that there are calderas in the northern portion of this area (Figure III-2). Most of the area within the Willow Creek Hills is mapped on a reconnaissance level; portions are unmapped.

The Willow Creek Hills area has a lower potential for ground water recharge than the Caribou Range because it receives much less precipitation. Most of the springs in this area are small, many of which dry up during the fall. There are also a few perennial medium-sized springs but no large springs are present.

Physical and Chemical Settings of Springs and Wells

Introduction

Twenty-three springs and two wells were inventoried in the study area (Figure III-4). Short descriptions of the physical setting and characteristics of the springs and wells are presented in Table III-1. Chemical analyses of these springs and wells are presented in Table III-2. Multiple analyses for several sites have been presented where the data are available. The springs inventoried in the study area have been divided into three groups for discussion purposes: thermal springs that discharge highly mineralized water, thermal springs or wells that discharge water with relatively low concentrations of dissolved solids, and nonthermal springs.

Thermal Springs with High Specific Conductivities

Seven spring sites are included in this group: H-3 (I-3), H-9 (H-10 and I-11), H-16, I-21 (I-22), H-23 (I-23), H-26 (W-26), and H-27 (Figure III-4). The temperatures and conductivity of the discharges range from 20 to 66°C and 6500 to 11,000 μmhos/cm, respectively.

Heise Hot Springs (H-3 and I-3). This 48°C spring is located at the foot of a 300 m escarpment. It has deposited a 10-meter high travertine mound which is being eroded at its base by the Snake River. Heise Hot Springs resort, located

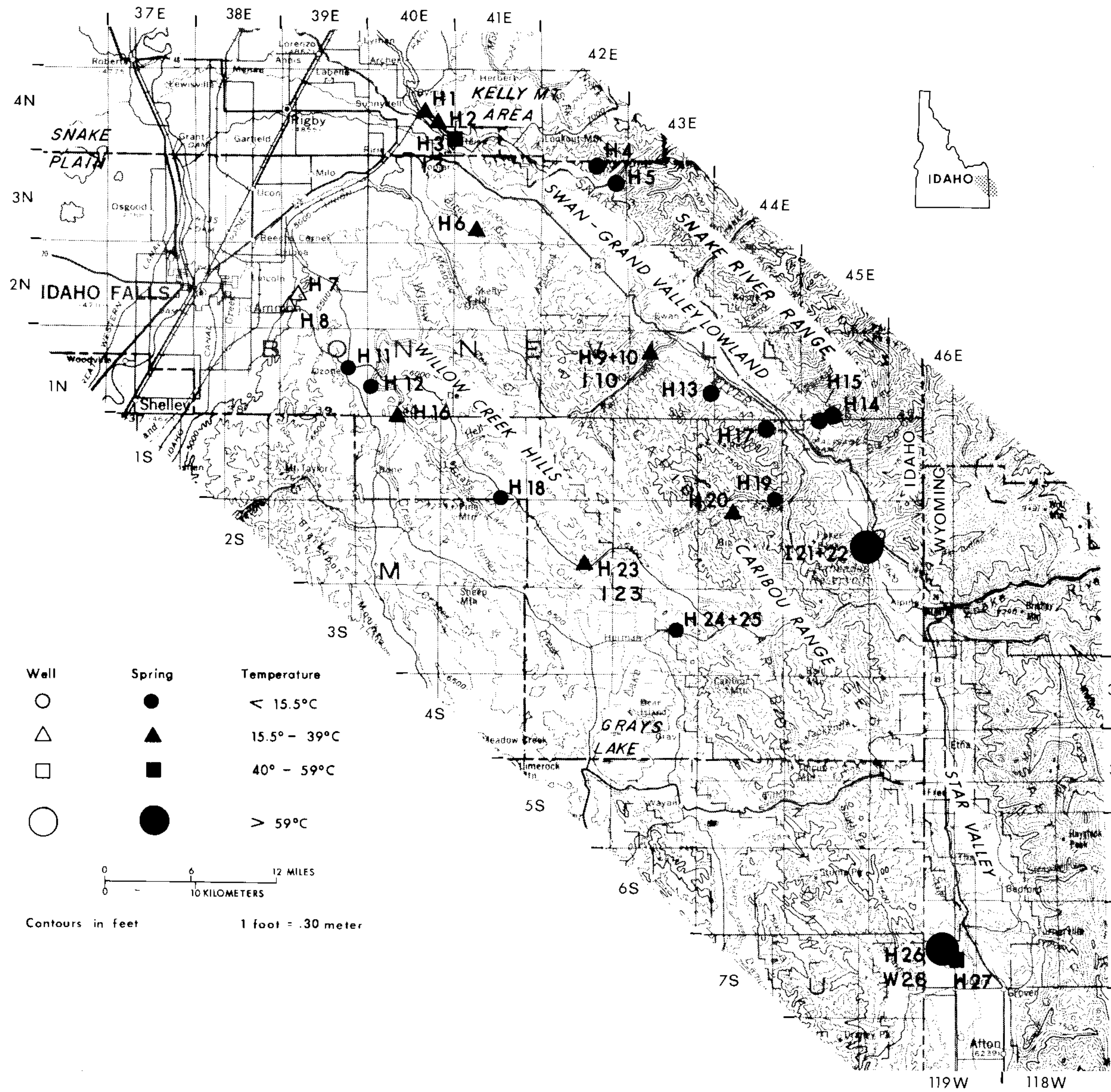

Figure III-4. Location and temperature of springs and wells in the vicinity of the Caribou Range, southeastern Idaho and western Wyoming.

Table III-1. Physical settings of springs and wells in the vicintiy of the Caribou Range, southeastern Idaho and western Wyoming.

Sample Number	Name, Location and Date Sampled	Water Temp. (°C)	Elevation (m above MSL)	Well Depth (m)	Depth to Water (m)	Discharge (l/s)		Site Description
H-1	Elkhorn Warm Spring 4N 30E 23cadS (7-31-80)	20	1580			10	E*	This spring is located 2.8 km northwest of Heise Hot Springs, 0.2 km north of the Heise fault and emerges from rhyolitic tuff. The spring is located within the southern edge of the Rexburg Caldera Complex.
H-2	Hawley Warm Springs 4N 40E 25bbdS (7-31-80)	16	1610			10	E	This spring is located 1.5 km northwest of Heise Hot Springs, 0.2 km north of the Heise fault and emerges from rhyolite tuff. The spring is located within the southern edge of the Rexburg Caldera Complex.
H-3	Heise Hot Springs 4N 40E 25ddaS (6-18-80)	48	1540			4	R	This spring issues from Tertiary silicic volcanic rocks within the southern edge of the Rexburg Caldera Complex. Two faults, the Heise fault and an unnamed northeast trending fault intersect at this site.
H-4	Lufklin Spring 3N 42E 2cbbS (6-30-80)	8	1770			2	E	This spring issues from the contact of Salt Lake formation and the Gallatin limestone formation. It is located 500 m southwest of the Grand Valley fault.
H-5	Buckland Warm Spring 3N 42E 12cca and ccdS (6-18-80)	11	1570			1000		This spring flows out of the Gallatin formation and may be the primary discharge point for a flow system controlled by the thrust plate to the north.
H-6	Unnamed Spring 3N 41E 32bbdS (6-18-80)	23	1710			6	E	This spring issues from a rhyolitic tuff. A large northeast trending fault is located 0.2 km to the south.
H-7	Dyer Well 2N 39E 21bcc (7-21-80)	21	1540	171	137			This well probably obtains water from a broken rhyolite zone as recorded in the drillers log from 140 to 171 m. There is a northeast trending fault mapped 150 m to the west of this well.
H-8	Anderson Well 2N 39E 29bac (7-21-80)	20	1520	109	76			This well is located 1.6 km southwest of the Dyer's well. The drillers log indicates rhyolite from 69 to 75 m, sandstone (presumably pumice) 95 to 107 m and rhyolite 107 to 109 m.

Table III-1. Continued.

Sample Number	Name, Location and Date Sampled	Water Temp. (°C)	Elevation (m above MSL)	Well Depth (m)	Depth to Water (m)	Discharge (l/s)	Site Description
H-9	Fall Creek Mineral Springs 1N 43E 9cbb1S (8-5-80)	24	1660			6 E	This spring is one of a series of warm springs along the south side of Fall Creek. These springs flow from Quaternary alluvium with travertine deposits above Mission Canyon Limestone. They are associated with the major northwest trending Snake River fault.
H-10	Fall Creek Mineral Springs 1N 43E 9cbb2S (8-5-80)	23	1660			4 R	This spring flows in the bottom of the northern most sink hole. See description under H-9.
H-11	Unnamed Spring 1N 39E 14acaS (7-22-80)	9	1770			3 E	This spring flows from the Salt Lake formation. It may originate from Tertiary rhyolite tuff outcropping 70 m north of this site.
H-12	Unnamed Spring 1N 40E 19cabS (7-22-80)	13	1680			4 E	This spring flows from the Salt Lake formation.
H-13	Unnamed Spring 1N 44E 30cbdS (7-7-80)	7	1840			0.7 E	This spring discharges from alluvium and travertine overlying Mission Canyon Limestone. The spring is associated with the northwest trending Snake River fault.
H-14	Unnamed Spring 1S 45E 4adaS (7-8-80)	6	1820			2 E	The spring flows from Salt Lake formation. The major northwest trending Grand Valley fault is located in this area, but it is concealed by the overlying Salt Lake formation.
H-15	Unnamed Spring 1S 45E 4acaS (7-8-80)	6	1880			4 E	This spring is located 300 m west of spring H-14. See description under H-14.
H-16	Unnamed Spring 1S 40E 4abcS (7-22-80)	21	1700			2 E	This spring flows from fractures in an outcrop of Ephriam Conglomerate. A minor fault is mapped at this site.
H-17	Unnamed Spring 1S 44E 1cbdS (7-7-80)	7	1800			10 E	This spring issues from the Twin Creek Limestone.

Table III-1. Continued.

Sample Number	Name, Location and Date Sampled	Water Temp. (°C)	Elevation (m above MSL)	Well Depth (m)	Depth to Water (m)	Discharge (l/s)	Site Description
H-18	Willow Spring 1S 41E 36cccS (6-29-80)	8	2010			6 E	This spring flows out of the Wayan formation, on the axis of a northwest trending syncline.
H-19	Unnamed Spring 2S 44E 1accS (6-20-80)	11	1780			100 E	This spring is flowing out of the Nugget formation.
H-20	Warm Spring 2S 44E 9aacS (7-23-80)	17	2180			10 E	This spring flows from near the contact of the Twin Creek Limestone and the Nugget formation. This site is 250 m east of the northwest trending axis of the Big Elk Mountain anticline.
I-21	Alpine Hot Spring 2S 46E 19bS (8-39)	56	1690			1.6 R	These springs are reported to discharge from alluvium and were depositing travertine; the springs are presently covered by waters of Palisades Reservoir. These springs are associated with the Snake River fault.
I-22	Alpine Hot Spring 2S 46E 19cadS (7-27-77)	37	1690			0.6 R	See description above.
H-23	Brockman Hot Spring 2S 42E 26dcdS (6-27-80)	35	1910			4 R	This spring flows out of either the Peterson or Bechler formation. The geology around this spring has been complexly folded and faulted by minor faults.
H-24	Unnamed Spring 3S 42E 15dccS (7-29-80)	10	2090			4 E	This spring issues from rocks of the Bechler formation on the west limb of a complexly faulted syncline.
H-25	Unnamed Spring 3S 42E 22abbS (7-6-80)	14	2080			3 E	This spring is located 100 m southwest of spring H-24. It flows from the contact of the Bechler and Peterson formation on the west limb of a complexly faulted syncline.

Table III-1. Continued.

Sample Number	Name, Location and Date Sampled	Water Temp. (°C)	Elevation (m above MSL)	Well Depth (m)	Depth to Water (m)	Discharge (l/s)	Site Description
H-26	Auburn Hot Springs 33N 119W 23dbdS (7-25-80)	57	1850			3 E	These springs discharge from the Dinwoody formation on the axis of the northwest trending Hemmert anticline. Two faults, the Hemmert fault and the Freedom fault join at this site. Extensive deposits of travertine and free sulphur are present at these springs.
H-27	Johnson Springs 33N 119W 26adS (7-25-80)	54	1850			0.01	This spring is located 1.6 km south of Auburn Hot Springs. The spring flows from a large travertine mound that overlies alluvium and at some depth, the Dinwoody formation. The trace of the Hemmert anticline and fault lie beneath this site.

*Accuracy of measurement
E = Estimated discharge
R = Reported Discharge
All others measured.

Table III-2. Hydrochemistry of springs and wells in the vicinity of the Caribou Range, southeastern Idaho and western Wyoming.

Sample Number	Name and Location	Water Temp. °C	Specific Conductance (μmho/cm)	TDS (mg/l)	pH	Concentration in mg/l (meq/l)[4] Ca	Mg	Na	K	Cl	F	HCO_3	SO_4	SiO_2	Error (%)**
H-1	Elkhorn Warm Spring 4N 40E 23cadS	20	390	340	6.6	30 (1.5)	10 (0.8)	14 (0.6)	0 (0)	5 (0.1)	0.78 (0)	190 (3.0)	7 (0.1)	83	7.1
H-2	Hawley Warm Spring 4N 40E 25bbdS	16	350	340	7.5	36 (1.8)	10 (0.8)	10 (0.4)	0 (0)	4 (0.1)	0.7 (0)	190 (3.1)	5 (0.1)	88	4.4
H-3	Heise Hot Springs 4N 40E 25ddaS	48	6500	7600	6.1*	680 (34)	81 (6.7)	1500 (65)	200 (5.2)	2300 (65)	3.1 (0.2)	2100* (35)	720 (15)	58	1.8
I-3	Heise Hot Springs[2] 4N 40E 25ddaS	49	8800	6500	6.7	450 (23)	82 (6.7)	1500 (65)	190 (4.9)	2400 (68)	3.1 (0.2)	1100 (18)	740 (15)	30	.99
H-4	Lufklin Spring 3N 42E 2cbbS	8	450	530	6.9	130 (6.6)	0 (0)	0 (0)	0 (0)	2 (0.1)	0 (0)	380 (6.2)	5 (0.1)	9	1.7
H-5	Buckland Warm Spring 3N 42E 12cca + ccdS	11	830	680	7.0	110 (5.6)	26 (2.1)	31 (1.3)	0 (0)	38 (1.1)	0.14 (0)	350 (5.7)	110 (2.3)	13	.04
H-6	Unnamed Spring 3N 41E 32bbdS	23	650	550	7.2	71 (3.5)	19 (1.6)	44 (1.9)	0 (0)	42 (1.2)	0.14 (0)	270 (4.4)	51 (1.1)	49	2.4
H-7	Dyer Well 2N 39E 21bcc	21	530	440	7.7	50 (2.5)	13 (1.1)	50 (2.2)	3 (0.1)	61 (1.7)	0.29 (0)	190 (3.1)	1 (0)	68	9.2
H-8	Anderson Well 2N 39E 29bac	20	520	470	7.7	50 (2.5)	10 (0.8)	45 (2.0)	7 (0.2)	45 (1.3)	0.44 (0)	200 (3.3)	0 (0)	110	9.0
H-9	Fall Creek Mineral Springs 1N 43E 9cbb1S	24	7800	5500	6.2	470 (24)	100 (8.2)	1100 (46)	120 (3.0)	1900 (52)	1.4 (0.1)	1500 (24)	330 (6.8)	15	1.4
H-10	Fall Creek Mineral Springs 1N 43E 9cbb2S	23	6800	5100	6.2	430 (22)	88 (7.2)	1100 (46)	110 (2.8)	1700 (46)	1.3 (0.1)	1300 (21)	330 (6.8)	17	2.1
I-10	Fall Creek Mineral Springs[2] 1N 43E 9cbbS	25	7900	5300	6.3	440 (22)	96 (7.9)	1110 (48)	120 (3.1)	1900 (54)	1.7 (0.1)	1200 (20)	390 (8.1)	11	.16
H-11	Unnamed Spring 1N 39E 14acaS	9	470	400	7.0	48 (2.4)	17 (1.4)	15 (0.7)	0 (0)	38 (1.1)	0.18 (0)	210 (3.4)	3 (0.1)	71	1.4
H-12	Unnamed Spring 1N 40E 19cabS	13	300	320	7.2	39 (1.9)	6 (0.5)	5 (0.2)	0 (0)	4 (0.1)	0.21 (0)	160 (2.6)	0 (0)	110	.44
H-13	Unnamed Spring 1N 44E 30cbdS	7	450	470	7.1	85 (4.2)	10 (0.8)	3 (0.1)	0 (0)	7 (0.2)	0.26 (0)	310 (5.0)	8 (0.2)	49	1.9
H-14	Unnamed Spring 1S 45E 4adaS	6	390	340	7.4	60 (3.0)	16 (1.3)	0 (0)	0 (0)	0 (0)	0 (0)	250 (4.2)	3 (0.1)	15	1.0

Table III-2. Continued.

Sample Number	Name and Location	Water Temp. °C	Specific Conductance (μmho/cm)	TDS (mg/l)	pH	Concentration in mg/l (meq/l)[4] Ca	Mg	Na	K	Cl	F	HCO_3	SO_4	SiO_2	Error (%)**
H-15	Unnamed Spring 1S 45E 4acaS	6	410	380	7.4	69 (3.4)	18 (1.5)	0 (0)	0 (0)	0 (0)	0 (0)	280 (4.5)	0 (0)	13	4.2
H-16	Unnamed Spring 1S 40E 4abcS	21	11000	9200	6.6	110 (5.5)	19 (1.6)	2800 (120)	40 (1.0)	880 (25)	4.6 (0.2)	2400 (40)	2900 (60)	62	3.0
H-17	Unnamed Spring 1S 44E 1cbdS	7	400	380	7.1	66 (3.3)	18 (1.5)	0 (0)	0 (0)	3 (0.1)	0.12 (0)	250 (4.1)	4 (0.1)	34	5.2
H-18	Willow Spring 1S 41E 36cccS	8	450	400	7.1	73 (3.6)	14 (1.2)	4 (0.2)	0 (0)	10 (0.3)	0.16 (0)	280 (4.6)	5 (0.1)	11	5.0
H-19	Unnamed Spring 2S 44E 1aacS	11	230	160	7.1	36 (1.8)	6 (0.5)	0 (0)	0 (0)	0 (0)	0 (0)	110 (1.8)	3 (0.1)	6	10.0
H-20	Warm Spring 2S 44E 9aacS	17	600	580	7.2	130 (6.4)	27 (2.2)	0 (0)	0 (0)	1 (0)	0.25 (0)	160 (2.7)	230 (4.9)	24	6.5
I-21	Alpine Hot Springs[3] 2S 46E 19bS	56		6800		530 (26)	93 (7.7)	1500 (67)	190 (4.8)	2400 (68)	2.8 (0.1)	920 (15.1)	1100 (22)	45	.10
I-22	Alpine Hot Springs[2] 2S 46E 19cadS	37	10000	7100	6.5	560 (28)	100 (8.2)	1500 (65)	180 (4.6)	2800 (79)	2.7 (0.1)	880 (14)	1000 (21)	40	3.8
H-23	Brockman Hot Spring 2S 42E 26dcdS	35	8800	7500	6.6	190 (9.3)	33 (2.7)	2000 (89)	38 (1.0)	550 (16)	2.3 (0.1)	2300 (37)	2400 (50)	38	.51
I-23	Brockman Creek W.S.[2] 2S 42E 26dcdS	35	8600	7300	6.4	150 (7.5)	41 (3.4)	2100 (91)	34 (0.9)	590 (17)	2.6 (0.1)	1900 (31)	2500 (52)	24	1.5
H-24	Unnamed Spring 3S 43E 15dccS	10	550	540	7.1	100 (5.2)	25 (2.1)	0 (0)	0 (0)	3 (0.1)	0.16 (0)	340 (5.6)	56 (1.2)	13	2.7
H-25	Unnamed Spring 3S 43E 22abbS	14	400	370	7.2	76 (3.8)	10 (0.8)	0 (0)	0 (0)	4 (0.1)	0.12 (0)	270 (4.5)	5 (0.1)	6	.71
H-26	Auburn Hot Springs 33N 119W 23dbdS	57	8000	5700	6.4	510 (25)	76 (6.3)	1300 (58)	160 (4.1)	1700 (49)	3.4 (0.2)	890 (14)	1000 (21)	68	5.1
W-26	Auburn Hot Springs[1] 33N 119W 23dbdS	62	6800	5700	7.5	400 (20)	70 (5.8)	1400 (61)	140 (3.6)	1700 (48)	0.6 (0)	860 (14)	1100 (23)	35	3.0
H-27	Johnson Springs 33N 119W 26adS	54	8100	6200	6.4	450 (23)	45 (3.7)	1500 (65)	180 (4.5)	1900 (55)	3.8 (0.2)	970 (16)	1100 (24)	88	.70

Table III-2. Continued.

* pH meter may have malfunctioned causing inaccurate pH and HCO_3 readings

** Charge-balance error, refer to page 58 in text

[1] Breckenridge and Hinkley, 1978

[2] Mitchell and others, 1980

[3] Ross, 1971

[4] Concentrations recorded as 0 mg/l imply a concentration less than 0.5 mg/l was present and that the procedure could not detect concentrations less than 0.5 mg/l.

0.2 km northeast of the springs, has used water from this spring since the late 1800's for recreational purposes.

Heise Hot Springs is located in a structurally complex area. This spring is associated with two faults. The Heise fault, a major northwest trending normal fault, runs through the spring site, and a smaller arcuate shaped fault meets the Heise fault from the north less than 100 m to the east of the spring. The area south of the Heise fault is covered by alluvial sediments deposited by the Snake River. The smaller northeast-trending fault north of the Heise fault separates Tertiary rhyolitic tuff to the northwest, and undifferentiated Mesozoic and Paleozoic rocks to the southeast. The springs flow from the Tertiary rhyolite cover at this site by a mantle of travertine and coluvium (Proskta and Embree, 1978). The spring site is located near older sedimentary rocks as indicated by a 100-meter well drilled about 100 m north of the springs in 1936. This well encountered only a small amount of water and drilled through what was desribed as gray, pink, and blue limestone (Stearns and others, 1938).

Utilizing the gravity and magnetic data Mabey reports:

> The most prominent local gravity and magnetic anomalies are highs within the Rexburg caldera complex in the area of Heise Hot Springs. Although the crests of the anomalies are coincident, the extent of the anomalies are different and they cannot reflect entirely the same mass. Meszoic sedimentary rocks overlain by Pliocene rhyolite flows and welded tuffs are exposed in the area of the anomalies. Rhyolite dikes are locally abundant. The

> northwest-trending Heise fault (Prostka and Hackman, 1974), which forms a southwest facing scarp locally 300 m high, is parallel to and near the crest of the anomalies. The correlation between the gravity high and outcropping Mesozoic sedimentary rock suggests that the gravity anomaly reflects in large part a structural high elevating the more dense pre-Tertiary rocks. The shape and extent of the magnetic anomaly, the abundant rhyolite dikes in the area, and the indication by the magnetic gradients that the source lies below the surface all suggest that a major part of the magnetic high is produced by a large buried intrusive body. Some features of the magnetic anomaly reflect the near-surface volcanic rocks.
>
> Heise Hot Springs and the warm springs to the northwest occur along the crest of the gravity and magnetic highs. The springs are in a structurally complex area where northwest-trending faults, probably related to the Basin and Range structure of Swan and Grand valleys, displace a structural high over the inferred intrusive body. Although the Heise fault forms a prominent southwest-facing scarp and the presence of the Snake River against this scarp attests to recent movement of the fault, the geophysical data indicate that the Heise fault is near the crest of the structural high... The gravity anomaly is attributed to a high on the surface of the pre-Cenozoic rocks at Heise Hot Springs and to an area of thicker Cenozoic rocks under the valley of the Snake River to the southwest. The depression containig the thicker Cenozoic rocks is parallel to and within a northwestward projection of the Swan-Grand Valley trend into the Rexburg caldera complex. The magnetic anomaly has two major components: a local high at Heise Hot Springs superimposed on broader, more deeply buried source. Both components probably reflect a large body of intrusive rock with the apex near Heise Hot Springs. The intrusive mass, which may be the same age as the rhyolite dikes, lies within the Rexburg caldera complex where the Swan-Grand valley trend intersects the caldera (Mabey, 1978, p. 12-16).

This spring deposits travertine, gypsum, and free sulfur and has a hydrogen sulfide odor. The mineralized water has a specific conductance of 6500 μmhos/cm and a pH of 6.7 (Young and Mitchell, 1973). Sodium and chloride are the dominant ions in this water. A subsurface temperature of 79°C was estimated using a silical geothermometer assuming quartz equilibrium and conductive cooling (Mitchell and others, 1980).

Fall Creek Mineral Springs (H-9, H-10, and I-10). Several springs and seeps discharge water along a 1.2 km reach of Fall Creek (Figure III-4). The warmest spring (H-9) is 24°C and flows from a travertine deposit located next to the creek. Sample H-10 was collected from the bottom of a sinkhole where the water emerges to the surface for the distance of a meter and then disappears into a solution channel in the cavernous rock. Travertine deposits fill the valley floor the entire length of the springs. The springs discharge from the Mission Canyon Limestone and are associated with the northwest-trending Snake River fault (Jobin and Schroeder, 1964a).

These springs deposit free sulfur and travertine and give off a strong hydrogen sulfide odor. Two other large deposits of travertine are located at a higher elevation on a ridge 0.5 and 1.6 km west of the springs. There are no springs associated with these deposits and their surface elevation ranges from 1680 to 1840 m.

The water from Fall Creek Mineral Springs have specific conductance values of 7800 and 6800 μmhos/cm and a pH of 6.2. The dominant ions are sodium and chloride. The subsurface temperature may be as high as 40°C as indicated by the quartz geothermometer (Mitchell and others, 1980).

Alpine Hot Springs (I-21 and I-22). These springs are presently located under Palisades Reservoir (Figure III-4). The data presented here are based upon an investigation of the site prior to the creation of the reservoir and during a visit when the water level was low in the reservoir. The springs flow from Quaternary alluvium and are associated with the Snake River fault (Gardner, 1961). The springs were located on both sides of the former channel of the river. Six springs on the west side of the river had temperatures ranging from 31 to 62°C. An excellent description of this area was given by Bradley (Hayden, 1873). His measurements are converted to metric units in the paragraph below to maintain consistency in this report.

> Here also is located a cluster of warm springs, making calcareous, sulphurous, and saline deposits. The largest spring, the Washtub, has built up a flaring table, 0.3 m high, of an oval form, measuring about 1.4 m by 2.3 m, upon a mound consisting of calcarious mud, scarcely solidified, of from 1.5 to 2.1 m above the creek bottom in which it stands. The central table has contracted so as to crack across diagonally, and the flow now escapes at its western base, depositing a fine mud tinged in the full pools with a faint sulphur-yellow, but pure white in the dry ones. These pools cover the mound in descending steps of great beauty. The present flow is southward, though it has been on all sides in succession. One mound, no longer active is 1.5 m high, with a circular base of about 1.5 m diamter and an oval summit of about 0.3 m by 2.4 cm. Many small springs escape along the bank for 90 m or more. The deposits vary greatly in color. At some points the odors of sulphuorous acid and of sulphureted hydrogen

> were quite noticeable. The older deposits have built up a bank 3 m high along the base of the terrace, and the beavers have taken possession and have dammed up on it the waters of the cold springs which flow from the second terrace at short intervals along this plain. On the opposite shore two considerable springs have built up their deposits against the foot of the mountain, one of which appears to be nearly dead. The highest temperature observed here was 62.2°C. The Washtub gave 61.6°C and others 61.1°, 32.2° and 31.1°, etc. (Hayden, 1873, p. 269).

On the east side of the river there were two main springs and several smaller ones with temperatures ranging from 49 to 66°C (Stearns and others, 1937). The wide range of temperatures in these springs indicate that warm and cold ground water is mixing before reaching the surface.

There are two analyses for Alpine Hot Springs. Ross (1971) reports an analysis (I-21) performed in August of 1939. This sample has a total dissolved solids of 6800 mg/l, no reading for specific conductance, and a temperature of 56°C. The dominant ions are sodium and chloride. The other analysis was obtained in 1977 when the water level in the reservoir was particularly low. The water has a specific electrical conductance of 10,000 μmhos/cm, a total dissolved solids of 7,100 mg/l, a temperature of 37°C, and a pH of 6.5. The dominant ions are sodium and chloride. The subsurface temperature as indicated by a chalcedony geothermometer (silica temperature assuming equilibrium with chalcedony and conductive cooling, i.e., no steam loss) may be as high as 61°C for I-22 (Mitchell and others, 1980).

Auburn Hot Springs and Johnson Springs (H-26, W-26, and H-27). Auburn Hot Springs is located 1.6 km north of Johnson springs (Figure III-4). Auburn Hot Springs flow from over 100 vents over a 1.2 hectacre area. The maximum temperature measured is 62°C (Breckenridge and Hinkley, 1978). Johnson Springs consist of five travertine cones, 1.5 to 2.4 m high, with a small spring and several seeps, on and around them. The temperature of this spring is 54°C. Both groups of springs give off the odor of hydrogen sulfide and deposit free sulfur along with the travertine.

These springs occur on the axis of the north-south trending Hemmert anticline. Two deep seated faults, the Hemmert fault which follows the crest of the anticline, and Freedom fault that roughly parallels this anticline one km to the west, join at Auburn Hot Springs. Both are westward dipping faults with 200 and 800 m of displacement, respectively. The Auburn fault, located 0.5 km west of the Freedom fault, is interpreted as an eastward dipping normal fault with as much as 2 km of displacement (Hinkley and Breckenridge, 1977). The springs emerge from the Dinwoody Formation of lower Triassic age (Mansfield, 1927). The roughly linear arrangement of these springs and other travertine deposits located 13 km north on the same trend suggest that these springs are structurally controlled. Breckenridge and Hinkley (1978) suggest a model whereby meteoric water are heated at depth, perhaps by a cooling magma body, and migrate to the surface.

Auburn Hot Springs has a specific electrical conductivity of 8,000 μmohs/cm and a pH of 6.4. The dominant ions are sodium and chloride. Johnson Springs has a similar chemical composition with a specific electrical conductance of 8,100 μmhos/cm and a pH of 6.4. The dominant ions are sodium and chloride. Using SiO_2 and Na-K-Ca geothermometry, Renner and other (1975) estimated a reservoir temperature of 150°C at Auburn Hot Springs.

Unnamed Springs at 1N 40E 4abcS (H-16). These springs are located in the bottom of a canyon formed by Willow Creek (Figure III-4). The springs discharge water at a temperature of 21°C from rocks of the Gannett Group. They flow from fractures in an outcrop of chert pebble conglomerate at the base of the Ephriam Conglomerate. A northeast-trending fault intersects this site from the north displacing the Peterson Limestone, placing Bechler Conglomerate against the Ephriam Conglomerate (Mansfield, 1952). The geology is complicated by rhyolite tuffs, basalts, and the Salt Lake Formation which conceal most of the older sedimentary rocks where they have been exposed by the erosion by Willow Creek.

The springs give off an odorless gas, presumably carbon dioxide. Travertine deposits are located in rocks of the Bechler Formation west of the present springs. Saline deposits surround the springs. These springs have a high specific electrical conductance of 11,000 μmhos/cm and a pH of 6.6. The dominant ions are sodium and sulfate.

Brockman Hot Springs (H-23 and I-23). These springs flow from several small seeps and a 1.2 m diameter pool into Brockman Creek (Figure III-4). The springs have a temperature of 35°C and they give off an odorless gas, presumbly carbon dioxide. Travertine deposits surround the spring and an inactive travertine mound is located a short distance to the south.

The area around the spring site is complexly folded and faulted. This spring flows out of Quaternary alluvium overlying Bechler Conglomerate or Peterson Limestone. Several minor faults run through the area, the nearest of which is 200 m to the north (Gardner, 1961). A major northwest trending fault is located 1.7 km northeast of the spring.

This spring has a specific electrical conductance of 8,800 μmhos/cm and a pH of 6.6. The dominant ions in this water are sodium and sulfate. The subsurface temperature from sample I-23 may be as high as 38°C as indicated by the chalcedony geothermometer (Mitchell and others, 1980).

Thermal Springs with Low Specific Conductivities

Four springs (H-1, H-2, H-6, and H-20) and two wells (H-7 and H-8) are included in this group (Figure III-4).

Temperatures ranged from 16 to 23°C with specific conductivities from 350 to 650 μmhos/cm.

Elkhorn and Hawley Warm Springs (H-1 and H-2). Elkhorn and Hawley Warm Springs are located 2.8 and 1.5 km northwest of Heise Hot Springs, respectively. Both springs are located on the escarpment formed by the Heise fault at an elevation of 40 to 70 m above Heise Hot Springs. The intrusive body suggested by Mabey (1978) to be under Heise Hot Springs is also believed to underlie these two springs. These springs emerge from relatively flat lying rhyolite tuffs on the southern edge of the Rexburg Caldera Complex (Proskta and Embree, 1978). These springs do not have associated travertine deposits and do not give off any gaseous odors.

Elkhorn Warm Spring has as specific conductance of 390 μmhos/cm, a temperature of 16°C, and a pH measurement of 6.6. The dominant ions are calcium and bicarbonate. Hawley Warm Spring has a specific electrial conductance of 350 μmhos/cm, a temperature of 20°C, and a pH of 7.5. The dominant ions are calcium and bicarbonate.

Unnamed Spring at 3N 41E 32bbdS (H-6). This 23°C spring discharges from a densely welded ash-flow tuff named Tuff of Spring Creek within the postulated Willow Creek caldera (Protska and Embree, 1978). This tuff may only form a thin covering overlying older Mesozoic and Paleozoic rocks. This is suggested by an exploration oil well (Sorenson No. 1) drilled 2 km to the east which intersected the Nugget

Formation at a depth of 6 meters (Savage, 1961). A 9.3 km long, northeast trending fault is located 0.2 km to the south of this spring site.

This spring has a specific electrical conductance of 650 μmhos/cm and a pH of 7.2. The dominant ions in this water are calcium and bicarbonate.

Dyer and Anderson Wells (H-7 and H-8). These two wells are representatives of a group of warm water wells located in a subdivision called Rim Rock Estates on the bench east of Idaho Falls. The wells are located 1.6 km apart with the Dyer well located northeast of the Anderson well. They have temperatures of 21 and 20°C, respectively. Tertiary Salt Lake Formation is mapped at the well sites with outcrops of rhyolite welded tuffs and associated ash nearby (Mansfield, 1952). The Salt Lake Formation mapped in this area appears to be a thin covering overlying the welded tuffs. The drill log for the Dyer well indicates that the water is obtained from fractured rhyolite. There is a northwest trending fault mapped 0.2 km west of this well. In the Anderson well, the drillers log reports that the water is coming from sandstone (pumice?) or rhyolite.

The chemistries of these wells are similar. The specific electrical conductivity values are 520-530 μmhos/cm and the pH is 7.7. The dominant ions present are calcium and bicarbonate.

Warm Spring (H-20). Warm Spring (H-20) is located at an elevation of 2180 m on the northwestern flank of Big Elk Mountain. Extensive deposits of travertine are present below the spring site. The spring surfaces near the contact of the Twin Creek Limestone and Nugget Sandstone. Beds of gypsum and anhydrite have been found at the base of the Twin Creek Limestone at some locations in Idaho and Wyoming. The presence of this bed would account for the high concentrations of calcium and sulfate in the water. This site is located 250 m west of the axis of the Big Elk Mountain anticline. Sun-Sinclair drilled an oil exploration well on the axis of the Big Elk Mountain anticline 4.8 km southeast of the spring site. The fluid from the Wells Formation was tested at a depth of 1534 to 1545 m at a recorded temperature of 103°C.

The water from this spring has a specific electrial conductance of 600 μmhos/cm. The pH is 7.2 and the dominant ions are calcium and sulfate.

Nonthermal Springs. Twelve springs in this study area have low temperatures and low specific conductivities: H-4, H-5, H-11, H-12, H-13, H-14, H-15, H-17, H-18, H-19, H-24, and H-25 (Figure III-4). Their temperatures range from 6 to 14°C with specific electrical conductivities from 230 to 830 mhos/cm. Detailed descriptions of these springs are given by Hubbell (1981).

Analysis of Data

Analysis of Springs and Wells Utilizing Physical Data

Introduction. The physical data collection at each site included information regarding the characteristics of the geologic setting such as the structural features near the springs and the formations from which they flow, the water temperature, the estimated or reported rate of discharge, the location, and the elevation. The geologic setting of the springs and wells provide information on the structural features influencing ground water flow and indicates which formations are aquifers. The relationship between temperature and discharge provides information regarding the amount of deep ground water flow.

Structural Controls on Springs and Wells. The most important factor influencing ground water flow paths is the spatial distribution of hydraulic conductivity. This distribution is controlled by structural features such as folds and faults and the hydraulic properties of the formations. Structural controls are geologic features produced in rocks after deposition and often after consolidation. Faults may affect ground water flow in three ways. A fault may act as a conduit to flow, as a barrier to flow, or may have no affect. In addition, the offset in beds produced by the fault may place formations of differing hydraulic characteristics against each other.

Thrust faults are pominant structural features in southeastern Idaho. The study area is bordered on three sides by the surface exposures of these faults and they pass beneath this area at various depths (Figure III-4, cross-section A-A'). Only one thrust fault has been mapped in the interior of the study area; there are no springs associated with this particular thrust fault. Data presented in Chapter II suggest that the Meade thrust fault may not act as a barrier to ground water flow except as a secondary control in positioning lithologies with high hydraulic conductivities against those with low hydraulic conductivities. The hydrogeologic importance of thrust faulting is probably markedly different near the surface where it cuts across individual units from the character of the faulting at depth where it is probably parallel to bedding.

Only one spring in the study area appears to be controlled by a thrust fault. Buckland Warm Spring (H-5) flows from a block of Gallatin Limestone thrust over Mission Canyon Limestone by the Baldy Mountain thrust fault. This overthrust plate covers 3 km^2 and is believed to be less than 200 m thick (Staatz and Albee, 1966). Buckland Warm Spring emerges at the surface trace of the thrust fault and may act as a drain, discharging ground water from the overthrust plate. However, calculations using the recorded discharge of 460 l/s along with the size of the overthrust plate (3 km^2)

indicate that the recharge must be approximately 7 m/year to maintain the discharge rate. The recharge area supplying water for this spring is obviously much larger than this overthrust plate.

The next most prominant structural features in the area are the graben forming faults along the Swan, Grand, and Star valleys. These faults probably create zones of high hydraulic conductivity along their paths. These faults extend very deep and probably influence all but the deepest flow systems (Figure III-3).

Five thermal springs are asociated with the faults along the edge of the Swan, Grand, and Star valleys. They are Heise Hot Springs (H-3 and I-3), Fall Creek Mineral Springs (H-9, H-10, and I-10), Alpine Hot Springs (I-21 and I-22), Auburn Hot Springs (H-26 and W-26), and Johnson Springs (H-27). Two other thermal springs, Elkhorn and Hawley warm springs (H-1 and H-2) are located near one of the major graben forming faults; however, these springs are not believed to be controlled by this fault but rather by zones of higher hydraulic conductivity in the Rexburg Caldera Complex. Five nonthermal springs (H-4, H-5, H-13, H-14 and H-15) are located near either the Snake River or the Grand Valley faults. It is not known if these springs are directly controlled by these faults.

Six more of the springs examined in this area are associated with minor faults. Four of these springs (H-6, H-7, H-16, and H-23) have warm temperatures; ground water is believed to move up the fault trace from depth. The remaining two springs (H-24 and H-25) are located in an intensely faulted area.

Geologic Formations Associated with Spring and Well Sites. The springs and wells sampled in the study area discharge from ten different formations ranging from Recent alluvial sediments to Cambrian Limestone (Table III-3). Most of the springs examined in the study area flow from zones of secondary hydraulic conductivity caused by faulting. The fault areas probably have considerably higher hydraulic coductivity than the undistrubed portions of the formations. The relationship between spring location and stratigraphic unit may thus be an indirect indicator of regional hyraulic properties of rocks.

Discharge of Springs. The total discharge of springs examined in this area is inversely proportional to the temperature. The springs in this study with temperatures less than 15.5°C have a total discharge of approximately 1200 l/s. The two largest springs have discharges of 100 and 1000 l/s. The springs with temperatures of 15.5 to 39°C have a total discharge of approximately 60 l/s. The largest of these springs has a discharge of 10 l/s. The total discharge

Table III-3. Geologic formation associated with springs and wells in the vicinity of the Caribou Range, southeastern Idaho and western Wyoming.

Geologic Formation or Rock Unit	Spring Number
Alluvium	I-21*, I-22*
Salt Lake	H-11, H-12, H-14*, H-15*
Rhyolite	H-1*, H-2*, H-3*, H-6*, H-7*, H-8
Wayan	H-18
Bechler	H-24*, H-23*
	or
Peterson	H-25*, H-23*
Ephriam	H-16*
Twin Creek Limestone	H-17, H-20
	or
Nugget	H-19, H-20
Dinwoody	H-26*, H-27*
Mission Canyon Limestone	H-9*, H-10*, H-13*
Gallatin Limestone	H-4*, H-5*

*spring is located near fault

of springs with temperatures above 39°C is approximately 9 l/s; the largest spring in this group has a discharge of 4 l/s. The small total discharge of the thermal water indicates that most ground water movement is relatively shallow.

The discharge-temperature relationship described for the study area in southeastern Idaho fits the general homogeneous models of flow systems as presented by Toth (1963) and Freeze and Witherspoon (1966, 1967). They found that approximately 90 percent of the total ground water in a homogeneous system circulates to very shallow depths and the remaining portion, in decreasing amounts, circulates to greater depths.

The rate of discharge varies over the course of the year for most springs. The amount of fluctuation in discharge is a function of the length of the flow path. The discharge from local flow systems fluctuates greatly, often ceasing during the year; intermediate flow systems have the least fluctuation of all. Only one of the springs in this area has been measured at different times of the year. The large discharge variation in Buckland Warm Springs indicates that at least a portion of the flow is supplied by ground water with a short flow path.

Elevation of Discharge. The elevations of springs and wells in this area range from 1530 to 2180 m. There appears to be no direct correlation between the elevation of spring discharge and water temperature. However, it is important to note that each spring is located in a local topographic low with one exception. Warm Spring (H-20) discharges at an elevation of 2180 m near the crest of the Caribou Range.

Analysis of Springs and Wells Utilizing Chemical Data

The chemical compositon of the water discharging from a spring is the result of a complicated set of interactions determined by the chemical characteristics of the porous media through which it moves, the rate at which it flows, and the temperature and pressure of the ground water along its flow path. The chemical analysis of the water from a spring or well provides information on the rocks that chemically interacted with the water, the relative length of the ground water flow path, the rate of flow, and the maximum temperature along the flow path. The combined interpretation of the chemical and physical data can be used to describe probable ground water flow systems.

Evolution of Major Ions in Ground Water Flow Systems. Chebolarev (1955) concluded that ground water changes its character chemically toward seawater as it moves along its flow path from recharge area to discharge area. He noted that dominant anion species evolve in the following manner along a ground water flow path (Freeze and Cherry, 1979, p. 242):

$$HCO_3^- \rightarrow HCO_3^- + SO_4^{2} \rightarrow SO_4^{2} + HCO_3^- \rightarrow SO_4^{2-} + Cl^- \rightarrow Cl^- + SO_4^{2-} \rightarrow Cl^-$$

Increasing age and distance of flow path →

Bicarbonate is the dominant ion in the beginning of the anion evolution. The sulfate concentration increases with increasing time and distance until it is the dominant anion and bicarbonate is secondary. This process proceeds until chloride is the dominant anion. The evolution of the anion species is controlled by two variables, the availability of minerals and the mineral solubility.

The cycle begins in the form of precipitation. Moisture moving through the soil zone is charged with carbon dioxide which reacts with the water to form a bicarbonate and a hydrogen ion. The hydrogen ion may react with calcite to form another bicarbonate plus a calcium ion. The upper limits of the concentrations attained by these reactions are controlled by the solubility of calcite and dolomite and the partial pressure of carbon dioxide. Sulfate concentrations increase in ground water along its flow path until it is the dominant ion. This process requires a long flow path because the major soures of sulfate in ground water, gypsum and anydrite, are generlly present only in trace amounts. Chloride may evolve to where it is the dominant anion species in some regions where the ground water is traveling through a deep ground water basin composed of sedimentary rocks.

The anion evolution can be correlated to Domenico's three ground water zones:

1. The upper zone - This zone is characterized by a high rate of ground water flushing through well leached

sediments. The dominant anion in this water is bicarbonate. This water commonly has a low total dissolved solids.

2. The intermediate zone - This zone has less flushing actions than the upper zone and a higher concentration of total dissolved solids. The dominant anion in this water is sulfate.

3. The Lower zone - The circulation of ground water at this zone is nearly stagnant with nearly unleached rocks. This water has highly mineralized water and the dominant anion is chlorided (Domenico, 1972, p. 292).

The anion evolution sequence provides information regarding the flow path of the ground water. It must be used with care because this process can be short circuited when the ground water comes in contact with soluble sediments such as evaporites. The use of the anion evolution sequence is also dependent upon the fact that the water flows through the same types of rocks throughout the system. Cation evolution is not used because the sequence is often reversed due to cation exchange.

The water analyses may be used to indicate the length of the ground water flow system in the study area by using the three dominant anion species, bicarbonate, sulfate, and chloride. The relative flow lengths are presented in Table III-4 with a bicarbonate water indicated as short system, a

Table III-4. Results of analyses tc determine relative length of flow paths by dominant anions and total dissolved solids and groups formed by cluster analysis in the vicintiy of the Caribou Range, southeastern Idaho and western Wyoming.

Sample Number	Sample Name and Location	Temp °C	Relative Length of Flow Path: Dominant Anion	Relative Length of Flow Path: Total Dissolved Solids	Cluster Analysis Group
H-1	Elkhorn Warm Spring 4N 40E 23cadS	20	short	short	1
H-2	Hawley Warm Spring 4N 40E 25bbdS	16	short	short	1
H-3, I-3	Heise Hot Springs 4N 40E 25ddaS	48	long	long	2
H-4	Lufklin Spring 3N 42E 2cbbS	8	short	short	1
H-5	Buckland Warm Spring 3N 42E 12cca and ccdS	11	short	short	1
H-6	Unnamed Spring 3N 41E 32bbdS	23	short	short	1
H-7	Dyer Well 2N 39E 21bcc	21	short	short	1
H-8	Anderson Well 2N 39E 29bac	20	short	short	1
H-9	Fall Creek Mineral Springs 1N 43E 9cbb1S	24	long	long	2
H-10, I-10	Fall Creek Mineral Springs 1N 43E 9cbbS	23	long	long	2
H-11	Unnamed Spring 1N 39E 14acaS	9	short	short	1
H-12	Unnamed Spring 1N 40E 19cabS	13	short	short	1
H-13	Unnamed Spring 1N 44E 30cbdS	7	short	short	1
H-14	Unnamed Spring 1N 45E 4adaS	6	short	short	1
H-15	Unnamed Spring 1N 45E 4acaS	6	short	short	1
H-16	Unnamed Spring 1S 40E 4abcS	21	intermediate	long	2
H-17	Unnamed Spring 1S 44E 1cbdS	7	short	short	1
H-18	Willow Springs 1S 41E 36cccS	8	short	short	1
H-19	Unnamed Spring 2S 44E 1accS	11	short	short	1
H-20	Warm Spring 2S 44E 9aacS	17	intermediate	short	1
I-21, I-22	Alpine Hot Springs 2S 46E 19cadS	56 37	long	long	2
H-23, I-23	Brockman Hot Springs 2S 42E 26dcdS	35	intermediate	long	2

Table III-4. Continued.

Sample Number	Sample Name and Location	Temp °C	Relative Length of Flow Path: Dominant Anion	Relative Length of Flow Path: Total Dissolved Solids	Cluster Analysis Group
H-24	Unnamed Spring 3S 43E 15dccS	10	short	short	1
H-25	Unnamed Spring 3S 43E 22abbS	14	short	short	1
H-26, W-26	Auburn Hot Springs 33N 119W 23dbdS	57	long	long	2
H-27	Johnson Springs 33N 119W 26adS	54	long	long	2

sulfate water as intermediate, and a chloride dominant water as a long flow system.

Total Dissolved Solids as an Indicator of Flow Path Length. The concentration of total dissolved solids can also be used as an indicator of the length of a ground water flow system. As ground water moves along its flow path from recharge area to discharge area it will attain higher concentrations of dissolved solids. Total dissolved solids cannot be specifically correlated to a time or distance in a flow path except to say that the concentrations of total dissolved solids increase with the distance of travel. This generalization assumes that the water does not come in contact with formations containing highly soluble minerals, the temperature is constant throughout the flow path, and that the water flows through the same type of rocks throughout the system. The results from this generalization are presented in Table III-4. The concentrations of total dissolved solids of 4000 to 11,000 mg/l (long flow systems) and a low total dissolved solids of 100 to 700 mg/l (shorter flow systems).

Classification of Springs and Wells Using WATEQF. WATEQF is the Fortran IV version of the WATEQ computer program written by Truesdell and Jones in 1973. It models the equilibrium distribution of inorganic ions and complex species in solution using the chemical analysis and measurements of pH and temperature as input. The calculation is performed in the following manner:

> The water analysis is read in and ion concentrations are converted to molality. All values of equilibrium constants are recalculated to the temperature of interest using the van't Hoff equation, unless experimental data are available. A cation-anion balance is calculated. If the charge balance error is greater than 30%, calculation is terminated at this point... As a final preparatory calculation, the Debye-Huckel solvent constants are corrected for temperature.
>
> During the next phase of computation, single-ion activity coefficients are calculated using the Davies equation or the Debye-Huckel approximation. With these, the activities of all possible aqueous species can then be computed. The distribution of these species is then calculated by means of a chemical model, which uses analytical concentrations, experimental solution equilibrium constants, mass balance equations, and the measured pH. This distribution is presented in the form of a table which contains the concentrations, in mg/l and molality, the activities, and the activity coefficients of all possible aqueous species.
>
> In the final phase of the calculation, saturation data are computed. Ion activity products for all possible reactions are calculated and compared with the temperature-corrected equilibrium constants. This information is, again, presented in a table containing ion activity products (K_{iap}), equilibrium constants (K_{eq}), the ratio of these two values (K_{iap}/K_{eq}) ... (Hounslow and others, 1978, p. 138-139).

The results of these computations can be used to group springs with the same saturation states.

The saturation index for the minerals aragonite, calcite, and dolomite as calculated by WATEQF for the samples obtained in the study area are presented in table III-5. These minerals were chosen because a large proportion of the

Table III-5. Saturation index of selected minerals for springs and well in the vicinity of the Caribou Range, southeastern Idaho and western Wyoming.

Sample Number	Sample Name and Location	Water Temp. (°C)	Aragonite	Calcite	Dolomite
H-1	Elkhorn Warm Spring 4N 40E 23cadS	20	.05	.07	.003
H-2	Hawley Warm Spring 4N 40E 25bbdS	16	.39	.61	.15
H-3	Heise Hot Springs 4N 40E 25ddaS	48	2.5	4.2	6.3
I-3	Heise Hot Springs 4N 40E 25ddaS	49	4.0	6.8	26
H-4	Lufklin Spring 3N 42E 2cbbS	8	.44	.74	--
H-5	Buckland Warm Spring 3N 42E 12cca + ccdS	11	.44	.72	.16
H-6	Unnamed Spring 3N 41E 32bbdS	23	.61	.92	.40
H-7	Dyer Well 2N 39E 21bcc	21	.96	1.5	.94
H-8	Anderson Well 2N 39E 29bac	20	.99	1.5	.76
H-9	Fall Creek Mineral Springs 1N 43E 9cbb1S	24	1.0	1.6	.98
H-10	Fall Creek Mineral Springs 1N 43E 9cbb2S	23	.82	1.2	.58
H-11	Unnamed Spring 1N 39E 14acaS	9	.13	.21	.02
H-12	Unnamed Spring 1N 40E 19cabS	13	.16	.26	.01
H-13	Unnamed Spring 1N 44E 30cbdS	7	.36	.62	.05
H-14	Unnamed Spring 1S 45E 4adaS	6	.42	.73	.17
H-15	Unnamed Spring 1S 45E 4acaS	6	.51	.90	.25
H-16	Unnamed Spring 1S 40E 4abcS	21	.56	.86	.22
H-17	Unnamed Spring 1S 44E 1cbdS	7	.24	.41	.05
H-18	Willow Spring 1S 41E 36cccS	8	.30	.51	.06
H-19	Unnamed Spring 2S 44E 1aacS	11	.08	.13	.004
H-20	Warm Spring 2S 44E 9aacS	17	.45	.70	.16
I-21	Alpine Hot Springs 2S 46E 19bS	56	2.7	5.0	15
I-22	Alpine Hot Springs 2S 46E 19cadS	37	1.8	2.8	3.5

Table III-5. Continued.

Sample Number	Sample Name and Location	Water Temp. (°C)	Aragonite	Calcite	Dolomite
H-23	Brockman Hot Spring 2S 42E 26dcdS	35	1.5	2.3	2.2
I-23	Brockman Creek W.S. 2S 42E 26dcdS	35	.66	1.0	.64
H-24	Unnamed Spring 3S 43E 15dccS	10	.51	.85	.23
H-25	Unnamed Spring 3S 43E 22abbS	14	.51	.80	.12
H-26	Auburn Hot Springs 33N 119W 23dbdS	57	2.1	4.0	8.3
W-26	Auburn Hot Springs 33N 119W 23dbdS	62	21	42	1200
H-27	Johnson Springs 33N 119W 26adS	54	2.0	3.6	4.1

study area is made up of carbonate rocks and because these three minerals are the most diagnostic minerals to divide these springs into separate groups. The saturation index (K_{iap}/K_{eq}) indicates whether a solution is undersaturated or saturated with respect to these specific minerals. Values less than one indicate that the solution is undersaturated and values more than one indicate the solution is oversaturated with respect to that mineral. Solutions oversaturated with a mineral species favors precipitation of that mineral while undersaturation favors dissolution.

The data indicate that all of the springs grouped as thermal springs with high specific conductivities in the previous chapter are oversaturated with respect to one or more of these three minerals except sample H-16, unnamed spring at 1S 40E 4abcS. These data are verified by the observation of active travertine deposition at each of these sites. As the water from hot springs rises to the surface the pressure drops and the water cools causing the precipitation of some dissolved minerals. The data also show that the two wells tested in this area (H-7 and H-8) are oversaturated with respect to calcite. The equilibrium of these samples was altered when the water was pumped to the surface so the results of WATEQF may not be representative of the water in the aquifer. All of the other springs in this area are undersaturated with respect to aragonite, calcite, and dolomite.

Correlation of Springs and Wells Utilizing Stiff Diagrams. Stiff diagrams graphically show the concentrations of major cations and anions in milliequivalents per liter. The width of the patterns are an approximate indication of the total ionic content. These diagrams are useful for analyzing gross similarities in water quality and thus ground water flow systems. Stiff diagrams for the springs and wells in the Caribou Range study area are presented in Figure III-5.

Seven of these springs, Heise Hot Springs (H-3 and I-3), Falls Creek Mineral Springs (H-9, H-10, and I-10), Unnamed Spring at 1S 40E 4abcS (H-16), Alpine Hot Springs (I-21 and I-22), Brockman Hot Springs (H-23 and I-23), Auburn Hot Springs (H-26 and W-26), and Johnson Springs (H-27), shown in Figure III-5 are drawn at one-half actual width. The significant differences between these stiff diagrams and those of the other springs in both size and major constituents suggest that these seven springs should be put into a separate group. This group could be further separated into two smaller groups, one with sodium and sulfate as their dominant ions (H-16 and H-23) and those with sodium and chloride as their dominant ions (H-3, I-3, H-9, H-10, I-10, I-21, I-22, W-26, H-26, and H-27). The similarities between the chemistries of the springs may be due to similar geologic controls on their flow paths. The

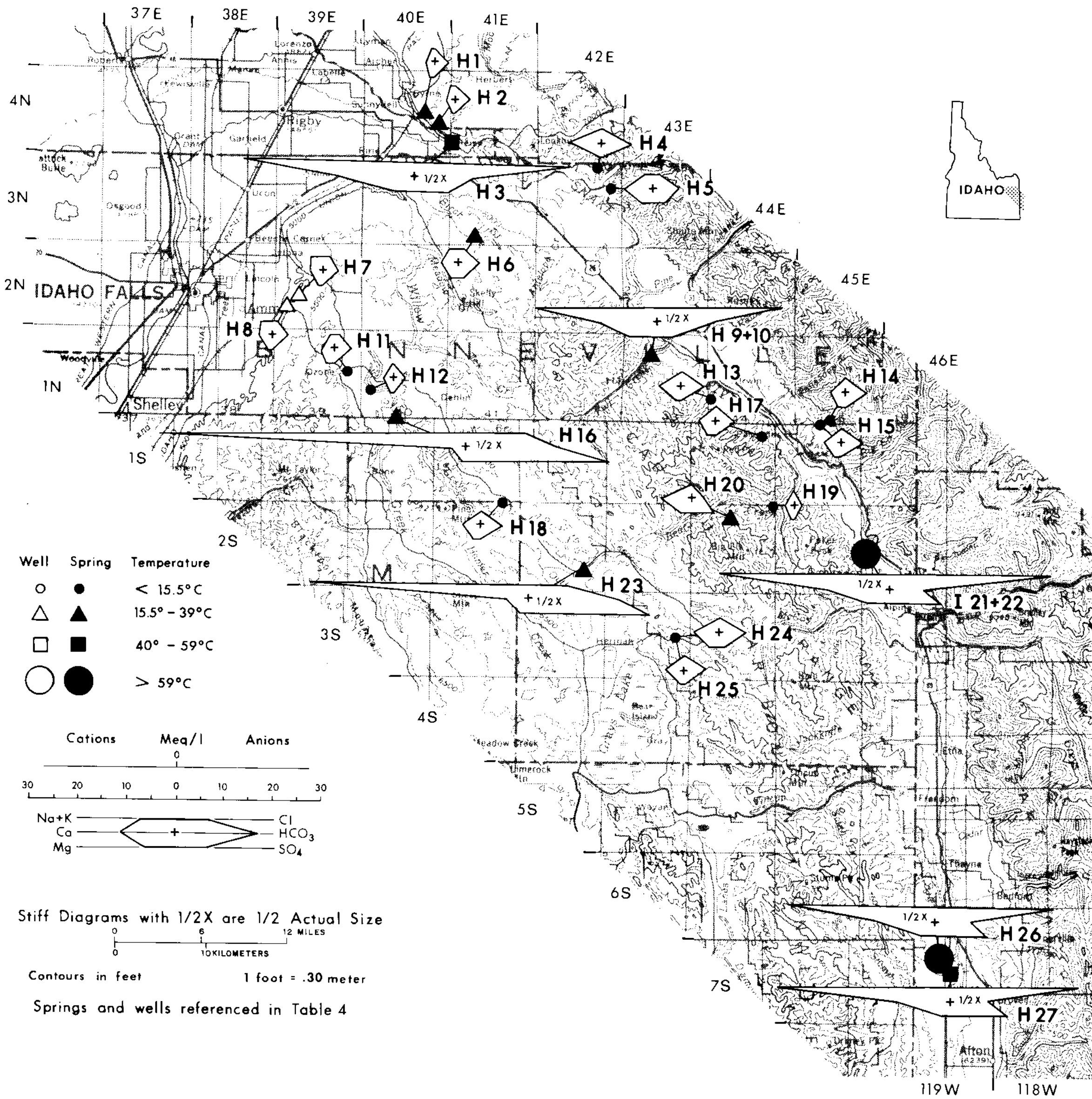

Figure III-5. Stiff diagrams of water chemistries of selected springs and wells in the vicinity of the Caribou Range, southeastern Idaho and western Wyoming springs with sodium and chloride as their dominant ions are associated with faults bordering the Swan, Grand, and Star valleys. The springs with sodium and sulfate as dominant ions flow from rocks of the Gannett group but are apparently not controlled by major faults. The group with sodium and chloride as their major ions can be further divided into two groups of like chemistries, one with higher concentrations of bicarbonate (H-3, I-3, H-9, I-10, and H-10) than the other group (I-21, I-22, H-26, W-26, and H-27).

It is more difficult to differentiate the stiff diagrams for waters with low concentrations of dissolved solids because of their small overall size. These diagrams have more subtle differences than do those with high total ionic contents. One of these springs, Warm Spring (H-20), can be differentiated from the other springs due to the differences in the major ions. This spring has calcium and sulfate as the dominant ions whereas other springs in this group have calcium and bicarbonate as their dominant ions.

The stiff diagrams with low total ionic contents are best used to relate springs located closely together. Elkhorn and Hawley Warm Springs (H-1 and H-2) are similar to each other yet distinct from the others as are Dyer and Anderson wells (H-7 and H-8). Two other springs that may be grouped this way are Unnamed Springs at 1S 45E 4adaS and 1N 45E 4acaS (H-14 and H-15). It should be noted that Heise Hot Springs (H-3) and Elkhorn and Hawley Warm Springs (H-1 and

H-2) do not have similar water chemistries despite the closeness in location, and the presence of thermal water in all three.

Statistical Analysis of Chemical Data

Introduction

The analysis of the chemical data requires the simultaneous examination of the twelve variables obtained at each site. The following steps were taken in the statistical analysis of the chemical data on springs and wells in the study area.

1. The data were summarized using the UNIVARIATE data summary program (SAS Institute Inc., 1979) to determine if they fulfill the assumptions that the data are normally distributed which is required for subsequent analyses.
2. The second step of the analysis was a cluster analysis which groups like samples.
3. A stepwise MANOVA analysis was performed using the groupings from the cluster analysis to determine which variables are most useful in discriminating between the specified groups and to test if the groups can be statistically separated by using the most discriminating variables. This step was accomplished by using SAS stepwise discriminate procedure (SAS Institute Inc., 1979).

UNIVARIATE Analysis

The UNIVARIATE data summary in the Statistical Analysis System was used to present the chemical data (Figure III-6). This program includes calculation of the descriptive statistics and the graphical summarization of the data with a stem-and-leaf plot, a box plot, and a normal probability plot. A listing of results is presented in Hubbell (1981, Appendix A).

The first three moments calculated in the descriptive statistics are the mean, the standard deviation, and the skewness. The mean and variance indicate the "center" of the data and variability of the data about that center, respectively.

The skewness indicates the symmetry of the data around its mean. Data with a normal distribution have a skewness equal to zero; data that are skewed to the left have a positive value (i.e. mean is larger than the median). The data from this study are all positively skewed except the variable pH. The positive skewness shown by the variables in the UNIVARIATE data summary indicates that a logrithmic transformation is appropriate for all variables except pH to approximate the normality assumptions required for subsequent tests of significance. Six of these variables have some concentrations equal to zero: magnesium, sodium, potassium, chloride, fluoride and sulfate. A concentration of 1 mg/l

S T A T I S T I C A L   A N A L Y S I S   S Y S T E M

UNIVARIATE

```
VARIABLE=TEMP

                MOMENTS                                              QUANTILES(DEF=4)                             EXTREMES

N               31   SUM WGTS        31     100% MAX   62    99%    62      LOWEST  ID          HIGHEST  ID
MEAN       24.2903   SUM            753      75% Q3    35    95%    59         6(H-15    )        49(I-3     )
STD DEV    17.2727   VARIANCE   298.346      50% MED   20    90%  55.6         6(H-14    )        54(H-27    )
SKEWNESS  0.923259   KURTOSIS -0.380486      25% Q1    10    10%     7         7(H-17    )        56(I-21    )
USS          27241   CSS        8950.39       0% MIN    6     5%     6         7(H-13    )        57(H-26    )
CV         71.1094   STD MEAN   3.10227                       1%     6         8(H-18    )        62(W-26    )
T:MEAN=0   7.82986   PROB>|T|    0.0001     RANGE      56
W:NORMAL  0.859252   PROB<W       <0.01     Q3-Q1      25
                                            MODE        6

      STEM LEAF                     #
         6 2                        1
         5 67                       2
         5 4                        1
         4 89                       2
         4
         3 557                      3
         3
         2 5                        1
         2 0011334                  7
         1 67                       2
         1 01134                    5
         0 6677889                  7
           ----+----+----+----+
```

BOXPLOT

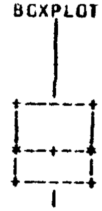

NORMAL PROBABILITY PLOT

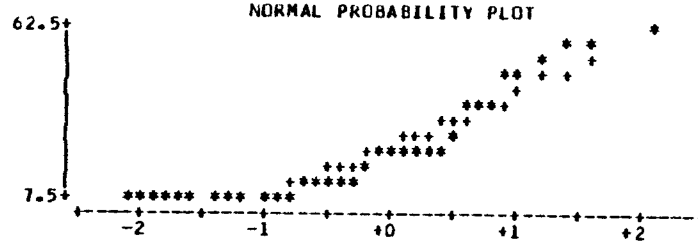

Figure III-6. UNIVARIATE data summary of the variable temperature for springs and wells in the vicinity of the Caribou Range, southeastern Idaho and western Wyoming has been added to each of the values of these variables before the transformation.

The stem-and-leaf plot is a histogram with the vertical axis, the stem, representing the leading digits of the data. The leaves are shown on the horizontal axis and are the last digits of the data.

The box plot indicates six summary points; the minimum, the lower quartile, the median, the mean (+), the upper quartile, and the maximum. This plot indicates whether the data are skewed positively or negatively and the relative variation of each variable. The normal probability plot graphs the raw data on the vertical scale versus the standard normal scores (Z scores) on the horizontal scale. The raw data are represented by asterisks versus the plus sign which represent normally distributed data. If the data are normal, one would expect the data to plot on a straight line. Any deviation from this line indicates non-normality.

The pH values and the log functions of the other variables are standardized by:

$$Z = \frac{X - \bar{X}}{S}$$

where:

Z = standardized log normal variable

X = sample value

$\bar{X}$ = mean of the variable

s = standard deviation of the variable (Huntsberger and Billingsley, 1977).

This procedure scales all values to a range of approximately -3 to +3, where each variable has a mean of zero and a standard deviation of one. In this way, each variable has equal weight in the subsequent cluster analysis.

Cluster Analysis

The chemical data in Table III-2 were run using the SAS hierarchical grouping, several variable cluster analysis (SAS Institute Inc., 1979). The clustering was performed on 31 samples in twelve dimensional space defined by pH, calcium, magnesium, sodium, potassium, chloride, fluoride, bicarbonate, sulfate, silica, total dissolved solids, and temperature. This technique reduced the data from 31 groups ultimately into one group. The cluster technique begins by the computation of a similarity or distance matrix between the samples. At each step two samples or clusters are joined, if they are the closest unjoined set. The final product is a dendrogram showing the stepwise joining of the samples (Figure III-7). If the diameter increases markedly when two clusters are joined the clustering process has gone too far. In Figure III-7 this occurs when two clusters are joined to make one (the diameter changes from 23 to 74).

The cluster analysis indicates that there are two distinguishable groups of chemistries (Table III-4). The first group is made up of samples with relatively low ionic

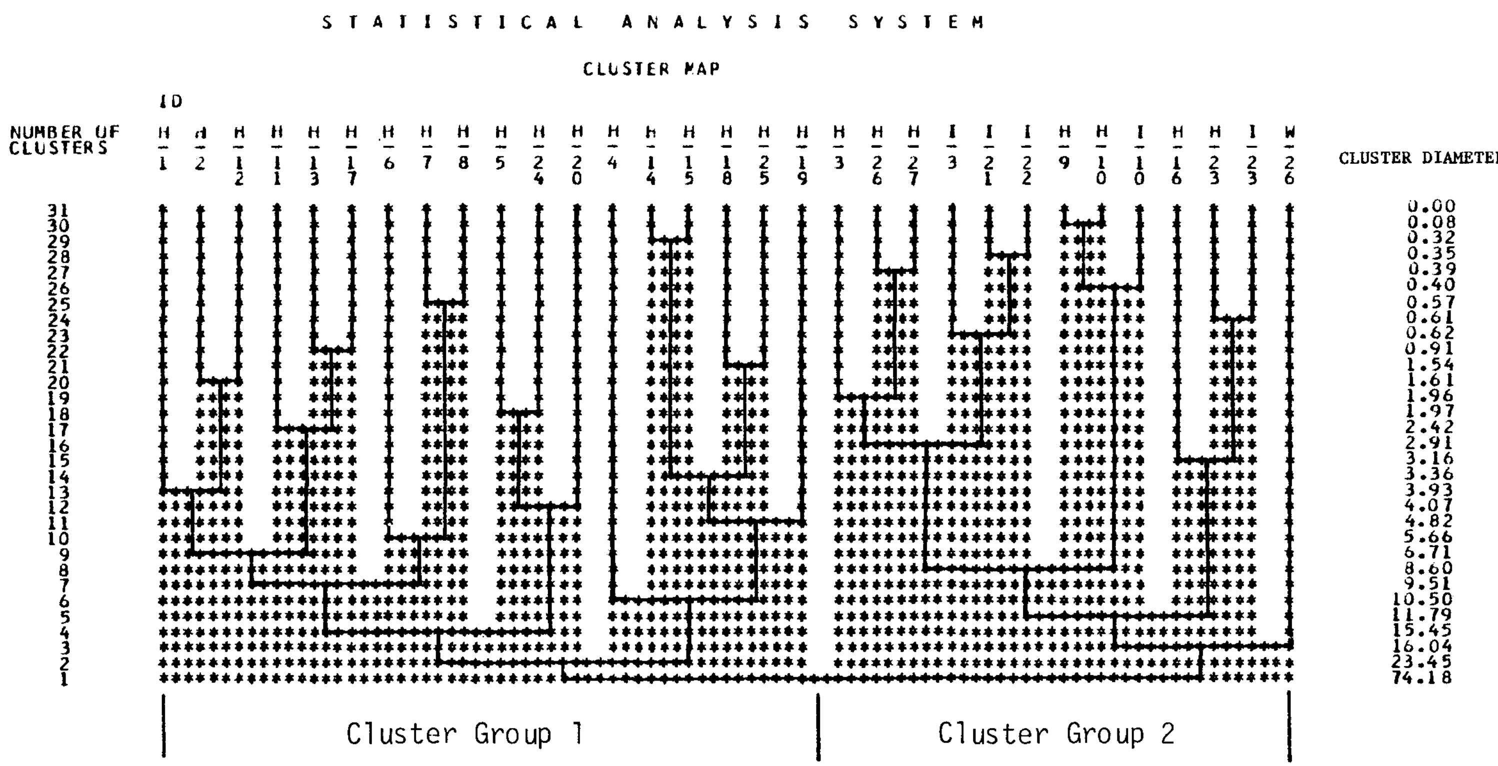

Figure III-7. Twelve variable cluster diagram for springs and wells in Caribou Range study area, southeastern Idaho and western Wyoming concentrations, lower temperatures, and higher pH's. The second group has relativey high ionic concentrations, higher temperatures, and lower pH's.

Stepwise MANOVA Analysis

A stepwise MANOVA analysis (SAS Institute Inc., 1979) was run to determine if the two groups formed by the cluster analysis can be differentiated statistically and to indicate the water quality variables most useful in separating these two groups. The hypothesis to be tested is that the mean of the combined distribution of chemial constituents of one group (μ_1) is equal to the mean of the constituents of the other (μ_2). The null hypothesis (Ho) can be stated as $\mu_1 = \mu_2$ and the alternate hypothesis is the converse $\mu_1 \neq \mu_2$.

The results of the test are listed in Table III-6. The first column lists the variables which are most useful in discriminating the two cluster groupings with the best discriminator at the top. The second column is the Wilk's lambda statistic. It is used to test for significance between the groups. A smaller value of the lambda statistic implies greater statistical significance between the groups. The statistical significance increases as more variables are added. The third column (Prob. <Lamba) is the probability of obtaining a Wilk's lambda statistic smaller than the observed statistic in column two when in fact the null hypothesis,

Table III-6. Results of stepwise MANOVA analysis for springs and wells in Caribou Range study area, southeastern Idaho and western Wyoming.

Variable	Wilk's Lambda	Prob.< Lambda
LTDS	.03476	0.0001
LK	.02214	0.0001
pH	.01914	0.0001
LCL	.01676	0.0001
LCA	.01383	0.0001
LF	.01098	0.0001

that the means are equal, is true. Thus by using the most discriminating variable, LTDS, the chance of obtaining a value of lambda less than .03476 is <.0001 if Ho is true. This implies that there is a difference between the two groups. The addition of the remaining variables essentially does not improve the ability to discriminate between the two groups.

Discussion of the Results

The cluster analysis indicates that there are at least two major clusters. These two groups are shown in Figure III-7. The stepwise MANOVA analysis indicates that the most discriminating variable is log TDS and that by using this variable alone that these two clusters can be separated.

Ground Water Flow Patterns

A ground water flow system is made up of three components: the recharge area, the flow path, and the discharge area. This investigation has concentrated on the physical characteristics and water quality at the discharge areas. Postulated ground water flow paths for the springs examined in the study area are presented in this section using the physical and chemical setting of the springs and wells and basic hydrologic concepts.

The cluster analysis discriminated two groups of springs with similar chemistries. The first group of springs to be examined have high concentrations of all the major ions, low pH values, and elevated temperatures.

Five of the springs in this group are associated with the graben forming faults along the Swan, Grand, and Star valleys: Heise Hot Springs (H-3 and I-3), Fall Creek Mineral Springs (H-9, H-10, and I-10), Alpine Hot Springs (I-21 and I-22), Auburn Hot Springs (H-26 and W-26), and Johnson Springs (H-27). Two hypotheses for the ground water flow to these springs may be stated.

1. Recharge occurs in the mountain ranges, where there are high rates of precipitation. The intense structural deformation of the ranges increase the vertical hydraulic conductivity allowing downward movement of ground water. The water moves laterally along bedding planes to the

fault systems bordering the Swan, Grand, and Star valleys where the fault provides a conduit of high hydraulic conductivity allowing the thermal water to move to the surface. Some mixing and cooling of the deep thermal ground water creates variations in temperature and water quality found along these systems.

2. Recharge occurs along the surface exposure of the major faults bordering the Swan, Grand, and Star valleys. The water moves downward following the vertical conduit formed by the major faulting. This deep thermal water follows the trace of the fault to move to the surface at a site some distance from the recharge area. And again, some cooling and mixing of the deep thermal ground water would create variations in temperature and water quality as seen in the springs in this system.

The remaining two thermal springs in the first group with high specific conductivities are Unnamed Spring at 1S 40E 4abcS (H-16) and Brockman Hot Springs (H-23). The water from these springs must circulate to depths where they can be heated; however there are no major faults closely associated with either of these sites. The closeness in their chemistries indicates that the processes which contribute to their chemistries are similar. Both springs issue from rocks of the Gannett Group and have minor faults near them. Their locations to one another, relative to the trend of the Swan and Grand Valley faults, implies that there may be a linear feature which may relate these two springs.

The second group differentiated by the cluster analysis is made up of springs with lower concentrations of all the major ions, and as a group have higher pH values and lower tempertures. This group can be further separated into three subgroups by their geologic setting and tempertures.

The first subgroup has three springs and two wells that emerge from rhyolite in the northwestern portion of the study area: Elkhorn Warm Spring (H-1), Hawley Warm Srping (H-2), Unnamed Spring at 3N 41E 32bbdS (H-6), Dyer well (H-7), and Anderson well (H-8). All of these have temperatures between 16 to 23°C. These springs and wells appear to be associated with caldera structures in this area. The calderas form closed basins filled with permeable materials with faults around their rims (Proskta and Embree, 1978). Precipitation in the mountains recharges the ground water system where some of it follows faults to the depths where it is heated. The water rises to form warm springs or, if the piezometric head is not great enough to force it to the surface, it may lie at depth where it may be pumped to the surface by wells. The similarity in chemistries and closeness of location suggests that this group can be further divided to group Elkhorn Warm Spring and Hawley Warm Spring into one group, Dyer and Anderson wells into a second, and Unnamed Spring at 3N 41E 32bbdS into a third group.

The second subgroup has one spring, Warm Spring (H-20). Warm Spring is unique in both its chemistry and its high elevation. The chemistry may be a function of the lithology and the elevated temperature may be a function of the lithology and the elevated temperture may be due to relatively shallow circulation of ground water in a region of high heat flow.

The third subgroup has twelve springs that probably represent shallow ground water flow systems controlled by the complex lithology and structure in this area. These springs are the result of local ground water flow systems formed by the discontinuous nature of the geologic units of this area. Their cool temperatures attest to shallow depths of circulation and the low ionic concentrations to short flow paths. Buckland Warm Spring (H-5) is associated with the Baldy Mountain thrust. This spring has a large discharge and a high ionic content relative to the other springs in this group which suggests that it has a longer flow path and a larger recharge area. The recharge area for this spring is located north of the study area in the Snake River Range.

CHAPTER IV

HYDROGEOLOGIC RECONNAISSANCE OF THE MEADE THRUST SUBAREA

Introduction

Ground water flow systems in the Meade thrust subarea have been evaluated both as a part of this study and as a research project related to phosphate mining under funding by the Idaho Mining and Minerals Resources Research Institute (Ralston and Mayo, 1981). The Meade thrust subarea includes the Meade Peak allochthon and is situated between the northern and southern subareas (Figures I-1 and IV-1). (An allochthon is a body of rocks that has been moved a long distance from their original place of deposition by a tectonic process such as overthrusting.) The study area consists of the large part of seven 15 minute quadrangles which cover approximately 3700 square kilometers and includes parts of Caribou and Bear Lake Counties, Idaho, and Lincoln County, Wyoming (Figure IV-2). The allochthon contains folded and faulted Mesozoic and Paleozoic sandy-shaly carbonate strata. The Meade thrust fault, previously known as a major segment of the Bannock thrust fault, underpins the allochthon and surfaces as thrust splays along its southern and eastern margins.

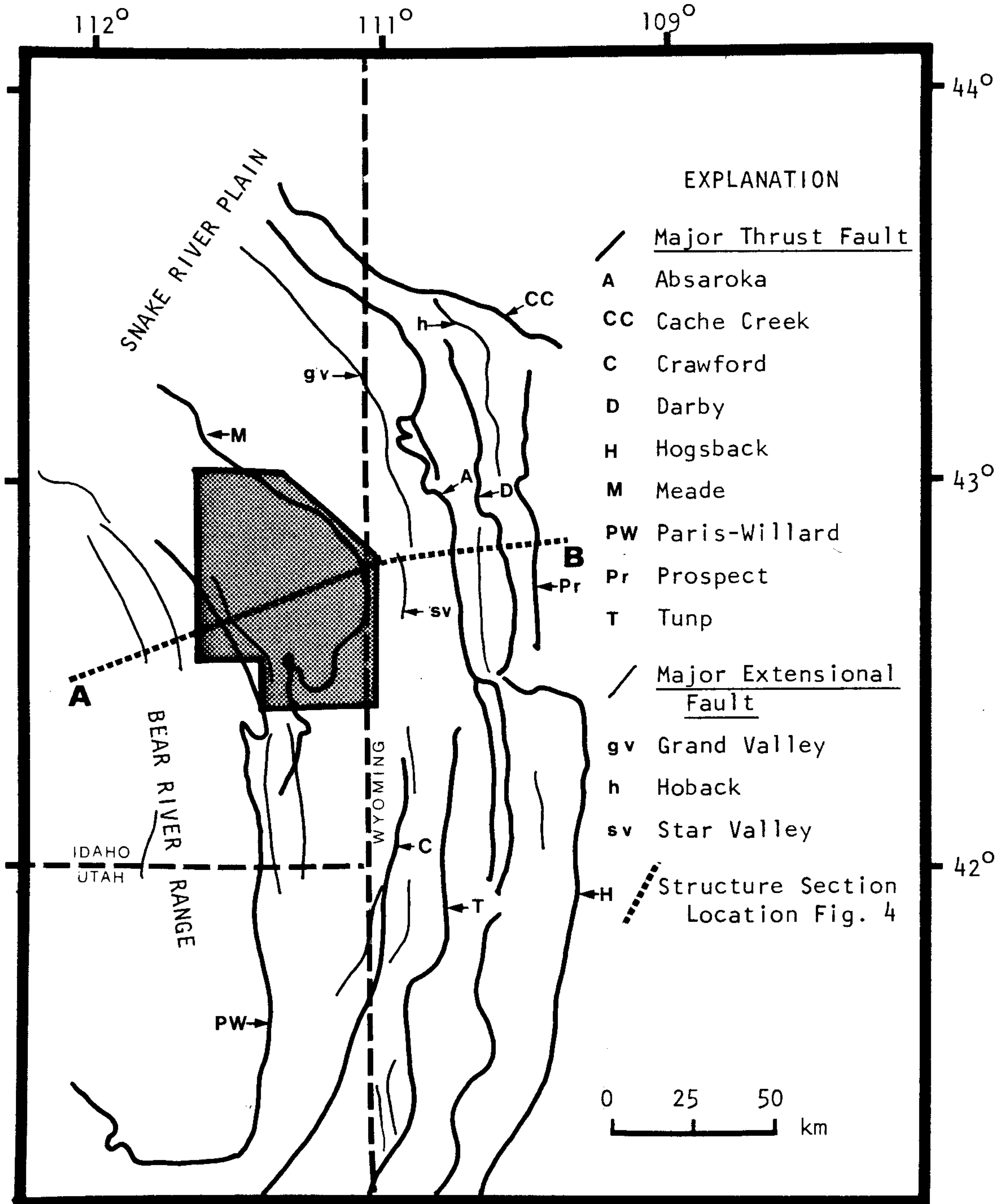

Figure IV-1. Generalized structural map of the overthrust belt in southeast Idaho and western Wyoming. Study area is shaded. Modified after Royse and others (1975).

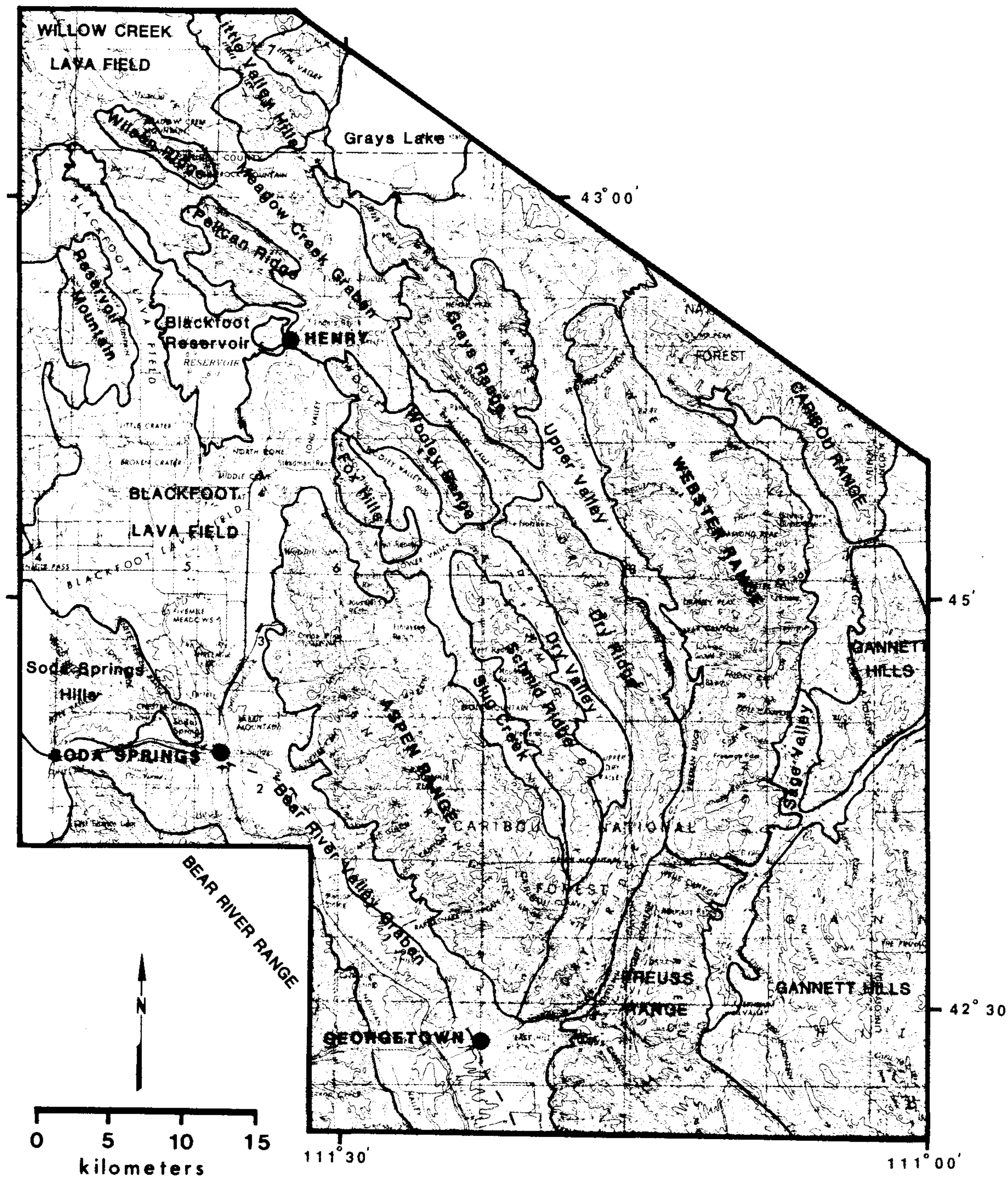

Figure IV-2. Map of physiographic regions of the Meade thrust area, southeastern Idaho.

Geologic Setting

The Meade thrust allochthon is defined here as that body of allochthonous strata transported by the Meade thrust fault. The Meade thrust fault is the principal structural feature of Blackstone's (1977) Meade unit and in the earlier literature is known as the major segment of Mansfield's (1927) Bannock thrust fault.

Numerous physiographic features are mentioned in this report; the locations of these features are shown in Figure IV-2.

Stratigraphy of the Allochthon and Adjacent Areas

The Meade thrust allochthon and surrounding areas contain a fairly continuous stratigraphic record representing Cambrian to Holocene time. Mansfield (1927) estimated that more than 14,000 m of calcareous, argillaceous and clastic sediments were deposited in the area. The Paleozoic through lower Mesozoic formations are predominantly of marine origins, and the upper Mesozoic and Cenozoic formations are predominantly of non-marine origins.

The upper Paleozoic and lower Mesozoic formations are of particular interest to this investigation because they are the principal strata in the Meade thrust allochthon.

The upper Paleozoic formations are, in ascending order, the Lodgepole, Monroe Canyon, Wells, Park City, and

Phosphoria. These formations have an aggregate maximum thickness of 1950 m. The Lodgepole, Monroe Canyon, and Wells formations predominantly include carbonate and sandy strata which have an aggregate maximum thickness of 1780 m. The Park City Formation is represented by the 25 m thick Grandeur Tongue. The Grandeur Tongue is composed of dolomite and is generally mapped as the uppermost part of the Wells Formation. The Phosphoria Formation has a maximum aggregate thickness of 145 m. This formation is one of the most significant hydrostratigraphic units in the study because it contains siliceous mudstones, cherts and phosphatic rocks which have hydraulic conductivities significantly less than the underlying and overlying strata. The Phosphoria Formation forms a hydrologic boundary between the aquifers above and below. This formation is mined for phosphate.

The lower Mesozoic formations which crop out in the allochthon are, in ascending order, the Dinwoody and Thaynes. These formations have a maximum aggregate thickness of 1675 m and have been subdivided into several members. The formations consist of carbonate and sandy, shaly strata which are generally less massively bedded than the strata of the upper Paleozoic formations.

Extensive geological mapping has been undertaken in the study area and adjacent areas because of the economic importance of the Phosphoria Formation. The stratigraphic nomenclature applied to the area has been continuously evolving since the time of the first geologic mapping in 1912. The only mapping which covered the entire allochthon was completed in 1927. Since 1927 numerous quadrangles have been remapped in greater detail. Some of the formation names have been changed, and members have commonly been named to meet the mapping requirements of a particular quadrangle. A stratigraphic correlation chart of the upper Paleozoic and lower Mesozoic formations mapped in the allochthon is presented by Mayo (1982) as part of this research effort.

Structure of the Allochthon

The Meade thrust allochthon is a body of upper Paleozoic and lower Mesozoic strata which is underlain by the Meade thrust fault. The allochthon is up to 40 km wide in an east-west direction and up to 80 km long in a north-south direction. The major structural features of the allochthon are shown on a generalized geologic map (Figure IV-3) and on two east-west structure sections (Figures IV-4 and IV-5). On the geologic map the rock units are shown as the upper Paleozoic and lower Mesozoic formations, lower plate strata, Pleistocene basalts, and surficial deposits.

The sole of the Meade thrust is thought to be continuous under the allochthon (Mansfield, 1927; Royse and others, 1975). Except for broad warping and a few steeply inclined thrust splays which cut upward from the thrust sole, the sole is generally believed to be flat lying. Structural sections

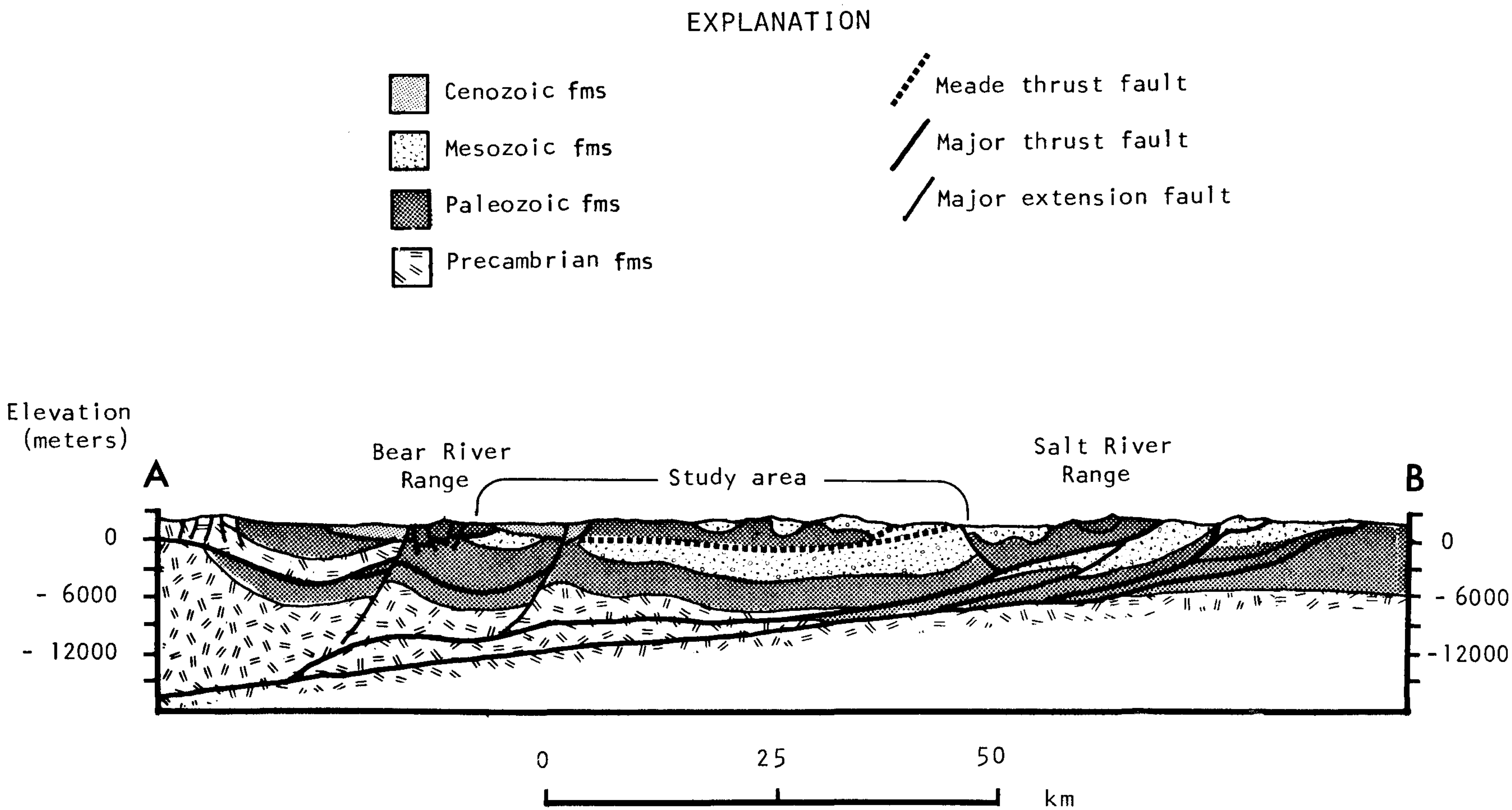

Figure IV-4. Generalized east west structure section through the overthrust belt of southeastern Idaho and western Wyoming. Total shortening (thrust) 50%. Extension faults are post Eocene. Location of the section is shown on figure IV-1. Modified after Royse and others (1975).

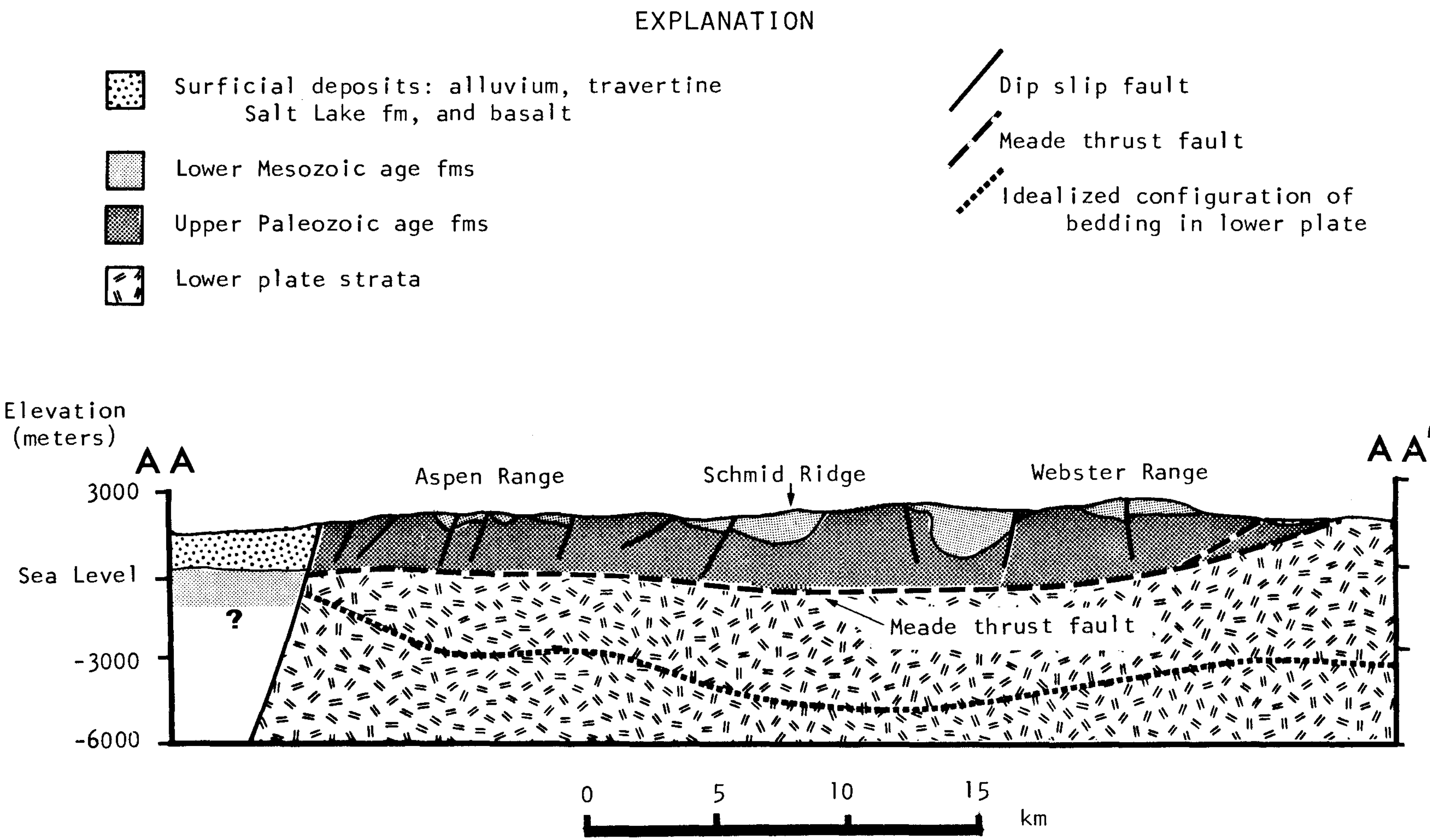

Figure IV-5. Generalized east-west structure section through the Meade thrust area, southeastern Idaho. The section is approximately perpendicular to the trend of the major folds in the allochthon. Location of the section is shown on Plate 1. Modified after Mansfield (1927) and Royse and others (1975).

by Mansfield (1927) and Cressman (1964) show the depth of the thrust sole from 910 to 2200 m below land surface. A more recent structure section by Royse and others (1975) shows the sole at depths ranging from 200 to 3300 m below land surface.

The Meade thrust fault surfaces as a series of steeply inclined thrust splays along the eastern and southern borders of the allochthon. The splays form an arcuate outcrop zone of discontinuous, branching, and subparallel thrust faults (Mansfield, 1927; Cressman, 1964; Conner, 1980; Hatch, 1980; and Jenkins, 1981). The eastern thrust zone is 1.5 to 4.5 km wide and extends southward from Grays Lake for a distance of 70 km along the eastern front of the Webster and Preuss Ranges. Armstrong and Cressman (1963) suggest that the northernmost of these splays may be normal faults.

The western portion of the allochthon is abruptly truncated by a major extension fault zone along the western front of the Aspen Range. The zone is more than 40 km long in a northwesterly direction and forms the border separating the Aspen Range horst to the east from the southern Blackfoot Reservoir and northern Bear River Valley grabens to the west. Armstrong (1969) suggested that there is at least 910 to 1500 m of stratigraphic throw along the frontal fault zone; Mabey and Oriel (1970) identified up to 1500 m of Tertiary sediments in the adjacent grabens.

The northern border of the allochthon is obscured by Tertiary basalt and geologic complexities. Mansfield (1927 and 1952) suggested that the Meade thrust fault extends northward to the Snake River Plain a distance of 110 km from Georgetown, Idaho. Armstrong and Cressman (1963, p. J8) reinterpreted the northern extent of the thrust fault, suggesting

> ...the eastward trending tear faults partially absorbed the movement along the thrust and they probably indicate the northern end of the thrust plate.

This reinterpretation limits the northern border to the vicinity of the Blackfoot Reservoir, a distance of 65 to 80 km from Georgetown. Allmendinger (1981) suggests extension of the Meade thrust to the Snake River Plain.

Normal faults have cut the allochthonous strata in many locations. These faults generally have stratigraphic throws of 200 m or less (Mansfield, 1927; Cressman and Gulbrandsen, 1955; Gulbrandsen and others, 1956; and others). The limited stratigraphic throws suggest the faults are restricted to the allochthonous strata and do not displace lower plate rocks. Strata below the Meade thrust fault are believed to be continuous and nearly horizontal (Cressman, 1964; Royse and others, 1975).

Strata within the allochthon have been folded into broad and open, northerly trending anticlines and synclines. Mansfield (1927), Cressman (1964) and others believe that folding accompanied thrusting; Rioux and others (1975) suggest the folding may have preceeded or accompanied thrusting.

The anticlines and synclines have been eroded into a ridge and valley system whose narrow, linear features dominate the topography of the allochthon's interior. Inverted relief is common in the ridges and valleys; anticlines have been eroded into valleys, and synclines have been eroded into ridges. These valleys and ridges share the names of the folds. The ridge and valley system extends almost the entire length and width of the allochthon, the longest ridge being 35 km long, 4 km wide and rising 460 m above its adjacent valley floor. Shallow seated extension faults commonly parallel the fold axes.

The Aspen and Webster Ranges are the western and eastern ranges of the allochthon, respectively. The ranges have intermontane valleys which have less relief than the valleys in the Ridge and Valley system. In the Aspen Range, extension faults having limited displacement have cut the folded strata into blocks. These faults generally parallel the fold axes. The Webster syncline and Boulder Creek anticline are the major structural features of the Webster Range. The two folds continue almost uninterrupted along the 50 km length of the Webster Range.

Physical and Chemical Characteristics of Springs and Wells

Overview

Water quality samples were collected from thirty-eight springs and three wells to determine the physical and chemical characteristics of representative discharge waters (Figure IV-6). Twenty-five of the springs and two flowing artesian wells issue from the peripheral region of the Meade thrust allochthon. The remaining well and springs issue from the interior of the allochthon. The periphery springs appear to flow from splays of the Meade thrust fault or from extension faults which intersect the thrust fault and are generally associated with the upper Paleozoic formations. The discharge locations of interior springs are generally not controlled by major faults. These springs are generally associated with the lower Mesozoic formations.

Within the two broad categories, periphery and interior, the springs have been organized into groups and subgroups on the basis of their geologic and physiographic characteristics. The wells have been included in the groups which are located closest to each well. The organizational structure is:

- Periphery Groups
    * Extension Fault Groups
        - Corral Creek
        - Western Frontal Fault Group

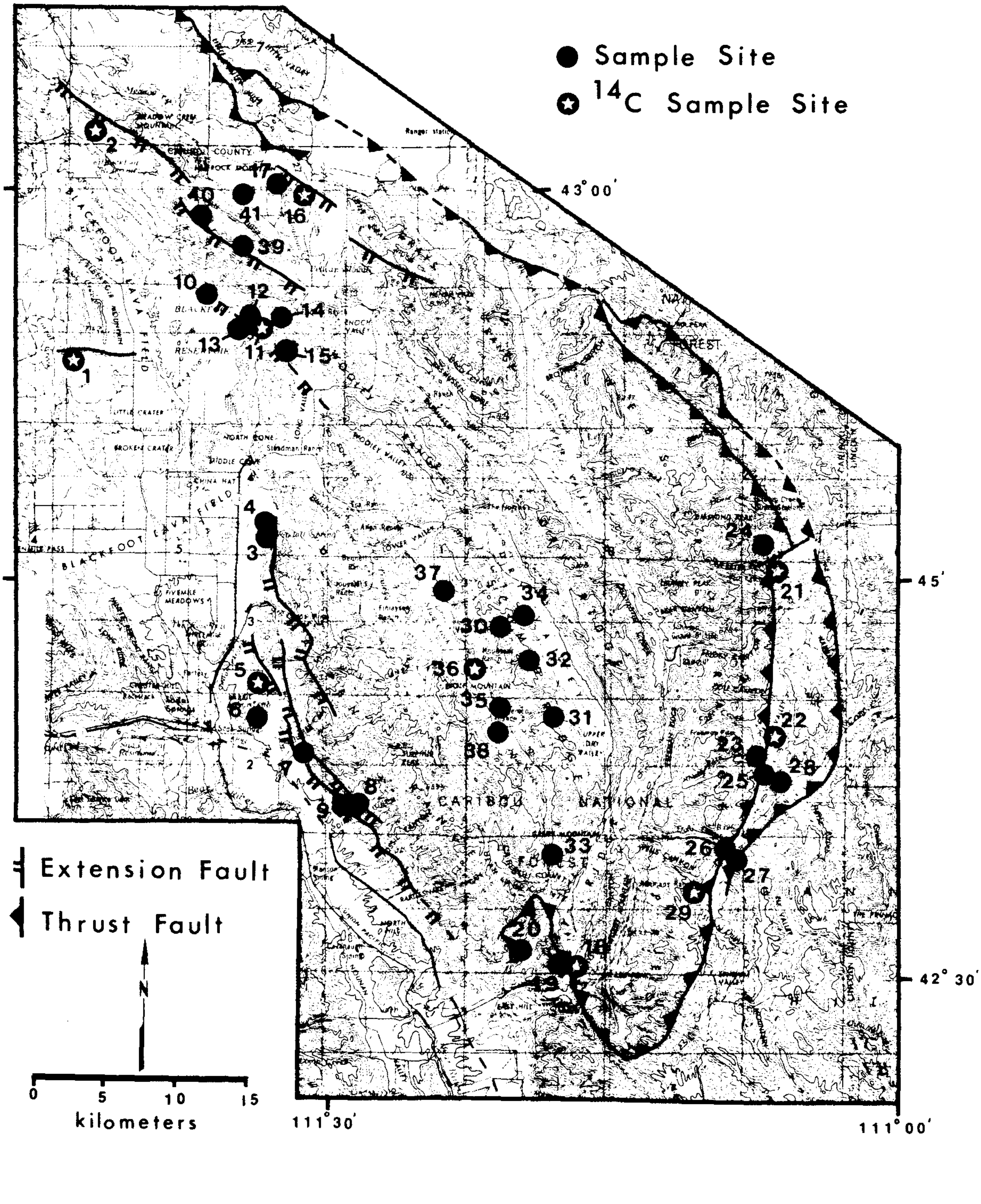

Figure IV-6. Location of water quality sampling sites in the Meade thrust area, southeastern Idaho.

- Henry Group
- Chubb Group

* Thrust Fault Splay Groups

- Georgetown Canyon Group
- Eastern Thrust Zone Group

- Interior Groups

* Dry Valley-Schmid Ridge-Slug Creek Group

* Pelican Ridge Group

Water samples from the forty-one sites were analyzed for the ions Ca^{2+}, Na^{+}, K^{+}, HCO_3^{-}, Cl^{-}, SO_4^{2-}, and F^{-}, SiO_2 and the stable isotopes D and ^{18}O. Samples from ten sites were analyzed for ^{13}C and ^{14}C. Results of the chemical analysis are listed in Table IV-1. Discharge measurements were taken at each site, and the stratigraphic and structural relationships of each site were obtained from the geologic literature. Table IV-2 is a summary of discharge magnitude, elevation, and major geologic features of each location.

Description of Springs and Wells

The general characteristics of the springs and wells are described below. One or more geologic sections which typify the discharge area of each group are included. The locations of the structure sections are shown on the generalized geologic map (Figure IV-3) and the locations of the springs and wells are shown in Figure IV-6.

Periphery Extension Fault Groups

Corral Creek (1). From 1966 to 1970 the FMC corporation drilled several dozen phosphate exploration boreholes along

Table IV-1. Chemical analysis of spring and well waters collected in the Meade thrust area, southeastern Idaho.[1]

Sample Number	Name and Location	Water Temp. °C	Specific Conductance (μmho/cm)	Total Dissolved Solids (mg/l)	pH	Concentration in mg/l (meq/l) Ca^{2+}	Mg^{2+}	Na^{+}	K^{+}	Cl^{-}	F^{-}	HCO_3^{-}	SO_4^{2-}	SiO_2
1	Corral Creek 6S 41E 19bbd	39.9	---	5369	6.6	900 (44.9)	275 (22.6)	88.5 (3.8)	250 (6.4)	38.7 (1.1)	1.9 (0.10)	2831 (46.4)	900.4 (18.7)	83
2	Sinkhole 4S 41E 32bbS	19	---	804	6.8	147 (7.3)	29 (2.4)	27 (1.2)	3 (0.1)	29 (0.8)	0.6 (0.03)	504 (8.3)	33 (0.7)	31
3	Woodall 7S 42E 34baS	13	1040	1137	6.6	232 (11.6)	35 (2.9)	1 (0.04)	0.3 (0.01)	2 (0.1)	0.4 (0.02)	790 (12.9)	37 (0.8)	39
4	North Woodall 7S 42E 27acS	17	1640	1701	6.3	382 (19.1)	49 (4.0)	4 (0.2)	1 (0.03)	3 (0.1)	1.0 (0.05)	1182 (19.4)	48 (1.0)	31
5	Formation 8S 42E 27cbS	11	920	931	6.6	190 (9.5)	29 (2.4)	0.4 (0.02)	1 (0.03)	6 (0.2)	0.3 (0.02)	622 (10.2)	57 (1.2)	25
6	East Soda 9S 42E 10acS	9	775	725	7	124 (6.2)	31 (2.6)	2 (0.1)	1 (0.03)	4 (0.1)	0.2 (0.01)	513 (8.4)	35 (0.7)	15
7	Sulphur Canyon 9S 42E 13bc	10	660	607	7.2	121 (6.0)	20 (1.6)	2 (0.1)	1 (0.03)	4 (0.1)	0.2 (0.01)	438 (7.2)	10 (0.2)	11
8	Swan Lake #1 (Lakey Res.) 9S 43E 30ccS	16	1020	1089	6.7	220 (11.0)	36 (3.0)	3 (0.1)	0.3 (0.01)	3 (0.1)	0.2 (0.01)	751 (12.3)	57 (1.2)	19
9	Swan Lake #2 9S 43E 30ccS	9	850	881	7.1	158 (7.9)	36 (3.0)	3 (0.1)	0 (0)	4 (0.1)	0.1 (0.01)	604 (9.9)	52 (1.1)	24
10	Lone Tree 6S 42E 6abS	26	1570	1506	6.4	314 (15.7)	39 (3.2)	26 (1.1)	18 (0.5)	26 (0.7)	1.7 (0.09)	989 (16.2)	75 (1.6)	17
11	Henry Warm #1 6S 42E 9acS	15	970	934	6.8	178 (8.9)	34 (2.8)	16 (0.7)	2 (0.05)	15 (0.4)	0.5 (0.03)	624 (10.2)	46 (1.0)	18
12	Henry Warm #2 6S 42E 9bcS	20	1410	1449	6.3	284 (14.2)	44 (3.6)	25 (1.1)	8 (0.2)	32 (0.9)	1.0 (0.05)	870 (14.3)	145 (3.0)	40
13	Warm Spring 6S 42E 81dbS	23	1510	1485	6.3	277 (13.8)	47 (3.9)	22 (1.0)	14 (0.4)	20 (0.6)	1.7 (0.09)	994 (16.3)	84 (1.7)	25
14	North Henry 6S 42E 10bcS	15	870	792	6.8	129 (6.4)	31 (2.6)	11 (0.5)	2 (0.05)	11 (0.3)	0.5 (0.03)	566 (9.3)	26 (0.5)	15
15	Little Blackfoot River 6S 42E 15baS	15	940	983	6.7	200 (10.0)	33 (2.7)	11 (0.5)	2 (0.05)	13 (0.4)	0.5 (0.03)	674 (11.0)	42 (0.9)	7
16	Chubb 5S 42E 11ccS	12	545	458	7.5	61 (3.0)	20 (1.6)	24 (1.0)	2 (0.05)	26 (0.7)	0.3 (0.02)	240 (3.9)	61 (1.3)	24

Table IV-1. Continued.

Sample Number	Name and Location	Water Temp. °C	Specific Conductance (μmho/cm)	Total Dissolved Solids (mg/l)	pH	Concentration in mg/l (meq/l)								
						Ca^{2+}	Mg^{2+}	Na^{+}	K^{+}	Cl^{-}	F^{-}	HCO_3^{-}	SO_4^{2-}	SiO_2
17	West Chubb 5S 42E 10daS	12	510	447	7.3	62 (3.1)	19 (1.6)	20 (0.9)	1 (0.03)	21 (0.6)	0.3 (0.02)	234 (3.8)	65 (1.4)	25
18	Georgetown Canyon 10S 44E 35dcS	7	---	361	7.4	63 (3.1)	15 (1.2)	trace (0)	0.5 (0.01)	0 (0)	0.1 (0.01)	195 (3.2)	69 (1.4)	18
19	Georgetown Canyon Tailings 10S 45E 35cdS	8	350	335	7.5	64 (3.2)	16 (1.3)	trace (0)	0.5 (0.01)	0 (0)	0.2 (0.01)	250 (4.1)	2 (0.09)	2
20	Big Spring 10S 44E 28ccS	8	505	465	7.3	90 (4.5)	16 (1.3)	trace (0)	0 (0)	2 (0.1)	0.1 (0.01)	244 (4.0)	96 (2.0)	17
21	Auburn Fish Hatchery 8S 46E 5baS	9	440	368	7.5	58 (3.9)	21 (1.7)	6 (0.3)	1 (0.03)	2 (0.1)	0.1 (0.01)	232 (3.8)	16 (0.3)	32
22	Sage Valley 9S 46E 18adS	12	460	397	7.5	64 (3.2)	21 (1.7)	6 (0.3)	0 (0)	7 (0.2)	0.4 (0.02)	232 (3.8)	38 (0.8)	29
23	South Fork 9S 46E 18daS	12	400	353	7.4	54 (2.7)	21 (1.7)	4 (0.2)	0.5 (0.01)	10 (0.3)	0.3 (0.02)	236 (3.9)	0 (0)	27
24	Star Valley Hatchery 7S 46E 32bdS	9	590	347	7.7	54 (2.7)	17 (1.4)	2 (0.1)	0.5 (0.01)	4 (0.1)	0.2 (0.01)	231 (3.8)	15 (0.3)	23
25	Fence Line 9S 46E 19adS	10	410	458	7.1	60 (3.0)	17 (1.4)	3 (0.1)	0.5 (0.01)	4 (0.1)	0.2 (0.01)	249 (4.1)	88 (1.8)	36
26	Brooks Spring 10S 45E 1daS	12	425	396	7.5	58 (2.9)	16 (1.3)	20 (0.9)	0 (0)	27 (0.8)	0.4 (0.02)	233 (3.8)	7 (0.7)	35
27	New Salt 10S 45E 1daS	11	1150	906	7.4	144 (7.2)	29 (2.4)	82 (3.6)	2 (0.05)	87 (2.5)	0.3 (0.02)	277 (4.5)	241 (5.1)	44
28	Nuggett 9S 46E 20caS	10	---	427	7.4	68 (3.4)	24 (2.0)	7 (0.3)	0 (0)	5 (0.1)	0.2 (0.01)	256 (4.2)	37 (0.8)	30
29	Crow Creek Ranch 10S 45E 15acS	7	360	338	7.4	59 (2.9)	14 (1.2)	2 (0.1)	0.5 (0.01)	2 (0.1)	0.1 (0.01)	226 (3.7)	22 (0.5)	12
30	Slump Spring 8S 44E 17ddS	5	460	413	7.1	82 (4.1)	13 (1.1)	6 (0.3)	0 (0)	12 (0.3)	0.1 (0.01)	262 (4.3)	19 (0.4)	19
31	Lower Lone Tree 8S 44E 28bbS	8	440	433	7.2	90 (4.5)	11 (0.9)	3 (0.1)	0.8 (0.02)	3 (0.1)	0.1 (0.01)	269 (4.4)	26 (0.5)	30
32	Lower Young Ranch 8S 44E 21acS	4	500	490	7	108 (5.4)	10 (0.8)	1 (0.04)	0.5 (0.01)	10 (0.3)	0 (0)	312 (5.1)	19 (0.4)	29

Table IV-1. Continued.

Sample Number	Name and Location	Water Temp. °C	Specific Conductance (µmho/cm)	Total Dissolved Solids (mg/l)	pH	Concentration in mg/l (meq/l) Ca^{2+}	Mg^{2+}	Na^{+}	K^{+}	Cl^{-}	F^{-}	HCO_3^{-}	SO_4^{2-}	SiO_2
33	Cold Spring 10S 44E 3ddS	4	---	385	7.5	74 (3.7)	5 (0.4)	4 (0.2)	4 (0.1)	0 (0)	0.3 (0.02)	238 (3.9)	14 (0.3)	46
34	FMC 8S 44E 15bd	8	430	372	7.4	51 (2.5)	18 (1.5)	3 (0.1)	0.8 (0.02)	3 (0.1)	0.1 (0.01)	257 (4.2)	18 (0.4)	21
35	Square Pond 9S 44E 5ddS	8	390	330	7.3	55 (2.7)	12 (1.0)	6 (0.3)	0.8 (0.02)	4 (0.1)	0.1 (0.01)	224 (3.7)	8 (0.2)	20
36	Kundsen Ranch 8S 44E 30dbS	12	360	367	7.5	63 (3.1)	15 (1.2)	8 (0.3)	2 (0.05)	5 (0.1)	trace (0)	238 (3.9)	17 (0.4)	19
37	Purple Spring 8S 43E 11cdS	11	440	376	7.3	50 (2.5)	21 (1.7)	7 (0.3)	2 (0.05)	4 (0.1)	0.2 (0.01)	254 (4.2)	21 (0.4)	17
38	Peterson Ranch 9S 44E 5cdS	8	320	187	6.4	8 (0.4)	7 (0.6)	14 (0.6)	18 (0.5)	9 (0.3)	0.2 (0.01)	89 (1.5)	11 (0.2)	31
39	Pelican Ridge #1 5S 42E 391dcS	7	465	440	7.2	70 (3.5)	19 (1.6)	4 (0.2)	1 (0.03)	6 (0.2)	trace (0)	294 (4.8)	17 (0.4)	29
40	Pelican Ridge #2 5S 42E 24dcS	7	540	489	7.2	77 (3.8)	23 (1.9)	3 (0.1)	1 (0.01)	8 (0.2)	0.1 (0.01)	325 (5.3)	34 (0.7)	18
41	North Pelican 5S 42E 17bcS	8	290	252	7.5	50 (2.5)	7 (0.6)	2 (0.1)	0.2 (0.01)	3 (0.1)	trace (0)	170 (2.8)	6 (0.1)	14

[1] Chemical samples collected during the summer of 1980.

Table IV-2. Physical settings of springs and wells in the Meade thrust area, southeastern Idaho.[2]

Sample Number	Name and Location	Water Temp. (°C)	Elevation (m above MSL)	Well Depth (m)	Depth to Water (m)	Discharge (l/s)	Site Description
1	Corral Creek 6S 41E 19bbd	39.9	1885		flowing	5	Artesian flow from phosphate test holes.
2	Sinkhole 4S 41E 32bbS	19	1890			292	Flows from Wells formation along the Enoch Valley fault.
3	Woodall 7S 42E 34baS	13	1900			365	Flows up an unnamed extension fault along the fault of the northern Aspen Range. Associated with Wells formation.
4	North Woodall 7S 42E 27acS	17	1900			28	Flows up an unnamed extension fault along the fault of the northern Aspen Range. Associated with Wells formation.
5	Formation 8S 42E 27cbS	11	1875			488	Flows up an unnamed extension fault along the fault of the northern Aspen Range. Associated with Wells formation.
6	East Soda 9S 42E 10acS	9	1840			85	Associated with Salt Lake formation; several extension faults have been mapped in the area.
7	Sulphur Canyon 9S 42E 13bc	10	1870	unknown	unknown	9	Artesian flow from Wells (?) formation in an area along the front of the Aspen Range which is bounded by extension faults.
8	Swan Lake #1 9S 43E 29ccS	16	1890			85	Flows from Wells formation along front of Aspen Range in an area of extension faulting.
9	Swan Lake #2 9S 43E 30ccS	9	1840			14	Flows from Wells formation along front of Aspen Range in an area of extension faulting.
10	Lone Tree 6S 42E 6abS	26	1870			3	Flows up the Slug Valley (?) fault.
11	Henry Warm #1 6S 42E 9acS	15	1867			88	Discharges on the Henry travertine terrace which conceals the intersection of the Henry and Slug Valley faults.
12	Henry Warm #2 6S 42E 9bcs	20	1870			55	Discharges on the Henry travertine terrace which conceals the intersection of the Henry and Slug Valley faults
13	Warm Spring 6S 42E 8dbS	23	1880			14	Discharges on the Henry travertine terrace which conceals the intersection of the Henry and Slug Valley faults

Table IV-2. Continued.

Sample Number	Name and Location	Water Temp. (°C)	Elevation (m above MSL)	Well Depth (m)	Depth to Water (m)	Discharge (l/s)	Site Description
14	North Henry 6S 42E 10bcS	15	1883			57	Discharges on the Henry travertine terrace which conceals the intersection of the Henry and Slug Valley faults.
15	Little Blackfoot River 6S 42 15baS	15	1880			7	Discharges from Wells formation along axis of Wooley Valley anticline.
16	Chubb 5S 42E 11ccS	12	1905			45	Flows from Monroe Canyon limestone along the Chubb springs fault.
17	West Chubb 5S 42E 10daS	12	1905			85	Flows from Monroe Canyon limestone along the Chubb springs fault.
18	Georgetown Canyon 10S 44E 35dcS	7	1997			408	Flows from the Wells formation along a splay of the Meade thrust.
19	Georgetown Canyon Tailings 10S 44E 35cdS	8	1997			448	Flows from the Wells formation along a splay of the Meade thrust.
20	Big Spring 10S 44E 28ccS	8	1970			60	Flows from a normal fault which cuts the Dairy Syncline and the Wells formation
21	Auburn Fish Hatchery 8S 46E 5baS	9	1980			142	Flows from Meade thrust and the Thaynes formation.
22	Sage Valley 9S 46E 18adS	12	2270			246	Flows from the Meade thrust and Wells (?) formation.
23	South Fork 9S 46E 18daS	12	2270			100	Flows from the Meade thrust and Wells (?) formation.
24	Star Valley Hatchery 7S 46E 32bdS	9	1975			100	Flows from contact of Portneuf (?) member and Timothy sandstone (?) member of Thaynes formation.
25	Fence Line 9S 46E 19adS	10	2120			25	Flows from the Meade thrust and Wells (?) formation.
26	Brooks Spring 10S 45E 1daS	12	2009			99	Flows from a splay of the Meade thrust (?) and the Wells (?) formation.
27	New Salt 10S 45E 1daS	11	2060			15	Flows from Twin Creek limestone.

Table IV-2. Continued.

Sample Number	Name and Location	Water Temp. (°C)	Elevation (m above MSL)	Well Depth (m)	Depth to Water (m)	Discharge (1/s)	Site Description
28	Nuggett 9S 45E 1daS	10	2090			15	Flows from slice of Nuggett sandstone near the Meade thrust.
29	Crow Creek Ranch 10S 45E 15acS	7	2048			161	Flows from the Wells formation at the contact with Monroe Canyon limestone.
30	Slump Spring 8S 44E 17ddS	5	2080			6	Flows from Thaynes formation along Schmid Syncline.
31	Lower Lone Tree 8S 44E 28bbS	8	2065			6	Flows from Thaynes formation along Schmid Syncline.
32	Lower Young Ranch 8S 44E 21acS	4	2080			17	Flows from Thaynes formation along Schmid Syncline.
33	Cold Spring 10S 44E 3ddS	4	2095			3	Flows from Wells formation along Schmid Syncline.
34	FMC 8S 44E 16bd	8	2000	435			Well penetrates only the Wells formation.
35	Square Pond 9S 44E 5ddS	8	1955			190	Flows from Dinwoody formation along Schmid Syncline.
36	Knudsen Ranch 8S 44E 30dbS	12	1940			100	Flows from Dinwoody formation along Schmid Syncline.
37	Purple Spring 8S 43E 11cdS	11	1935			35	Flows from Wells formation along Schmid Syncline.
38	Peterson Ranch 9S 44E 5cd	8	1955	unknown			Well in shallow alluvium in Slug Creek Valley.
39	Pelican Ridge #1 5S 42E 39dcS	7	1920			9	Flows from a fault bounded slice of the Dinwoody formation.
40	Pelican Ridge #2 5S 42E 24dcS	7	1985			3	Flows from a fault bounded slice of the Dinwoody formation.
41	North Pelican 5S 42E 17bcS	8	1915			14	Flows from Dinwoody formation in the Meadow Creek graben.

[2] Data collected during the summers of 1979 and 1980.

the western edge of Reservoir Mountain west of the Blackfoot Reservoir (Mitchell, 1976) (Figure IV-6). Drilling penetrated the phosphate ore bearing Meade Peak Member of the Phosphoria Formation and terminated in the upper portion of the Wells Formation. A generalized north-south structure section through the Corral Creek area is shown in Figure.IV-7.

The boreholes were drilled through older travertine deposits and many encountered warm water and artesian conditions. J. Spalding (oral communication, 1981) reported that warm water and gas (99% CO_2) were encountered in the Meade Peak Member of the Phosphoria Formation, and the warm water was found only in boreholes in an area of a few hectares. The nearby Pelican fault is the likely avenue for the upward movement of the warm water. The water probably moves laterally into the Wells Formation.

One flowing well (FMC 166), known in this report as Corral Creek (1), was sampled. The well was discharging about l l/s, depositing travertine, and evolving copious amounts of CO_2 gas. X-ray diffraction analysis of the layered travertine near the flowing well and from a nearby pond indicated the new deposits are virtually pure calcite.

Western Frontal Fault Group (2-9). Eight springs along the western periphery of the Meade thrust allochthon have been placed into this group (Figure IV-6). The springs issue from deep seated extension faults which form the boundary

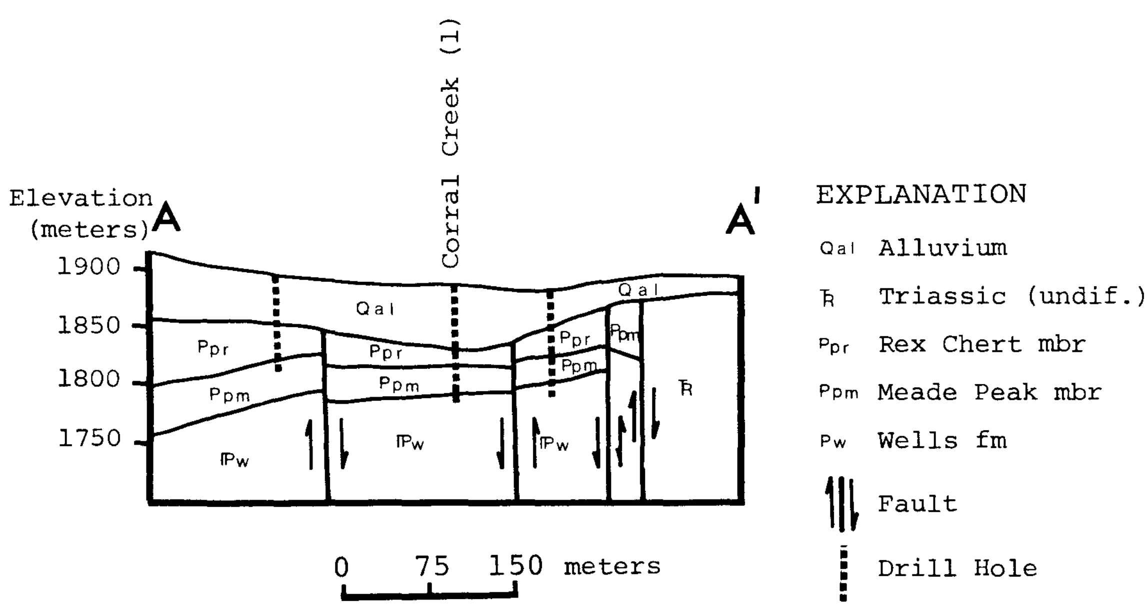

Figure IV-7. North-south structure section through the Corral Creek area, southeastern Idaho. Courtesy of FMC Natural Resources Department, Denver, Colorado.

between the allochthon and the grabens to the west. One spring, Sinkhole (2), issues from the Enoch Valley fault at the base of Wilson Ridge. The Enoch Valley fault, along which Wilson and Pelican Ridges have been uplifted, forms the northeastern boundary of the Blackfoot Reservoir graben.

The remaining seven springs (3-9) of this group issue from steeply westward dipping frontal extension faults of the Aspen Range. The frontal faults separate the Aspen Range from the southern portion of the Blackfoot Reservoir graben and the northern portion of the Bear River Valley graben.

All of the springs in this group are either actively depositing or have deposited large travertine terraces covering hundreds to thousands of hectares each. Several large travertine deposits not assoicated with active springs are located along the front of the Aspen Range. These deposits indicate spring migration along the frontal fault zone. In all, the frontal fault travertine terraces extend for more than 50 km along the base of the Aspen Range, covering 4320 hetares. The maximum thickness of the travertine deposits is not known; more than 25 m of travertine may be seen in a collapse structure in the Swan Lake terrace.

Sinkhole spring (2), located at the base of Wilson Ridge, is named in this report after a large sinkhole which formed 120 m from the spring on the lower slope of Wilson

Ridge. The circular, vertical walled sink resulted from the collapse of solution cavities in the steeply inclined Wells Formation. The topographic map of the area, made in 1917, does not show the sinkhole, nor does Mansfield's 1927 work mention it. An examination of oblique aerial photographs of the area suggests the main sink is in the hub of an area, perhaps 750 to 1000 m across, undergoing subsidence. A reconnaissance of the area suggests the solution weathering is a continuing phenomenon.

Waters from Sinkhole spring have precipitated an extensive travertine terrace on the Cenozoic basalt flows of the Blackfoot lava field which abut the base of Wilson Ridge (Figure IV-8a). Approximately 450 hectares of the terrace are visible, and an additional 80 to 160 hectares have been inundated by the waters of Blackfoot Reservoir. The spring currently issues midway along the 2.5 km long travertine front at the base of Wilson Ridge. Ground water flow appears to move along the Enoch Valley fault. Flow emerges from three closely spaced orifices at the base of the ridge and from four to five holes in the bottom of a several hundred meter diameter pool which has formed on the terrace about 9 m from the ridge base. Measured discharge was 292 l/s; an estimated 30 to 100 l/s could not be measured.

Woodall (3) and North Woodall (4) springs issue along the frontal extension fault zone at the base of the northern Aspen Range. A minimum of 640 m of displacement between the

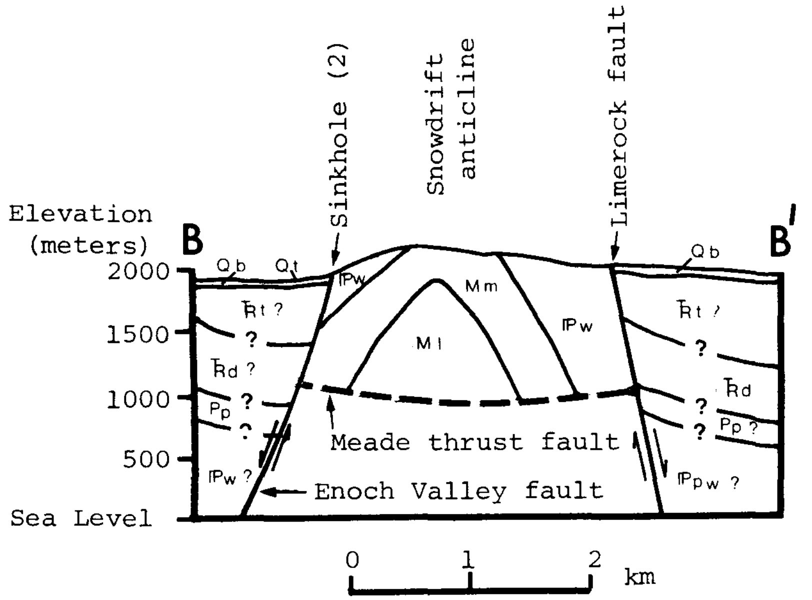

EXPLANATION

Qal Alluvium

Qt Travertine

Qb Basalt

Tsl Salt Lake fm

Ȓt Thaynes fm

Ȓd Dinwoody fm

Pp Phosphoria fm

IPw Wells fm

Mm Monroe Canyon fm

Ml Lodgepole fm

Fault

(2) Spring

Figure IV-8a. North-south structure section through Sinkhole spring (2) area. Modified after Mansfield (1927).

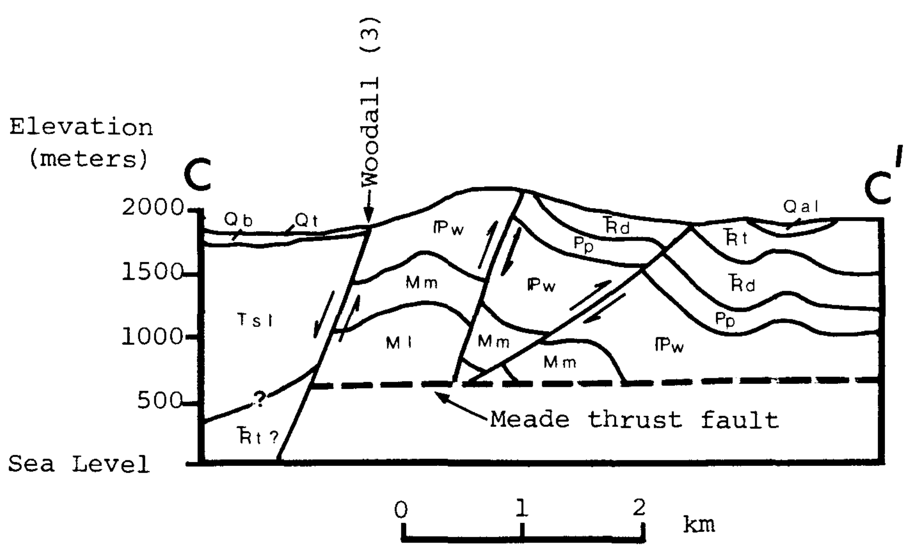

Figure IV-8b. East-west structure section through Woodall spring (3) area. Modified after Mansfield (1927).

Aspen Range horst and the Blackfoot Reservoir graben is indicated by Mansfield (1927) in a structure section covering the area just south of the springs. Greater displacement along the frontal fault zone is suggested by Mabey and Oriel (1970), who identified a major gravity low centered about 8 km northwest of the springs. They suggest as much as 1500 m of Tertiary strata and overlying basaltic lava flows would account for the gravity low.

The structural and stratigraphic relationships at the springs are typical of those along the Aspen Range front: the upper Paleozoic formations in the uplifted block and the upper Paleozoic and lower Mesozoic formations in the downdropped graben. Surficial deposits of Cenozoic age cover most of the graben (Figure IV-8b).

Active travertine deposition apears to be occurring from the Woodall springs. The springs are located in the southern portion of a 950 hectare, 16 km long travertine terrace which abuts the base of the Aspen Range. Woodall spring (3) issues from the bottom of a .6 to 1.6 m deep, one hectare pond. Water samples were taken at the north end of the pond where gas, presumably CO_2, was actively evolving. North Woodall spring (4) issues from a 1.5 m diameter pool, about 1.5 km north of Woodall spring. North Woodall is located in an area containing numerous inactive travertine ledges, pool structures, and minor seeps. Both springs discharge from the upland area of the terrace where it abuts the Aspen Range. A discharge of 365 l/s was measured for Woodall in two irrigation diversion ditches which flow from the pond. Discharge from north Woodall was estimated to be 30 l/s. Total discharge from the Woodall terrace may be two to three times the measured discharge, based on an airplane reconnaissance of the area. In 1923, the total discharge from the pond at Woodall was approximately 700 l/s (Mansfield, 1927). Damming of the pond for agricultural diversions since 1923 may have raised the pond level, inducing leakage from the travertine bottom of the pond.

Formation spring (5), located at the base of the Aspen Range 6.5 km northeast of the town of Soda Springs, is one of the major sources of water for that community as well as for irrigation for several local ranchers. The spring, which issues from the frontal fault zone, forms a small stream having a nearly constant flow of 680 to 710 l/s. Mansfield (1927) reported that similar discharges were measured several times during 1923. Rocks of the Wells Formation have been elevated at least 1000 m above similar rocks in the adjacent graben along the frontal fault zone. Surficial rocks covering the Paleozoic and Mesozoic rocks in the graben are Cenozoic basaltic lavas and travertine. Figure IV-9 is an east-west structure section through the spring area.

Formation spring is associated with a 515 hectare travertine terrace, although the spring does not currently

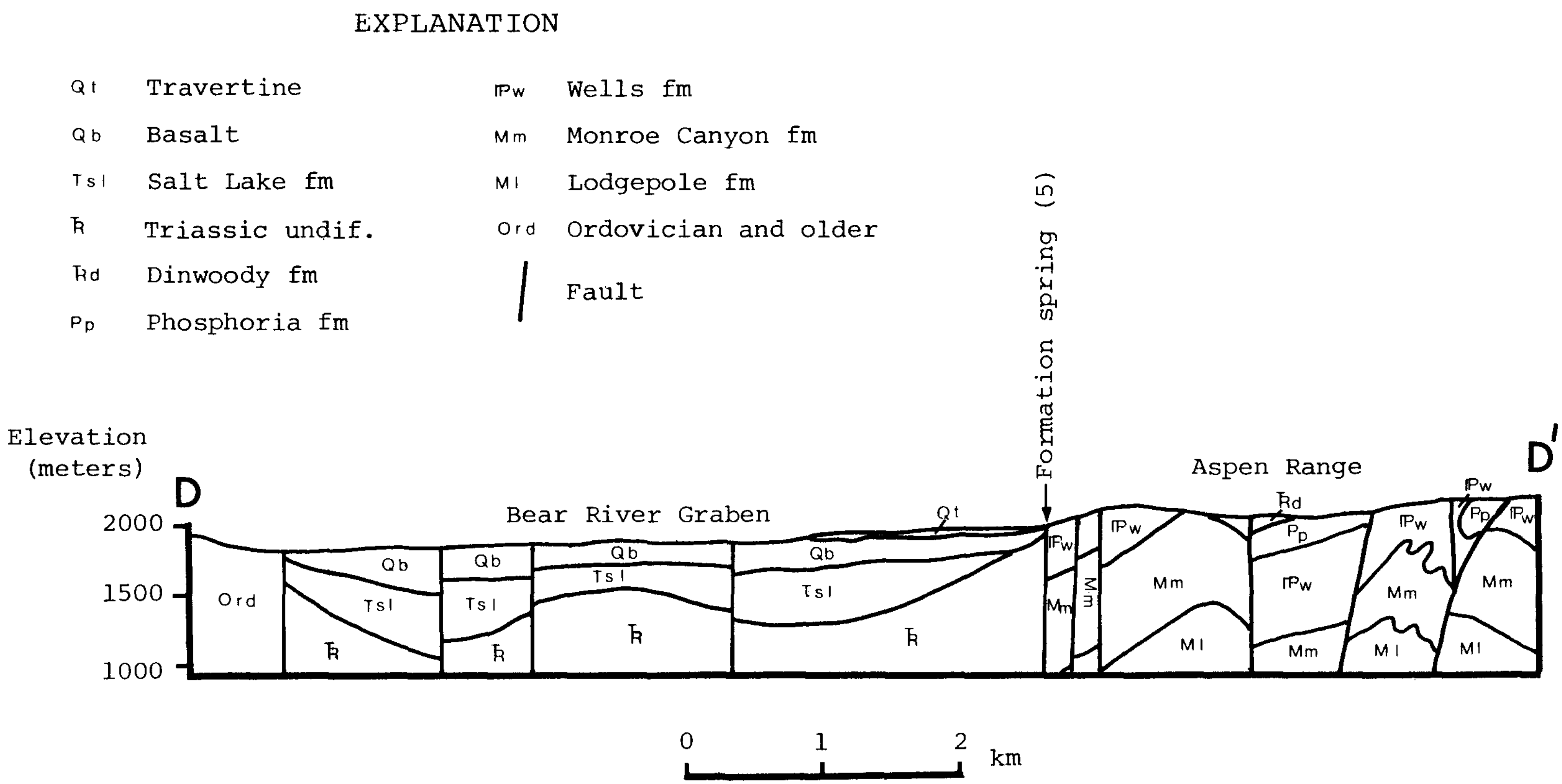

Figure IV-9. East-west structure section through Formation spring (5), Aspen Range, and Bear River graben, southeastern Idaho. Modified after Arstrong (1969).

appear to be depositing travertine. Numerous well preserved travertine ledges and associated pool structures occurring in the area suggest that travertine deposition occurred in the not too distant past. Many of the structures appear to be so fresh that the early settlers called them formation rock and named the spring after them.

East Soda spring (6) is located east of Soda Springs in the travertine belt along the front of the Aspen Range. The spring is actually several seepage areas in a one hectare wet land at the head of a small draw cut into low hills of Tertiary Salt Lake Formation near the base of the Aspen Range. A 300 hectare older travertine terrace, partially covered by more recent alluvium and soil, is present about 200 m to the south. The deposit may extend to the spring area; however, the alluvial cover obscures this relationship. Armstrong (1969) suggests that a trace of frontal fault may be concealed by the surficial deposits near the spring area. Mabey and Oriel (1970) have identified a gravity low whose border is coincident with the spring area. The gravity low further suggests the existence of a buried frontal fault as the spring source.

The springs of Sulphur Canyon (7) are bounded to the east and west by two frontal faults of the Aspen Range (Armstrong, 1969). The springs were investigated by Peale (1872), Richards and Bridges (1911), and Mansfield (1927);

they are, for the most part, small, milky, cloudy pools of cool water which emit large volumes of CO_2 and hydrogen sulphide gas. Gas also emanates from dry vents in surficial gravel deposits. In some locations sulfur has been deposited in the interstices of the gravels and in nearby deposits of the Salt Lake Formation. Only small quantities of water discharge from the pools.

The floor of Sulphur Canyon is underlain by travertine which has been partially covered by more recent alluvium. This travertine forms the northwestern border of the most areally extensive terrace in the study area. In all, the terrace covers 2000 hectares and extends to the south for 10 km. Formation of the terrace is most likely the result of numerous now inactive springs. Geologic mapping by Cressman (1964) and Armstrong (1969) and gravity work by Mabey and Oriel (1970) suggest more than 1500 m of vertical displacement along the frontal faults of the Aspen Range in the area covered by the terrace. Rocks in the Aspen Range horst are the upper Paleozoic formations. Cenozoic deposits of basaltic lavas, travertine, and alluvium form the surficial deposits of the graben. The Tertiary Salt Lake Formation and Mesozoic formations underlie the surficial graben rocks.

Water samples at Sulphur Canyon were taken from a flowing artesian well in the spring area. Depth of the well is unknown.

Swan Lake #1 (8) and Swan Lake #2 (9) springs issue from a travertine terrace in the bottom of Swan Lake Gulch. The gulch has been cut into the front of the Aspen Range where several faults of the frontal fault zone have been mapped (Cressman, 1964). The stratigraphic sequence in the area is similar to that found elsewhere along the Aspen Range front.

Swan Lake Gulch travertine terrace is part of the 2000 hectare terrace connecting with Sulphur Canyon to the north. Swan Lake spring #1 issues from Upper Swan Lake (Lakey Reservoir) which has formed on travertine deposits. Swan Lake spring #2 issues from the terrace about 1.5 km west and 50 m lower than Upper Swan Lake. Swan Lake spring #2 is not affected by the irrigation diversions from Upper Swan Lake which suggests that the spring is not part of an interterrace flow system.

Henry Group (10-15). Six springs (10-15) in the vicinity of Henry have been placed into this group (Figure IV-6). All of the springs are warm, with water temperatures in the range of 14 to 26°C. Four of the springs issue from a 420 hectare travertine terrace at Henry, one from a 90 hectare terrace 5 km northwest of Henry, and one from a small travertine area along the Little Blackfoot River 1.5 km southeast of Henry.

Surficial Cenozoic deposits and the waters of the Blackfoot Reservoir cover most of the Henry area and obscure bedrock relationships. The springs occur along the northeast border of the Blackfoot Reservoir graben which Mansfield (1927) identified as a modified graben.

Faults mapped by Mansfield (1927) in the spring area include the normal Slug Valley and Pelican faults and the Henry thrust (a minor splay of the Meade thrust). The Pelican fault has been reinterpreted by Armstrong and Cressman (1963) as a tear fault.

Lone Tree (10), associated with a concealed terrace of the Slug Valley fault, is located on a 90 hectare travertine terrace. Water of the Blackfoot Reservoir has inundated the southern portion of the terrace, making determination of its total area impossible. Discharge from a pool that is the main spring discharge point was measured at 3 l/s. Figure IV-10 is a north-south structure section through the spring area.

Water samples were taken from the bottom of the pool in an area evolving gas (presumably CO_2). Active travertine deposition by the spring appeared to be minor (if occurring at all) and only a few small ledges and pool structures, considerably broken down by cattle, were in the area.

Henry Warm #1 (11), Henry Warm #2 (12), and Warm Spring (13) discharge from the 420 hectare travertine terrace at Henry. The terrace overlies a wedge shaped intersection of the Slug Valley and Henry faults. Most of the borders of the terrace are bounded by waters of Blackfoot Reservoir, making an estimate of the terrace's total extent impossible. Two

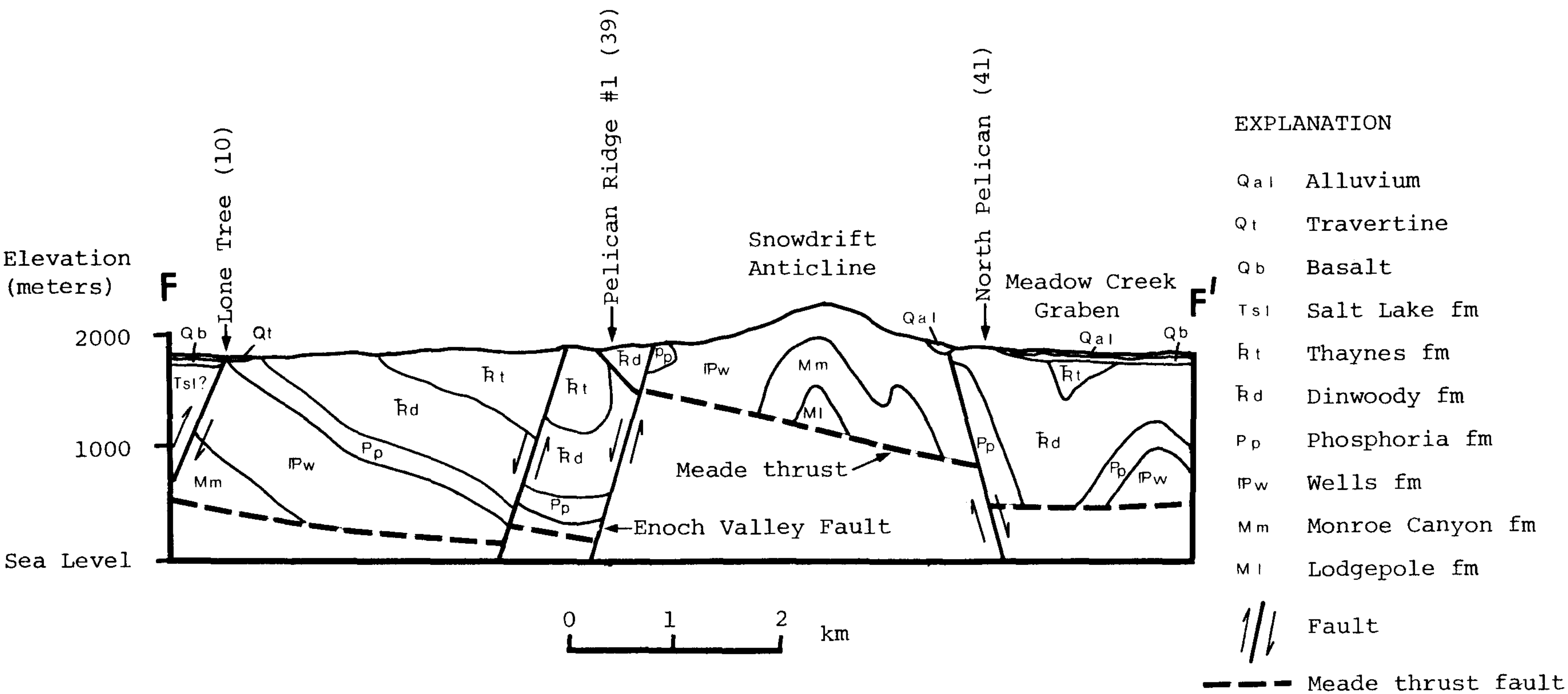

Figure IV-10. North-south structure section through Lone Tree (10), Pelican Ridge #1 (39) and North Pelican (41) springs, southeastern Idaho. Modified after Mansfield (1927).

small exposures of Wells Formation crop out in the "wedge" area.

Henry Warm #1 (11) flows from two small pools about 6 m apart in the northeast portion of the terrace. Active travertine deposition does not appear to be occurring and the pools are evolving some gas (presumbly CO_2). Water samples were collected from the bottom of the larger pool.

Discharge from the two pools flows into a small creek, where the flow was measured as 88 l/s in July, 1979. Visual inspections of the creek flow the following winter and summer suggested that the discharge from the pools remains fairly constant.

Henry Warm #2 (12) is located about 800 m west of Henry Warm #1 (11) in a nearly flat lying, one to two hectare area, which contains numerous travertine cones and small active springs. The cones, many of which stand as much as 2 m high and contain stagnant water in their central craters, were not active springs during Mansfield's (1927) field investigations. Six active springs, all having discharges of 10 l/s or less issue from slightly elevated, irregularly shaped travertine structures which may be the eroded remains of small travertine cones. None of the springs appeared to be depositing travertine and all were evolving CO_2 gas. The spring selected for sampling was the most northwesterly one of the group and was discharging approximately 10 l/s during visits in the winter and summer of 1980.

Warm Spring (13), located about 650 m west of Henry Warm #2 (12), issues from a relatively flat travertine mound of about 15 hectares which has been built on the Henry terrace. The mound rises about 9 m above the terrace and currently issues water from a 2.5 m deep, 6 m wide pool. Approximately 15 l/s was discharging from the pool, and some CO_2 gas was evolving from the bottom. Water samples were collected from the bottom of the pool.

North Henry (14) discharges from a single orifice, located about 150 m north of the Little Blackfoot River, and flows across the northeasterly edge of the Henry terrace. The spring issues from the Wells Formation which abuts the Henry terrace along an extension of the concealed Wooley Valley anticline; it is probably related to the Little Blackfoot River spring (15), although the travertine deposits at this site are connected to the Henry terrace. Active travertine deposition does not appear to be occurring.

Little Blackfoot River spring (15) is one of more than a dozen small springs and seeps which occur along a 1000 m reach of the Little Blackfoot River southeast of Henry. Small travertine ledges crop out along the banks and the bottom of the river. A travertine mound covering a few hectares has also formed on the lava flows south of and adjacent to the river. Most of the observed springs flow near river level along the north bank where the Wells Formation is exposed. Also observed were some springs discharging from the channel's bottom and from the travertine deposits along the south bank and the southern mound. Flow from each spring is generally small, appearing to be less than 8 l/s. In late July, 1980, total spring discharges accounted for approximately 1/3 to 1/2 of the river's estimated 225 to 275 l/s flow. Water samples were collected from one of the larger springs on the north bank.

Chubb Spring Group (16 and 17). Five springs issue along a two mile section of the Chubb Spring fault at the base of Little Gray Ridge (Figure IV-5). Water samples were collected from two sites, Chubb Spring (16) and West Chubb (17), which are located about 800 m apart. All of the springs have discharge temperatures of about 12°C and appear to have fairly constant discharges. Flow at Chubb Spring was measured at 45 l/s, and flow at West Chubb was estimated to be 8 l/s. Several site visits during the summer of 1979 and the following winter and summer indicated no obvious discharge variations.

Four of the springs flow from the Monroe Canyon Formation along the base of Little Gray Ridge, whereas the fifth spring flows from Cenozoic basaltic lava which covers the fault trace of the Chubb Spring fault. No travertine is associated with any of the springs.

Periphery Thrust Fault Splay Groups

Georgetown Canyon Group (18-20). The Georgetown Canyon area is one of the more geologically complex regions of the study area. In simplest terms the geology of the area consists of a series of north-trending anticlines and synclines resting on the sole of the Meade thrust fault (Cressman, 1964). Many of the folds have at least one overturned limb and have axial plane surfaces dipping generally westwards. Because folding was contemporaneous with thrusting, the bedding surfaces of the lowermost formations involved in folding crudely parallel the sole of the thrust sheet. In this area the sole of the thrust is warped into an anticline-shaped flexure. Splays of the thrust fault cut upward from the thrust sole and cut through the folded strata. The splays are closely spaced and their traces generally crop out parallel to the fold axis. Folding of the overthrust sheet was also accompanied by some normal faulting of the folded strata. For the most part, the folds plunge gently, 2° to 3° northward, so that the southerly drainage of the area exposes increasingly older strata to the south.

The folded rocks in the overthrust sheet are the lower Mesozoic and upper Paleozoic formations common throughout the Meade thrust region. The Jurassic Twin Creek Limestone lies nearly horizontally below the overthrust sheet (Cressman, 1964).

Springs in the area issue from faults and appear to be related to the Georgetown and Dairy synclines. Gerogetown Canyon (18) issues from a discontinuous splay of the Meade thrust separating slices of the Wells and Monroe Canyon Formations in the closed end of the Georgetown Canyon syncline. This thrust splay is one of a group of closely spaced splays whose outcrop pattern generally parallels the west limb of the Georgetown syncline and which have as much as 500 m of total stratigraphic throw (Cressman, 1964). The splays turn eastward, cutting across the syncline in the spring area. Georgetown Canyon spring (18) issues from a point in the canyon where Twin Creek crosses the thrust splay.

Georgetown Canyon Tailings (19) issues along the base of an abandoned phosphate mill tailings pile which fills a small tributary canyon. The pile, located between an exposure of the Meade thrust and a splay of the thrust, lies on the Lodgepole Formation.

Water from both springs is cool, 7 to 8°C. Neither spring is associated with travertine deposits, although the small hill through which the Meade thrust passes along the south side of the tailings pile contains a fault breccia zone and some small exposures of travertine not mapped by

Mansfield (1927) or Cressman (1964). Total discharges from Georgetown Canyon (18) and Georgetown Canyon Tailings (19) were measured as 408 and 448 l/s, respectively, in August, 1979, when there was no upstream surface flow in Twin Creek.

Big Spring (20) issues from the left fork of Twin Creek where a normal fault crosses the creek bed. The fault has a stratigraphic throw of about 90 m (Cressman, 1964). Triassic strata of the lower plate crop out north of the fault, and the folded Wells Formation of the upper plate crops out south of the fault. Water from the spring is cool, 8°C, and the spring is not associated with travertine deposits.

Eastern Thrust Zone Group (21-29). The eastern periphery of the Meade thrust allochthon is delineated by an arcuate outcrop zone of splays of the Meade thrust. Nine springs in the central and southern segments of this zone were sampled. Three of the springs issue from thrust splays, and the remaining six issue from slices of strata bounded by thrust splays. All of the springs discharge less than 300 l/s, have cool water and generally are not associated with travertine deposits. Auburn Hatchery (21), Sage Valley (22) and South Fork (23) springs issue from the Sage Valley branch of the Meade thrust. Auburn Hatchery (21) flows from the Thaynes Formation, and Sage Valley (22) and South Fork (23) flow from the Wells Formation. Figure IV-11 is an east-west structure section through Sage Valley. Auburn and Sage Valley springs were sampled for ^{14}C.

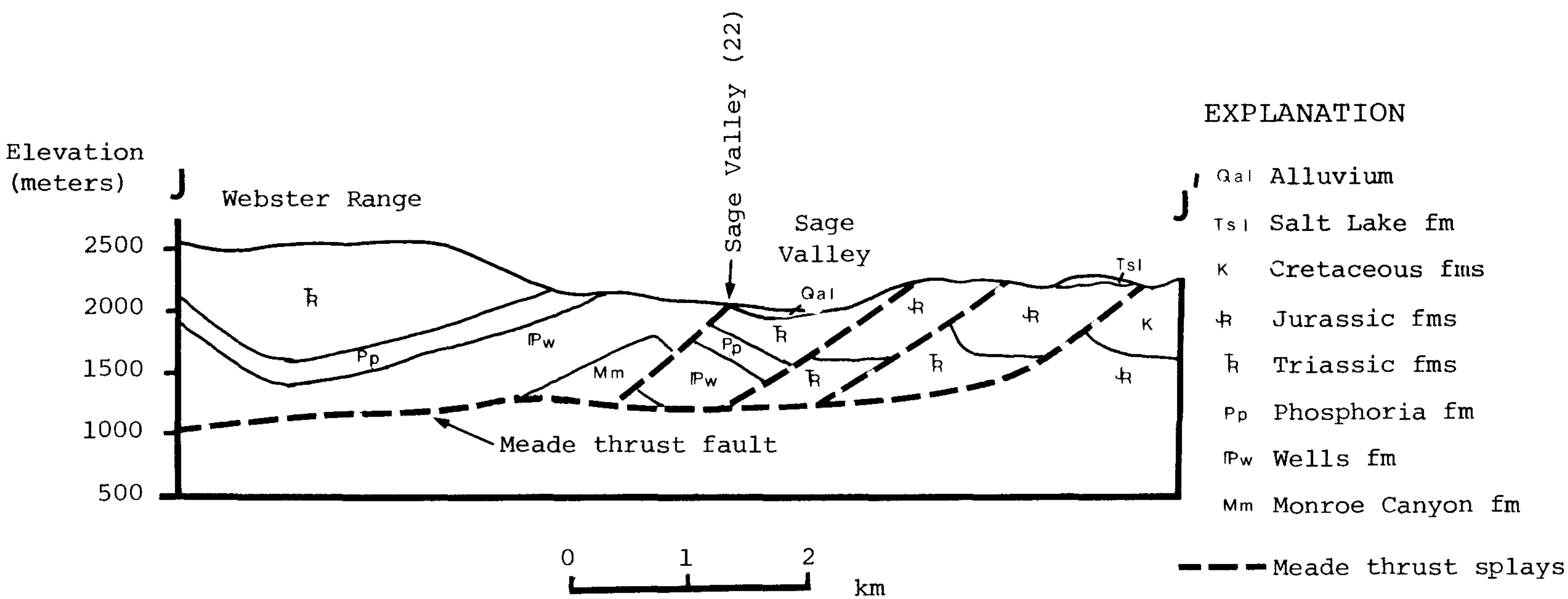

Figure IV-11. East-west structure section through Sage Valley (22) area, southeastern Idaho. Modified after Mansfield (1927) and Conner (1980).

Star Valley Hatchery (24), Fence Line (25), Brook (26), New Salt (27), and Nuggett (28) springs issue from slices of strata bounded by thrust splays. Discharge at Star Valley Hatchery is reported by hatchery personnel to be fairly constant throughout the year. Brook spring (26) issues from the bottom of a half hectare pond and may be associated with an alluvially concealed thrust trace in the Monroe Canyon Formation. New Salt (27) issues from the Twin Creek Limestone, has a salty taste and flows over a small travertine deposit on the steep western slope of Crow Creek Canyon. Nuggett (28) discharges from an exposure of the Nuggett Sandstone along the outlet of Sage Valley. Crow Creek (29) issues from the Wells Formation near the contact with the Monroe Canyon Formation. Neil Stewart (oral communication, 1980) reports a nearly constant discharge of about 60 l/s from this spring. Crow Creek was sampled for ^{14}C.

Interior Groups (30-41)

Springs and wells assigned to the interior groups are those which are located in the interior regions of the allochthon and are not associated with a major extension or periphery thrust fault. All of these springs discharge cold water and are associated with local structural-stratigraphic features. Detailed descriptions of these sites are presented by Mayo (1982).

Analysis of Chemical Data

Graphical Analysis and Hydrochemical Facies

Major ion analyses were plotted on Piper (1944) and Stiff (1951) diagrams for visual inspection. The Piper plot, or trilinear diagram, represents the major ion concentrations as percentages of total anion or cation equivalents on three distinct fields (Figure IV-12). Two triangular fields at the lower left and right are cations and anions respectively, and the center diamond shows the overall chemical character. Each analysis plots as a single point in each field, so the ionic distribution of numerous analyses may be conveniently represented on the same diagram. Differences in the magnitude of ionic concentrations between analyses with the same ionic distribution are not, however, presented.

Trilinear plots of the 41 analyses from the Meade thrust area are shown on Figure IV-13. All of the analyses except two (27 and 38) fall in the calcium bicarbonate type facies in the cation and anion fields. The sample taken at New Salt (27), from the Twin Creek Limestone in the Crow Creek area, falls in the no dominant type anion field as a result of the high chloride content. The high chloride content most likely results from the overlying Preuss Formation. The Peterson Ranch sample (38), taken from a shallow alluvial aquifer in

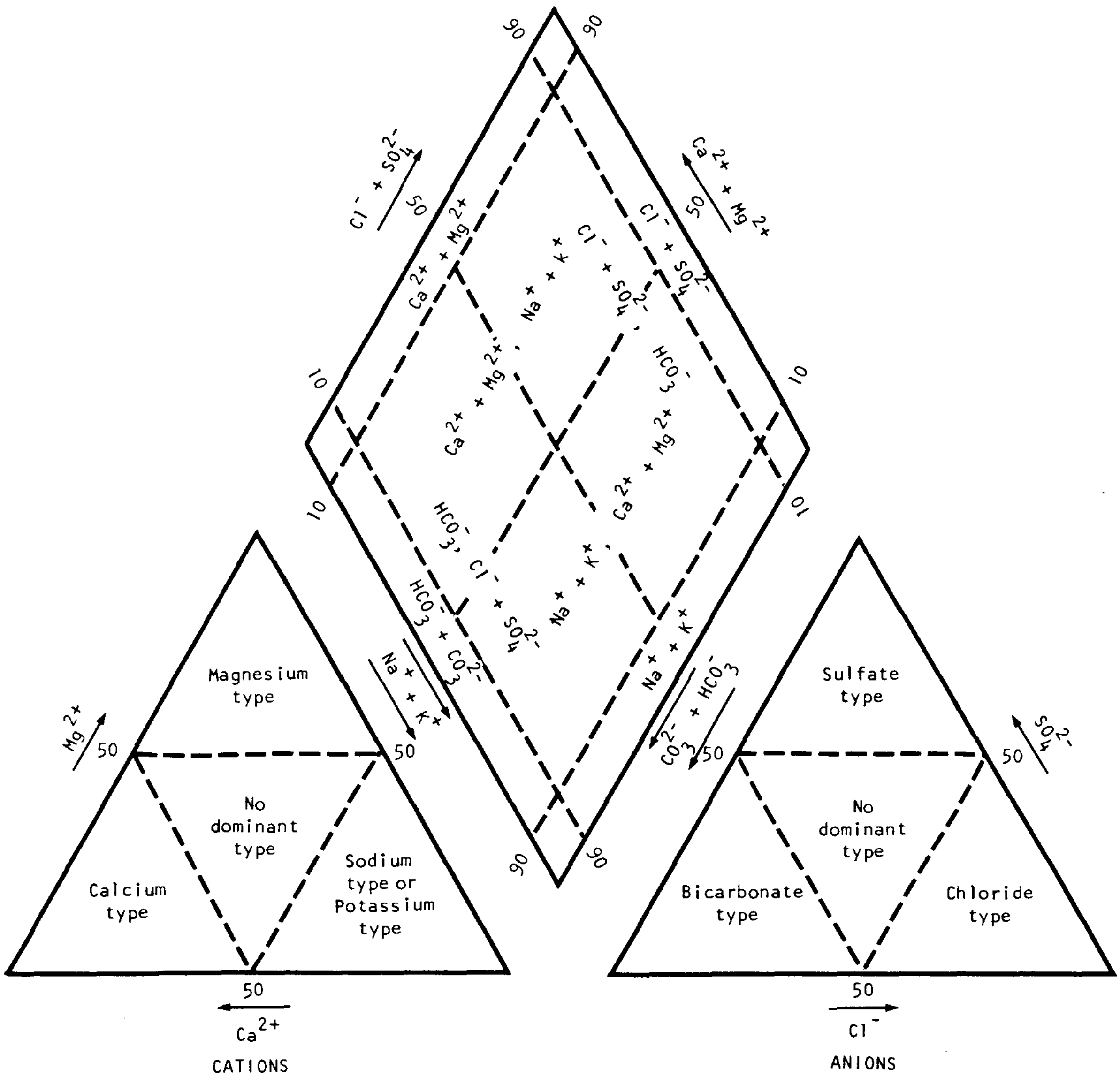

Figure IV-12. **Classification diagram for anion and cation facies in terms of major-ion percentages (after Freeze and Cherry, 1979).**

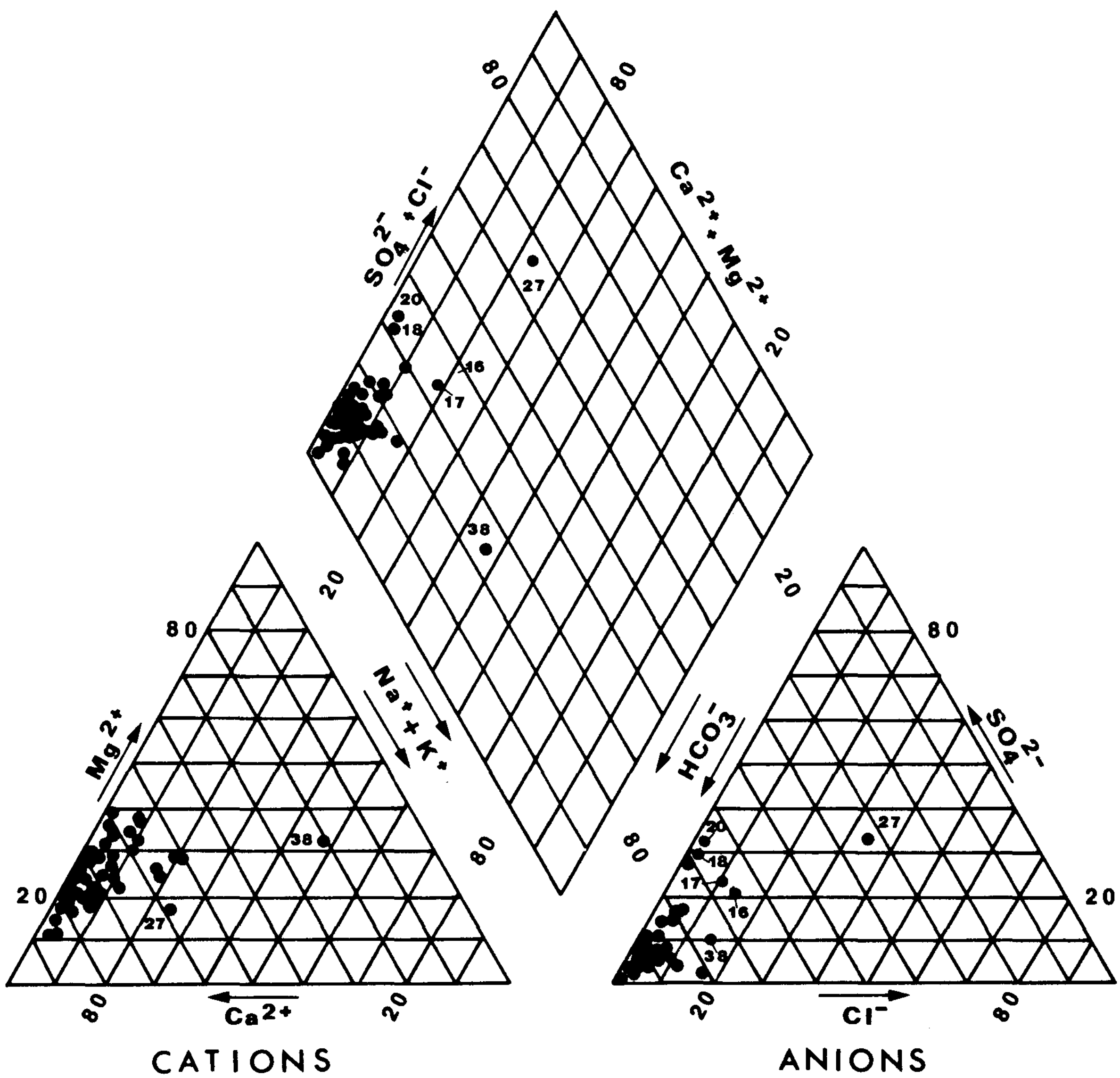

Figure IV-13. Trilinear diagram of chemical analyses of discharge waters from 3 wells and 38 springs in the Meade thrust area, southeastern Idaho.

Slug Creek, falls in the no dominant type cation field, perhaps because of agricultural contamination.

The data presentations on the trilinear diagram are consistent with the fact that the aquifers are predominantly carbonate. The data form a fairly tight cluster about the calcium-magnesium cation and the bicarbonate to lowermost bicarbonate-chloride sulfate anion facies. Interior groups, which are largely restricted to the lower Mesozoic strata, have discharge waters which tend toward the calcium-magnesium and bicarbonate facies. Periphery extension and periphery thrust groups, which are largely restricted to the upper Paleozoic strata, generally have discharge waters which fall in the calcium-magnesium cation facies. Waters at Chubb (16, 17) and Georgetown Canyon (18, 20) belong to the bicarbonate-chloride sulfate anion facies. Waters from the remaining periphery extension and periphery thrust groups tend to cluster in the bicarbonate anion facies.

Stiff diagrams facilitate the comparison of total concentration and ionic composition by the utilization of graphical shapes (Figure IV-14). The shape of the diagram represents composition, while the size reflects concentration. All of the analyses except two (27 and 38) have the same general form, suggesting a predominantly limestone aquifer with minor amounts of dolomite. There are, however, significant differences in concentrations between samples from the periphery extension group and the other two

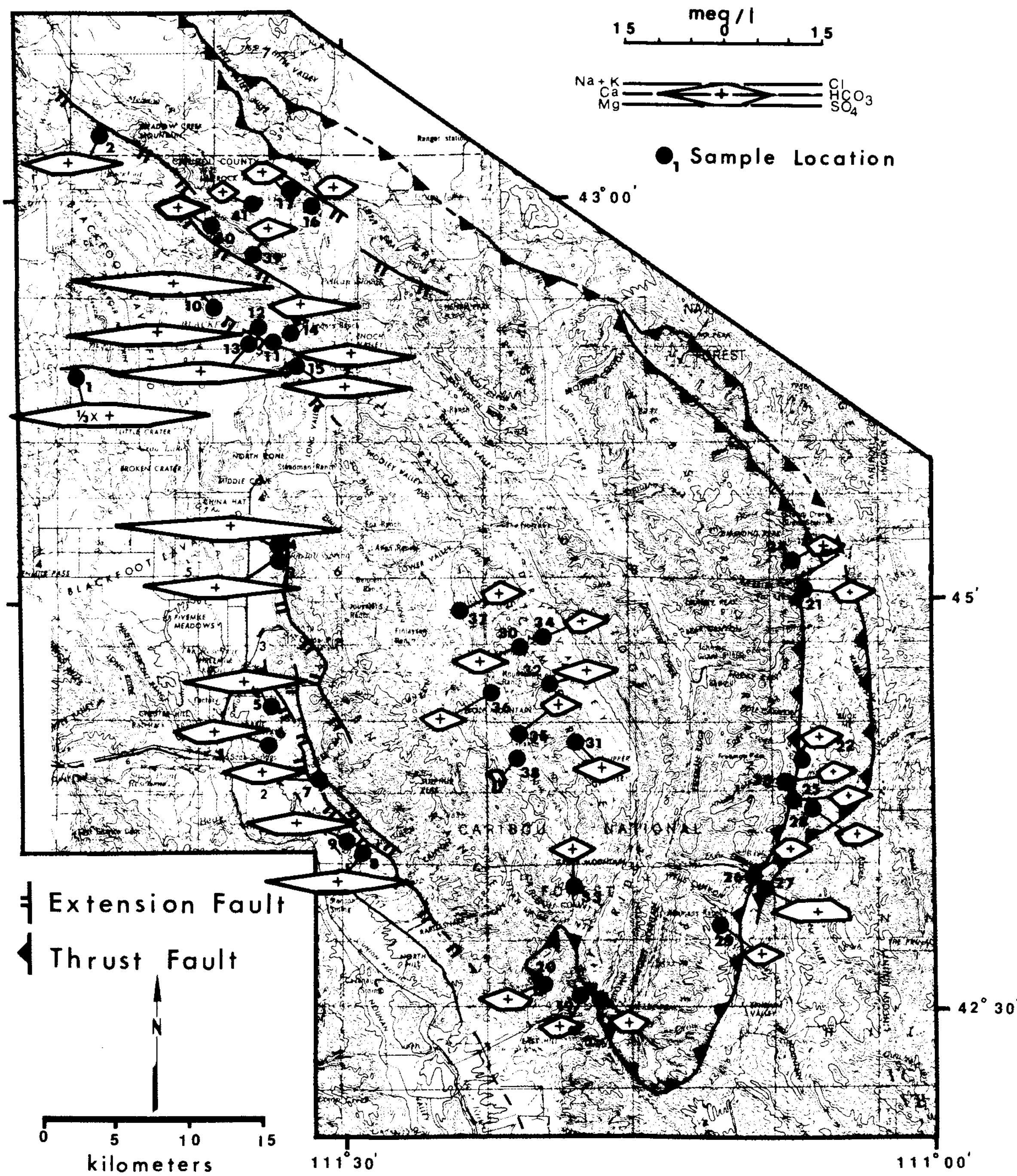

Figure IV-14. Stiff diagrams of chemical analyses of waters from 3 wells and 38 springs in the Meade thrust area, southeastern Idaho.

groups. The higher concentrations occur in springs with large travertine deposits, elevated discharge temperatures, and increased PCO_2 levels.

Ca/Mg Ratios

Typical ranges of concentration ratios of some major ions in ground water samples are characteristic of many diagenetic, metamorphic and magmatic processes (White, 1957a, 1957b, 1960; White and others, 1963; and Hem, 1970). Of particular interest to the study area is the Ca/Mg ratio, which Meisler and Becher (1967) and Jacobson and Langmuir (1970) demonstrated to be useful in identifying limestone and dolomite aquifers. The stoichiometric molar ratio of calcium to magnesium in pure dolomite is 1; higher ratios are obtained from limestone, siltstone, clay and shale. White and others (1963) report Ca/Mg ratios of water samples taken from limestone aquifers may be as high as 50 and are commonly above 10, whereas argillaceous aquifers commonly have ground water whose Ca/Mg ratios are in the range of 1 to 3.

The Ca/Mg ratios of the samples analyzed are listed in Table IV-3 and are shown in cumulative-frequency distribution plots grouped according to the major spring groups (Figure IV-15). Trends 1, 2, and 3 represent the periphery extension, periphery thrust and interior (excluding eastern Schmid Ridge Thaynes Formation springs and Cold Spring (33)

Table IV-3. SI, Ca/Mg ratios, and P_{CO_2} of water samples collected in the Meade thrust area, southeastern Idaho.

Spring identification number and name		Ca/Mg	Log P_{CO_2} (atm)	Saturation Index (SI)							
				Anhydrite	Aragonite	Calcite	Dolomite	Fluorite	Gypsum	Halite	Magnesite
1	Corral Creek	1.98	-0.2	0.57	0.52	17.90	225.90	1.21	0.67	0.00	6.90
2	Sinkhole	3.07	-0.2	0.01	0.61	1.13	0.43	0.16	0.02	0.00	0.19
3	Woodall	3.97	-0.8	0.01	0.64	1.25	0.33	0.13	0.03	0.00	0.01
4	North Woodall	4.76	-0.3	0.02	0.83	1.58	0.51	0.88	0.05	0.00	0.16
5	Formation	3.91	-0.9	0.02	0.41	0.82	0.14	0.06	0.42	0.00	0.09
6	East Soda	2.47	-1.4	0.01	0.59	1.20	0.43	0.03	0.02	0.00	0.18
7	Sulphur Canyon	3.76	-1.7	0.00	0.83	1.69	0.57	0.01	0.01	0.00	0.17
8	Swan Lake #1	3.67	-0.9	0.02	0.76	1.46	0.55	0.02	0.04	0.00	0.19
9	Swan Lake #2	2.64	-1.5	0.01	1.03	2.19	1.25	0.01	0.03	0.00	0.30
10	Lone Tree	4.92	-0.5	0.04	1.02	1.85	0.84	1.67	0.06	0.00	0.22
11	Henry Warm #1	3.17	-1.1	0.02	0.72	1.38	0.55	0.15	0.03	0.00	0.20
12	Henry Warm #2	3.91	-0.6	0.06	0.71	1.31	0.46	0.58	0.12	0.00	0.17
13	Warm Spring	3.57	-0.4	0.04	0.67	1.22	0.47	1.64	0.06	0.00	0.19
14	North Henry	2.56	-1.2	0.01	0.52	1.00	0.35	0.09	0.01	0.00	0.17
15	Little Blackfoot River	3.71	-1.0	0.02	0.76	1.47	0.53	0.17	0.03	0.00	0.18
16	Chubb	1.87	-2.2	0.01	0.52	1.04	0.48	0.02	0.02	0.00	0.24
17	West Chubb	1.99	-2.1	0.35	0.35	0.69	0.20	0.02	0.01	0.00	0.15
18	Georgetown Canyon	2.53	-2.2	0.01	0.27	0.57	0.09	0.00	0.03	0.00	0.08
19	Georgetown Canyon Tailings	2.50	-2.3	0.00	0.60	1.24	0.43	0.01	0.00	0.00	0.18
20	Big Spring	3.39	-2.1	0.02	0.44	0.92	0.18	0.01	0.05	0.00	0.10
21	Auburn Fish Hatchery	1.70	-2.3	0.01	0.48	0.97	0.42	0.01	0.01	0.00	0.22
22	Sage Valley	1.87	-2.2	0.01	0.53	1.04	0.50	0.05	0.01	0.00	0.24
23	South Fork	1.57	-2.2	0.01	0.43	0.86	0.34	0.03	0.00	0.00	0.23
24	Star Valley Hatchery	1.94	-2.5	0.00	0.69	1.42	0.78	0.01	0.01	0.00	0.28
25	Fence Line	2.14	-1.8	0.00	0.21	0.41	0.06	0.15	0.00	0.00	0.08
26	Brooks Spring	2.18	-2.3	0.00	0.59	1.16	0.51	0.04	0.00	0.00	0.22
27	New Salt	3.03	-2.1	0.06	0.80	1.60	0.70	0.05	0.13	10^{-6}	0.22
28	Nuggett	1.72	-2.1	0.01	0.48	0.97	0.42	0.01	0.01	0.00	0.22

Table IV-3. Continued

Spring identification number and name		Ca/Mg	Log P_{CO_2} (atm)	Saturation Index (SI)							
				Anhydrite	Aragonite	Calcite	Dolomite	Fluorite	Gypsum	Halite	Magnesite
29	Crow Creek Ranch	2.52	-2.2	0.00	0.32	0.67	0.12	0.01	0.01	0.00	0.09
30	Slump Spring	3.98	-1.9	0.00	0.28	0.06	0.56	0.01	0.01	0.00	0.50
31	Lower Lone Tree	5.13	-1.9	0.01	0.35	0.74	0.07	0.00	0.01	0.00	0.05
32	Lower Young Ranch	6.47	-1.7	0.00	0.28	0.62	0.36	0.00	0.00	0.00	0.31
33	Cold Spring	8.51	-2.3	0.00	0.54	1.19	0.10	0.05	0.01	0.00	0.04
34	FMC	1.75	-2.1	0.00	0.33	0.69	0.19	0.00	0.00	0.00	0.14
35	Square Pond	2.71	-2.0	0.00	0.24	0.51	0.07	0.00	0.00	0.00	0.07
36	Knudsen Ranch	2.60	-2.2	0.00	0.57	1.13	0.41	0.00	0.00	0.00	0.18
37	Purple Spring	1.42	-2.0	0.00	0.33	0.66	0.25	0.01	0.00	0.00	0.19
38	Peterson Ranch	0.71	-1.6	0.00	0.00	0.00	0.00	0.00	0.00	0.00	0.00
39	Pelican Ridge #1	2.26	-.19	0.00	0.30	0.64	0.12	0.00	0.00	0.00	0.10
40	Pelican Ridge #2	2.28	-1.8	0.01	0.35	0.73	0.17	0.01	0.15	0.00	0.12
41	North Pelican	4.27	-2.4	0.00	0.28	0.58	0.56	0.00	0.00	0.00	0.50

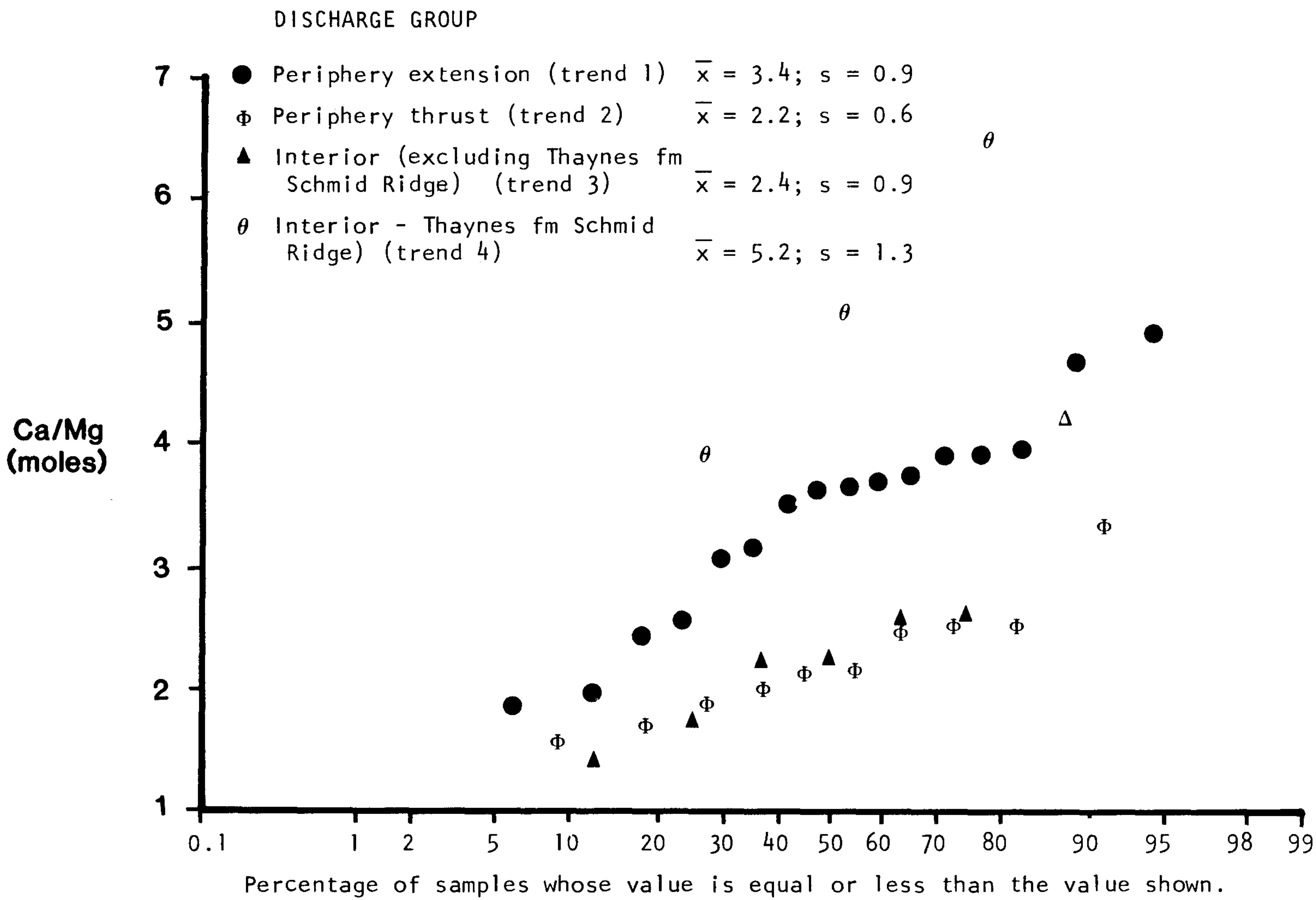

Figure IV-15. Cumulative frequency distribution of calcium-magnesium molar ratios in ground water samples collected from springs and wells in the Meade thrust area, southeastern Idaho. Ca/Mg molar ratios are grouped by discharge groups. Mean ($\overline{x}$) and standard deviation (s) are shown for each group.

groups, respectively. Trend 4 represents eastern Schmid Ridge Thaynes Formation springs.

Statistical t tests were performed on the data in trends 1, 2, and 3 to determine if there is a statistical difference between the average values of Ca/Mg ratios among the trends. Procedures used are those described by Natrella (1963). The t test is based on the t probability distribution and compares the difference of the sample means with test criteria calculated using preselected confidence interval. Details of the testing are presented by Mayo (1982).

Trends 1 vs 2, 1 vs 3, and 2 vs 3 were tested utilizing 0.95 confidence interval. The t test demonstrated that a statistical difference exists between trends 1 and 2 and 1 and 3, and thus we may conclude that a statistical difference exists between the Ca/Mg ratios of the discharge waters of the periphery extension aquifers and the periphery thrust and interior aquifers.

Cumulative frequency distribution diagrams commonly provide useful information for single-variant analysis and they are a convenient form for displaying data (Figure IV-15). The linearity of a data trend is an indicator of the normality of the distribution of a population. A normally distributed population will plot on a straight trend. The slope of the trend indicates the degree of variation in the population. A significant deviation of a data point from a population trend may suggest the data point has been assigned to the wrong population.

The periphery extension (trend 1) and the periphery thrust (trend 2) groups generally discharge from the upper Paleozoic formations which tend to be more carbonaceous and less argillaceous than the lower Mesozoic formations. The interior groups (trend 3) generally discharge from the lower Mesozoic formations, although discharge from the upper Paleozoic formations is not uncommon.

The periphery extension springs (trend 1) have higher Ca/Mg ratios and thus appear to draw their water from purer limestone facies than do the springs of the periphery thrust and interior groups. Abundant siltstone and shale facies reported in the lower Mesozoic strata (Mansfield, 1927; Cressman, 1964; Montgomery and Cheney, 1964; and others) probably account for the increased magnesium content of the waters from these formations. Argillaceous facies are commonly rich in magnesium bearing minerals and commonly yield ground waters with low Ca/Mg ratios. Dissolution of dolomite is probably not responsible for the low Ca/Mg ratios in the lower Mesozoic strata; dolomite is seldom reported in the formations. Ca/Mg ratios from flow systems in the Thaynes Formation along eastern Schmid Ridge (trend 4) and from Cold Spring (33) are not typical of most of the flow systems investigated. Additional geochemical investigations of the Schmid Ridge area are needed to explain the Ca/Mg anomaly.

Mineral Equilibrium

The saturation index is a powerful tool for evaluating the hydrochemistry of a ground water system. A SI less than 1 means the water is undersaturated with respect to the mineral and the water would ideally dissolve the mineral when encountered in the aquifer. An index greater than 1 indicates the water is supersaturated and has a thermodynamic tendency to precipitate the mineral.

Natural waters from carbonate aquifers are frequently not at chemical equilibrium and are commonly undersaturated or supersaturated with respect to carbonate minerals. Calcite solubility is at least two times greater than dolomite solubility, which helps account for dolomite undersaturation in many waters saturated with respect to calcite. Numerous investigations of carbonate saturation have been done (Rauch and White, 1977; Drake and Harmon, 1973; Back and Hanshaw, 1971, 1970; Langmuir, 1971; Hostetler, 1964; Hsu, 1963; Back, 1963; and others). In general these investigators concluded that carbonate saturation is influenced by kinetic effects as well as thermodynamic equilibrium, allowing nonequilibrium conditions to exist. Kinetic factors may be temperature, ground water mixing, flow rates, CO_2 exsolution, reaction rates, lithology and grain size, or others. Armoring of carbonate mineral surfaces by inorganic species may also be a factor.

WATEQ, a computer program developed by Truesdell and Jones (1974), was used to calculate the ionic equilibrium (saturation index) of the water samples with respect to 34 minerals, Ca/Mg molar ratios, and PCO_2 for the 41 water samples. The minerals selected for discussion include the six carbonate species, fluorite, gypsum, which is a likely source of SO_4^{2-}, and halite, which is locally associated with lower Mesozoic formations in the Auburn Hatchery-Crow Creek areas. The SI of the six minerals, PCO_2, and Ca/Mg ratios are listed in Table IV-3.

Back and Hanshaw (1970), Langmuir (1971), Harmon and others (1975), and others have suggested defining saturation at SI = 1 $\pm$ 0.1 to allow for measurement error; this convention has been adopted here. Twenty-five of the samples analyzed are saturated or supersaturated with respect to calcite. Two samples, (1) and (9), are supersaturated with respect to dolomite and three samples, (1), (9), and (13), are supersaturated with respect to fluorite.

The areal distributions of calcite and fluorite saturation are shown on Figure IV-16. The periphery extension springs tend to be saturated or supersaturated with respect to calcite, the periphery thrust springs are undersaturated to supersaturated with respect to calcite, and

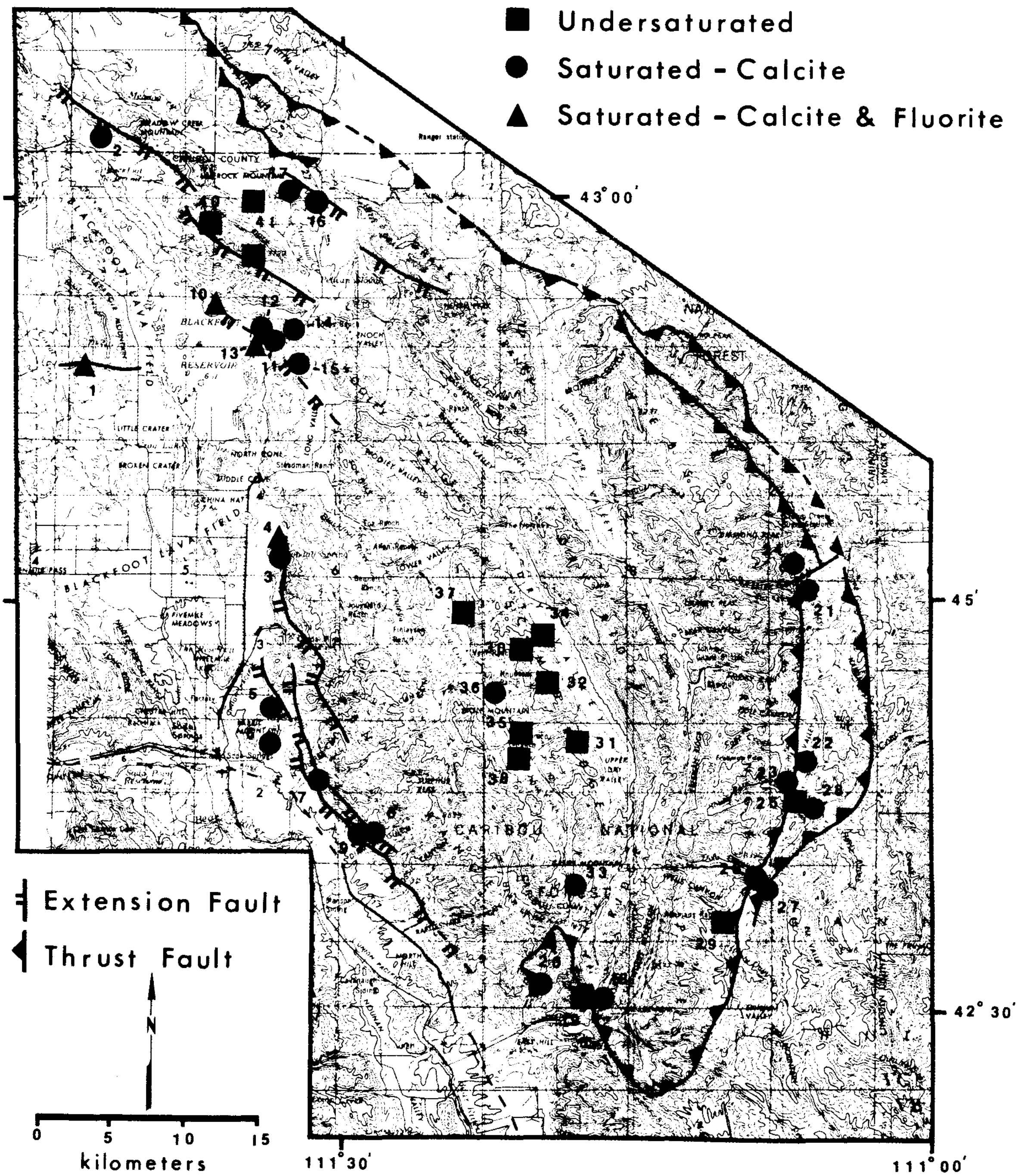

Figure IV-16. Saturation of water samples with respect to calcite and fluorite for 41 sites in the Meade thrust area, southeastern Idaho.

the interior springs are almost exclusively undersaturated with respect to calcite. The mean saturation index of calcite (SI_c) of the periphery extension springs is 1.33, and 87 percent of the springs are above 0.90. The periphery thrust springs have a mean SI_c of 0.93; however, only 60 percent of the springs are above 0.90. Undersaturation with respect to calcite is characteristic of most interior springs, which have a mean SI_c of 0.74. Only two springs in this group have a SI_c above 0.90.

Statistical one sided t tests were performed on the data to determine whether there is a statistical difference between the average saturation indices among the three different groups of springs. The t tests demonstrated that a statistical difference exists between trends 1 and 2 and 1 and 3. The tests did not show a statistical difference between trends 2 and 3. Thus we may conclude that waters discharging from periphery extension springs may be statistically differentiated from waters discharging from periphery thrust and interior springs.

There appears to be a relationship between SI_c and bedrock lithology. The periphery extension springs which discharge from the upper Paleozoic formations, tend to be saturated and supersaturated. The periphery thrust springs, which discharge from the upper Palezoic and lower Mesozoic formations, have discharge waters which are undersaturated to supersaturated. Most of the interior springs, which discharge primarily from the lower Mesozoic formations, have discharge waters that are generally undersaturated.

The apparent relationship between SI_C and bedrock lithology is not casual, however; it may be explained as a function of the thermal regime of the aquifers. Unlike most minerals, calcite tends to be less soluble in warmer waters and the control of calcite saturation is primarily thermal rather than aquifer dependent. Most of the carbon in ground water is taken up by solution in the cool, unsaturated recharge zone, which fixes the SI_C for that temperature. This is reflected by the observed SI_C of the waters of the interior aquifers. Those waters which underwent some warming in the path to the surface became more saturated in calcite not by further uptake, but due to the reduction of calcite solubility at these higher intermediate temperatures. This conclusion is supported by WATEQ calculations for temperatures different than ones observed, and by the apparent lack of change in the SI_C of noncarbonate minerals, which do not track the high SI in warm waters (Table IV-3). These warm water temperatures need not have been high enough to cause an ^{18}O shift, because calcite saturation is much more temperature sensitive. Therefore the high degree of calcite saturation observed in the discharge waters of many periphery springs must have resulted from greater cirulation depths.

Fluorite saturation of three analyses, (1), (10), and (13), and near saturation of a fourth (3) may indicate that these waters have at some time been in contact with the Phosphoria Formation. The Phosphoria Formation is the only known source of fluorite in the study area. All of these springs and the well discharge from the Wells Formation, which underlies the Phosphoria Formation. Lowell (1952) identified abundant fluourapathite and fluorite in thin section and x-ray analyses of the Phosphoria Formation in the Meade thrust area.

The saturation indices for anhydrite, gypsum, and magnesite indicate that the discharge waters of all sites, excluding Corral Creek (1), are substantially undersaturated with respect to these minerals. Such low saturation indices may suggest that these minerals are not in high concentrations in the aquifers. Halite saturation (SI_h) is less than 10^{-6} for all samples analyzed. The SI_h of 10^{-6} for the water of New Salt (27) suggests that the discharge water does not flow through halite beds which have been reported in the spring area or that ground water mixing is occurring.

$Ca\text{-}Mg\text{-}HCO_3$ Concentrations

Substantial differences exist between the concentration of carbonate dissociation products in the discharge water of the periphery extension group and the water of the other two groups. These differences are represented graphically as Stiff diagrams in Figure IV-14. The discharge waters of the periphery extension group have a mean Ca-Mg-HCO_3 concentration of 23.3 meq/l (standard deviation 9.4). The discharge waters of the periphery thrust and interior groups have mean concentrations ranging from 8.5 to 8.9 meq/l (standard deviations of 0.7 and 1.6, respectively).

Mayo (1982) discusses potential responsible mechanisms for the variation in concentrations of carbonate dissociation products. He concludes that the differences may reflect differences in recharge histories of the three aquifer groups.

Deuterium-Oxygen Analysis

Hydrogen has two stable isotopes, 1_H and 2_H (deuterium or D), whose terrestrial isotopic abundances average 99.985 and 0.015 percent, respectively. Oxygen has three stable isotopes, ^{16}O, ^{17}O, and ^{18}O, whose terrestrial isotopic abundances average 99.756, 0.039, and 0.205 percent, respectively. Water molecules therefore have nine different stable isotopic configurations whose atomic masses range from 18 to 22. The physio-chemical behaviors of these various isotopic forms of water depend on their chemical activities, which are related to their vapor pressures (Faure, 1977). The lightest water molecule, $^{1}H_2\,^{16}O$, has a significantly higher vapor pressure than does the heaviest water molecule,

$D_2^{18}O$. The differences in chemical activity tend to concentrate water molecules containing the isotopes ^{18}O and D in certain reservoirs (e.g., atmosphere, surface water, ocean, ground water, etc.) in the hydrologic cycle by isotope fractionation.

Knowledge of the absolute abundance of these isotopes of hydrogen and oxygen is extremely difficult to obtain and has proven not to be necessary to hydrologic and geologic studies (Faure, 1977). Rather, mass ratio mass spectrometry permits the determination of certain isotopic ratios in water with relative ease. The ratios most important in the study of the water within the water cycle are $^{18}O/^{16}O$ and $D/^{1}H$. In each case this is the ratio of the abundance of the second most common stable isotope to the most common one. This allows these ratios to be comparable in different studies using different mass spectrometers. Without determining any absolute abundances, the $^{18}O/^{16}O$ and $D/^{1}H$ are expressed in terms of the parameter δ, which is defined:

$$\delta^{18}O\ ^{o}/oo = \left(\frac{(^{18}O/^{16}O)\ \text{sample}}{(^{18}O/^{16}O)\ \text{standard}} - 1\right) 10^3$$

$$\delta D\ ^{o}/oo = \left(\frac{(D/^{1}H)\ \text{sample}}{(D/^{1}H)\ \text{standard}} - 1\right) 10^3$$

By convention, the reporting standard has become SMOW (Standard Mean Ocean Water), which was originally a defined value and was not based on a physical standard (Craig, 1961a). The IAEA (International Atomic Energy Agency) in Vienna has recently prepared a physical standard. The standard is a $CO_{2(g)}$ and has been equilibrated with SMOW. All stable isotopic compositions presented in this investigation are reported with respect to SMOW.

The tendency for species of different isotopic composition, but identical chemical composition, not to equilibrate identically in a chemical or physical phase change (i.e., isotopic fractionation) is temperature dependent. This temperature dependence is important to this investigation in two ways. First, it controls the occurrence of certain isotopes in the precipitation-evaporation-ground water recharge cycle. Second, it controls the occurrence of certain isotopes in ground water in geothermal regimes.

During evaporation, the more volatile light water molecules (primarily ${}^{1}H_2{}^{16}O$) tend to enter the vapor phase, concentrating the heavier and less volatile molecules of $DH^{16}O$ and $H_2{}^{18}O$. We may neglect the molecules $D_2{}^{16}O$, $DH^{18}O$, $D_2{}^{18}O$ and all molecules containing ${}^{17}O$, since they cumulatively make up less than 0.06 percent of water molecules, as opposed to 99.7 percent made up by ${}^{1}H_2{}^{16}O$ and about 0.3 percent made up by the D and ${}^{18}O$ species. This concentration results in a residual phase in evaporation enriched in heavy isotopes and a vapor phase depleted of them. At high temperatures, approaching boiling, the difference in escaping tendency diminishes toward zero. A second fractionation important in hydrogeology is that which occurs in the equilibration between oxygen in ground water and silicate minerals of the aquifer matrix. At low temperatures the reaction rates are too slow to show any appreciable equilibration. Above about 80°C, an equilibration takes place which tends to concentrate ^{18}O in the water and to deplete the silicate minerals. Unlike evaporation, during which both D and ^{18}O are concentrated in the water, only ^{18}O of the water increases, since there is no appreciable hydrogen in the rocks of the aquifer matrix (Craig, 1963, 1966).

In a detailed study of continental precipitations, Craig (1961b) observed a linear relationship in ^{18}O/D space. The band in which over 1000 analyses fell has an equation of:

$$\delta D = 8\delta^{18}O + 10$$

It is important to remember that not all continental precipitation will fall directly upon this line, but tend to group near it. The line is frequently called the Craig or Meteoric Water line. Notice that the standard SMOW does not lie upon this line (since it plots $\delta^{18}O = \delta 0$ o/oo, D = 0 o/oo) because it is not meteoric water, but lies beneath, on the isotopically enriched side of it. The location of meteoric waters upon the Craig line is a function of the conditions under which the precipitation falls. During condensation the lighter isotopes tend to remain in the vapor phase, and this fractionation is also temperature dependent. Precipitation falling in areas with higher temperatures or at lower latitudes tend to have higher δD and $\delta^{18}O$ values than does precipitation falling in areas with lower temperatures or higher latitudes. In a particular region the lowest δD and $\delta^{18}O$ values tend to occur at the higher elevations where the air temperatures are generally lower. At a single location a seasonal migration along the meteoric water line may be observed, as recently demonstrated by the semiseasonal variations in δD and $\delta^{18}O$ observed by Turner and others (1980) in the Tucson basin, Arizona.

The δD and $\delta^{18}O$ values of geothermal water and steam have been investigated by Craig (1963, 1966). Geothermal water heated above 70 to 90°C displays oxygen isotope shifts of +5 o/oo or more due to the progressive equilibration of oxygen in the water with oxygen in carbonate and silicate rocks. The δD value of the water remains unchanged because of the low hydrogen content of these rocks. The magnitude of the oxygen shift increases with temperature and residence time.

The results of the stable isotopic analysis for thirty-eight samples from the study area are summarized in Table IV-4 and are shown graphically on Figure IV-17. The analytical error bars of ±0.2 o/oo for $\delta^{18}O$ and ±3 o/oo for δD are too small to appear with each data point. All the results fall into the narrow range of -16 to -19 o/oo in $\delta^{18}O$

Table IV-4. Deuterium and oxygen-18 analyses of spring and well waters in the Meade thrust areas, southeastern Idaho.

Spring identification number and name	$\delta^{18}O$ ($^o/oo$)	δD ($^o/oo$)
1 Corral Creek	-18.4	-119
2 Sinkhole	-18.2	-132
3 Woodall	-18.2	-130
4 North Woodall	-17.6	-124
5 Formation	-18.3	-139
6 East Soda	-18.1	-139
7 Sulphur Canyon	-17.6	-128
8 Swan Lake #1	-18.3	-140
9 Swan Lake #2	-17.7	-131
10 Lone Tree	-18.5	-133
11 Henry Warm #1	-18.1	-140
12 Henry Warm #2	-18.4	-133
13 Warm Spring	-18.4	-135
14 North Henry	-18.4	-139
15 Little Blackfoot River	-18.3	-132
16 Chubb	-18.3	-136
17 West Chubb	--	--
18 Georgetown Canyon	-18.0	-131
19 Georgetown Canyon Tailings	--	--
20 Big Spring	-17.9	-129
21 Auburn Fish Hatchery	-18.5	-131
22 Sage Valley	-19.0	-130
23 South Fork	-18.6	-121
24 Star Valley Hatchery	-18.2	-129
25 Fence Line	-17.8	-128
26 Brooks Spring	-17.2	-123
27 New Salt	--	--
28 Nuggett	-18.8	-143
29 Crow Creek Ranch	-17.6	-128
30 Slump Spring	--	--
31 Lower Lone Tree	-17.3	-137
32 Lower Young Ranch	-17.5	-136
33 Cold Spring	-17.1	-122
34 FMC	-16.8	-134
35 Square Pond	--	--
36 Knudsen Ranch	-17.5	-131
37 Purple Spring	-17.7	-138
38 Peterson Ranch	--	--
39 Pelican Ridge #1	-17.9	-130
40 Pelican Ridge #2	--	--
41 North Pelican	-17.8	-116

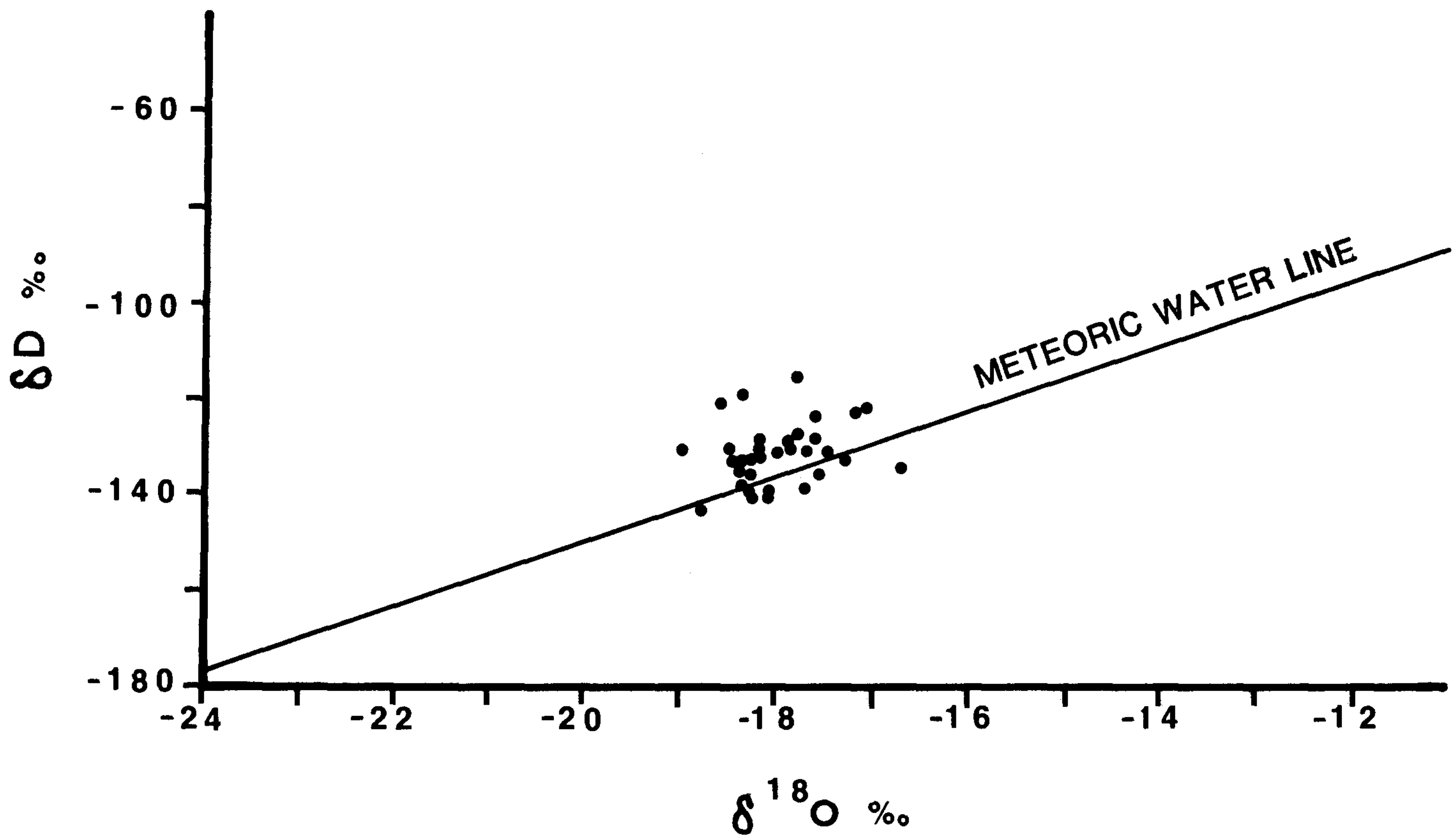

Figure IV-17. δD and $\delta^{18}O$ values from spring and well waters in the Meade thrust area, southeastern Idaho.

and -116 to -143 o/oo in δD. Although these are not meteoric waters, they have not undergone any process which has moved their stable isotopic composition appreciably away from the meteoric water line. The small scatter in the data permit the following conclusions to be drawn:

1. variations in recharge altitudes cannot be determined;
2. summer versus winter recharge can not be distinguished; and
3. the waters have not been elevated above approximately 80°C.

Radiocarbon Chronometry

Origin of Carbon-14. Carbon-14 or radiocarbon, is produced in nature by the bombardment of atmospheric nitrogen-14 with secondary neutrons from cosmic ray spallation reactions. Libby (1946) suggested that atmospheric production of radiocarbon is continuous and occurs at a constant rate. He assumed a constant cosmic radiation intensity over a long period of time and a constant neutron flux.

As is the case with stable isotopes, the absolute abundance of ^{14}C is not determined in an analysis. This hypothetical atmospheric equilibrium concentration has been arbitrarily assigned a value of 100 percent modern. This corresponds to a ^{14}C decay rate of 13.56 disintegrations per minute per gram of carbon (Bq/g) (Olsson, 1974). All ^{14}C

activities in the environmental sciences are reported with respect to this standard in units of percent modern carbon (pmc).

Direct verification of the paleoatmospheric ^{14}C content is not possible. Paleontological and stratigraphic studies suggest that there has been a relatively stable relationship between the atmosphere and atmospheric CO_2 during the past 1.0×10^7 years (Cloud, 1968). The ^{14}C analysis of bristle cone pine tree rings, which reflect the ^{14}C content of the atmosphere in the year they were formed, has allowed a detailed reconstruction of the ^{14}C variations in the atmosphere in the last 8,000 years (Klein and others, 1980). Suess (1955) has shown twentieth-century wood formed prior to nuclear weapons testing to be almost 2 pmc lower in ^{14}C activity than nineteenth-century wood. He attributed this to the introduction of CO_2 containing no ^{14}C into the atmosphere by the combustion of fossil fuels. This phenomenon is known as the "Suess effect". In 1958 deVries demonstrated that the radiocarbon of the atmosphere has varied systematically and that ^{14}C activity was about 2 pmc greater around 1500 and 1700 AD than in the ninteenth-century. These periods correspond to periods of increased cosmic ray flux. Explosion of nuclear devices raised the ^{14}C activity in the atmosphere to over 200 pmc at the peak in the 1960's. The atmospheric ^{14}C content has decreased since then to about 120 pmc, due to the transfer of ^{14}C from the atmosphere to the ocean reservoir of carbon. This great pulse of ^{14}C into the hydrologic cycle serves as an ideal tracer of post bomb waters and has proven of great value in this investigation.

<u>Principles of Radiocarbon Chronometry</u>. Radiometric dating using ^{14}C is based on the principle that material such as water which is open to the atmosphere and exchanging with it has a ^{14}C content similar to that of the atmosphere. When the material is no longer in contact with the atmospheric reservoir, the ^{14}C which decays is no longer replenished by that reservoir and the C content begins to decrease according to the law of radioactive decay. The law may be used to predict the time since the sample was isolated from the atmospheric reservoir. This equation may be written as follows:

$$t = \frac{\tau}{\log 2} \log \frac{A_o}{A_t}$$

where:

t = time since the sample was isolated from the atmosphere (or age),

τ = radioactive half life,

A = specific activity at time zero (initial activity), and

A = specific activity at time t.

Carbon-14 has a half life of 5730 ±30 years (Godwin, 1962), which allows the above equation to be simplified to:

Inherent assumptions in radiocarbon chronometry are:

1. A_0 is known;
2. there is no loss of activity except for natural disintegration.

These assumptions are seldom met since most dissolved carbon is not of direct atmospheric origin in natural ground water systems. The mechanisms controlling the initial ^{14}C activity in ground water are described in the next section. Mayo (1982) provides a more detailed discussion of the subject.

Mechanisms Controlling the Initial ^{14}C Activity in Ground Water. There are two fundamental reasons why the ^{14}C activity of water issuing from a spring is not equal to the atmospheric ^{14}C activity of 100 pmc. First, some ^{14}C has undergone radioactive decay, as described above. Second, the water has undergone interactions with various reservoirs of carbon of different isotopic compositions, altering the chemical and isotopic carbon composition of the solution. The law of radioactive decay can be used to determine the age of the sample after accounting for all these interactions because the only change in activity unaccounted for is due to decay. Therefore, an understanding of these interactions is essential to ground water dating (Wigley, 1975).

Garrels and Christ (1965) show that because of pH constraints, a falling rain droplet can take up only a very small amount of atmospheric CO_2. This small amount, on the order of 1 meq/l HCO_3^-, cannot account for the total bicarbonate normally found in ground waters, which is on the order of 5 to 8 meq/l HCO_3^- (Vogel and Ehhalt, 1963). The rest of this bicarbonate must be taken up farther along the path of the water, either in the soil zone during recharge or in the aquifer itself.

From a mass balance perspective, recharge through the soil in the Meade thrust area may be considered as a system open to a reservoir of 100 pmc phytogenic CO_2 in contact with a small to medium (but finite) reservoir of dead mineral carbonate. Humic acids and silicate minerals are also potential sources of CO_2 (Gehy, 1970; Vogel and Ehhalt, 1963). They are unlikely sources in the Meade thrust area because they are commonly associated with swampy conditions or crystalline rock areas. The recharging water becomes closed to the CO_2 reservoir when it passes into the phreatic zone. In the case of waters in the study area, the amount of $CO_{2(aq)}$ retained in solution is small compared to a relatively infinite reservoir of $CaCO_3$ in the aquifer matrix. Further uptake of dead carbon may occur here, but since a soure of H^+ for this reaction is no longer available, the total amount contributed here probably is small.

The sources and contribution of carbon to solution in the study area are thus well defined. The influence of isotopic fractionation during these processes must also be considered.

Isotopic Fractionation. Chemical and isotopic equilibrium are not necessarily synonymous. Each of the chemical processes that occur in a ground water system is accompanied by an isotopic fractionation (Muller, 1977, 1980, 1981). The isotopes of carbon tend also, like those of oxygen and hydrogen presented earlier, to prefer some phases over others. This preference is reflected in the isotopic enrichment factor ε.

Only one enrichment factor of the isotopes ^{14}C and ^{13}C needs to be determined because of a linear relationship between the fractionation behaviors of the two (Wigley and Muller, 1981). The values for ^{13}C are conventionally used. Fractionation (and thus ε) is temperature dependent; this dependence must be considered when treating for the redistribution of isotopes in the system. The method for accomplishing this treatment is through modeling the initial activity of the water A_0. If this is done correctly, the difference between A_0 and A_t in the radiometric dating equation will be the age of the water.

Modeling A_0. From the previous discussion it is clear that the problem of radiocarbon hydrochronometry is estimating A_0. A number of models have been developed for estimating the initial ^{14}C activity of ground waters. These models are based on: 1) empirical relationships, 2) carbonate stoichiometry, 3) carbonate equilibrium, 4) isotopic mixing, 5) isotopic fractionation, and 6) combinations thereof. Reviews of the current models are presented by Mook (1976) and Fontes and Garnier (1979).

Two models, that of Tamers (1975) and that of Pearson (Pearson and Hanshaw, 1970) were used in this investigation. The actual model calculations were done by using a preliminary form of the SAGE (Sandia Age of Ground Water Estimator) code being developed at Sandia National Laboratories, Albuquerque, New Mexico (Muller, 1980). The Tamers model calculates A_0 using stoichiometry and isotopic equilibrium considerations. The model is a simple mixing model which sets A_0 as the activity of dissolved original organic carbon diluted by dissolved inorganic carbon. In the SAGE code, the Tamers model has been modified to account for isotopic fractionation between $CO_{2(aq)}$ and bicarbonate and between mineral carbonate and bicarbonate (Muller, oral and written communication, 1981). The Pearson model is an isotopic mixing model which calculates A_0 on the basis of ^{13}C. This model uses the stable ^{13}C content of the water, which is not subject to radioactive decay, as an analogy to ^{14}C content. The ^{13}C content of carbonates dissolved in the ground water was determined in the laboratory at the time of the ^{14}C analyses, and is represented in terms similar to the notation used for stable hydrogen and oxygen:

$$\delta^{13}C\ o/oo = \frac{(^{13}C/^{12}C)\ \text{sample}}{(^{13}C/^{12}C)\ \text{standard}} - 1 \quad 10^{3}$$

The standard is the conventionally accepted reference of Pee Dee Bellenite (PDB). All ^{13}C values are expressed with respect to this standard in this study. The model accounts for mixing (under stoichiometric and non-stoichiometric conditions) and is based on linear mixing of ^{13}C and ^{14}C from the soil gas and aquifer reservoirs. A discussion of these models and other models is included in Mayo (1982).

Ground Water Ages from the Meade Thrust Allochthon. Nine springs and one flowing well were sampled for radiocarbon dating. Site selection was based on three criteria:

1. a wide areal distribution of sites,
2. representative of the flow systems being evaluated,
3. minimal potential for atmospheric contamination of the samples.

One site, Corral Creek (1), was selected because it represents a thermal flow system from the adjacent Paris thrust block. Four springs, Sinkhole (2), Formation (5), Henry Warm #2 (12) and Chubb (16), are representative of springs of the periphery extension group. Four springs, Georgetown Canyon (18), Auburn Hatchery (21), Sage Valley (22), and Crow Creek (29), are representative of the periphery thrust group. One spring, Knudsen Ranch (36), is from a shallow interbasin ground water flow system of the interior group. Samples of mineral carbonates from the aquifer were collected at sites (2) and (22) for ^{13}C analysis. The ^{14}C content of the carbonate was taken to be zero.

Chemical and isotopic parameters for the models were obtained from field and laboratory analysis and from WATEQ calculations. Certain isotopic parameters were estimated and adjusted during the computational process. The sources of parameters are listed below.

Parameter	Source
CO_2 (mm/l)	WATEQ
HCO_3^- (meq/l)	Field
CO_3^{2-} (meq/l)	WATEQ
γHCO_3^-	WATEQ
pH	Field
Temperature (C°)	Field
Sample $\delta^{13}C$ (o/oo)	Laboratory
Aquifer $\delta^{13}C$ (o/oo)	Laboratory
Soil gas $\delta^{13}C$ (o/oo)	Estimate (adjustable)
Sample $A^{14}C$ (pmc)	Laboratory
Aquifer $A^{14}C$ (pmc)	Estimate (adjustable); assumed 0 pmc for old marine carbonates

Soil gas $A^{14}C$ (pmc)   Estimate (adjustable); assumed 100 pmc for prebomb water.

Computer runs of both models were made for each site by an iterative process. For the first iteration the adjustable parameters were set at soil gas $\delta^{13}C$ = -20 o/oo, $A^{14}C$ = 100 pmc and the mineral phase $A^{14}C$ = 0 pmc. The mineral phases ^{13}C was set at 3.97 o/oo for Sinkhole (2) and 3.28 o/oo for Sage Valley (22), which correspond to the $\delta^{13}C$ contents of the aquifer carbonate samples at these sites. An average of the two values (3.6 o/oo) was used for the remainder of the analyses. A convergence between the Tamers and Pearson models was checked. If the models did not converge, the soil gas $\delta^{13}C$ parameter was adjusted and the models were rerun. Iterations continued in this manner until A_0 convergence occurred. Convergence of these models is of great importance and physical meaning, since it indicates that two completely independent approaches to modeling A_0 have predicted the same value under the same (and reasonable) input conditions. The implications of this convergence are further discussed by Mayo (1982). The final soil gas $\delta^{13}C$ parameter at each site was adjusted to maintain consistent input values for similar ground water flow systems.

After convergence was obtained, the ground water age was calculated from the general law of radioactive decay. Final input parameters and estimated ground water ages of the ten sites are listed in Table IV-5 and the distribution of radiocarbon age is shown on Figure IV-18.

Caution should be used when considering the concept of "age" as applied to ground water. The concept of "age" is only clearly defined in linear, one directional, non-mixing, confined ground water flow systems. Such systems are uncommon in nature. In all other cases the "age" of ground water, as predicted by the methodology developed here, is an indication of the mean travel time, or "mean age" of the various parcels of water issuing from the spring. Spring discharge is an integration of many events, over a period of time, and with diverse physical and chemical histories. As such the predicted ground water age also reflects this integration. In some environments like fracture rocks, the fundamental assumptions implied in this integration become questionable. The ground water flow systems being studied here are partiularly well suited for ^{14}C dating because of their size, geometry, and confinement.

A_0 convergence of the two models was not possible at Corral Creek (1), Sinkhole (2), Formation (5), and Henry Warm #2 (12). The results from the extended Tamers model are considered more reliable, since the springs at these sites were actively evolving CO_2 gas. The Pearson model asumes linear mixing between the gaseous and mineral phases in the

Table IV-5. Ground water ages and dating input parameters of nine springs and one flowing well in the Meade thrust area, southeastern Idaho.

Sample Name and Number	Estimated Age (years; BCI-Bomb Carbon Identified)	Model Used T-Tamers; TP-Tamers & Pearson	P_{CO_2} (mm/l)	HCO_3^- (meq/l)	CO_3^{-2} (meq/l)	γHCO_3	pH	Temperature (°C)	$\delta^{13}C$ sample (°/oo)	$\delta^{13}C$ mineral (°/oo)	$\delta^{13}C$ soil gas (°/oo)	$A^{14}C$ sample (pmc)	$A^{14}C$ mineral (pmc)	$A^{14}C$ soil gas (pmc)
Corral Creek (1)	36,500 ± 3,000	T	16.40	46.6	0.000	0.793	6.58	31.0	2.2	3.60	--	0.80 ± 0.14	0	100
Sinkhole (2)	12,500 ± 1,000	T	2.70	8.3	0.003	0.890	6.81	19.0	-3.1	3.97	--	13.9 ± 0.2	0	100
Formation (5)	14,500 ± 1,000	T	6.22	10.2	0.002	0.887	6.60	11.3	-1.7	3.60	--	12.2 ± 0.1	0	100
Henry Warm #2 (12)	20,500 ± 2,000	T	10.40	14.3	0.002	0.864	6.44	19.5	-2.4	3.60	--	6.19 ± 0.23	0	100
Chubb (16)	1,850 ± 200	TP	0.29	3.9	0.606	0.913	7.52	12.3	-9.0	2.58	-19.0	44.1 ± 0.6	0	100
Georgetown Canyon (22)	<300; BCI	TP	0.36	3.2	0.003	0.920	7.40	7.0	-9.6	3.28	-21.5	59.87 ± 0.63	0	110
Crow Creek (24)	<300; BCI	TP	0.04	3.7	0.004	0.923	7.41	6.8	-10.4	3.28	-21.5	61.3 ± 0.8	0	110
Sage Valley (28)	450 ± 50	TP	0.29	3.8	0.000	0.917	7.51	11.5	-10.0	3.28	-21.5	52.7 ± 0.9	0	100
Auburn Fish Hatchery (29)	<300; BCI	TP	0.29	3.8	0.005	0.921	7.54	9.5	-10.2	3.28	-21.5	52.7 ± 0.9	0	110
Knudsen Ranch (39)	<300; BCI	TP	0.29	3.9	0.006	0.921	7.52	7.5	-11.25	3.60	-23.5	61.7 ± 0.8	0	110

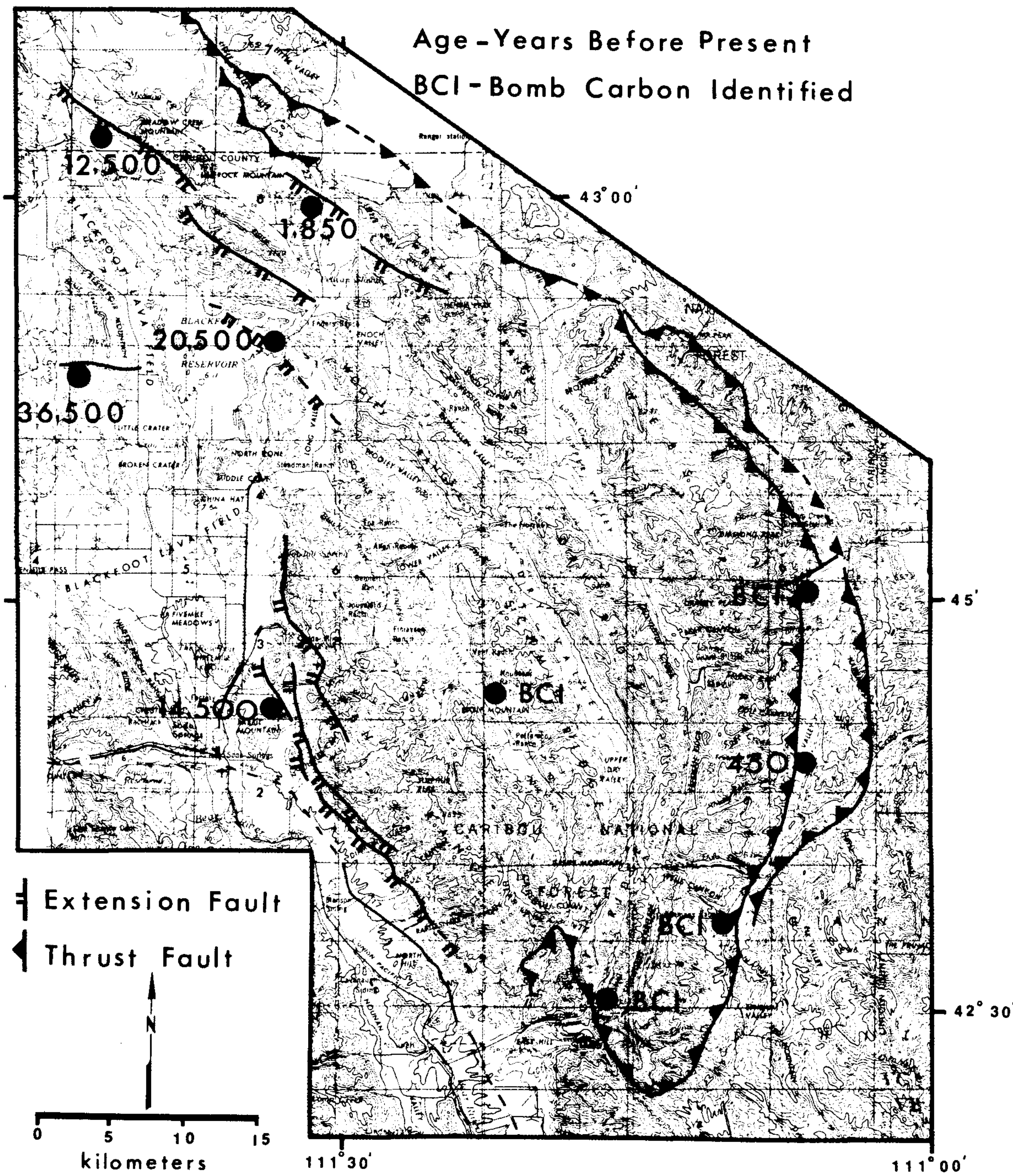

Figure IV-18. Radiocarbon ground water ages of nine springs and one flowing well in the Meade thrust area, southeastern Idaho.

reservoir and will not account for isotopic enrichment of the residual phase as CO_2 gas is evolved.

Four sites, Georgetown Canyon (18), Auburn Hatchery (21), Crow Creek (29) and Knudsen Ranch (36), required an adjustment of the soil gas $A^{14}C$ to 110 pmc. Without this adjustment the models would not converge and the ground water age calculations resulted in rechage ages that are in the future - obviously an error. A soil gas $A^{14}C$ of 110 pmc is consistent with post-bomb recharge conditions (i.e., the last 20 years); however, it is unlikely that these waters are less than 20 years old. The 110 pmc value probably indicates mixing of modern and prebomb water. A 20% component of 150 pmc mixed with an 80% component of modern but prebomb soil gas, at 100 pmc, could yield the apparent 110 pmc. The 150 pmc contribution could only have occurred for a short period. The proposed 150 pmc mixture is highly unlikely, but it does bound the "modern" age of the waters to no greater than about 300 years mean age.

Aquifer Temperatures

Discharge temperatures of springs and wells in the Meade thrust allochthon are 26°C or less. Many of the springs may be classified as geothermal. Maximum aquifer temperatures of several springs and wells in the Blackfoot Reservoir area were estimated by Mitchell (1976) using geochemical thermometers. Corral Creek (1), Woodall (3) and Sulphur

Canyon (7) were included in Mitchell's investigation. Mitchell used the following geochemical thermometers: silica, Na^+/K^+, Ca^{2+} and HCO_3^-, Cl^-/F^-, Mg^{2+}:Mg^{2+}/Ca^{2+}, $Na^{2=}/Ca^{2=}$, Cl^-/HCO_3^- +CO_3^{2-}, and Fournier and Truesdell geochemical thermometer mixing models (Mitchell, 1976). Mitchell concluded: 1) the chalcedony equilibrium thermometer was the most reliable for the area and 2) aquifer temperatures do not exceed 50°C. The D/^{18}O analyses presented earlier support this conclusion. It appears that aquifer temperatures do not exceed 80°C and many are probably less than 50°C.

Cumulative-frequency distribution trends of discharge temperature by spring groups (Figure IV-19) show that the periphery extension springs (trend 1) have higher temperatures and greater temperature variations between the springs than do those of the periphery thrust (trend 2) and interior (trend 3) groups. Statistical one sided t tests were performed on the data in trends 1, 2, and 3 to determine if there is a statistical difference between the average values of the temperatures among the trends. A 0.95 confidence interval was used for the test. The t test demonstrated that statistical differences exist between trends 1 and 2, and 1 and 3. It is thus possible to conclude that discharge waters from periphery extension springs may be statistically differentiated from discharge

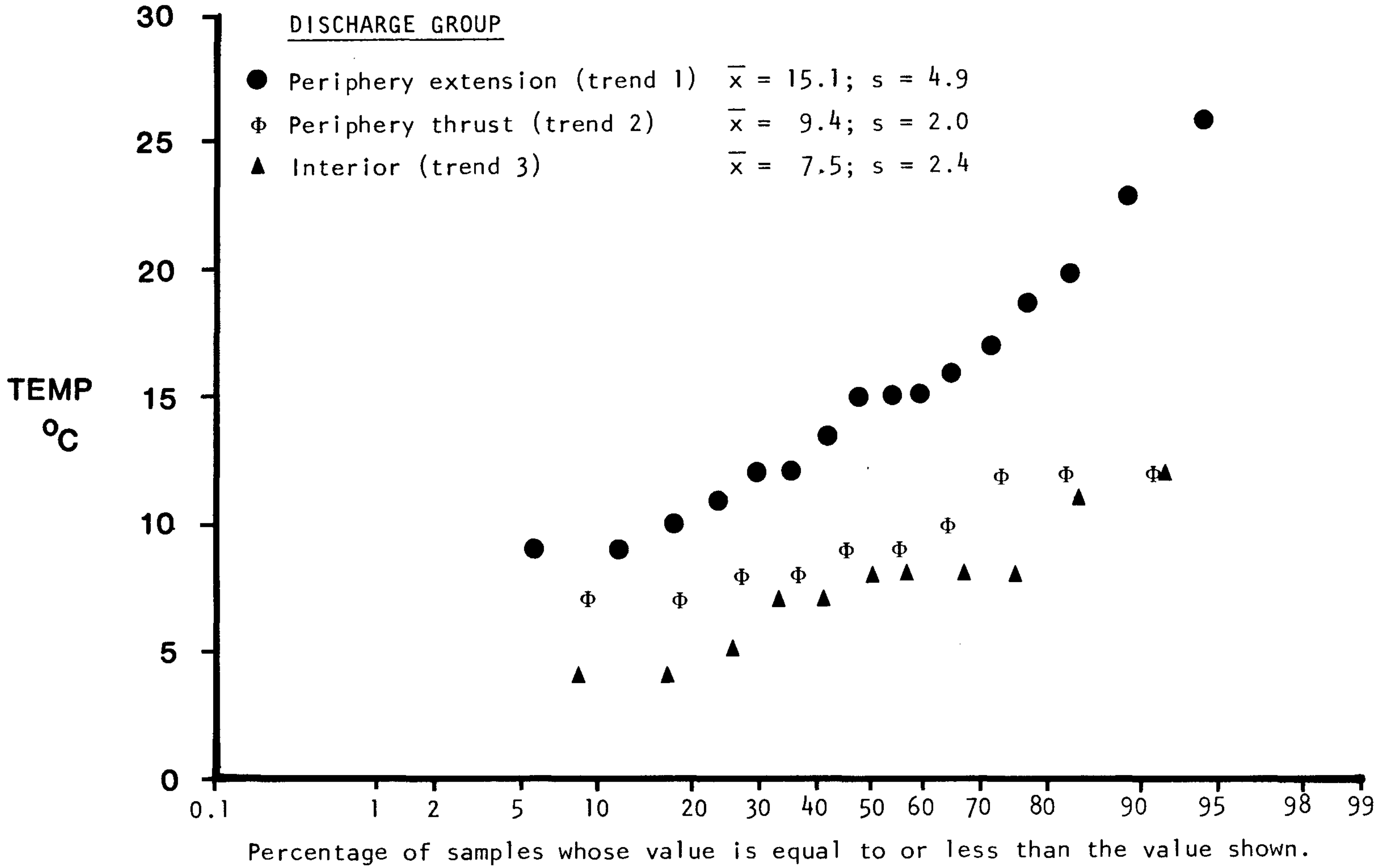

Figure IV-19. Cumulative frequence distribution of discharge temperature grouped by discharge groups. Mean ($\bar{x}$) and standard deviation (s) are shown for each group.

waters from periphery thrust and interior springs. A summary of t test results is shown in Table IV-6.

Table IV-6. Results of discharge temperature t tests

Trends Tested	(X - X)	U Test Criteria
1 vs 2	5.73	2.87
1 vs 3	7.68	2.99
2 vs 3	1.95	2.07

Two mechanisms, heat loss from Pleistocene volcanics and the geothermal gradient, are the most likely sources of heat responsible for the warming of the discharge water of the periphery extension springs. Mabey and Oriel (1970) report two cycles of volcanism in the Blackfoot Reservoir graben. During the first cycle basalt accumulated in a local depression east of the present reservoir; the basalt has been dated by reverse remnant magnetism as greater than 700,000 years before the present. During the second phase, basaltic volcanics accumulated in depressions south and west of the present reservoir. The three prominent volcanic cones, China Hat, North Cone and South Cone, have been dated by K-Ar methods as about 100,000 years old (Armstrong and others, 1975). The cones are located near the center of the graben. They are chiefly rhyolitic and are thought to be older than the second cycle of basaltic deposition in the lava field.

Four lines of evidence suggest the shallow basalts are not the heat source for the periphery extension group. First, springs 5-9 are located considerably south of the volcanics in the graben. Second, the water chemistry of the periphery extension springs is not typical of basaltic waters. Basaltic aquifers generally have high Ca/Mg ratios and high Cl^- concentrations (White and others, 1963), whereas the periphery extension springs do not. Third, spring discharge elevations are above nearby elevations of the lava field. Fourth, water table contours in the basalt, developed by Dion (1974) a part of an investigation of leakage from the Blackfoot Reservoir, and independently developed contours by Seitz and Norvitch (1979) indicate shallow ground water flow paths in the basalt are to the southwest, away from the periphery extension springs.

The regional geothermal gradient can account for maximum estimated aquifer tempreatures. Temperature variations between spring groups may be explained by variations in the depth of circulation patterns. Mansfield (1927) and Mitchell (1976) estimated a regional geothermal gradient of 40°C/km for the Meade thrust area. Brott and others (1976) estimated geothermal gradients just north of the area, near Rexburg, Idaho, to be in the range of 16 to 80°C/km. (Rexburg is on the edge of the Snake River Plain.) Ralston and others (1981) calculated geothermal gradients in the range of 19 to 61°C/km from oil and gas exploration borehole data from the overthrust belt in southeastern Idaho.

Flow Patterns Suggested by Chemical and Physical Data

The complex rock-water interactions that occur in ground water flow systems may be described by an analysis of the chemical and physical characteristics of the discharge waters from the system. In a geologically complex region such as this study area, the chemical-physical characteristics of an individual discharge are very complex. However, properly organized and analyzed chemical-physical data allow the classification of characteristics associated with the various aquifer types in the region and the analysis of ground water flow patterns.

Three aquifer types have been identified in the study area. The types are: 1) aquifers discharging along periphery extension faults, called periphery extension aquifers, 2) aquifers discharging along or near periphery thrust faults, called periphery thrust aquifers, and 3) aquifers discharging in the upland, interior regions of the allochthon, called interior aquifers. This classification scheme, originally selected on the basis of apparent structural and stratigraphic controls regulating the location of springs, has served well as an organizational umbrella for the characterization of the chemical-physical signatures of the waters analyzed. The chemical-physical characteristics of the aquifer types are summarized in Table IV-7.

Periphery Extension Aquifers. The periphery extension springs are the discharge area of a major group of deep circulating, regional type aquifers whose individual flow systems have similar patterns and encounter similar geologic conditions and whose waters have similar chemical-physical properties. The aquifers are restricted to the upper Paleozoic formations. Circulation patterns are largely controlled by the configuration of the bedding in these formations; however, discharge patterns are fault controlled. The aquifers have calcium-bicarbonate type water resulting from the dissolution of limestone. The discharge waters have the highest Ca/Mg ratios and concentrations of carbonate dissociation products in the study area. The discharge waters are also saturated or supersaturated with respect to calcite. Discharge waters are generally in the low thermal range, and appear to be heated as a result of the geothermal gradient. Calcite saturation appears to result from the decreased solubility of calcite at the elevated temperatures encountered deep in the aquifer. Dissolution of carbonate minerals probably occurs under open system conditions in the presence of CO_2 soil gas during the slow movement of water through the unsaturated zone. This suspected slow movement through the unsaturated zone may be the cause of the

Table IV-7. Summary of the chemical and physical characteristics of discharges from springs and wells in the Meade thrust area, southeastern Idaho.

	Periphery extension	Periphery thrust	Interior
Number of samples	16	10	11
Discharge temperature			
mean (°C)	15.1	9.4	7.5
standard deviation	4.9	2.0	2.4
Discharge elevation			
mean (meters)	1880	2065	varies greatly
standard deviation	19	117	na
Discharge volume			
% springs having discharge less than 20 l/sec	18.2	0	67.1
% springs having discharge 21 - 99 l/sec	36.4	30.0	14.3
% springs having discharge 100 - 200 l/sec	18.2	40.0	28.6
% springs having discharge 200 - 625 l/sec	27.2	30.0	0
Ca/Mg ratio			
mean	3.4	2.2	2.4
standard deviation	0.9	0.6	0.9
Calcite saturation Index (SI_c)			
mean	1.33	0.93	0.74
standard deviation	0.38	0.31	0.22
% less than 0.9	12.5	40.0	81.8
% 0.9 - 1.1	12.5	30.0	0
% greater than 1.1	75.0	30.0	18.2
Ca-Mg-HCO_3 concentration			
mean (meq/l)	23.2	8.5	8.9
standard deviation	9.4	0.7	1.6
Radiocarbon age (y.b.p.)	12,500 to 20,500	less than 450	less than 300
Discharge control	Deepseated extension faults.	Splays of the Meade thrust fault; some bedding plane.	Bedding plane and shallow extension fault.
Remarks	Massive travertine deposits.		Interbasin discharges are less than 20 l/sec; intrabasin discharges are usually greater than 100 l/sec.

increased concentration of calcite dissolution products. Mean ground water residence times are in the range of 12,700 to 20,500 radiocarbon years.

Ground water storage capacity of these systems is great, as shown by the nearly constant and large spring discharges. As a group of these aquifers support the largest springs in the Meade thrust area. Ground water flow paths are primarily bedding plane controlled, and discharge is controlled by the extension fault system, which truncates the upper Paleozoic formations at depth, along the western periphery of the allochthon. The ascent of ground water along the extension structures in the discharge area lowers the water temperature and the confining pressure. Lowered temperatures and confining pressures trigger a series of chemical reactions resulting in the deposition of extensive travertine deposits and the evolution of CO_2 gas. The deposition of travertine periodically seals spring discharge vents, causing a migration of discharge areas along the extension fault system. In the discharge areas the flow systems appear to have a common hydraulic head at about 1900 m.

Periphery Thrust and Interior Aquifers. The periphery thrust and interior springs are the discharge areas of shallow to possibly moderately deep circulating, local and intermediate type ground water systems. The aquifer systems are contained by the upper Paleozoic and lower Mesozoic formations. Classification of the interior aquifers into interbasin and intrabasin types, as proposed by Winter (1979) and others, is useful when describing their flow paths. The Meak Peak Phosphatic Shale Member of the Phosphoria Formation is believed to form a hydraulic barrier separating individual aquifers within the interior and periphery thrust aquifer systems. In general, interior intrabasin ground water flow systems occur above this barrier, and interior interbasin ground water flow systems occur below it.

The periphery thrust and interior aquifers have many common chemical-physical properties. Both aquifer groups have calcium-bicarbonate type waters that are nonthermal and low in carbonate mineral dissociation products, and have low Ca/Mg ratios. Despite these similarities, there are differences between the two aquifer groups. The most significant chemical difference is the degree of saturation with respect to calcite; discharge waters from the periphery thrust aquifers are generally saturated, whereas those of the interior aquifers are not. Discharge volumes and temperatures also help distinguish between the two groups. Periphery thrust springs have slightly greater discharge temperatures and greater discharge volumes.

Dissolution of carbonate minerals generally occurs under open system conditions. Much of the recharge may occur on steeper slopes where the residual material in the unsaturated zone is relatively thin. A thin layer of unconsolidated material in the unsaturated zone may allow water to move fairly rapidly through the unsaturated zone. Rapid movement through the unsaturated zone would result in the water of the saturated zone having a low concentration of carbonate dissolution products and being undersaturated with respect to calcite. A consequence of this undersaturation and the shallow circulation of the periphery thrust and interior aquifers, which limits significant warming of the ground water, is the sustained undersaturation of the water along the flow path. Travertine deposits do not develop because the discharge waters are undersaturated with respect to calcite.

Mean carbon-14 ages of interior interbasin and periphery thrust ground waters are generally less than 300 years, although a mean age of 450 years was determined for the waters of one periphery thrust spring. A mixing of recharge water containing "bomb" carbon with other recharge waters in these aquifers suggests that the flow systems are not hydraulically isolated along the entire length of their flow paths.

Ground water flow patterns of both groups of aquifers are primarily bedding plane controlled. Discharge locations of the interior aquifers are typically at the intersection of a topographic low and a bedding surface, although some discharge locations are along shallow extension faults. Splays of the Meade thrust fault regulate the discharge location of many periphery thrust aquifers. These thrust splays appear juxtapose strata of differing hydraulic conductivities and thus form high hydraulic conductivity zones parallel to the thrust surface.

Proposed Three Tier Ground Water Flow Model

This investigation has documented the occurrence and flow patterns of three major bedrock aquifers systems. These systems are: 1) the interior aquifers described by Winter (1979) and others, 2) previously undescribed system of shallow aquifers along the eastern and southern borders of the allochthon, and 3) the deep circulating aquifers which have been postulated by some previous investigators.

The three tier model proposed in this report incorporates the three major aquifer systems documented in this report and the regional hydraulic barrier formed by the Meade Peak Phosphatic Shale Member of the Phosphoria Formation (Figure IV-20). The top two tiers describe ground water flow patterns in the Meade thrust allochthon, and a third, lower tier describes the possible existence of very deep flow systems. Tiers one and two are restricted to bedrock aquifers and are defined by their relative positions to the low hydraulic conductivity zone created by the Meade Peak Phosphatic Shale Member.

Tier one ground water flow systems include most aquifers which discharge as springs in the interior regions of the allochthon as well as a few aquifers which discharge along

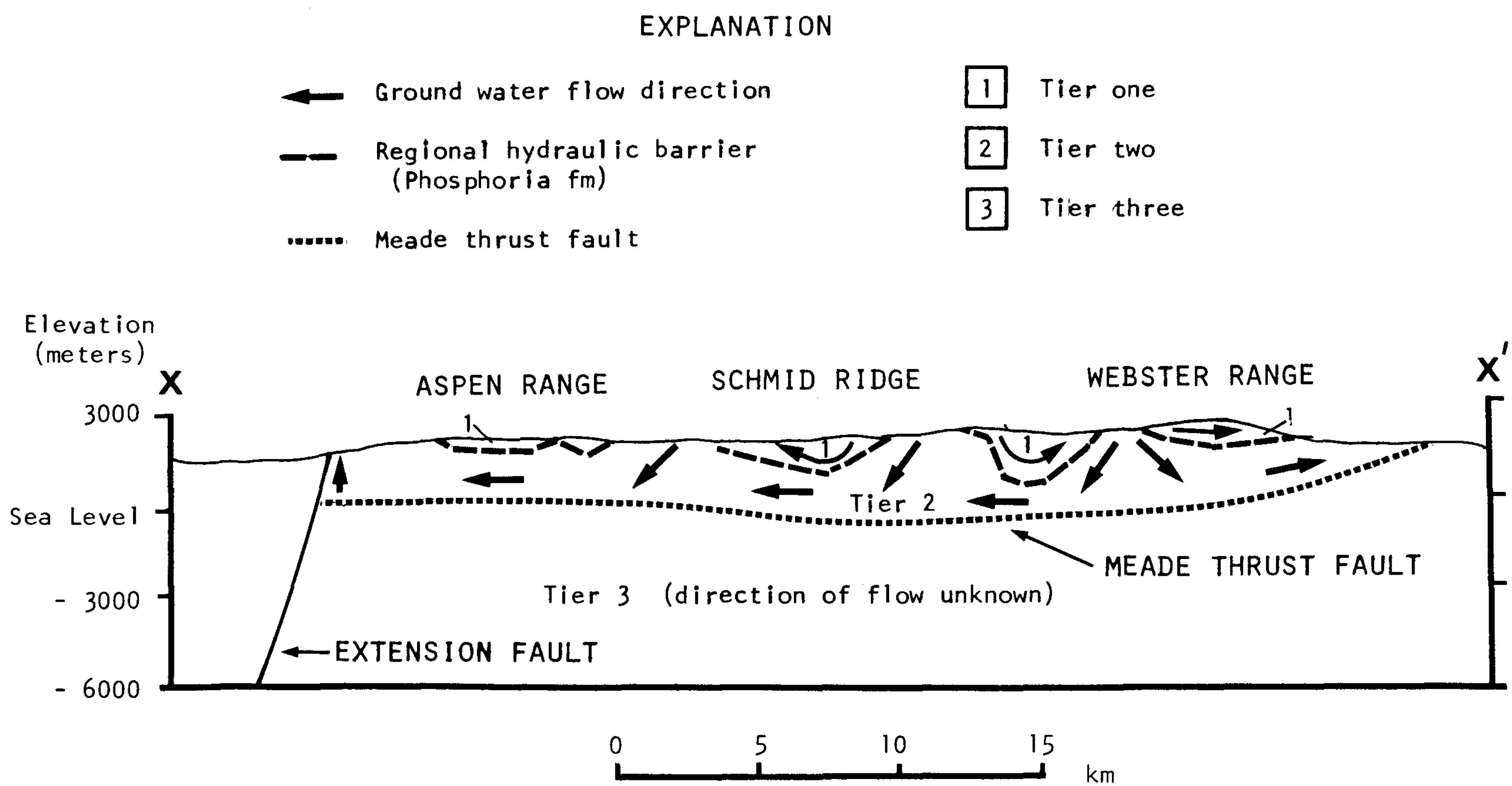

Figure IV-20. Postulated three tier ground water flow model in the Meade thrust area, southeastern Idaho. See Figure 34 for location.

the periphery thrust splays. As previously mentioned, these systems tend to be shallow to moderately deep circulating, intermediate type flow systems. Flow paths generally tend to follow beding planes and are perpendicular to the fold axial traces. Flow paths are also perpendicular to the trend of the ridge and valley system, since topographic trends are coincident with fold trends.

Two tier one springs, Auburn Hatchery (21), and Star Valley (24), have been identified in the periphery thrust group. These springs discharge along the northern portion of the Webster Range where erosion has not exposed the upper Paleozoic formations. It is uncertain if the two springs discharge from the same aquifer. The system(s) are recharged at higher elevations in the Webster Range. The discharge waters are saturated with respect to calcite, suggesting deeper circulating flow paths than most interbasin systems; however, bomb carbon identified in the discharge water suggests the aquifer(s) are not continuously hydraulically isolated from the surface along the flow path.

Tier two ground water flow systems include a few aquifers which discharge as springs in the interior regions of the allochthon, most aquifers which discharge as springs along periphery thrust splays and all aquifers which discharge along periphery extension faults.

Interior discharging tier two aquifers have flow patterns similar to the intrabasin and interbasin types of tier one. These aquifers have very short flow paths and their waters circulate shallowly. Periphery discharging tier two aquifers may be divided into west and east lobes. The west lobe includes all aquifers discharging as periphery extension springs and the east lobe includes the periphery thrust aquifers supported by the uppper Paleozoic formations. Both lobes have been further divided into sublobes on the basis of similar geologic and hydrologic characteristics and probably similarities in flow directions.

Determinations of flow path directions and recharge areas are hampered by the complex folding and faulting and the absence of potentiometric data. It is possible, however, to speculate about some flow directions and recharge areas by making two assumptions: 1) the bedding plane flow path control mechanism which dominates tier one systems also dominates tier two, and 2) the deep geologic structure sections published on the area are reasonably accurate. Using these assumptions, probable flow directions of the subtiers were developed and are shown diagrammatically in Figures IV-20 and IV-21. The degree of certainty of the suggested flow directions and recharge areas varies substantially. A higher degree of certainty may be assigned in southern portion of the allochthon than in the northern

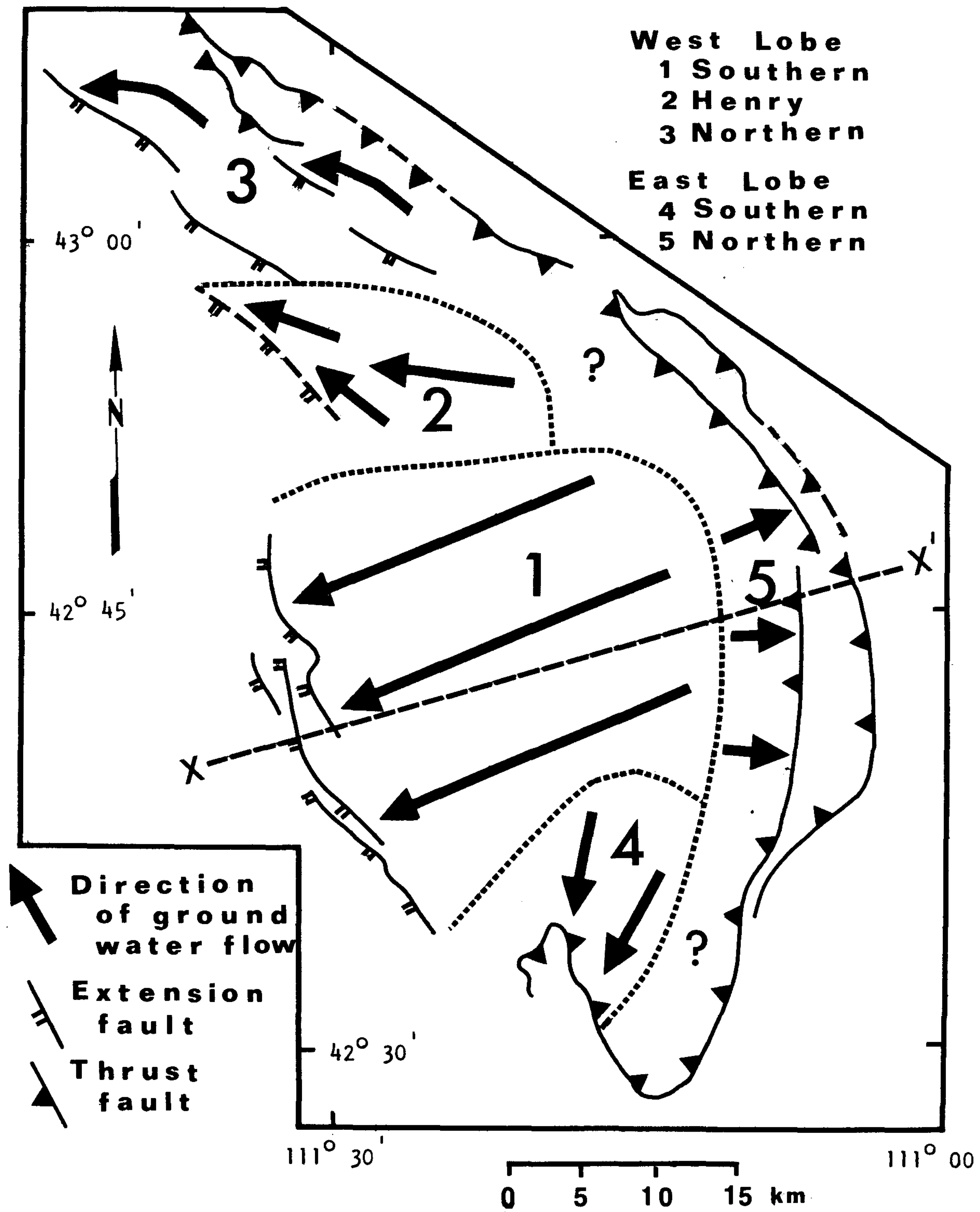

Figure IV-21. Postulated ground water flow directions in tier two. Flow directions of tier two aquifers which discharge in the interior of the Meade thrust allochthon are not shown. See text for description of sublobes. Structure section X - X' is shown on Figure 33. Dotted line shows approximate sublobe boundaries.

portion. In the southern portion, folding is the subsurface structure, whereas faulting is more pronounced in the northern portion. Potential recharge areas are restricted to outcrops of the upper Paleozoic formations or areas where soil, alluvium, etc., cover these formations.

The western lobe has been divided into three sublobes, the southern, Henry, and northern; the eastern lobe has been divided into the northern and southern sublobes. Characteristics of the sublobes are described below:

Lobe	Sublobe	Spring ID #	Characteristics
West	Southern	3-9	Discharge from the Aspen Range frontal fault system; large storage capacity aquifers having individual discharges up to 625 l/sec; discharge temperatures range from 9° to 17°C; extensive travertine deposits; common discharge head of 1905 m; radiocarbon age about 15,000 years; probable recharge in the interior valleys and valleys in eastern Aspen Range; total estimated discharge about 1100 l/sec.
	Henry	10-15	Discharge related to Henry fault; storage capacity unknown; discharge volumes up to 88 l/sec; discharge temperatures range from 15° to 26°C; massive common travertine area; common discharge head of 1905 m; radiocarbon age about 20,000 years; recharge area unknown; total estimated discharge about 225 l/sec.
	Northern	2,16, 17	Isolated aquifers discharging unconnected extension faults; discharge volumes up to 246 l/sec;

			storage capacities vary; discharge temperatures 19° to 20°C; some with extensive travertine deposits; others without travertine; radiocarbon age dated at about 1,800 and 13,000 years; recharge areas unknown; total estimated discharge 425 l/sec.
East	Southern	18,19, 20	Discharge long splays of Meade thrust; discharge volumes up to 448 l/sec; discharge temperatures 7° to 8°C; bomb carbon identifed in radiocarbon analysis - oldest ground water age estimated at 300 to 450 years; no recent travertine and only minor older travertine; probable recharge areas in southern Aspen Range and southern Dry Ridge; total estimated discharge 900 l/sec.
	Northern	20,23, 25,26, 29	Discharge along splays of Meade thrust and thrust fault bound slices of strata; discharge volumes up to 246 l/sec; discharge temperature up to 12°C; oldest radiocarbon age 450 years - bomb carbon identified in most analyses; recharge area in Webster Range; total esti-mated discharge 900 to 1200 l/sec.

Tier three has been identified largely by interference. Diagnostic thermochemical characteristics of water circulating deeply in the lower plate have not been detected in any tier one or tier two waters. Because the allochthonous formations and adjacent formations are repeated in the lower plate, it is reasonable to expect the lower plate strata to contain ground water flow sytems. Oil and gas exploration boreholes have encountered ground waters with temperatures above 100°C below the Meade thrust. These temperatures confirm the existence of flow systems in the lower plate strata, but provide little information concerning their flow directions or other characteristics. It is likely that ground water movement and recharge and discharge volumes in this tier are very small.

CHAPTER V

HYDROGEOLOGIC RECONNAISSANCE OF THE SOUTHERN SUBAREA

Introduction

This portion of the study is a hydrogeological reconnaissance of the region bordered roughly by the Blackfoot River on the north, Cache Valley on the west and the Idaho state line on the south and east (Figures I-1 and V-1. The study area encompasses approximately 4,700 square kilometers in parts of Bear Lake, Caribou, and Franklin counties, Idaho.

The southern subarea is characterized by north and northwest trending mountain ranges and valleys. The principle mountain ranges in the study area are the Bear River Range trending north-south from Soda Springs into Utah, and the Chesterfield Range trending northwest from Soda Springs to the Blackfoot River. The Portneuf Range joins the Bear River Range in a hilly region on the western side of the study area.

Elevation generally increases from the southwest to the east and northeast. The lowest elevation is about 1,395 m near Franklin in the southwest corner, and the highest elevation is 2,998 m at the summit of Sherman Peak in the northern Bear River Range. Local reliefs of 300 to 600 m are common in the area.

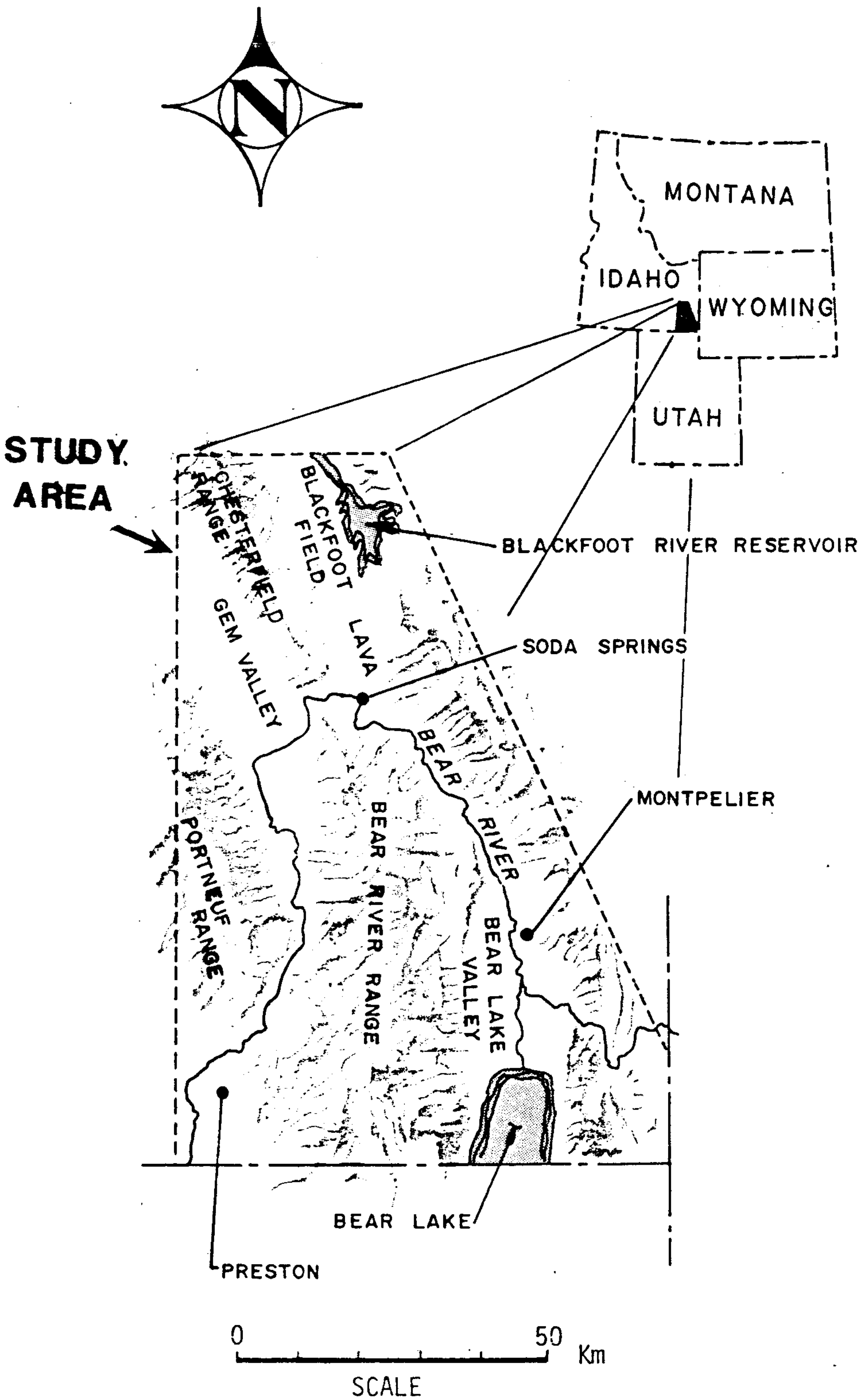

Figure V-1. Location map of study area in southeastern Idaho.

Geologic Setting

The study area lies in a region of southeastern Idaho that is transitional between the Basin and Range and Middle Rocky Mountains Physiographic Provinces. It consists primarily of wide, deeply-filled intermontane basins (grabens) separating folded, block-faulted ranges (horsts).

The Bear River Range and Chesterfield Range combine to form a major north-northwest trending horst. The Paris thrust, trending north-south on the eastern side of the Bear River Range is the first of the series of great thrust faults that comprise the overthrust belt to the east. The rocks of the overthrust belt have intense folds, many of which are overturned to the east and are cut by younger thrust faults of great length and displacement. In the Bear River Range and to the west, folding decreases in intensity and frequency, and normal faulting increases (Keller, 1963). The Portneuf Range joins the Bear River Range in an intensely faulted, hilly divide in the southwestern portion of the study area.

Stratigraphic units recognized in southeastern Idaho span in age from Precambrian to Recent and are describe in Table V-1. Precambrian metasediments outcrop in a few isolated locations in the southwestern corner of the study area (Figure V-2). Lower Paleozoic marine sediments are the most extensive rocks in the study area and comprise most of

Table V-1. Stratigraphic column for Bear River Range and surrounding areas, southeastern Idaho.

System	Symbol	Group or Formation	Thickness (m)	Lithology
Quaternary	Qal	Stream alluvium		Unconsolidated, well to poorly sorted, gravel, sand, silt, and clay
	Qtg	Terrace gravels		
	Qls	Landslide debris	0-100	
	Qf	Alluvail fan deposits		
	Qc	Colluvium		
	Qdm	Diamictite		
	Qtr	Travertine		
		Gentile Valley Group		
	Qb	Gem Valley basalt	0-1000(?)	Dark gray, vesicular, porphyritic, massive olivine basalt
	Qbc	Basalt cinders		Loose scoriaceous red-weathering cinders
	Qmc	Main Canyon formation	0-20	Poorly consolidated silt and marl, grades into sand and gravel
		Lake Bonneville Group		
	Qp	Provo formation	0-30	Unconsolidated gravel and sand deposited along shoreline of Lake Bonneville in the Provo stage
	Qpb	Pink silt	?	Unconsolidated, thinly bedded silt and clay in deeper parts of Lake Bonneville
	Qbo	Bonneville and Alpine formations, undifferentiated	0-30	Poorly consolidated gravel and sand deposited along shoreline of Lake Bonneville in the Alpine and Bonneville stages
	Qtr	Rhyolite domes	?	Tan-weathering, partly devitrified glass, Quaternary and Tertiary
Tertiary		Salt Lake formation	0-3000(?)	Conglomerate, volcanic ash, marl, calcareous clay, and sandstone
		Wasatch formation	0-450	Red conglomerate and sandstone interbedded with tan limestone
Upper Jurassic	Js	Stump formation	50-100	Gray-green silty limestone, calcareous siltstone and sandstone
	Jp	Pruess formation	0-200	Red shaley sandstone and siltstone
	Jsp	Stump/Pruess formations, undifferentiated		
Middle Jurassic	Jtc	Twin Creek formation	200-500	Dark-gray shaley limestone, oolitic limestone and siltstone
Lower Jurassic	Jn	Nugget formation	100-500	Reddish-brown, well-sorted, fine-grained sandstone
Upper Triassic	Tra	Ankareh formation	90-200	Red calcareous shale and siltstone
Lower Triassic	Trt	Thaynes formation	250-300	Upper Member, gray limestone interbedded with brownish-gray siltstone; Middle Member, brownish-gray siltstone and silty limestone; Lower Member, black to gray shale and siltstone
	Trw	Woodside formation	100-400	Reddish-brown siltstone and shale

Table V-1. Continued.

System	Symbol	Group or Formation	Thickness (m)	Lithology
Lower Triassic (cont'd)	Trd	Dinwoody formation	100-600	Upper Member, gray limestone interbedded with olive-brown siltstone; Lower Member, olive-brown calcareous siltstone interbedded with gray limestone
Permian	Pp	Phosphoria formation	70-100	Rex Chert Member, black to white chert interbedded with black cherty mudstone; Phosphatic Shale Member, dark-brown to black mudstone, limestone and oolitic phosphate rock
Pennsylvanian	PPw	Wells formation	300-900	Upper Member, light-gray to reddish-brown sandstone interbedded with light brown limestone; Lower Member, gray limestone and silty limestone with interbedded sandstone
Mississippian	Mm	Mission Canyon formation	300-800	Light- to dark-gray cherty limestone and dolomite
	Ml	Lodgepole formation	200-400	Dark-gray limestone and dolomite
Upper Devonian	Db	Beirdneau formation	200-275	Gray and tan dolomite and sandy dolomite with pink sandstone and gray limestone in lower part
Middle Devonian	Dh	Hyrum formation	350-500	Light- to dark-gray, finely crystalline dolomite
	Dbh	Beirdneau/Hyrum, undifferentiated		
Silurian	Sl	Laketown formation	300-400	Very light- to medium-gray, finely crystalline dolomite
Upper Ordovician	Of	Fish Haven formation*	80-150	Dark-gray dolomite with interbeds of light-gray dolomite and dark-gray chert
Middle Ordovician	Osp	Swan Peak formation*	200-300	White, tan, and pink, well sorted, well rounded fine- to medium-grained quartzite
Lower Ordovician	Ogc	Garden City formation*	350-400	Medium-gray, medium crystalline dolomite and dark-gray chert with dark-gray limestone in lower part
Upper Cambrian	Ꞓsc	Saint Charles formation*	300-550	Medium-gray medium crystalline limestone with interbeds of chert and conglomerate
Middle Cambrian	Ꞓn	Nounan formation*	200-300	Gray and blue-gray domomite and dark-gray silty limestone and sandstone
	Ꞓbo	Bloomington formation*	250-300	Green shaley micaceous mudstone with interbeds of brown siltstone, sandstone and limestone
	Ꞓbl	Blacksmith formation*	270-400	Medium-gray to buff, finely to coarsely crystalline limestone
	Ꞓu	Ute formation*	100-200	Medium-gray limestone with interbeds of shale and silt

Table V-1. Continued.

System	Symbol	Group or Formation	Thickness (m)	Lithology
Middle Cambrian	Ꞓl	Langston formation*	100-120	Light-gray coarsely-crystalline dolomite with interbeds of dark-gray limestone
	Ꞓul	Ute/Langston formations, undifferentiated		
Lower Cambrian	Ꞓq	Brigham formation*	3000+	White, buff, purple, and pink, poorly sorted quartzite with interbeds of conglomerate and phylite
Pre-Cambrian	pꞒql and pꞒq	Quartzite and limestone	?	Mainly gray, pink, and green, poorly sorted quartzite, and thin, dark-gray limestone units
	pꞒmd	Metadiabase	?	Medium- to coarsely-crystalline diabase with alabitized plagioclase and actinolite in chloritic matrix
	pꞒmg and pꞒs	Metagraywacke and shale	?	Very poorly sorted detrital rock with clasts of quartz and feldspar in chloritic matrix

* Principle Pre-Tertiary formation in study area

(Arrigo, 1982; Cressman and Gulbrandsen, 1955; Hubbell, 1982; Jobin and Schroeder, 1964a; Mansfield, 1927; Oriel, 1968; Oriel and Lucian, 1980; Oriel and Platt, 1968, 1980; Pampeyan and others, 1967; Staatz and Albee, 1966) the Bear River and Portneuf Ranges. These rocks probably comprise the basement rocks of the Cache and Gem Valleys. Upper Paleozoic and Mesozoic rocks occur in the northern part and to the east of the study area. Tertiary strata consisting of semi-consolidated to unconsolidated conglomerates, sandstones, and siltstones fill the intermontane basins and cover some higher areas. Quaternary alluvium, colluvium, basalts and rhyolites comprise a major portion of the surficial geology. Extensive fine-grained lacustrine sediments cover the surface in the southern portion of the Gem Valley and in Cache Valley from Pleistocene lakes Thatcher and Bonneville, respectively (Bright, 1960 and 1963).

The horst and graben structures of this region have produced ranges and basins comprised of different lithologies and structures. These horsts and grabens include the: 1) Bear River Range horst, 2) Portneuf Range horst, 3) Chesterfield Range horst, 4) Bear River Valley graben, 5) Gem Valley graben, and 6) Cache Valley graben. The geology of these units is described in the following paragraphs.

The Bear River Range is bounded on the east and west by Bear Lake and Bear River Valleys, on the south by Cache Valley and on the north by Gem Valley. An east-west hilly divide north of the village of Mink Creek joins the Bear River and Portneuf Ranges. The Bear River Range is "a deeply eroded, synclinal, karst plateau, with wide basins and occasional ridges and peaks on top" (Keller, 1963, p. 60). The range consists mostly of Cambrian to Ordovician marine sediments of the Fish Haven syncline.

The portion of the Portneuf Range within the study area is bordered by the Cache Valley to the south and Gentile and Mound Valleys to the northeast. North of the junction with the Bear River Range, the Portneuf Range is composed of relatively simple, faulted homoclines of lower Paleozoic rocks dipping generally to the northeast. At the range junction, the structure is complex with a very high intensity of normal and reverse faults. Precambrian metasediments outcrop in several localities in this area.

Bear River Valley is a long narrow graben extending from Bear Lake north to near the Blackfoot Reservoir. It is bordered on the east by a high angle normal fault extending in length at least 90 km. The characteristics of the western border of the graben are uncertain. Keller (1963) calls the Bear River Valley a half-graben downdropped on the east side by the East Bear Lake fault and with the bedrock unbroken by normal faulting on the west side. Witkind (1975) shows the western border of the graben as an en echelon series of short, high-angle normal faults.

The graben is filled predominantly with sediments of the Tertiary Salt Lake Group. The surface of the valley from several kilometers south of the town of Soda Springs northward into the Blackfoot Lava Field is covered predominantly with Quaternary basalt. An area of high magnetic intensity about 1550 m (5,000 ft) deep near China Hat, shown on Figure V-2, indicates a possible deep intrusive body related to the basalt vents on the Blackfoot Lava Field (Armstrong, 1969; Mabey and Oriel, 1970). The surface in the southern portion of the valley is covered predominantly by Quaternary colluvial, fluvial, and lacustrine sediments.

Gem Valley graben is bordered on the east by the East Gem Valley fault, a high angle normal fault extending about 50 km, and on the west by the West Gem Valley fault extending about 40 km (Witkind, 1975). Gem Valley is almost entirely covered with Quaternary basalts which are thin near the edges and thicken to about 620 m in the center. Gravity lows south of the town of Grace suggest light rocks, probably Tertiary sediments, about 2,500 m thick (Mabey and Oriel, 1970).

The northern Cache Valley is a complex half graben bounded on the east by the East Cache fault (Keller, 1963). The western boundary of the graben is covered by Pleistocene Lake Bonneville alluvium; the East Cache fault is covered in places by Tertiary sediments. The East Cache fault separates the Cache Valley basin from the Fish Haven syncline of the Bear River Range. The graben is filled with an estimated 3,100 m (10,000 ft) of Tertiary sediments (Stanley, 1972).

The surface materials are primarily Pleistocene Lake Bonneville deposits (Keller, 1963).

Physical and Chemical Characteristics of Springs and Wells

This study included analysis of the hydrogeologic settings and hydrochemistry of 32 spring and well sites. Data on eight springs analyzed during a concurrent study by Souder (1982), and 13 wells sampled by Dion (1969) were also included. Thousands of springs and wells are present in this portion of southeastern Idaho; the 53 sites used for this study were selected to represent the full range of thermal and non-thermal ground water systems in the area. The locations of the springs and wells sampled are shown on Figure V-3. Hydrogeologic data on the sites are presented in Table V-2. Hydrochemical data are presented in Table V-3.

Analysis of Physical Data

Introduction

Geologic formations and structures associated with springs and wells are examined in this section for trends that may identify important stratigraphic and structural controls on the distribution of ground water discharges. Discharge rates are compared with water temperatures. Variations in the hydrochemical characteristics of the ground water discharges are explored and quantified using

Table V-2. Inventory of and hydrogeologic data from springs and wells sampled in southeastern Idaho.

Sample Number	Name and Location	Water Temp. (°C)	Elevation (m above MSL)	Well Depth (m)	Depth to Water (m)	Discharge (l/s)	Site Description
B-1	Corral Creek Well 6S 41E 19bbd	40	1880	?	flowing	< 1	One of many phosphate exploration holes drilled by FMC into a broad north-northwest trending anticline of upper-Paleozoic rocks. The holes average 57 m in depth.
B-2	Gem Valley Spring #1 8S 40E 26bdcS	13	1710			5.7	Flows out of extensive flat travertine deposit over-Quaternary basalt, approximately on the East Gem Valley fault. Ordovician Garden City limestone out-crops in range near spring.
B-3	Thermal Gradient Well 8S 40E 26dbc	15	1710	61	flowing	1.4	Well drilled by Phillips Petroleum as thermal grad-ient hole. Located just south of spring B-2 along same graben-forming normal fault.
B-4	Gem Valley Spring #2 8S 40E 26dcbS	16	1720			14	Flows out of base of 3m high bluff in Quaternary basalt just south of sites B-2 and B-3. Spring is depositing thin layer of white calcareous tufa on the basalt.
B-5	Soda Creek Headwaters 8S 41E 26dabS	13	1810			140	One of many springs that well up through thin veneer of alluvium overlying basalt of Blackfoot Lava Field.
B-6	Hooper Spring 8S 41E 36dddS	10	1800			23	Flows out of Quaternary basalt of Blackfoot Lava Field near contact with Paleozoic sediments forming Soda Springs Hills.
B-7	Soda Springs Geyser 9S 41E 12adaS	29	1770			?	One of several small springs occurring along a north-south trending fracture trace through a large traver-tine mound in downtown Soda Springs.
B-8	Unnamed Spring 10S 42E 12ccbS	8	1800			0.8	Flows out of Tertiary Salt Lake formation, composed of large rounded quartzitic boulders, near contact with Bear River floodplain.
B-9	Cold Spring 10S 42E 31daaS	7	1950			160	Flows out of base of hill marking the contact be-tween shallow alluvium of Cow's Fork and Cambrian Blacksmith limestone.

Table V-2. Continued.

Sample Number	Name and Location	Water Temp. (°C)	Elevation (m above MSL)	Well Depth (m)	Depth to Water (m)	Discharge (l/s)		Site Description
B-10	Trout Creek Spring 11S 41E 15cdaS	5	1710			200	E	Flows out of Cambrian Nounan limestone. A short distance down the canyon is a large apparently old travertine deposit.
B-11	Unnamed Spring 12S 41E 18acdS	13	1510			440		Flows out of thin Quaternary alluvium in shallow broad valley overlying Paleozoic rocks, either the Cambrian Nounan or Cambrian St. Charles limestone.
B-12	Harris Spring 11S 41E 8dbcS	10	1600			<10	E	Spring emerges high on Quaternary basalt bluff where the lavas of the Gem Valley terminate above Gentile Valley.
B-13	Pescadero Warm Spring 11S 43E 36bdaS	23	1820			<1	E	Spring flows from top of large travertine bluff overlooking Bear River. Extensive travertine mound overlies lower Triassic Thaynes limestone.
B-14	Unnamed Spring 12S 44E 7baaS	12	1940			3		Flows out of Tertiary Salt Lake formation and is piped about 90 m into watering trough.
B-15	Unnamed Spring 13S 43E 8daaS	11	1820			20		Spring occurs at the contact between the Quaternary alluvium and lower Triassic Thaynes limestone.
B-16	Williams Creek Spring 12S 41E 27bbaS	7	1710			420	E	Flows out of Cambrian Nounan limestone dipping approximately 10-15° to the northeast.
B-17	Unnamed Spring 12S 41E 31abcS	18	1540			10	E	Flows out of large travertine mound overlying Quaternary lacustrine sediments which also overlay Cambrian Blacksmith (?) limestone.
B-18	Mink Creek Spring 13S 41E 24bbcS	6	1800			280	E	Flows out of Cambrian Nounan limestone dipping 10-20° to the northeast. Highly faulted and fractured area.
B-19	Paris Creek Spring 14S 42E 13badS	9	2000			850	E	Issues from base of very high cliff at head of Paris Creek. Cliff is mostly Cambrian Bloomington limestone.
B-20	Jarvis Spring 14S 43E 19bcdS	7	1930			410		Flows out of Cambrian Blacksmith limestone in Bloomington Canyon.

Table V-2. Continued.

Sample Number	Name and Location	Water Temp. (°C)	Elevation (m above MSL)	Well Depth (m)	Depth to Water (m)	Discharge (l/s)	Site Description
B-21	Unnamed Spring 14S 41E 15acdS	8	1910			10 E	Flows out of Cambrian Brigham Quartzite dipping approximately 30° to the east. Rock is very hard and appears highly fractured.
B-22	Burgquist Spring 15S 41E 10aadS	6	1780			420 E	Flows out of Cambrian Nounan limestone dipping about 10-20° to the northeast.
B-23	Sadducee Spring 16S 43E 8cbbS	6	2100			230	Issues from side of canyon and out of middle to lower section of Ordivician Garden City limestone.
B-24	Unnamed Spring 16S 40E 15ddbS	9	1440			3 E	Seeps out of Quaternary alluvium next to Maple Creek. Cement holding tank and pump house constructed over spring for domestic water supply.
B-25	Bear Lake Hot Spring #1 15S 44E 13ccaS	40	1810			<10 E	Located along escarpment of East Bear River Valley fault. Mississippian Brazier limestone forms the slope.
B-26	Bear Lake Hot Spring #2 15S 44E 13cbaS	39	1810			<10 E	Located about .3 km north of spring number B-25 along the escarpment.
B-27	Bear Lake Hot Spring #3 15S 44E 12ccdS	33	1810			<10 E	Located 1.3 km north of spring B-25 along the escarpment. The spring seeps out of colluvium.
B-28	Gentile Valley Spring #1 11S 40E 5aaaS	22	1510			140	Flows at contact of Bear River alluvium and Ordovician Garden City limestone. Extensive travertine deposit on opposite side of hill, apparently unrelated to the spring.
B-29	Gentile Valley Spring #2 10S 40E 32abdS	14	1520			48	Spring flows out of fracture in Ordovician Swan Peak quartzite dipping 38° to the northeast at contact with Quaternary terrace gravels.
B-30	Gentile Valley Spring #3 11S 40E 8dddS	30	1520			45	Flows out of alluvium through clean gravel bottom, closest Paleozoic outcrop is Cambrian Blacksmith limestone, is about one mile to the northwest.

Table V-2. Continued.

Sample Number	Name and Location	Water Temp. (°C)	Elevation (m above MSL)	Well Depth (m)	Depth to Water (m)	Discharge (l/s)	Site Description
B-31	Ben Meek Well 14S 39E 36ada	40	1380	12	1.8	?	Well drilled into Bear River alluvium about .3 km south of the river. Several wells in the vicinity also contain hot water. Well is located along Mink Creek lineament.
B-32	Orvil Rallison Well 16S 40E 16cac	15	1370	24	flowing	?	Well drilled into alluvium of Cub River about .5 km southeast of the river.
S-2	Blackfoot River W. S. 5S 40E 14bcdS	28	1850			0.3 E	Spring discharges out of large travertine mound on side of basalt bluff southeast of spring S-3 about 12-16 m above Blackfoot River.
S-3	Unnamed Spring 5S 40E 15bacS	18	1880			0	Water is standing in a 5 m high travertine mound at top of Quaternary basalt bluff just north of Blackfoot River, and is evolving CO_2 gas.
S-7	Mound Valley Warm Spring 12S 40E 13dcdS	34	1530			<0.1 E	Trickles out of large travertine mound about 30 m tall above Bear River floodplain about 150 m east of the river.
S-8	Cleveland Hot Springs 12S 41E 31cacS	55	1520			100 E	One of many discharges through a large travertine bluff overlooking Bear River. Discharges can be seen welling up in river also.
S-9	Unnamed Warm Spring 12S 41E 31badS	21	1510			30 E	Flows out of extensive travertine mound further down the hill from spring B-17.
S-10	Treasureton Warm Spring 12S 40E 36acdS	40	1510			20 E	One of several springs discharging through Quaternary alluvium on west side of Bear River from springs at S-8.
S-11	Maple Grove Hot Spring 13S 41E 7acaS	75	1500			2 E	One of many springs issuing from Cambrian Brigham quartzite. Spring is actively depositing tufa.
S-12	Unnamed Hot Spring 13S 41E 7dabS	62	1520			<1 E	About .5 km south of spring S-11 and also flows out of Cambrian Brigham quartzite. Associated small tufa deposits.

E = estimated discharge, all others are measured discharge.

Table V-3. Hydrochemical data from springs and wells sampled in southeastern Idaho.

Sample Number	Name and Location	Water Temp. °C	Specific Conductance (μmho/cm)	TDS (mg/l)	pH	Concentration in mg/l (meq/l) Ca	Mg	Na	K	Cl	F	HCO_3	SO_4	SiO_2	Error %
B-1	Corral Creek Well 6S 41E 19bbd	40	4900	5267	6.9	745 (37.2)	244 (20.1)	53 (2.3)	222 (5.7)	39 (1.1)	1.8 (0.09)	3016 (49.5)	915 (19)	31	-3.2
B-2	Gem Valley Spring #1 8S 40E 26bdcS	13	1775	1806	6.6	261 (13)	126 (10.4)	23 (1)	8 (0.2)	13 (0.4)	0 (0)	1231 (20.2)	123 (2.6)	21	3.1
B-3	Thermal Gradient Well 8S 40E 26dbc	15	2400	2221	6.5	345 (17.2)	118 (9.7)	26 (1.1)	12 (0.3)	2 (0.07)	0 (0)	1529 (25.1)	147 (3.1)	42	0.3
B-4	Gem Valley Spring #2 8S 40E 26dcbS	16	2400	2320	6.5	361 (18)	120 (9.9)	28 (1.2)	12 (0.3)	13 (0.4)	0 (0)	1592 (26.1)	153 (3.2)	41	-0.4
B-5	Soda Creek Headwaters 8S 41E 26dabS	13	1450	1595	6.2	124 (6.2)	141 (11.6)	49 (2.1)	16 (0.4)	10 (0.3)	0.4 (0.02)	1106 (18.1)	37 (0.8)	112	2.8
B-6	Hooper Spring 8S 41E 36dddS	10	1300	1406	6.3	106 (5.3)	111 (9.1)	36 (1.6)	11 (0.3)	9 (0.3)	0.5 (0.03)	1007 (16.5)	41 (0.9)	85	-4.0
B-7	Soda Springs Geyser 9S 41E 12adaS	29	4025	4694	6.8	925 (46.2)	150 (12.4)	3 (0.1)	18 (0.5)	3 (0.08)	0.4 (0.02)	2778 (45.6)	771 (16)	46	-2.2
B-8	Unnamed Spring 10S 42E 12ccbS	8	460	451	7.7	79 (3.9)	13 (1.1)	9 (0.4)	2 (0.05)	5 (0.1)	0.2 (0.01)	297 (4.9)	10 (0.2)	36	2.1
B-9	Cold Spring 10S 42E 31daaS	7	250	217	7.9	47 (2.4)	6 (0.5)	2 (0.09)	0 (0)	0 (0)	0 (0)	155 (2.5)	0 (0)	7	6.9
B-10	Trout Creek Spring 11S 41E 15cdaS	5	325	311	7.0	63 (3.1)	12 (1)	4 (0.2)	0 (0)	9 (0.3)	0 (0)	223 (3.7)	0 (0)	0	4.8
B-11	Unnamed Spring 12S 41E 18acdS	13	425	372	7.1	52 (2.6)	20 (1.6)	7 (0.3)	0 (0)	7 (0.2)	0 (0)	277 (4.5)	0 (0)	9	-2.6
B-12	Harris Spring 11S 41E 8dbcS	10	650	543	7.1	111 (5.5)	0 (0)	9 (0.4)	0 (0)	17 (0.5)	0 (0)	361 (5.9)	18 (0.4)	27	-6.6
B-13	Pescadero Warm Spring 11S 43E 36bdaS	23	1475	1380	7.0	194 (9.7)	46 (3.8)	70 (3)	13 (2.9)	74 (2.1)	2.3 (0.1)	749 (12.3)	215 (4.5)	17	1.1
B-14	Unnamed Spring 12S 44E 7baaS	12	550	464	7.0	72 (3.6)	21 (1.7)	11 (0.5)	0 (0)	10 (0.3)	0.2 (0.01)	317 (5.2)	0 (0)	33	2.8
B-15	Unnamed Spring 13S 43E 8daaS	11	440	346	7.0	42 (2.1)	19 (1.6)	22 (0.9)	0 (0)	8 (0.2)	0.2 (0.01)	236 (3.9)	4 (0.08)	15	4.9
B-16	Williams Creek Spring 12S 41E 27bbaS	7		325	7.2	55 (2.7)	17 (1.4)	0 (0)	0 (0)	3 (0.08)	0 (0)	250 (4.1)	0 (0)	0	-0.6
B-17	Unnamed Spring 12S 41E 31abcS	18	775	666	7.1	94 (4.7)	28 (2.3)	37 (1.6)	3 (0.07)	30 (0.9)	0.3 (0.02)	439 (7.2)	26 (0.5)	9	0.4

Table V-3. Continued.

Sample Number	Name and Location	Water Temp. °C	Specific Conductance (μmho/cm)	TDS (mg/l)	pH	Concentration in mg/l (meq/l) Ca	Mg	Na	K	Cl	F	HCO_3	SO_4	SiO_2	Error %
B-18	Mink Creek Spring 13S 41E 24bbcS	6	245	205	7.4	46 (2.3)	5 (0.4)	3 (0.1)	1 (0.03)	2 (0.05)	0 (0)	148 (2.4)	0 (0)	0	7.3
B-19	Paris Creek Spring 14S 42E 13badS	9	325	256	6.9	58 (2.9)	5 (0.4)	2 (0.1)	0 (0)	1 (0.03)	0 (0)	190 (3.1)	0 (0)	0	3.8
B-20	Jarvis Spring 14S 43E 19bcdS	7	350	284	7.0	48 (2.4)	17 (1.4)	0 (0)	0 (0)	6 (0.2)	0 (0)	213 (3.5)	0 (0)	0	1.6
B-21	Unnamed Spring 14S 41E 15acdS	8	440	361	7.2	77 (3.8)	9 (0.7)	2 (0.1)	0 (0)	4 (0.1)	0 (0)	259 (4.2)	3 (0.06)	7	2.9
B-22	Burgquist Spring 15S 41E 10aadS	6	300	271	7.7	56 (2.8)	11 (0.9)	1 (0.04)	0 (0)	4 (0.1)	0 (0)	195 (3.2)	4 (0.08)	0	4.9
B-23	Sadducee Spring 16S 43E 8cbbS	6	300	251	7.2	49 (2.5)	12 (1)	0 (0)	0 (0)	1 (0.03)	0 (0)	189 (3.1)	0 (0)	0	4.6
B-24	Unnamed Spring 16S 40E 15ddbS	9	310	221	7.3	40 (2)	8 (0.7)	0 (0)	0 (0)	3 (0.1)	0 (0)	159 (2.6)	2 (0.04)	9	-1.5
B-25	Bear Lake Hot Spring #1 15S 44E 13ccaS	40	2250	1625	7.0	230 (11.5)	41 (3.4)	155 (6.7)	48 (1.2)	72 (2)	4.2 (0.2)	263 (4.3)	769 (16)	43	0.6
B-26	Bear Lake Hot Spring #2 15S 44E 13cbaS	39	1975	1634	7.2	227 (11.3)	41 (3.4)	151 (6.5)	44 (1.1)	75 (2.1)	4.2 (0.2)	255 (4.2)	791 (16.5)	46	-1.3
B-27	Bear Lake Hot Spring #3 15S 44E 12ccdS	33	1900	1621	7.1	227 (11.3)	41 (3.4)	163 (7.1)	43 (1.1)	74 (2.1)	4 (0.2)	271 (4.4)	758 (15.8)	40	0.8
B-28	Gentile Valley Spring #1 11S 40E 5aaaS	22	1825	1698	6.1	239 (11.9)	47 (3.9)	92 (4)	34 (0.9)	78 (2.2)	0.2 (0.01)	1086 (17.8)	104 (2.2)	18	-3.5
B-29	Gentile Valley Spring #2 10S 40E 32abdS	14	625	524	7.0	60 (3)	30 (2.5)	29 (1.3)	0 (0)	33 (0.9)	0.1 (0.01)	332 (5.4)	23 (0.5)	17	-1.0
B-30	Gentile Valley Spring #3 11S 40E 8dddS	30		930	6.6	132 (6.6)	38 (3.1)	54 (2.3)	3 (0.07)	43 (1.2)	0.2 (0.01)	594 (9.7)	40 (0.8)	26	1.4
B-31	Ben Meek Well 14S 39E 36ada	40	1900	1349	7.4	23 (1.2)	5 (0.4)	348 (15.1)	20 (0.9)	321 (9.1)	11 (0.6)	526 (8.6)	5 (0.1)	90	-2.3
B-32	Orvil Rallison Well 16S 40E 16cac	15	455	374	7.6	42 (2.1)	18 (1.5)	20 (0.9)	7 (0.2)	31 (0.9)	0.4 (0.02)	199 (3.3)	14 (0.3)	43	2.0
S-2***	Blackfoot River W. S. 5S 40E 14bcdS	28	4600	4915	6.4	700 (34.9)	224 (18.4)	164 (7.1)	201 (5.1)	72 (2.0)	1.9 (0.1)	2371 (38.9)	1178 (23.9)	33	0.5
S-3	Unnamed Spring 5S 40E 15bacS	18		4851	6.3	688 (33.3)	312 (25.7)	149 (6.5)	182 (4.7)	64 (1.8)	1.3 (0.1)	2287 (37.5)	1171 (24.4)	17	4.8

Table V-3. Continued.

Sample Number	Name and Location	Water Temp. °C	Specific Conductance (µmho/cm)	TDS (mg/l)	pH	Concentration in mg/l (meq/l) Ca	Mg	Na	K	Cl	F	HCO_3	SO_4	SiO_2	Error %
S-7	Mound Valley Warm Spring 12S 40E 13dcdS	34	3100	2441	6.1	353 (17.6)	52 (4.3)	267 (11.6)	51 (1.3)	309 (8.7)	0.8 (0)	1106 (18.1)	278 (5.8)	24	5.2
S-8	Cleveland Hot Springs 12S 41E 31cacS	55	3600	2554	6.2	259 (12.9)	41 (3.4)	444 (19.3)	90 (2.3)	574 (16.2)	1.7 (0.1)	565 (9.3)	517 (10.8)	62	2.0
S-9	Unnamed Warm Spring 12S 41E 31badS	21	750	619	6.7	82 (4.1)	25 (2.1)	32 (1.4)	0 (0)	27 (0.8)	0.3 (0)	410 (6.7)	23 (0.5)	15	-1.9
S-10	Treasureton Warm Spring 12S 40E 36acdS	40	4550	3179	6.4	336 (16.8)	48 (3.9)	542 (23.6)	110 (2.8)	629 (17.7)	2 (0.1)	726 (11.9)	735 (15.3)	54	2.3
S-11	Maple Grove Hot Spring 13S 41E 7acaS	75	3000	2177	6.3	132 (4.4)	24 (1.8)	550 (23.9)	71 (1.8)	586 (16.5)	0.3 (0)	466 (7.6)	282 (5.9)	66	3.1
S-12	Unnamed Hot Spring 13S 41E 7dabS	62	3150	2107	5.9	82 (4.1)	22 (1.8)	499 (21.7)	77 (2)	585 (16.5)	1 (0.1)	454 (7.4)	323 (6.7)	64	-1.8
D-1**	A. M. Thompson Well 11S 44E 7ccb	*	511	350	7.7	74 (3.7)	30 (2.5)	5 (0.2)	1 (0.03)	3.3 (0.09)	0 (0)	310 (5.1)	48 (1)	12	1.9
D-2	Rebecca Buhler Well 12S 43E 25daa	*	539	351	7.8	61 (3)	27 (2.2)	16 (0.7)	4.6 (0.1)	17 (0.5)	0.1 (0.01)	292 (4.8)	30 (0.6)	40	3.1
D-3	Dave Gerber Well 12S 44E 33dcc	*	652	426	7.8	91 (4.5)	30 (2.5)	10 (0.4)	1 (0.03)	6.7 (0.2)	0.1 (0.01)	336 (5.5)	74 (1.5)	12	1.6
D-4	Dean Roberts Well 13S 43E 16dcc	*	576	351	7.7	66 (3.3)	20 (1.7)	30 (1.3)	1 (0.03)	27 (0.8)	0.2 (0.01)	340 (5.6)	0 (0)	23	-0.5
D-5	Karel Thomas Well 14S 43E 35bba	*	556	336	7.9	67 (3.3)	26 (2.2)	17 (0.7)	1.9 (0.05)	12 (0.3)	0.1 (0.01)	356 (5.8)	12 (0.3)	19	-1.3
D-6	Oscar Arnell Well 14S 44E 12ccc	*	765	475	7.7	83 (4.1)	34 (2.8)	39 (1.7)	2.1 (0.05)	40 (1.1)	0.1 (0.01)	352 (5.8)	74 (1.5)	15	1.4
D-7	Al Butterfield Well 8S 42E 7bda	*	718	422	7.3	75 (3.7)	50 (4.2)	8.2 (0.4)	3 (0.08)	8.1 (0.3)	0.3 (0.02)	464 (7.6)	23 (0.5)	29	0
D-8	Monsanto Chem Well 8S 42E 31adb	*	1000	684	7.6	88 (4.4)	60 (4.9)	48 (2.1)	6.9 (0.2)	59 (1.7)	1.5 (0.08)	392 (6.4)	147 (3.1)	44	1.6
D-9	Dewey Mansfield Well 10S 40E 14bba	*	760	454	7.8	59 (2.9)	48 (3.9)	34 (1.5)	4.9 (0.1)	38 (1.1)	0.5 (0.03)	360 (5.9)	51 (1.1)	23	2.7
D-10	Alvin Kingsford Well 10S 40E 36dcc	*	852	520	7.8	62 (3.1)	57 (4.7)	39 (1.7)	5.2 (0.1)	42 (1.2)	0.5 (0.03)	412 (6.8)	70 (1.5)	27	0.9
D-11	Clark Mickelson Well 11S 41E 30bdd	*	1430	998	7.8	128 (6.4)	78 (6.4)	89 (3.9)	3.6 (0.1)	98 (2.8)	0.3 (0.02)	520 (8.5)	228 (4.7)	28	2.2

Table V-3. Continued.

Sample Number	Name and Location	Water Temp. °C	Specific Conductance (μmho/cm)	TDS (mg/l)	pH	Concentration in mg/l (meq/l)									Error %
						Ca	Mg	Na	K	Cl	F	HCO_3	SO_4	SiO_2	
D-12	Mack Hymas Well 13S 40E 30acb	*	625	368	7.6	69 (3.4)	30 (2.7)	21 (0.9)	1.9 (0.05)	30 (0.9)	0.4 (0.02)	326 (5.4)	22 (0.5)	21	1.4
D-13	Byron Tanner Well 14S 39E 25add	*	866	550	7.9	89 (4.4)	35 (2.9)	58 (2.5)	5.6 (0.1)	30 (0.9)	0.5 (0.03)	496 (8.1)	40 (0.8)	45	0.7

* not reported

** Numbers D-1 through D-13 are modified from Dion (1969).

*** Numbers S-2 through S-12 are from Souder (1983) multivariate data analysis methods. The spring and well discharges are statistically grouped by similarities in their hydrochemical characteristics. Spatial distributions of the groups are then compared with the regional geologic framework.

Associated Geologic Features

The springs and wells sampled in the study area discharge from eleven geologic formations ranging from the Precambrian/Cambrian Brigham quartzite to Recent alluvium. A summary of the geologic formations associated with springs and wells, and the frequency of discharges within the study area is presented in Table V-4. Springs and wells which are in close proximity to major normal faults are also indicated in the table.

The most prominent structural features in the study area are the normal faults which have created the horst/graben structures that comprise the ranges and valleys. Most of these faults show surficial evidence of recent movement (Witkind, 1974) and may be considered active based upon the high frequency of earthquakes centered within and near the study area (Smith and Shar, 1974). The seismic evidence suggests that these faults extend to great depths (3 to 16 km) and may act as conduits for the deep circulation of ground water.

Table V-4. Geologic formation associated with springs and wells in the vicinity of the Bear River Range, southeastern Idaho.

Age	Formation	Spring or Well
Quaternary	Alluvium	D-1, D-2, D-3, D-4, D-5, D-6, D-13, B-15, B-17*, B-30*, B-31*, B-32, S-7(?)*, S-8*, S-9*, S-10*
Quaternary and Tertirary	Basalt	D-7, D-8, D-9, D-10, B-1*, B-2*, B-3*, B-4*, B-5*, B-6*, B-7*, B-12, S-2, S-3
Tertiary	Salt Lake	D-8, B-24
Triassic	Thaynes	B-13, B-15(?)
Mississippian	Brazier	B-25*, B-26*, B-27*
Ordovician	Garden City	B-23, B-28*, B-29
Cambrian	St. Charles	B-11
Cambrian	Nounan	B-10, B-16, B-18, B-22
Cambrian	Bloomington	B-19
Cambrian	Blacksmith	B-9, B-20
Cambrian/ Pre-Cambrian	Brigham	B-21, S-11*, S-12*

* Indicates close proximity of spring or well to major fault.

The springs and wells in close proximity to major faults are indicated in Table V-4. Twenty of the fifty one springs and wells examined are located near faults and discharge through alluvium, basalt, the Mississippian Brazier limestone and the Cambrian Brigham quartzite. Sixteen of the twenty fault-associated springs and wells have surface temperatures greater than or equal to 15.5°C. The association of the thermal springs and wells with these faults tends to orient them along the edges of the valleys. The thermal springs which extend from Gentile Valley (B-28) to Mound Valley (S-8 and S-10) are all aligned toward the western edge of the valleys along the West Gem Valley fault. Maple Grove Hot Springs (S-11 and S-12) in Onieda Narrows occurs in the intensely faulted area that forms the junction of the Bear River and Portneuf Ranges at the southern end of the same graben structure.

Mineralized warm springs and wells located in the northern Gem Valley and Blackfoot Lava Field occur along the east and west sides of the Soda Springs Hills. The well (B-3) and two springs (B-1 and B-2) on the west side of the range are aligned along a three-meter break in the basalt, probably an expression of the East Gem Valley fault. The springs on the east side of the Soda Springs Hills include the warm spring at Soda Springs geyser (B-7), Hooper Spring (B-6) and the headwaters of Soda Spring (B-5). These springs are all in close proximity to the northern extension of the West Bear Lake fault. The three springs sampled at the Bear Lake Hot Springs resort (B-25, B-26, B-27) all align along the East Bear Lake fault.

Thrust faulting and associated folding of the pre-Tertiary rocks of the mountain ranges are also prominent structural features. The Paris thrust fault which extends through the study area along the eastern edge of the Bear River Range appears to have little, if any, direct control over ground water flow systems. Large folds in the Paleozoic rocks caused by the Paris thrust fault, however, affect ground water flow patterns through these rocks. The axis of the broad, northward plunging Fish Haven syncline follows roughly along the center of the Bear River Range. The many large springs, such as Trout Creek spring (B-10), Paris Creek Spring (B-17) and Burgquist Spring (B-22) that discharge on both sides of the Bear River Range, reflect the controls of the syncline on ground water flow patterns in the range. The fold has caused the higher hydraulic conductivity formations such as the Nounan Limestone and the Blacksmith Limestone which overlay the dense and lower hydraulic conductivity Brigham quartzite to outcrop on both the east and west sides of the range. The springs that do occur in the Brigham quartzite are much smaller in discharge than the springs in the overlying carbonate rocks. These stratigraphic, structural and discharge relationships indicate that probably most of the ground water in the Bear River Range is discharged to the surface above the Brigham quartzite, and little ground water flows through the Brigham into lower flow systems.

Discharge of Springs

The total discharge of springs and wells sampled during this study is inversely proportional to temperature. The springs and wells with temperatures less than 15.5°C have a total discharge of about 3670 l/s. The largest of these is Paris Creek Spring with a discharge of approximately 850 l/s. The springs and wells with temperatures between 15.5°C and 39°C have a total discharge of about 250 l/s. The springs and wells with temperatures greater than 39°C have a total discharge of approximately 20 l/s. The contrast between thermal and non-thermal discharges are even greater than expressed here because only a small percentage of the springs with temperatures below 15.5°C were visited; most of the thermal springs in the area were sampled.

Analysis of Chemical Data

Introduction

The chemical composition of ground water discharging from a spring or well is the product of dynamic hydrogeochemical reactions. The environment in which these reactions occur is controlled by the chemical and physical properties of the rocks through which the ground water flows, the rate of ground water flow, and the temperatures and pressures encountered along the flow path. Knowledge of the hydrogeologic environment of the discharging ground water can thus be obtained from its chemical composition. A comparison of the hydrochemistry with the local and regional geologic structure can provide a description of the probable ground water flow system.

Treatment of the chemical characteristics of ground water samples as random variables and treatment of the ground water discharges as random samples of different hydrogeologic systems are conducive to a multivariate analysis of the hydrochemical data to quantify differences between the flow systems. A suite of multivaiate data analyses was applied to the hydrochemical data listed in Table V-3 in order to: 1) identify the most important variables in determining the hydrochemistry, 2) group spring and well sites based on these hydrochemical differences and finally 3) correlate the groups to regional lithologic types and/or geologic structures.

First, the variables were subjected to a logarithmic transformation and then standardized. This procedure assures that large values will not dominate the statistical analyses and that assumptions of normality are satisfied. Details of the procedure for standardization of data are presented by Baglio (1983). Second, factor analysis and cluster analysis of the data were applied to identify important variables by which to group the samples. Finally, a multiple discriminant analysis was applied to test the statistical significance of the defined groups.

Multivariate Methods

Four multivariate data analysis methods were applied to the hydrochemical data. Factor analysis and cluster analysis are exploratory methods used to examine the relative importance of the hydrochemical properties in determining the variations among the samples. Multivariate analysis of variance (MANOVA) and multiple discriminant analyses are confirmatory methods used to make statistical tests of the sample variations.

Factor Analysis. The general purpose of factor analysis is to condense the information contained in a number of original variables (in this case 12) into a smaller set of composite dimensions (factors) with a minimum loss of information. A discussion of the mathematical theory of factor analysis can be found in Giri (1977), and discussions on applications can be found in Comrey (1973) and Hair and others (1979).

Factor analysis begins with the calculation of a correlation matrix. The correlation matrix is an array of correlation coefficients between all pairs of constituents. The squared correlation coefficient is a measure or a proportion of the variance of one variable that can be explained by another variable. Correlation coefficients range in value from -1 to 1. The correlation coefficients are arranged in the matrix so that the entry in row i and column j is the computed correlation coefficient r_{ij} for the ith and jth variables. The correlation matrix is a measure of simple relationships of each variable with all the other variables.

The correlation coefficient matrix for the twelve variables temperature, TDS, pH, calcium, magnesium, sodium, potassium, chloride, fluoride, bicarbonate, sulfate and silica is presented in Table V-5. Many of the variables in the matrix are highly correlated. These correlations indicate that the dominant cation/anion combinations are highly, positively related. Sodium and chloride, for example, have a correlation coefficient of .91. Also, calcium, magnesium and bicarbonate are all highly, positively correlated. TDS is highly correlated with calcium and bicarbonate, probably because the highest TDS concentrations occur in samples dominated by calcium and bicarbonate in the Soda Springs area. Temperature is highly correlated with sodium, potassium and chloride, and is poorly correlated with calcium, magnesium and bicarbonate. These relationships may be influenced by solubilities of these ions. The solubilities of sodium and chloride increase with temperature

Table V-5. Correlation coefficient matrix for the hydrochemical parameters: temperature, total dissolved solids (TDS), pH, calcium, magnesium, sodium, potassium, chloride, fluoride, bicarbonate, sulfate, and silica.

	Temp	TDS	pH	Ca	Mg	Na	K	Cl	F	HCO_3	SO_4	SiO_2
Temp	1.00	.78	-.54	.54	.43	.88	.82	.86	.50	.47	.80	.72
TDS		1.00	-.70	.88	.79	.77	.92	.64	.34	.88	.93	.71
pH			1.00	-.57	-.60	-.62	-.62	-.54	.08	-.66	-.59	-.45
Ca				1.00	.79	.49	.76	.36	.04	.84	.86	.46
Mg					1.00	.46	.67	.28	.01	.82	.71	.46
Na						1.00	.82	.91	.51	.48	.78	.76
K							1.00	.74	.44	.69	.90	.65
Cl								1.00	.50	.33	.68	.61
F									1.00	.08	.29	.39
HCO_3										1.00	.71	.54
SO_4											1.00	.69
SiO_2												1.00

whereas calcium, magnesium and sodium decrease with temperature.

The next step of factor analysis is to determine the factor constructs needed to account for the pattern of variances observed in the correlation matrix. These factors are linear combinations of the original variables. Details of this step of factor analysis are presented by Baglio (1983). The factor loadings indicate that there are essentially two sets of variables in the data set: one characterized by TDS, calcium, magnesium, bicarbonate and sulfate and the other characterized by sodium, chloride, fluoride and temperature. The total contribution of the two factors in defining the variance in the data is equal to 79.8 percent. The factors represent the two end members of hydrochemical types present within the study area. These are: 1) calcium plus magnesium and bicarbonate and 2) sodium and chloride.

Cluster Analysis. Cluster analysis is an exploratory multivariate data analysis technique used for grouping a number of individuals or samples by several variables with which they are measured. An agglomerative (hierarchical), polythetic (several variable) clustering technique was used for this analysis.

This cluster analysis was performed with the CLUSTER procedure available from SAS (Goodnight and others, 1979).

The variables used in the analysis to define the groups were temperature, sodium, chloride, calcium, magnesium and bicarbonate. These six variables, as defined by the factor analysis, are the more significant in determining the hydrochemical types of ground water found throughout the study area. A dendrogram of the resultant clusters is presented in Figure V-4.

The determination of the correct number of clusters within the data as suggested by Everett (1974) is accomplished by an examination of the dendrogram for large changes in the cluster diameter (or maximum distance within a cluster) between successive fusions. The largest change in the maximum cluster diameter is between the formation of 3 clusters and 2 clusters.

These three groups as labeled in Figure V-4 represent different hydrochemical types determined by the six variables. Group 1 represents ground waters that are relatively warm, high in dissolved solids and dominated by calcium, calcium plus magnesium, or magnesium plus bicarbonate. Group 2 represents ground waters that are relatively cold, low in dissolved solids and dominated by calcium, calcium plus magnesium, or magnesium bicarbonate. Group 3 represents ground waters that are relatively warm or hot, moderate to high in dissolved solids and with higher sodium and chloride concentrations although not necessarily dominated by these ions.

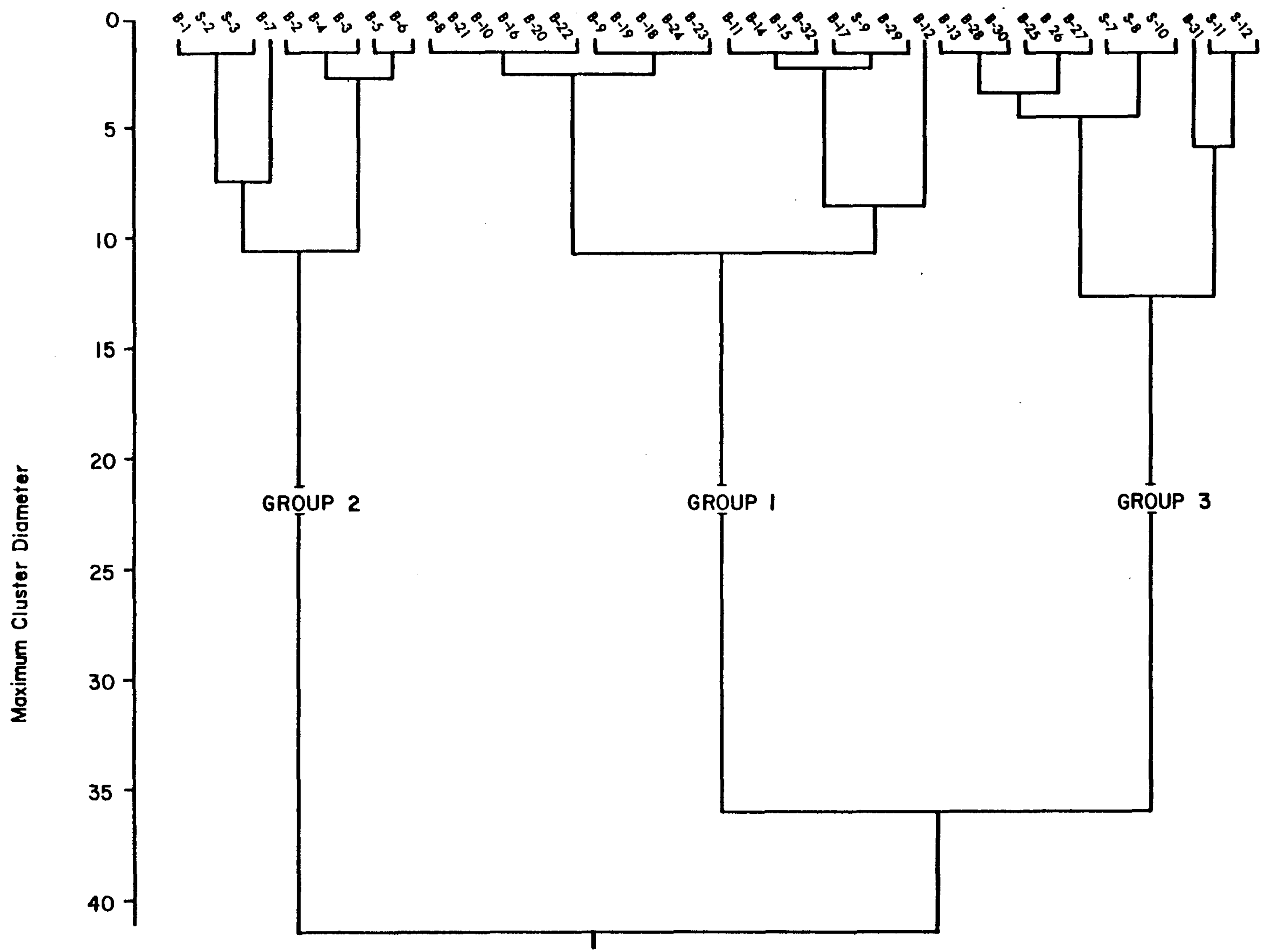

Figure V-4. Dendrogram of hydrochemical groups resulting from a cluster analysis using the variables: temperature, sodium, chloride, calcium, magnesium, and bicarbonate

Multiple Discriminant Analysis. Multiple discriminant analysis is a confirmatory multivariate data analysis technique that tests whether two or more groups are indeed different. The analysis is based on the linear discriminant function (LDF). The analysis involves the derivation of a linear combination of the variables that will discriminate best between a priori defined groups.

The discriminant analysis was performed by the DISCRIM procedure of SAS (Goodnight and others, 1979). The six variables (temperature, calcium, magnesium, bicarbonate, sodium and bicarbonate), determined by the factor analysis as important in controlling variation among the samples and also used in the cluster analysis, are used for this analysis. Eight samples (B-2, B-6, B-12, B-13, B-17, B-25, B-27 and S-9) were included as ungrouped samples. A discriminant function was derived from the 32 samples in three a priori defined groups (i.e. grouped by the clustering procedure). The function was then used to classify the ungrouped samples into one of the three groups (Table V-6). Of the a priori defined groups, 7 samples were in group 1, 16 samples were in group 2 and 9 samples were in group 3. The eight ungrouped samples fell into the same groups in which they were classified by the clustering procedure.

Table V-6. Comparison of geologic formations and structures with statistically derived hydrochemical groups.

	Sample Number	Discharge Temperature (°C)	Associated Geologic Formation	Associated Geologic Structure
Group 1	B-1	40	Quaternary basalt (thin)	
	B-2	13	Quaternary basalt (thin?)	East Gem Valley fault
	B-3	15	Quaternary basalt (thin?)	East Gem Valley fault
	B-4	16	Quaternary basalt (thin?)	East Gem Valley fault
	B-5	13	Quaternary basalt (thin?)	West Bear Lake fault
	B-6	10	Quaternary basalt (thin?)	West Bear Lake fault
	B-7	29	Quaternary basalt (thin?)	West Bear Lake fault
	S-2	18	Quaternary basalt	
	S-3	28	Quaternary basalt	
Group 2	B-8	8	Tertiary Salt Lake	
	B-9	7	Cambrian Blacksmith limestone	
	B-10	5	Cambrian Nounan limestone	
	B-11	13	Cambrian St. Charles limestone	
	B-14	12	Quaternary alluvium (thin?) Triassic Thaynes limestone	
	B-15	11	Quaternary alluvium (thin?)	
	B-16	7	Cambrian Nounan limestone	
	B-17	18	Quaternary alluvium (thin?)	West Gem Valley fault (?)
	B-18	6	Cambrian Nounan limestone	
	B-19	9	Cambrian Bloomington limestone	
	B-20	7	Cambrian Blacksmith limestone	
	B-21	8	Cambrian Brigham quartzite	
	B-22	6	Cambrian Nounan limestone	
	B-23	6	Ordovician Garden City limestone	
	B-24	9	Tertiary Salt Lake formation	
	B-29	14	Ordovician Swan Peak quartzite	
	B-32	15	Quaternary alluvium (thin?)	
	S-9	21	Quaternary alluvium (thin?)	West Gem Valley fault (?)
Group 3	B-12	10	Quaternary basalt	
	B-13	23	Triassic Thaynes limestone	
	B-25	40	Mississippian Brazier limestone	East Bear Lake fault
	B-26	39	Mississippian Brazier limestone	East Bear Lake fault
	B-27	33	Mississippian Brazier limestone	East Bear Lake fault
	B-28	22	Ordovician Garden City limestone	West Gem Valley fault
	B-30	30	Quaternary alluvium (thin?)	West Gem Valley fault
	B-31	40	Quaternary alluvium (thin?)	Mink Creek fault (?)
	S-7	34	Quaternary alluvium (thin?)	West Gem Valley fault
	S-8	55	Quaternary alluvium (thin?)	West Gem Valley fault
	S-10	40	Quaternary alluvium (thin?)	West Gem Valley fault
	S-11	75	Cambrian Brigham quartzite	Highly faulted area at junction of Portneuf Range and Bear River Range
	S-12	62	Cambrian Brigham quartzite	

Two of the ungrouped samples (B-17 and S-9) had posterior probabilities of membership in group 1 of only .61 and .52, repsectively. These samples had posterior probabilities of membership in group 3 of .39 and .48, respectively. The physical and chemical characteristics of these springs suggest that they may be the result of mixing of the thermal waters in group 3 and the nonthermal waters of group 1.

Discussion of Results

Quantitative statistical analysis of the hydrochemical data using the variables of temperature, calcium, magnesium, bicarbonate, sodium and chloride has resulted in the establishment of three groups of ground water discharges with differing chemical character. Two of these three groups represent thermal ground water systems and the other, the largest group, represents the non-thermal ground water systems of the area (Table V-7).

The areal distribution of the three groups is presented in Figure V-5. The major ion concentrations are illustrated for each site utilizing Stiff diagrams. The patterns graphically represent the major ions in milliequivalents per liter on three parallel axes.

Table V-7. Summary of physical and chemical characteristics of springs and wells in southeastern Idaho

	Group 1 (Nonthermal)	Group 2 (Soda Springs)	Group 3 (Gem Valley)	Group 3 (Bear Lake and Cache Valleys)
Number of Samples	19	9	7	5
Mean Surface Temp. (°C)	10	20	45	35
Elevation Range (m)	1370 - 2000	1710 - 1880	1500 - 1530	1380 - 1820
Approximate Combined Discharge Rate (l/s)	3500	190	300	30
Mean TDS (mg/l)	370	3230	2160	1520
Predominant Ions	$Ca^{+2} + HCO_3^-$	$Ca^{+2} + HCO_3^-$	$Ca^{+2} + HCO_3^-$ $Na^+ + Cl^-$	$Ca^{+2} + SO_4^{-2}$ $Na^+ + Cl^-$
Predominant Discharge Control	Stratigraphic and Structural	Structural	Structural	Structural
Remarks		Active Travertine Deposition		Inactive Travertine Deposits

Ground Water Flow Patterns

The patterns of ground water flow are described in this section for the three major groups of discharges delineated by analsysis of chemical data. These groups are: 1) the non-thermal systems throughout the region, 2) the Soda Springs group, and 3) the Gem Valley group. Isolated thermal discharges within the study area in Bear River Valley and Cache Valley are discussed separately.

Non-Thermal Systems

The occurrence, distribution, and potential for development of regional shallow, non-thermal ground water systems within the major basins of the area have been discussed in detail by previous investigators. These shallow systems occur primarily in basalt and alluvium, and have been extensively developed as water supplies throughout the region. Ground water in the mountainous areas has not been examined in detail because of ample water supplies in the valleys. Most of the non-thermal springs sampled during this study are located along the flanks and foothills of the ranges.

Ground water flow paths in the carbonate rocks of the Bear River Range are probably localized by solutional modification into well integrated systems of conduits. Discharge occurs at the many large springs surrounding the range. The Brigham quartzite impedes downward movement of ground water, and the broad synclinal structure of the range directs the movement of ground water towards the flanks of the range. The northern end of the Bear River Range is an eastward dipping monocline; only one large spring exists in this area, indicating that deeper circulation may occur. Recharge to these systems occurs by infiltration of precipitation (primarily snowmelt) and by runoff draining into a number of sinkholes and closed basins.

Soda Springs Group

The thermal and non-thermal discharges of the Soda Springs system probably comprise several flow systems. Springs are located on the south, east, and west sides of Soda Springs Hills. The springs, however, must have similar hydrogeologic environments at depth because of their similar hydrochemical characteristics and limited areal distribution. The unique hydrochemistries of these springs and wells are the result of high carbon dioxide concentrations in the ground water.

Lang (1959) studied the $^{12}C/^{13}C$ isotopic abundance ratios of several carbon dioxide gas sources throughout the country, including Soda Springs, to determine the origins of the gases. The $^{12}C/^{13}C$ isotopic ratios for the carbon in the carbon dioxide gas from Soda Springs was 89.9, indicating a marine carbonate source for the carbon.

The ^{13}C values for carbon dissolved in the samples from Corral Creek (B-1) (Mayo, 1982), Soda Springs Geyser (B-7), Blackfoot River Warm Spring (S-2), and a spring in Gem Valley (B-4) (Souder, 1983) were +2.2, +5.6, +2.1, and +2.2, respectively. These values, with the possible exception of the Soda Springs Geyser which may be high, are all in the range of carbon from marine carbonate rock.

The difference in major ion and TDS concentrations of the springs and wells in the Soda Springs/Blackfoot Lava Field areas are probably the result of differences in CO_2 input to the systems and the succeeding rock/water interactions. The chemical characteristics of the high TDS sites (S-2, S-3, B-1, B-7) are all similar indicating similar hydrogeochemical environments at depth. The discharges all occur along tear faults associated with the Paris thrust fault, and all occur where the surficial covers (basalts and unconsolidated sediments) are thin. The springs and wells also occur in association with Paleozoic or Mesozoic carbonate rocks.

The chemical characteristics of the Soda Springs area discharges, nevertheless, are indicative that both the ground water flow patterns and hydrochemical evolutions of these systems are complex. Recharge to these systems most likely occurs in the Chesterfield Range and Soda Springs Hills. Ground water systems probably flow through the sedimentary strata of the ranges until intercepted by permeable fault zones, where flow is directed towards the surface. Deep flow systems may also occur in the basin-fill sediments under the basalts of the Blackfoot Lava Field. The occurrence of such systems, however, has not been confirmed.

Gem Valley Group

The discharges are confined to the west side of Gem Valley aligned along the West Gem Valley fault and also occur in the narrows at the southern end of the valley near the junction of the Bear River and Portneuf Ranges. The springs of this group discharge primarily from Ordovician and Cambrian strata. The northernmost spring (B-28) occurs just below the southern terminous of the Gem Valley basalts.

Springs in the Gem Valley evolve hydrochemically from calcium and bicarbonate water at the northern sites (B-28, B-30, S-7) to sodium and chloride water at the southern sites (S-8, S-10, S-11, S-12). The sodium and chloride concentrations increase progressively southward. Surface temperatures of the springs also increase southward from 22°C at spring B-28 to 75°C at Maple Grove Hot Spring (S-11). Travertine is associated with all the springs. Mound Valley Warm Spring (S-7) has developed a travertine mound 30 m high; although, the spring is not presently depositing any travertine. Springs S-8, S-10, and S-11 appear to be actively depositing travertine.

The gradual and progressive increase in sodium and chloride concentrations with increasing water temperature from north to south along the West Gem Fault suggests that similar mechanisms are controlling the hydrochemical characteristics of these springs. The mechanisms causing this trend may be mixing phenomena, carbonate equilibria, or natural hydrochemical evolution.

Recharge to the spring systems aligned along the West Gem Valley Fault probably occurs in the Portneuf Range. The ground water probably flows through the lower Paleozoic strata of the range until intercepted and directed to the surface by the fault. Depths of circulation of these systems may increase southward in accordance with the increasing temperatures of the surface discharges. Recharge to the thermal systems located in the faulted and fractured area at the junction of the Bear River and Portneuf Ranges may occur in either the Bear River or Portneuf Ranges.

Isolated Thermal Discharges

Thermal discharges within the study area for which insufficient data prevent descriptions of the systems occur in the Bear Lake and Cache Valleys. These discharges are the Pescadero Warm Spring (B-13) and a group of springs at Bear Lake Hot Springs (B-25, B-26, B-27) in the Bear Lake Valley, and one of several thermal wells (B-31) in the community of Riverdale in the northern Cache Valley.

CHAPTER VI

HYDROCHEMISTRY OF THERMAL FLOW SYSTEMS

Introduction

This portion of the study is an examination of the hydrochemistry of the thermal waters within a broad region including portions of southeastern Idaho, western Wyoming and northern Utah (Figure VI-1). This study area includes the subareas described in Chapters III, IV and V plus additional areas on all sides. For purposes of this study, 15°C was defined as the lowest temperature described as thermal. The purpose of this portion of the study is to provide a better understanding of the geothermal flow systems in the thrust belt and adjacent areas through an analysis of the hydrochemistry of the thermal waters.

The study area is roughly bounded by the margin of the Snake River Plain on the northwest, latitude 44° 00' on the north, longitude 110° 30' on the west, latitude 41° 30' on the south, and longitude 113° 30' on the east. This includes an area of approximately 52,000 square kilometers. This area is drained on the north and east by the Snake River and its tributaries the Raft, Portneuf, Blackfoot, Teton, and Salt rivers. To the south, the study area is drained predominantly by the Bear River which flows into the Great Salt Lake.

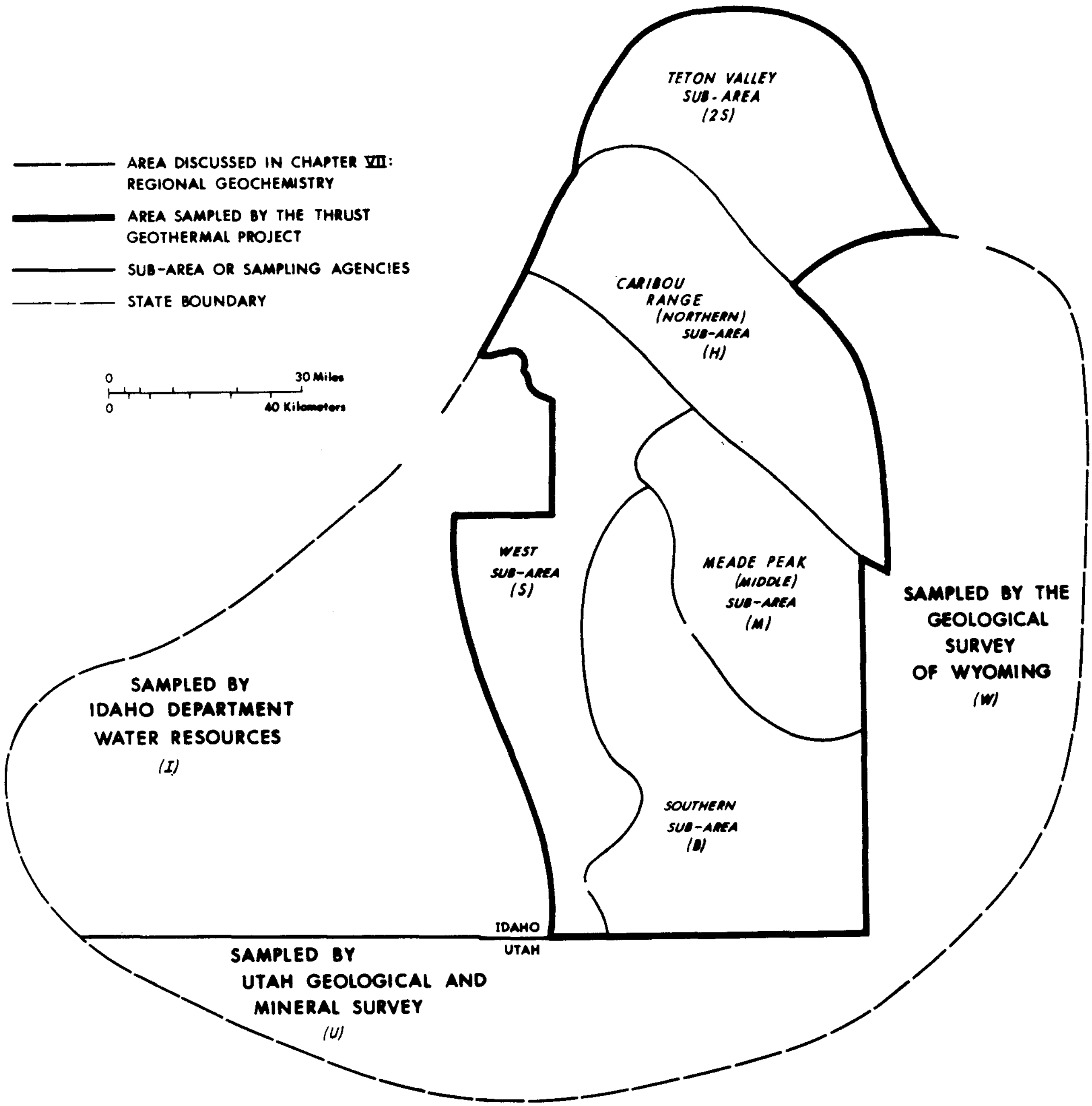

Figure VI-1. Data sources and subareas

The major mountain ranges are north-south trending in the western and southern portions of the study area, and northwest-southeast trending in the northeastern portion of the area. These ranges include (from west to east): the Raft River Range, the Sublette Range, the Hansel Mountains, the Bannock Range, the Portneuf Range, the Bear River Range, the Wasatch Range, the Blackfoot Mountains, the Caribou Range, the Snake River Range, the Salt River Range, and the Tunp Range (Figure VI-2). The study area lies within the Basin and Range and the Middle Rocky Mountain physiographic provinces and is bordered by the Snake River Plain (on the northwest) and Green River Basin on the east. Elevation in the valleys varies from about 1500 to 1900 m. Mountains typically are about 2300 m high, with the maximums being near 3100 m in several locations.

Regional Hydrogeologic Setting

The geologic development of the study area has occurred in at least three major stages: 1) deposition of about twenty kilometers of marine sediments in a miogeosyncline during Paleozoic time (Armstrong and Oriel, 1965), 2) folding and thrusting of this material along a north-south to northwest-southeast axis during Mesozoic time, and 3) Basin and Range style block faulting during Cenozoic time continuing to the present. The eastern portion of the study

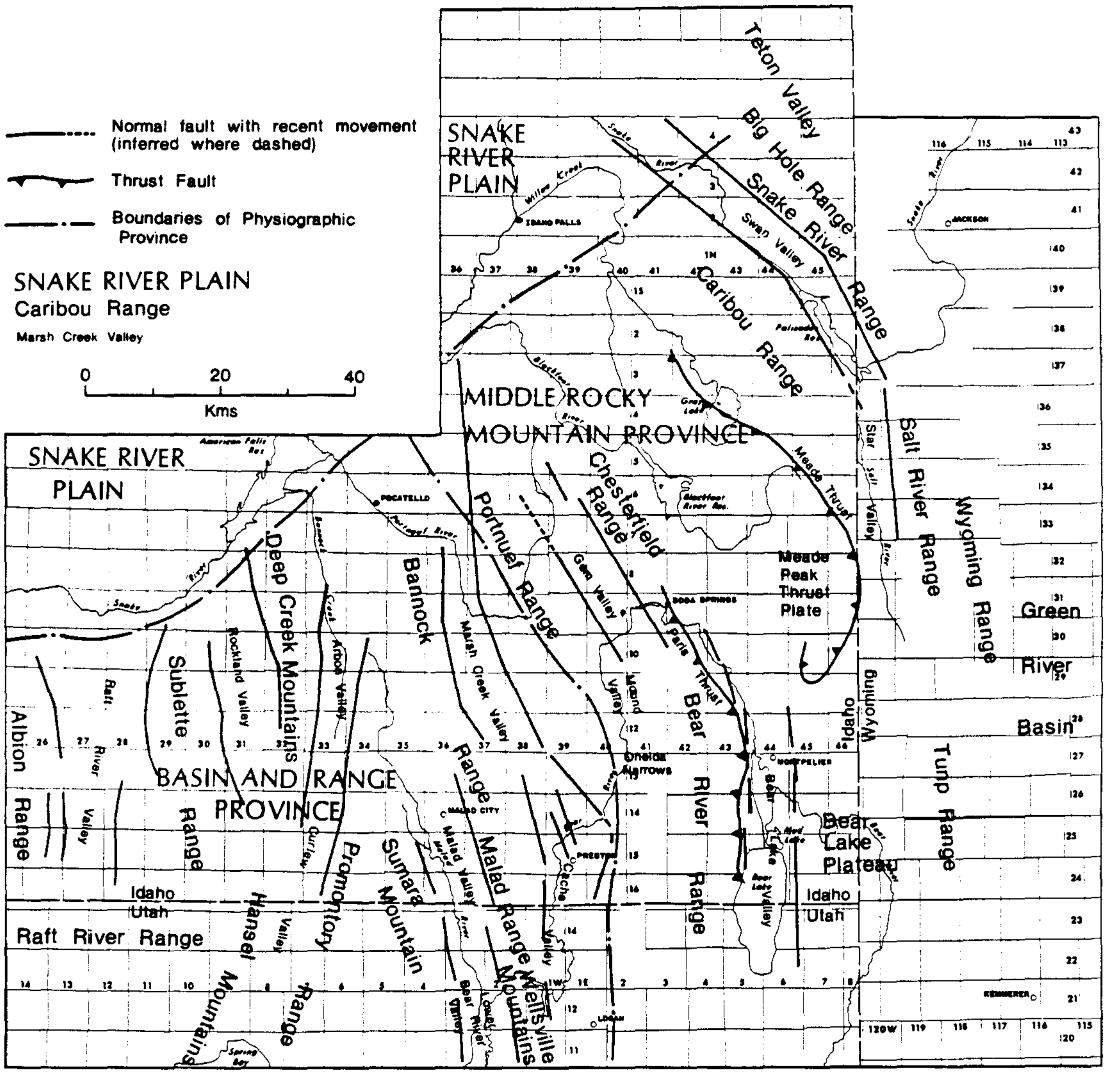

Figure VI-2. Major geologic structures in southeastern Idaho, northern Utah and western Wyoming area is characterized by thrust and fold features without major normal faulting. These features have been described in Chapters III, IV and V. The western and south-central portions of the study area are characterized by Basin and Range style mountains and valleys. The normal faults which have created these block mountains are thought to reach great depths.

Presentation of Chemical and Physical Data

Introduction

This section brings together information on the characteristics of thermal sites within the Idaho-Wyoming thrust belt, and selected data from adjacent areas. The contributions of various agencies and participants in this project are acknowledged in Table VI-1. The letter prefix to the site number indicates the sampling agency or sub-area within the project. Sites are listed by agency and generally in order from north to south. Spring or well locations are indicated in the second column according to the system used by IDWR and the United States Geological Survey (USGS). It is based on the township and range divisions of lands in the respective states (Mitchell and others, 1980). An S following the location number indicates that the site is a spring. In all other cases the site represented is a well.

Table VI-1. Sources of water quality data used in this report.

Prefix	Agency or Sampler	Sub-area or Data Type
2S	Karl Souder - 1981 field season	Teton Valley and miscellaneous springs
AQ	American Quasar	Oil well data
H	Joel Hubbell	Northern sub-area (chapter III)
M	Alan Mayo	Meade Peak sub-area (chapter IV)
B	Joseph Baglio	Southern sub-area (chapter v)
S	Karl Souder - 1980	Western sub-area
R	U.S. Department of Energy	Raft River site
I	Idaho Department of Water Resources	Other Idaho sites
W	Geological Survey of Wyoming	Western Wyoming sites
U	Utah Geological and Mineral Survey	Northern Utah sites

Water Quality Data

Water quality data are presented in Table VI-2. Constituents are expressed in milligrams per liter and in parentheses, in milliequivalents per liter. All concentrations have been rounded to two significant figures. Concentrations shown as zero are below the level of detection. Spaces for which no value is found indicate that the analysis was not performed or was not available.

Data taken from American Quasar (prefix AQ) oil wells are from drill stem test samples or from down-hole samplers. Drill stem test samples may not be representative of the actual formation water. Samples taken from as close to the tool as possible or from the sampler were taken to be most representative of the formation water.

The figure shown for silica (SiO_2) in Table VI-2 is the value obtained by atomic absorption spectrometry for total silica. Silica actually exists as H_4SiO_4 or to a much lesser extent, $H_3SiO_4^-$ at typical pH values for these waters (Hem, 1970).

Physical Characteristics of Thermal Discharge Sites

The geologic setting and physical characteristics of spring and well sites are described in Table VI-3. The geologic formation or structure from which a spring occurs is described wherever possible. In some cases this information is lacking due to mantling by alluvium or by

Table VI-2. Hydrochemical data for thermal springs and wells of the study area.

Sample Number	Name and Location	Water Temp. °C	Specific Conductance (μmho/cm)	TDS (mg/l)	pH	Concentration in mg/l (meq/l) Ca	Mg	Na	K	Cl	HCO_3	SO_4	SiO_2
AQ-1	26-1 Cook 5N 44E 26ba 2497'-2584' interval	46	--	3900	8.3	61 (3.0)	22 (1.8)	1200 (53)	21 (0.5)	30 (0.8)	590 (9.6)	2200 (46)	
AQ-2	26-1 Cook 5N 44E 26ba 2962'-2997' interval	49	--	640	7.9	76 (3.8)	19 (1.6)	100 (4.5)	20 (0.5)	14 (0.4)	244 (4.0)	280 (5.9)	
AQ-3	26-1 Cook 5N 44E 26ba 4210'-4230' interval	70	--	590	7.5	58 (2.9)	12 (1.0)	100 (4.5)	31 (0.8)	50 (1.4)	150 (2.4)	260 (5.4)	
AQ-4	Black Mountain Federal #1 3S 45E 36cc 13,550'-13,703' interval	65	--	24000	6.9	130 (6.5)	6 (0.5)	8600 (370)	490 (12)	11000 (300)	2300 (38)	2800 (59)	
AQ-5	2-1 King 2S 41E 2bc 8550'-8660' interval	116	--	28000	7.4	430 (22)	46 (3.8)	9400 (410)	470 (12)	6900 (190)	3300 (54)	9400 (200)	
AQ-6	2-1 King 2S 41E 2bc 11,375'-11,519' interval	160	--	52000	6.6	170 (8.6)	43 (3.5)	19000 (810)	2100 (53)	27000 (770)	4000 (66)	1800 (37)	
AQ-7	2-1 King 2S 41E 2bc 12,830'-12,884' interval	249	--	50000	8.0	210 (10)	0 (0)	18000 (760)	2600 (66)	26000 (730)	4500 (74)	1800 (36)	
AQ-8	North Eden Federal 21-11 16S 45E 21aa 8214'-8469' interval	92	--	19000	9.8	39 (2.0)	2 (0.2)	6500 (280)	130 (3.2)	600 (17)	3100[1] (51)	11000 (220)	
AQ-9	22-1 Jensen 13S 44E 22cc 10,900'-10,931' interval	74	--	29000	10.5	30 (1.5)	0 (0)	8400 (370)	93 (2.4)	1100 (31)	7000[1] (110)	11000 (220)	
2S1	O. J. Neeley Well 7N 43E 30ccc	22	450	360	7.4	51 (2.5)	23 (1.9)	19 (0.8)	2.6 (0.1)	61 (1.7)	150 (2.5)	24 (0.5)	34
2S2	Walz Warm Spring 5N 43E 7acS	35	690	630	7.3	120 (5.9)	31 (2.6)	3.3 (0.1)	4.0 (0.1)	26 (0.7)	160 (2.6)	260 (5.4)	22
2S3	Stinking Spring 3N 41E 10bbbS	20	180	220	6.9	26 (1.3)	7.2 (0.6)	7.1 (0.3)	3.2 (0.1)	19.7 (0.5)	110 (1.8)	6 (0.1)	47
2S4	Taylor Warm Spring 3N 44E 7baaS	21	340	310	6.8	49 (2.4)	19 (1.6)	2.0 (0.1)	1.8 (0.0)	18 (0.5)	170 (2.8)	38 (0.8)	14

Table VI-2. Continued.

Sample Number	Name and Location	Water Temp. °C	Specific Conductance (μmho/cm)	TDS (mg/l)	pH	Concentration in mg/l (meq/l) Ca	Mg	Na	K	Cl	HCO_3	SO_4	SiO_2
2S5	Queedup Springs 4S 38E 32ddbS	20	940	1100	6.6	170 (8.3)	61 (5.0)	27 (1.2)	24 (0.6)	28 (0.8)	560 (9.2)	220 (4.6)	18
2S6	Steamboat Springs[1] 9S 41E 10ddaS	31	1100	890	6.1	130 (6.4)	61 (5.0)	26 (1.1)	6.7 (0.2)	0 (0.0)	530 (8.7)	120 (2.5)	20
H-1	Elkhorn Hot Spring 4N 40E 23cadS	20	385	335	6.6	30 (1.5)	10 (0.8)	14 (0.6)	0 (0)	5 (0.1)	186 (3)	7 (0.1)	83
H-2	Hawley Warm Spring 4N 40E 25bbdS	16	350	341	7.5	36 (1.8)	10 (0.8)	10 (0.4)	0 (0)	4 (0.1)	188 (3.1)	5 (0.1)	88
H-3	Heise Hot Springs 4N 40E 25ddaS	48	6500	7667	6.1	676 (33.7)	81 (6.7)	1498 (65.2)	204 (5.2)	2299 (64.9)	2125 (34.8)	723 (15.1)	58
H-6	Unnamed Spring on Birch Creek 3N 41E 32bbdS	23	650	547	7.2	71 (3.5)	19 (1.6)	44 (1.9)	0 (0)	42 (1.2)	271 (4.4)	51 (1.1)	49
H-7	Dyer Well 2N 39E 21bccS	21	530	434	7.7	50 (2.5)	13 (1.1)	50 (2.2)	3 (0.1)	61 (1.7)	188 (3.1)	1 (0)	68
H-8	Anderson Well 2N 39E 29bacS	20	520	467	7.7	50 (2.5)	10 (0.8)	45 (2.0)	7 (0.2)	45 (1.3)	199 (3.3)	0 (0)	111
H-9	Fall Creek Mineral Spring 1N 43E 9cbb1S	24	7800	5416	6.2	473 (23.6)	100 (8.2)	1058 (46)	118 (3)	1851 (52.2)	1473 (24.1)	327 (6.8)	15
H-10	Fall Creek Mineral Spring 1N 43E 9cbb2S	23	6750	4961	6.2	431 (21.5)	88 (7.2)	1065 (46.3)	108 (2.8)	1650 (46.5)	1272 (20.8)	329 (6.8)	17
H-16	Unnamed Spring on Rock Creek 1S 40E 4abcS	21	10500	9229	6.6	110 (5.5)	19 (1.6)	2843 (123.7)	40 (1)	876 (24.7)	2416 (39.6)	2858 (59.5)	62
H-20	Warm Spring 2S 44E 9aacS	17	600	576	7.2	128 (6.4)	27 (2.2)	0 (0)	0 (0)	1 (0)	163 (2.7)	233 (4.9)	24
H-23	Brockman Hot Spring 2S 42E 26dcdS	35	8750	7562	6.6	186 (9.3)	33 (2.7)	2044 (88.9)	38 (1)	553 (15.6)	2255 (37)	2413 (50.2)	38
H-26	Auburn Hot Springs 33N 119W 23dbdS	57	8000	5760	6.4	509 (25.4	76 (6.3)	1327 (57.7)	162 (4.1)	1737 (49)	822 (14.5)	996 (20.7)	68
H-27	Johnson Springs 33N 119W 26adS	54	8100	6310	6.4	454 (22.7)	45 (3.7)	1494 (65)	176 (4.5)	1947 (54.9)	973 (15.9)	1129 (23.5)	88
M-1	Sink Hole 4S 41E 32bbS	19		804	6.8	147 (7.3)	29 (2.4)	27 (1.2)	3 (0.1)	29 (0.8)	504 (8.3)	33 (0.7)	31

Table VI-2. Continued.

Sample Number	Name and Location	Water Temp. °C	Specific Conductance (μmho/cm)	TDS (mg/l)	pH	Ca	Mg	Na	K	Cl	HCO_3	SO_4	SiO_2
						Concentration in mg/l (meq/l)							
M-2	North Woodall 7S 42E 27caS	17	1640	1701	6.3	382 (19.1)	49 (4.0)	4 (0.2)	1 (0.04)	3 (0.07)	1182 (19.4)	48 (1)	31
M-7	Swan Lake #1 (Lakey Res.) 9S 43E 29ccS	16	1020	1089	6.7	220 (11)	36 (3)	3 (0.1)	0.3 (0.01)	3 (0.1)	751 (12.3)	57 (1.2)	19
M-9	Lone Tree 6S 42E 6abS	26	1570	1506	6.4	314 (15.7)	39 (3.2)	26 (1.1)	18 (0.5)	26 (0.7)	989 (16.2)	75 (1.6)	17
M-10	Henry Warm #1 6S 42E 9acS	15	970	934	6.8	178 (8.9)	34 (2.8)	16 (0.7)	2 (0.06)	15 (0.4)	624 (10.2)	46 (1)	18
M-11	Henry Warm #2 6S 42E 9bcS	20	1410	1449	6.4	284 (14.2)	44 (3.6)	25 (1.1)	8 (0.2)	32 (0.9)	870 (14.3)	145 (3)	40
M-12	Warm Spring 6S 42E 8dbS	23	1510	1485	6.3	277 (13.8)	47 (3.9)	22 (1)	14 (0.4)	20 (0.6)	994 (16.3)	84 (1.7)	25
M-14	Little Blackfoot River 6S 42E 15baS	15	940	982	6.7	200 (10)	33 (2.7)	11 (0.5)	2 (0.04)	13 (0.4)	674 (11.1)	42 (0.9)	7
B-1	Corral Creek Well 6S 41E 19bbd	40	4900	5267	6.9	745 (37.2)	244 (20.1)	53 (2.3)	222 (5.7)	39 (1.1)	3016 (49.5)	915 (19)	31
B-3	Thermal Gradient Well 8S 40E 26dbc	15	2400	2221	6.5	345 (17.2)	118 (9.7)	26 (1.1)	12 (0.3)	2 (0.07)	1529 (25.1)	147 (3.1)	42
B-4	Gem Valley Spring #2 8S 40E 26dcbS	16	2400	2320	6.5	361 (18)	120 (9.9)	28 (1.2)	12 (0.3)	13 (0.4)	1529 (26.1)	153 (3.2)	41
B-7	Soda Springs Geyser 9S 41E 12ada	29	4025	4694	6.8	925 (46.2)	150 (12.4)	3 (0.1)	18 (0.5)	3 (0.08)	2778 (45.6)	771 (16)	46
B-13	Pescadero Warm Spring 11S 43E 36bdaS	23	1475	1380	7.0	194 (9.7)	46 (3.8)	70 (3)	13 (2.9)	74 (2.1)	749 (12.3)	215 (4.5)	17
B-17	Unnamed Spring 12S 41E 31abcS	18	775	666	7.1	94 (4.7)	28 (2.3)	37 (1.6)	3 (0.07)	30 (0.9)	439 (7.2)	26 (0.5)	9
B-25	Bear Lake Hot Spring #1 15S 44E 13ccaS	40	2250	1625	7.0	230 (11.5)	41 (3.4)	155 (6.7)	48 (1.2)	72 (2)	263 (4.3)	769 (16)	43
B-28	Gentile Valley Spring #1 11S 40E 5aaaS	22	1825	1698	6.1	239 (11.9)	47 (3.9)	92 (4)	34 (0.9)	78 (2.2)	1086 (17.8)	104 (2.2)	18
B-30	Gentile Valley Spring #3 11S 40E 8dddS	30		930	6.6	132 (6.6)	38 (3.1)	54 (2.3)	3 (0.07)	43 (1.2)	594 (9.7)	40 (0.8)	26

Table VI-2. Continued

Sample Number	Name and Location	Water Temp. °C	Specific Conductance (μmho/cm)	TDS (mg/l)	pH	Ca	Mg	Na	K	Cl	HCO_3	SO_4	SiO_2
						Concentration in mg/l (meq/l)							
B-31	Ben Meek Well 14S 39E 36ada	40	1900	1349	7.4	23 (1.2)	5 (0.4)	348 (15.1)	20 (0.9)	321 (9.1)	526 (8.6)	5 (0.1)	90
B-32	Orvil Rallison Well 16S 40E 16cac	15	455	374	7.6	42 (2.1)	18 (1.5)	20 (0.9)	7 (0.2)	31 (0.9)	199 (3.3)	14 (0.3)	43
S-1	Unnamed on Wolverine Creek 2S 38E 11bbcS	18	640	502	6.8	85 (4.2)	21 (1.7)	3 (0.1)	3 (0.1)	5 (0.1)	268 (4.4)	102 (2.1)	15
S-2	Blackfoot River Warm Spring 5S 40E 14bcdS	28	4600	4915	6.4	700 (34.9)	224 (18.4)	164 (7.1)	201 (5.1)	72 (2)	2371 (38.9)	1148 (23.9)	33
S-3	Unnamed on Blackfoot River 5S 40E 15bacS	18		4851	6.3	668 (33.3)	312 (25.7)	149 (6.5)	182 (4.7)	64 (1.8)	2287 (37.5)	1171 (24.4)	17
S-4	Portneuf River Warm Spring 7S 38E 26cbdS	41	2200	1849	6.3	275 (13.7)	48 (3.9)	85 (3.7)	60 (1.5)	53 (2.4)	1060 (17.4)	259 (5.4)	47
S-5	Lava Hot Spring 9S 38E 21ddaS	43	1590	1179	6.7	103 (5.1)	29 (2.4)	176 (7.7)	37 (0.9)	179 (5)	528 (8.9)	91 (1.9)	35
S-6	Downata Hot Spring 12S 37E 12ccdS	43	450	392	7.1	61 (2.7)	15 (1.2)	26 (1.1)	3 (0.1)	22 (0.6)	211 (3.5)	26 (0.5)	28
S-7	Mound Valley Warm Spring 12S 40E 13dcdS	34	3100	2441	6.1	353 (17.6)	52 (4.3)	267 (11.6)	51 (1.3)	309 (8.7)	1106 (18.1)	278 (5.8)	24
S-8	Cleveland Warm Springs 12S 41E 31cacS	55	3600	2554	6.2	259 (12.9)	41 (3.4)	444 (19.3)	90 (2.3)	574 (16.2)	565 (9.3)	517 (10.8)	62
S-9	Unnamed near Cleveland 12S 41E 31badS	21	750	619	6.7	82 (4.1)	25 (2.1)	32 (1.4)	5 (0.1)	27 (0.8)	410 (7.7)	23 (0.5)	15
S-10	Treasureton Warm Spring 12S 40E 36acdS	40	4550	3179	6.4	336 (16.8)	48 (3.9)	542 (23.6)	110 (2.8)	626 (17.7)	726 (11.9)	734 (15.3)	54
S-11	Maple Grove Hot Spring 13S 41E 7acaS	75	3000	2177	6.3	132 (6.6)	24 (1.8)	550 (23.9)	71 (1.8)	586 (16.5)	466 (7.6)	282 (5.9)	66
S-12	Unnamed near Maple Grove 13S 41E 7dabS	62	3150	2107	5.9	82 (4.1)	22 (1.8)	499 (21.7)	77 (2)	585 (16.5)	454 (7.4)	323 (6.7)	64
S-13	Battle Creek (Wayland) H. S. 15S 39E 8bdcS	77	16550	9581	6.5	179 (8.9)	16 (1.3)	2985 (129.8)	493 (12.6)	5092 (143.6)	631 (11.2)	39 (0.8)	90
S-14	Squaw Hot Spring Well 15S 39E 17bdc	82	24800	13167	6.9	261 (13)	21 (1.7)	3996 (173.8)	694 (17.7)	7291 (205.7)	725 (11.9)	35 (0.7)	139

Table VI-2. Continued.

Sample Number	Name and Location	Water Temp. °C	Specific Conductance (μmho/cm)	TDS (mg/l)	pH	Concentration in mg/l (meq/l) Ca	Mg	Na	K	Cl	HCO_3	SO_4	SiO_2
I-1	Yandell Springs 3S 37E 31dbbS	32	950	714	7.1	150 (7.5)	35 (2.9)	22 (1)	7.2 (0.2)	29 (0.8)	240 (3.8)	330 (6.9)	32
I-2	Alkali Warm Springs 4S 38E 28dddS	34	1529	1040	6.6	210 (10.5)	68 (5.6)	34 (1.5)	37 (1)	17 (0.5)	640 (10.2)	340 (7.1)	34
I-4	Shoal Subdiv. Well 5S 34E 26dba	26		973		93 (4.6)	39 (3.2)	176 (7.7)	25 (0.7)	228 (6.4)	425 (6.8)	156 (3.2)	38
I-5	Dean Morris Well 9S 36E 3cdb	22	349	200	7.2	44 (2.2)	9.2 (0.8)	13 (0.6)	1.9 (0)	24 (0.7)	143 (2.3)	13 (0.3)	25
I-6	Indian Springs 8S 31E 18dabS	32	1099	599	7.5	76 (3.8)	19 (1.6)	110 (4.8)	10 (0.3)	220 (6.2)	254 (4.1)	19 (0.4)	20
I-7	Rockland Warm Spring 10S 30E 13cdcS	38	1109	575	7.6	92 (4.6)	33 (2.7)	62 (2.7)	14 (0.4)	250 (7)	160 (2.6)	23 (0.5)	22
I-8	C & Y Ranch Well 11S 27E 5bab	29	655	432	7.6	26 (1.3)	7.2 (0.6)	100 (4.4)		90 (2.5)	230 (3.7)	14 (0.3)	78
I-9	6-S Ranch Well 11S 25E 11cca	60	574	372	7.7	8.2 (0.4)	0.5 (0)	110 (4.8)	3.9 (0.1)	55 (1.5)	125 (2.6)	59 (1.2)	60
I-11	Ward Warm Spring 13S 26E 17ccdS	21	217	176	8.7	34 (1.7)	0.6 (0)	14 (0.6)	3 (0.1)	25 (0.7)	92 (1.5)	9.5 (0.2)	45
I-12	Malad Warm Spring 14S 36E 27cdaS	24	7589	4345	6.5	240 (12)	79 (6.5)	1200 (52.2)	210 (5.5)	2100 (58.8)	958 (15.3)	25 (0.5)	19
I-13	Pleasantville Warm Spring 15S 35E 3aabS	25	2187	1217	6.8	110 (5.5)	33 (2.7)	280 (12.2)	29 (0.8)	470 (13.2)	331 (5.3)	110 (2.3)	21
I-14	M. Fonnesbeck Well 15S 39E 7dbcS	23	889	566	6.8	78 (3.9)	27 (2.2)	68 (3)	18 (0.5)	91 (2.5)	418 (6.7)	4.3 (0)	7.4
I-15	E. Bingham Well 16S 38E 24abcS	63	27999	14103	6.2	320 (16)	36 (3)	4600 (200.1)	770 (20)	7800 (218.4)	930 (14.9)	48 (1)	68
I-16	Woodruff Warm Spring 16S 36E 10bbcS	27	5369	3084	7.3	130 (6.4)	45 (3.7)	910 (39.6)	87 (2.3)	1600 (44.8)	454 (7.4)	58 (1.2)	29
I-17	Robert Brown Well 5S 34E 26dab	41	1170	706	7.7	70 (3.5)	25 (2)	150 (6.5)	21 (0.5)	87 (2.4)	478 (7.6)	95 (2)	20
I-18	Kent Warm Spring 12S 34E 36bcbS	24	479	292	6.7	56 (2.8)	19 (1.6)	15 (0.7)	43 (1)	35 (1)	226 (3.6)	18 (0.4)	33

Table VI-2. Continued

Sample Number	Name and Location	Water Temp. °C	Specific Conductance (μmho/cm)	TDS (mg/l)	pH	Concentration in mg/l (meq/l) Ca	Mg	Na	K	Cl	HCO_3	SO_4	SiO_2
I-19	Green Canyon (Pincock) W. S. 5N 43E 6bcaS	44	850	620	6.8	140 (7.0)	32 (2.7)	3 (0.2)	3.6 (0.1)	1.7 (0)	170 (2.7)	330 (6.9)	25
I-22	Alpine Warm Spring 2S 46E 19cadS	37	10499	6615	6.5	560 (27.9)	100 (8.2)	1500 (65.3)	180 (4.6)	2800 (79)	880 (14.4)	1000 (20.8)	40
R-1	RRGE-1 15S 26E 23caa	138	2987	1478	7.8	53 (2.6)	0.6 (0)	469 (20.4)	33 (0.9)	709 (19.9)	34 (0.6)	40 (0.8)	134
R-2	RRGE-2 15S 26E 23aaa	139	2157	1330	7.6	32 (1.6)	0.7 (0)	331 (14.4)	31 (0.8)	701 (19.6)	42 (0.7)	29 (0.6)	155
R-3	RRGE-3 15S 26E 25bdc	147	7997	3824	7.2	127 (6.3)	1 (0)	1245 (54.2)	103 (2.7)	2116 (59.2)	26 (0.4)	44 (0.9)	158
R-4	RRGP-5B 15S 26E 22dda	130	2857	1076	7.5	50 (2.5)	0.5 (0)	179 (7.8)	34 (0.9)	590 (16.5)	40 (0.6)	40 (0.8)	136
R-5	RRGI-6 15S 26E 25ada	122	11594	6107	7.3	199 (9.9)	1.4 (0.1)	2020 (87.9)	32 (0.8)	3636 (101.8)	62 (1)	60 (1.2)	91
W-1	Big Fall Creek Warm Spring 28N 115W 20dcaS	16	712	524	7.8	110 (5.5)	29 (2.4)	4 (0.2)	1 (0)	4 (0.1)	160 (2.6)	260 (5.4)	13
W-2	Granite Hot Spring 39N 113W 6dabS*	41	1050	670	8.3	32 (1.6)	46.4 (3.8)	180 (7.8)	8.6 (0.2)	140 (3.9)	200 (3.3)	150 (3.1)	49
W-3	Astoria Warm Spring 39N 116W 32daaS	37	1550	1160	7.8	170 (8.5)	43 (3.5)	120 (5.2)	13 (0.3)	97 (2.7)	300 (4.9)	520 (10.8)	
W-4	Boyles Hill Warm Spring 41N 117W 36caaS	30	2380	2480	7.6	430 (21.5)	120 (9.9)	28 (1.2)	13 (0.3)	3.9 (0.1)	160 (2.6)	1600 (33.3)	
U-1	Crystal Hot Springs 11N 2W 39dadS	56	58000	43500		830 (41.4)	230 (18.9)	15000 (652.5)	790 (20.2)	26000 (733.4)	479 (7.7)	480 (10)	32
U-2	Cutler Warm Spring 13N 2W 27dbd	23	3670	2120	7.6	84 (4.2)	43 (3.5)	620 (27)	22 (0.6)	1000 (28.2)	320 (5.1)	65 (1.4)	17
U-3	Morning Glory Pool 13N 3W 23acb	51	15000	15000	7.2	220 (11)	70 (5.8)	2900 (126.2)	120 (3.1)	4800 (135.4)	360 (5.8)	98 (2)	29
U-4	Bemont Ward Well 13N 3W 35dda	15.5	2390	1560	7.8	66 (3.3)	35 (2.9)	440 (19.1)	28 (0.7)	470 (13.2)	485 (7.8)	220 (4.6)	47
U-5	Blue Springs 13N 5W 29	28	3410	2010	7.9	56 (2.8)	24 (2)	636 (27.7)	22 (0.6)	895 (25.2)	329 (5.3)	84 (1.7)	19

Table VI-2. Continued

Sample Number	Name and Location	Water Temp. °C	Specific Conductance (μmho/cm)	TDS (mg/l)	pH	Concentration in mg/l (meq/l) Ca	Mg	Na	K	Cl	HCO_3	SO_4	SiO_2
U-6	R. W. Tolman Well 15N 6W 34ccc	20.5	1610	938	7.9	60 (3)	25 (2)	247 (10.7)	5.7 (0.1)	375 (10.6)	259 (4.1)	40 (0.8)	41
U-7	Chas Taylor Well 12N 1E 16ddd	22	534	336	7.4	56 (2.8)	26 (2.1)	32 (1.4)	0 (0)	12 (0.3)	327 (5.2)	16 (0.3)	17
U-8	Cache Valley Well 13N 1E 33aca	21	1480	789	6.8	42 (2.1)	36 (3)	204 (8.9)	49 (1.3)	342 (9.6)	286 (4.6)	1.2 (0)	13
U-9	D. J. Gancheff Well 14N 1W 33aca	31	7230	4380	7.6	132 (6.6)	46 (3.8)	1400 (60.9)	110 (2.8)	2280 (64.3)	548 (8.8)	71 (1.5)	23
U-10	Coyote Spring 14N 10W 33bccS	43.5	5590	5990	7.6	87 (4.3)	19 (1.6)	1070 (46.5)	56 (1.4)	1620 (45.7)	352 (5.6)	70 (1.5)	29
U-11	Ethyl Taylor Well 15N 9W 31abc	16	626	626	7.8	70 (3.5)	17 (1.4)	31 (1.3)	0 (0)	99 (2.8)	181 (2.9)	20 (0.4)	63
U-12	Peter Mayo Well 15N 10W 36bbb	16.5	502	324	7.4	59 (2.9)	17 (1.4)	18 (0.8)	0 (0)	51 (1.4)	198 (3.2)	23 (0.5)	56

[1]Spring emerges in Soda Point Reservoir. Water sample is probably mixed with surface water from the reservoir.

Table VI-3. Physical characteristics of thermal spring and well sites in the study area.

Sample Number	Name and Location	Date Sampled	Temp. °C	Elevation (meters)	Estimated Discharge (l/s)	Site Description
AQ-1	26-1 Cook 5N 44E 26ba 2497'-2584' interval	12/01/77	46	1842	-	Upper Triassic Dinwoody formation.
AQ-2	26-1 Cook 5N 44E 26ba 2962'-2997' interval	12/01/77	49	1842	-	Lower Triassic Dinwoody formation.
AQ-3	26-1 Cook 5N 44E 26ba 4210'-4230' interval	12/01/77	70	1842	-	Mississippian Lodgepole formation.
AQ-4	Black Mountain Federal #1 3S 45E 36cc 13,550'-13,703' interval	4/13/77	65	2523	-	Contact between Triassic Dinwoody and Permian Phosphoria formations.
AQ-5	2-1 King 2S 41E 2bc 8550'-8660' interval	6/00/78	116	2031	-	Jurassic Gypsum Springs (lower Twin Creek) formation.
AQ-6	2-1 King 2S 41E 2bc 11,375'-11,519' interval	6/00/78	160	2031	-	Triassic basal Thaynes.
AQ-7	2-1 King 2S 41E 2bc 12,830'-12,884' interval	8/00/78	249	2031	-	Permeian upper Phosphoria formation.
AQ-8	North Eden Felderal 21-11 16S 45E 21aa 8214'-8469' interval	5/15/80	92	2139	-	Overturned Triassic Thaynes formation.
AQ-9	Jensen 13S 44E 22cc 10,900'-10,931' interval	1/25/78	74	1823	-	Permeain-Pennsylvanian Wells formation.
2S1	O. J. Neeley Well 7N 43E 30ccc	9/07/81	22	1749	-	Pliocene rhyolite near the edge of the Moody Creek Caldera complex on northeast trending fault.
2S2	Walz Warm Spring 5N 43E 7acS	9/07/81	35	1894	9.2	Pliocene rhyolite on northwest trending Warm Creek fault.
2S3	Stinking Spring 3N 41E 10bbbS	9/07/81	20	1754	0.05	Tertiary rhyolite.
2S4	Taylor Warm Spring 3N 44E 7baaS	9/05/81	21	1874	35	Colluvium underlain by Wells formation or Mission Canyon limestone. The trace of the Jackson Thrust is very close as is an inferred normal fault.

Table VI-3. Continued.

Sample Number	Name and Location	Date Sampled	Temp. °C	Elevation (meters)	Estimated Discharge (l/s)	Site Description
2S5	Queedup Springs 4S 38E 32ddbS	10/02/81	20	1759	42	Permian-Pennsylvanian Wells formation.
2S6	Steamboat Springs 9S 31E 10ddaS	9/29/81	31[1]	1757	-	Basalt overlying Ordovician and upper Cambrian rocks in an area of numerous extensionl faults. Emerges in Soda Point Reservoir.
H-1	Elkhorn Hot Spring 4N 40E 23cadS	7/31/80	20	1580	13	Rhyolite tuff near Heise fault. Spring is associated with the Rexburg Caldera Complex.
H-2	Hawley Warm Spring 4N 40E 25bbdS	7/31/80	16	1610	13	Same as above.
H-3	Heise Hot Springs 4N 40E 25ddaS	6/18/80	48	1536	3.8	Tertiary silicic volcanics, associated with the Heise fault and a northeast trending fault.
H-6	Unnamed Spring on Birch Creek 3N 31E 32bbdS	6/18/80	23	1707	6.3	Rhyolitic Spring Creek tuff near a large northeast trending fault.
H-7	Dyer Well 2N 39E 21bccS	7/21/80	21	1537	-	Well produces from broken rhyolite near a northeast trending fault.
H-8	Anderson Well 2N 39E 29bacS	7/21/80	20	1524	-	Similar to above.
H-9	Fall Creek Mineral Spring 1N 43E 9cbb1S	8/05/80	24	1658	6.3	Mission Canyon limestone, associated with the Swan Valley fault. Springs are depositing travertine.
H-10	Fall Creek Mineral Spring 1N 43E 9cbb2S	8/05/80	23	1658	4.4	Same as above
H-16	Unnamed Spring on Rock Creek 1S 40E 4abcS	7/22/80	21	1699	1.8	Ephraim conglomerate associated with a minor fault.
H-20	Warm Spring 2S 44E 9aacS	7/23/80	17	2182	13	Twin Creek limestone-Nugget sandstone contact (= Gypsum Springs), near axis of northwest trending anticline.
H-23	Brockman Hot Spring 2S 42E 26dcdS	6/27/80	35	1908	3.8	Peterson or Bechler formation in an area of complex folding and minor faulting.
H-26	Auburn Hot Springs 33N 119W 23dbdS	7/25/80	57	1853	2.5	Dinwoody formation at intersection of Hemmert and Freedom faults. Spring is depositing travertine and free sulfur.
H-27	Johnson Springs 33N 119W 26adS	7/25/80	54	1853	0.01	Paleozoic sedimentary rocks. Spring issues from Hemmert fault and is depositing travertine.
M-1	Sink Hole 4S 41E 32bbS		19	1890	292	Wells formation along Enoch Valley fault.

Table VI-3. Continued.

Sample Number	Name and Location	Date Sampled	Temp. °C	Elevation (meters)	Estimated Discharge (l/s)	Site Description
M-2	North Woodall 7S 42E 27caS		17	1900	28	Wells formation along an extension fault in the Aspen Range.
M-7	Swan Lake #1 (Lakey Res.) 9S 43E 29ccS		16	1890	85	Same as above.
M-9	Lone Tree 6S 42E 6abS		26	1870	3	Flows from Slug Valley(?) fault.
M-10	Henry Warm #1 6S 42E 9acS		15	1867	88	Flows from intersection of Slug Valley and Henry faults. Is depositing travertine.
M-11	Henry Warm #2 6S 42E 9bcS		20	1870	55	Same as above.
M-12	Warm Spring 6S 42E 8dbS		23	1880	14	Same as above.
M-14	Little Blackfoot River 6S 42E 15baS		15	1883	57	Wells formation along axis of Wooley Valley anticline.
B-1	Corral Creek Well 6S 41E 19bbd		40	1884	1.2	Wells-Phosphoria contact in a highly faulted area. This spring produces large amounts of gas, probably CO_2.
B-3	Thermal Gradient Well 8S 40E 26dbc		15	1707	1.4	Garden City limestone (Ordovician) along East Gem Valley graben fault.
B-4	Gem Valley Spring #2 8S 40E 26dcbS		16	1722	22	Quaternary basalt-Garden City contact near above.
B-7	Soda Springs Geyser 9S 41E 12ada		29	1770	0.1	Occurs along a north trending fracture trace. The well is rapidly depositing travertine and is a large CO_2 producer.
B-13	Pescadero Warm Spring 11S 43E 36bdaS		23	1820	0.6	Triassic Thaynes formation overlain by travertine.
B-17	Unnamed Spring 12S 41E 31abcS		18	1540	-	Cambrian Blacksmith(?) limestone overlain by travertine.
B-25	Bear Lake Hot Spring #1 15S 44E 13ccaS		40	1810	-	Mississippian Lodgepole limestone along East Bear River Valley graben fault.
B-28	Gentile Valley Spring #1 11S 40E 5aaaS		22	1510	140	Ordovician Garden City limestone overlain by alluvium.
B-30	Gentile Valley Spring #3 11S 40E 8dddS		30	1520	45	Cambrian Blacksmith(?) limestone overlain by alluvium.

Table VI-3. Continued.

Sample Number	Name and Location	Date Sampled	Temp. °C	Elevation (meters)	Estimated Discharge (l/s)	Site Description
B-31	Ben Meek Well 14S 39E 36ada		40	1380		Possible intersection of Mink Creek lineament and inferred northwest trending extension faults.
B-32	Orvil Rallison Well 16S 40E 16cac		15	1370		Alluvium overlying Cambrian rocks near Cub River lineament.
S-1	Unnamed on Wolverine Creek 2S 38E 11bbcS	7/24/80	18	1554	71	Mississippian Mission Canyon limestone. The area is intensely faulted and folded.
S-2	Blackfoot River Warm Spring 5S 40E 14bcdS	7/11/80	28	1874	0.1	Triassic Thaynes(?) overlain by basalt. This spring has deposited large amounts of travertine.
S-3	Unnamed on Blackfoot River 5S 40E 15bacS	7/09/80	18	1898		Same as above. This "spring" was not flowing, but was degassing. It has deposited a large travertine mound.
S-4	Portneuf River Warm Spring 7S 38E 26cbdS	6/27/80	41	1637	28	Basalt and colluvium over Garden City(?) limestone. This spring is evolving considerable gas. Smells of H_2S.
S-5	Lava Hot Spring 9S 38E 21ddaS	6/27/80	43	1508		Ordovician Swan Peak quartzite near the intersection of north and west trending faults.
S-6	Downata Hot Spring 12S 37E 12ccdS	7/21/80	43	1477	31	Tertiary sediments overlain by alluvium. The spring is associated with an east-west trending lineament.
S-7	Mound Valley Warm Spring 12S 40E 13dcdS	7/14/80	34	1530	0.01	Large travertine mound overlying alluvium and probably Cambrian rocks at depth. This spring was not flowing at 9/81.
S-8	Cleveland Warm Springs 12S 41E 31cacS	7/15/80	55	1520		Travertine over alluvium over Cambrian(?) rocks.
S-9	Unnamed near Cleveland 12S 41E 31badS	7/14/80	21	1510	30	Extensive travertine underlain by Cambrian rocks. The area is extensively faulted.
S-10	Treasureton Warm Spring 12S 40E 36acdS	7/14/80	40	1510	0.2	Same as above.
S-11	Maple Grove Hot Spring 13S 41E 7acaS	7/14/80	75	1500	2	Cambrian Brigham quartzite. The area is extensively faulted. The spring is depositing tufa.
S-12	Unnamed near Maple Grove 13S 41E 7dabS	7/16/80	62	1520	1	Same as above.
S-13	Battle Creek (Wayland) H. S. 15S 39E 8bdcS	7/24/80	77	1383	57	Spring emerges near inferred intersection of the Clifton Hill faults and the Mink Creek lineament.
S-14	Squaw Hot Spring Well 15S 39E 17bdc	7/21/80	82	1380	1.9	Same as above.

Table VI-3. Continued.

Sample Number	Name and Location	Date Sampled	Temp. °C	Elevation (meters)	Estimated Discharge (l/s)	Site Description
I-1	Yandell Springs 3S 37E 31dbbS	8/18/77	32	1514	95	Wells formation(?).
I-2	Alkali Warm Springs 4S 38E 28dddS	8/18/77	34	1738	0.6	Wells formation.
I-4	Shoal Subdiv. Well 5S 34E 26dba	6/20/79	26	1391	-	Quaternary loess near Snake Plain boundary fault.
I-5	Dean Morris Well 9S 36E 3cdb	8/07/76	22			
I-6	Indian Springs 8S 31E 18dabS	7/27/72	34	1369	-	Paleozoic limestone along northwest trending fault.
I-7	Rockland Warm Spring 10S 30E 13cdcS	7/27/72	38	1462	-	Alluvium over Permian-Pennsylvanian Oquirrh formation in Cenozoic graben.
I-8	C & Y Ranch Well 11S 27E 5bab	9/00/66	29	1342	88	Alluvium and basalt over Tertiary sediments in a Cenozoic graben.
I-9	6-S Ranch Well	7/26/72	60	1415	68	Precambrian fractured quartzite near north trending fault.
I-11	Ward Warm Spring 13S 26E 17ccdS	8/08/75	21	1532	0.3	Tertiary rhyolite(?) near east trending fault zone.
I-12	Malad Warm Spring 14S 36E 27cdaS	5/16/72	24	1415	-	Flows from alluvium and travertine near graben boundary.
I-13	Pleasantville Warm Spring 15S 35E 3aabS	5/10/72	25	1362	240	Same as above.
I-14	M. Fonnesbeck Well 15S 39E 7dbcS	9/03/73	63	1390	69	Similar to S-14
I-15	E. Bingham Well 16S 38E 24abcS	8/24/77	63	1415	37	
I-16	Woodruff Warm Spring 16S 36E 10bbcS	5/11/72	27	1354	-	Same as I-12 and I-13
I-17	Robert Brown Well 5S 34E 26dab	7/27/72	41	1390	11	Same as I-4
I-18	Kent Warm Spring 12S 34E 36bcbS	5/17/72	24	1608	12	Upper Paleozoic rocks.

Table VI-3. Continued.

Sample Number	Name and Location	Date Sampled	Temp. °C	Elevation (meters)	Estimated Discharge (l/s)	Site Description
I-19	Green Canyon (Pincock) W. S. 5N 43E 6bcaS	8/09/72	44	1846	-	Tertiary rhyolite near edge of Moody Creek Caldera and Warm Creek fault.
I-22	Alpine Warm Spring 2S 46E 19cadS	9/27/77	37	1689	1.6	Issues under Palisades Reservoir near northwest trending graben boundary fault (Swan Valley fault). Other discharge vents were reported to be as hot as 65°C.
R-1 - R-5	Raft River Geothermal Wells 15S 26E 23caa, 23aaa, 25bdc, 22dda, 25ada		122- 147	1508	3	Tertiary Salt Lake sediments overlying Precambrian gneiss complex. Wells are near the intersection of two fault zones.
W-1	Big Fall Creek Warm Spring 28N 115W 20dcaS	10/07/76	16	2569	170	Lower Triassic Dinwoody formation within the Cabin Creek over-thrust.
W-2	Granite Hot Springs 39N 113W 6dabS*	9/22/76	41	2166	19	Fractured Cambrian Death Canyon formation near contact with Flat Head formation and perhaps in contact with underlying granites.
W-3	Astoria Warm Spring 39N 116W 32daaS	9/22/76	37	1808	≥6.3	Mississippian Mission Canyon limestone near crest of north trending anticline at a regional topographic low for the formation
W-4	Boyles Hill Warm Spring 41N 117W 36caaS	9/23/76	30	1940	3.2	Cambrian Gallatin limestone near Jackson thrust fault.
U-1	Crystal Hot Springs 11N 2W 39dadS	10/27/51	56	1375	101	Issues from alluvium about 2.4 km from the Wasatch fault.
U-2	Cutler Warm Spring 13N 2W 27dbd	2/02/68	23	1385	0.6	Issues from Paleozoic limestone about 1.6 km from the Wasatch fault.
U-3	Morning Glory Pool 13N 3W 23acb	9/08/71	51	1346	13	Paleozoic limestone near a buried, north-trending fault along the Malad River Valley.
U-4	Belmont Ward Well 13N 3W 35dda	8/25/64	16	1360	30	Similar to above.
U-5	Blue Springs 13N 5W 29	7/07/70	28	1353	295	Permian-Pennsylvanian Oquirrh formation.
U-6	R. W. Tolman Well 15N 6W 34ccc	7/07/70	21	1631	-	
U-7	Chas Taylor Well 12N 1E 16ddd	4/17/68	22	1369	2.3	Alluvium.
U-8	Cache Valley Well 13N 1E 33aca	7/09/57	21	1369	4.7	Tertiary rocks, undifferentiated.

Table VI-3. Continued.

Sample Number	Name and Location	Date Sampled	Temp. °C	Elevation (meters)	Estimated Discharge (l/s)	Site Description
U-9	D. J. Gancheff Well 14N 1W 33aca	1/12/68	31	1392	-	Alluvium near Dayton fault zone.
U-10	Coyote Spring 14N 10W 33bccS	5/28/68	44	1354	1.3	Pleistocene basalt overlying upper Paleozoic rocks. An intrusive body is inferred at depth.
U-11	Ethyl Taylor Well 15N 9W 31abc	9/00/69	16	1415	145	Same as above.
U-12	Peter Mayo Well 15N 10W 36bbb	5/24/56	17	1415	135	Same as above.

spring deposits, or because information was not included in the reports summarized on this table. Spring discharges noted in this table were obtained by various methods, but are often estimates.

<u>Comparability of Water Quality Data</u>

Many of the thermal occurrences sampled by this project had been previously sampled by IDWR. In addition, sampling by this project occurred over two field seasons involving different personnel and different analytical techniques. In order to assure the comparibility of these data, a statistical comparison was done using the General Linear Models (GLM) computer program developed by SAS (SAS Institute, Inc., 1979). This program compares the variances of the values obtained for a given analysis as done by different agencies. Variances are compared by the F statistic:

$$F = \frac{s_1^2}{s_2^2}$$

where:

s_1^2 = the variance within the set of values obtained for a given analysis as done by Agency 1, and

s_2^2 = the corresponding variance for the analysis as done by Agency 2 (Ott, 1977).

Prior to performing this test the concentration values were converted to their log value in order to smooth the difference between values. Concentrations of zero (undetectable) were changed to one to avoid an undefined operation (log 0). The data were then standardized according to the formula:

$$Z = \frac{x - \bar{x}}{s}$$

where:

Z = the standardized variable,

x = the original value,

$\bar{x}$ = the mean for that variable, and

s = the standard deviation of the variable (Huntsberger and Billingsley, 1977)

In this GLM test, the null hypothesis (H) states that the variance of a particular analysis for a given constituent as done by Agency 1 (IDWR) equals the variance of the same analysis as done by Agency 2 (this project, 1980, samples analyzed by researchers): $s_1^2 = s_2^2$. The alternate hypothesis is the converse: $s_1^2 \neq s_2^2$. This same type of test is also done to compare Agency 2 with Agency 3 (this project, 1981, samples analyzed by the University of Idaho Agricultural Science Analytical Laboratory). Tables VI-4 and VI-5 are the results of these GLM analyses.

Table VI-4. Comparison of IDWR and Thrust Geothermal project chemical analysis (1980 samples)

Chemical Species	F Value	Probability of a Greater F Value	Accept Null Hypothesis
pH	2.34	0.1453	yes
Ca	0.00	0.9830	yes
Mg	35.55	0.0001	no
Na	1.37	0.2587	yes
K	4.89	0.0420	no
Cl	4.20	0.0571	yes
HCO_3	2.28	0.1510	yes
SO_4	1.07	0.3157	yes
SO_2	1.34	0.2640	yes

Table IV-5. Comparison of Thrust Geothermal project (1980 samples) and University of Idaho Agricultural Science Analytical Laboratory chemical analysis (1981 samples)

Chemical Species	F Value	Probability of a Greater F Value	Accept Null Hypothesis
Ca	14.02	0.0028	no
Mg	0.14	0.7119	yes
Na	0.59	0.4571	yes
K	0.04	0.8373	yes
Cl	0.89	0.3649	yes
SO_4	0.31	0.5863	yes
SiO_2	0.35	0.5637	yes

The comparison indicates that differences between the analyses are not generally significant, i.e., the null hypothesis is accepted. These results appear quite good considering that it was not always possible to sample the exact same spring outlet sampled by previous workers, samples were collected over a number of years at different times of the year and by different researchers.

Deuterium and Oxygen-18 Data

Twenty-two samples were collected and analyzed for stable isotope ratios of deuterium (D) to H and oxygen-18 to oxygen-16 in addition to those reported in Chapter IV. Souder (1983) compared these results to the standard SMOW line (see Chapter IV for an explanation of the method). Only samples S-13 and S-14 (Battle Creek (Wayland) Hot Springs and Squaw Hot Springs well) showed any evidence of an oxygen-18 shift caused by heating above 80°C. Distinguishable effects caused by differences in recharge latitude or elevation were not noted.

Carbon Isotope Analysis

Twelve samples were collected and analyzed for carbon-14 age data analysis in addition to those reported in Chapter IV. The data are presented on Table VI-6. Analysis and interpretation of results followed the procedures outlined

Table VI-6. Isotopic and geochemical characteristics, and estimated ages of selected thermal and non-thermal waters in southeastern Idaho

Name/Location	Site ID No.	pCO_2 (atms)	HCO_3^- (meq)	$CO_3^=$ (meq)	pH	Temp (°C)	Sample ^{13}C (o/99 PDB)	Mineral ^{13}C (o/oo PDB)	Soil Gas ^{13}C (o/oo PDB)	Sample $A^{14}C$ (pmc)	Mineral $A^{14}C$ (pmc)	Soil Gas $A^{14}C$ (pmc)	Estimated Age/Error (yrs BP)
Treasureton Warm Spring 12S 40E 36acdS	S-10	.30	11.3	$10^{-2.5}$	6.4	49	+1.9		+20.0	0.96 ±0.07	0	100	36,000 ±3,000
Williams Creek Spring 12S 41E 27bbaS	B-16	.01	3.8	$10^{-2.6}$	7.8	6	-11.7		+20.0	76.8 ±0.7	0	150	post bomb
Soda Springs Geyser 9S 41E 12adaS	B-7	.36	39.5	$10^{-1.5}$	7.2	30	+5.6			0.24 ±0.07	0	100	45,000 +3,000
Gem Valley Spring #2 8S 40E 26dcbS	B-4	.39	22.9	$10^{-2.3}$	7.1	16	+2.2			2.17 ±0.10	0	100	27,000 ±2,000
Blackfoot River Warm Spring 5S 40E 15bacS	S-2	.78	35.7	$10^{-2.1}$	6.6	28	+2.1			0.35 ±0.12	0	100	43,000 ±3,000
Brockman Warm Spring 2S 42E 26dcdS	H-23	.53	34.1	$10^{-1.8}$	6.6	36	-2.7			0.32 ±0.09	0	100	44,000 ±3,000
Wolverine Spring 2S 38E 11bbcS	S-1	.04	4.0	$10^{-2.8}$	7.7	19	-7.5			45.5 ±0.90	0	100	1,500 +400 -200
Schluter Spring 3N 41E 32bbdS	H-6	.02	3.6	$10^{-2.4}$	7.4	22	-10.4			59.4 ±0.80	0	100	50-200
Heise Hot Spring 4N 40E 25ddaS	H-3	1.80	16.2	$10^{-2.3}$	6.3	48	+1.2			0.31 ±0.10	0	100	45,000 ±3,000
Fall Creek Mineral Spring 1N 43E 9cbblS	H-9	.73	20.1	$10^{-2.5}$	6.2	24	-0.7			2.20 ±0.13	0	100	30,000 ±2,000
Auburn Hot Spring 33N 119W 23dbdS	H-26	.43	13.5	$10^{-2.4}$	6.3	60	-0.2			0.32 ±0.10	0	100	45,000 ±3,000
Maple Grove Hot Spring 13S 41E 7acaS	S-11	.46	7.8	$10^{-2.8}$	6.4	70	-0.8			2.79 ±0.45	0	100	26,000 ±2,500
Corral Creek Well* 6S 41E 19bbd	B-1	.36	46.6	0	6.6	31	+2.2	+3.6	--	0.80 ±0.14	0	100	36,500 ±3,000
Sinkhole Spring* 4S 41E 22bbS	M-1	.06	8.3	$10^{-2.5}$	6.8	19	-3.1	+3.97	--	13.9 ±0.2	0	100	12,500 ±1,000
Formation Spring* 8S42E 27cbS	M-5	.14	10.2	$10^{-2.7}$	6.6	11	-1.7	+3.6	--	12.2 ±0.1	0	100	14,500 ±1,000
Henry Warm Spring #2 6S 42E 9bcS	M-11	.23	14.3	$10^{-2.6}$	6.4	20	-2.4	+3.6	--	6.19 ±0.23	0	100	20,500 ±2,000

*Data reported in Chapter IV.

in Chapter IV. Most of the thermal discharges had estimated ages greater than 10,000 years.

Thermal Water Groups Delineated By Major Ion Data and Site Geology

Introduction

The large body of hydrochemical and physical data presented in this chapter provides a good basis upon which to begin to interpret the characteristics of geothermal flow systems in the study area. It should be noted that each sample point represents a unique hydrochemistry which is acquired in response to the following controls: 1) rock type through which the water passes, 2) temperature, 3) length of flow path and residence time, 4) relative time of encounter of a given rock type and 5) soil and biological charcateristics of the recharge zone. Souder (1983) discusses these controls in detail. The water quality varies somewhat from site to site even within a particular flow system or discrete hydrochemical environment, but consistent trends are recognizable for a particular system.

Graphic Analysis Techniques

For this study, stiff diagrams presented on a map of the study area (Figure VI-3) were considered to be the most useful means of displaying the hydrochemical information. The stiff diagrams shown on Figure VI-3 indicate that several configurations of ion proportions dominate. In the southern portion of the Basin and Range province, the thermal springs are almost inevitably dominated by two ions -- sodium and chloride. In the center of the study area, the Meade Peak block and adjacent area, calcium and bicarbonate ions dominate with varying amounts of magnesium and sulfate ions also present. Thermal springs along the Swan Valley to Star Valley trend have a very similar hydrochemical make-up which can be represented as Na>Ca>Mg and $Cl>HCO_3>SO_4$. Five widely scattered springs along the western portion of the study area are dominated by calcium and sulfate ions with ion abundance being Ca>Mg>Na> and $SO_4>HCO_3>Cl$. The remaining sites have a lower TDS, generally less than 25 meq/l and are of variable composition. They are found along the margin of the Snake River Plain and scattered throughout the Basin and Range area, but in particular they are concentrated in the northern portion of the Basin and Range area. These springs are difficult to correlate except in the case of proximate sites. It is interesting to note that the low TDS sites in the southern portion of the Basin and Range are all from wells rather than springs. This may indicate that salt concentrations in the upper alluvium are responsible for high TDS in many of the springs in this area.

Statistical Analysis of Major Ion Groups

A statistical analysis was done in order to place the sites into discrete groups. This process requires the simultaneous examination of the nine concentration variables. The statistical analysis procedure followed is describe in Chapter III.

Groups were delineated on the basis of similar geologic settings and similar stiff diagram patterns. The groups are as follows: Group 1 - Meade Peak block calcium bicarboante springs; Group 2 - Adjacent (Paris block) calcium-bicarbonate springs; Group 3 - Swan Valley to Star Valley graben springs; Group 4 - Basin and Range high TDS springs (>25 meq/l); Group 5 - low TDS thermal occurrences from the Basin and Range, Snake River Plain margins; and Group 6 - Maple Grove and Mound Valley area. The calcium-sulfate springs were not considered since they are few in number and widely separated.

A stepwise MANOVA analysis (SAS Institute Inc., 1979) was run to determine if the groups chosen from an examination of the stiff diagrams and the geologic setting can be differentiated statistically, and which hydrochemical variables are the most useful in discriminating between the groups. The hypothesis tested was that the mean of the combined distribution of chemical constituents of one group (μ_1) is equal to the means of the constituents of the others

(μ_2, μ_3, ...). The null hypothesis (H_0) can thus be stated as $\mu_1 = \mu_2 = \mu_3 = \ldots$ and the alternate hypothesis is the converse (Hubbell, 1981).

A discriminant analysis (SAS Institute Inc., 1979) was run using the most significant variables (Souder, 1983). Such an analysis enables determination of whether an observation falls statistically into the group into which it was placed on the basis of geological setting and stiff diagram pattern. Observations which are not statistically consistent with the groups into which they were originally placed are reclassified. The results of this test indicated that 84 percent of the observations are statistically consistent with the groups into which they were originally placed. Seven observations were statistically reclassified into groups which could not be justified geologically (Souder, 1983). In particular, the discharges in Mound Valley and those along the West Gem Valley were reclassified from Group 6 to Group 1. Group 1 thus represents moderate carbonate springs.

<u>WATEQF Analysis of Chemical Equilibria and Speciation</u>

WATEQF, a FORTRAN IV version of a computer program that models thermodynamic speciation of inorganic ions and complex species in solution for a given water analysis was run utilizing the data presented in this chapter (see Chapter III for a description of the program).

Results of the WATEQF analysis indicate that the site groups mentioned earier have distinctive saturation characteristics (see Souder (1983) for tabulated results). The Swan Valley to Star graben (Group 3) thermal springs are all supersaturated (H-3) to slightly undersaturated (I-22) with respect to aragonite, calcite, and dolomite. The Meade Peak thrust block thermal springs (Group 1) are saturated to slightly supersaturated with respect to calcite and aragonite. The adjacent Paris thrust block calcium-bicarbonate thermal springs (Group 2) are all supersaturated with respect to aragonite, calcite, and dolomite. The Basin and Range high-TDS thermal springs and wells (Group 4) are almost all supersaturated with respect to aragonite, calcite, dolomite, talc, and tremolite. The exceptions being that springs B-31, S-13, and I-15 are at saturation with respect to aragonite, springs S-13 and I-15 are undersaturated with respect to talc and tremolite and the thermal springs of the Malad Valley generally are undersaturated in all of the minerals. The low-TDS springs of the Basin and Range and along the margin of the Snake River Plain (Group 5) also tend to be saturated with respect to talc and tremolite, exceptions being I-4 and H-1. These springs and wells are highly variable as to their degree of saturation with respect to the other minerals under discussion.

Ground Water Geochemical Environments in the Study Area

Introduction

The thermal waters of the study area were seen in the preceeding sections to fall into several hydrochemical types which correspond to geologic environments. These hydrochemical environments are summarized in this section. Additional details on the hydrogeologic controls for the theremal systems is presented for areas not discussed in previous chapters.

Thermal Waters of the Swan Valley to Star Valley Graben and Adjacent Areas (Group 3)

The four groups of thermal springs along Swan Valley to Star Valley have temperatures ranging from 66°C at Alpine Hot Spring (I-21) to 23°C at Fall Creek Mineral Springs (H-9 and H-10) (Chapter III). All of these springs emerge along the southwest side of a graben along the Snake River fault, except Heise Hot Springs (H-3) which is along the Heise fault.

The Swan to Star Valley thermal springs have TDS values ranging from 6,000 to 9,000 mg/l. The dominant ions are sodium and chloride but the other major ions are also well represented. The relative ionic concentrations are generally Na>Cl>Mg and $Cl>HCO_3^- >SO_4$. However at Alpine Hot Spring (I-21) and Auburn Hot Spring (H-26), sulfate exceeds bicarbonate. The estimated ages of the discharges are all greater than 25,000 years.

An unnamed spring on Rock Creek (H-14) and Brockman Warm Spring (H-23) to the west of the Caribou Range have water chemistries which are statistically grouped with those of the Swan Valley to Star Valley graben. These two thermal springs have very similar chemistries which differ from those of the Swan Valley to Star Valley springs primarily in their high sodium to chloride ratio (6:1) and high sulfate concentration (50 and 60 meq. respectively).

Thermal Waters of the Meade Peak Thrust Block (Group 1)

The thermal waters of the Meade Peak thrust block all emerge from extensional faults along the western margin of the thrust block (Chapter IV). The temperatures of these springs vary from 15 to 26°C. The thermal waters of the Meade Peak thrust block are uniformly of the calcium bicarbonate type. The TDS of these springs generally varies from between 800 to 1500 mg/l. Sodium, chloride, and sulfate concentrations are negligible in all of the springs.

The thermal springs of the West Gem Valley fault system, also placed in Group 1, have bicarbonate concentrations of 10-18 meq/l and TDS values of 900-2,400 mg/l. Temperatures of these waters vary from 22°C at B-28 up to 41°C at S-4. Sodium and potassium account for between 20-30% of the cation equivalents (versus no more than 18% at the most saline of the high bicarbonate group). Partial pressures of

CO_2 in these discharges are 0.15-0.85 atmospheres. The WATEQF saturation analysis for aragonite, calcite, and dolomite indicated that conditions varied from slightly supersaturated (at S-4) to unsaturated (at B-28). Springs along this trend are not large travertine depositors at this time, but apparently were in the past as evidenced by extensive travertine deposits in the vicinity of B-28, B-30, S-7 and further south at the end of the valley. Souder (1983) presents additional discussion of the CO_2 levels in the area.

Mitchell (1976) has found that aquifer temperature based on silica geothermometry in the Blackfoot Reservoir area do not exceed 50°C. Stable isotope results confirm this conclusion indicating that the water has never attained temperatures of greater than 80°C.

Thermal Waters of the Areas Adjacent to the Meade Peak Block (Group 2)

Several thermal springs and wells arise from the Paris thrust block west of the Meade Peak block. The southern portion of this block is discussed in Chapter V. This thrust block is composed of 1000 to 3500 m of Mississippian through Precambrian rocks thrust over lower Triassic to upper Paleozoic rocks (Armstrong, 1969; Royse and others, 1975). The Paris block is bounded on the east by the Bear Valley graben and by extensional faults along the Blackfoot Lava Field. The western margin is uncertain but the block is truncated by the Gem Valley graben (Armstrong, 1969). The Portneuf Range, which lies just west of the Gem Valley, is composed of the same sequence of rocks as the Paris Block.

The pattern of discharge locations in the Paris Block area is more complicated than that of the Meade Peak block. Two springs and two flowing artesian wells (S-2, S-3, B-7 and B-1) emerge along a trend of extensional faults which runs from the west side of the Bear River Valley graben north along the west side of the Blackfoot Reservoir. Two springs and a flowing artesian well (B-3 and B-4) arise from the East Gem Valley fault just east of the Soda Springs Hills. Four springs (S-4, B-28, B-30 and S-7) emerge near the trace of the West Gem Valley boundary fault system.

All of the calcium bicarbonate type springs were initially grouped for purposes of the discriminant statistical analysis. However, the SAS discriminant analysis placed the springs and well on the west side of the Blackfoot Reservoir (S-2, S-3 and B-1), Soda Springs "Geyser" (B-7), and the spring and well along the East Gem Valley fault (B-3 and B-4) in a group distinct from the springs of the Meade Peak block (Group 1). These springs and wells are referred to here as the "high bicarbonate thermal waters". The springs on the West Gem Valley fault system are grouped with those of the Meade Peak block but may be distinguished by their appreciable sodium chloride content.

Springs in the high bicarbonate group have bicarbonate concentrations which vary from 25-50 meq/l and TDS values which range from 2,200-5,300 mg/l. Temperatures of the waters of this group vary from 15°C at B-3 to 40°C at B-1. Sites S-2, S-3, B-1 and B-7 have a rather high ratio of sulfate to bicarbonate--up to 0.6. All of these thermal occurrences have calculated PCO_2 values of at least 0.29 atmospheres and at one site, S-3, the PCO_2 is 0.84. The results of the WATEQF calculations show that all of these springs are supersaturated with respect to aragonite, calcite, and dolomite and that the high sulfate springs are over 50% saturated with respect to anhydrite and gypsum.

The results of the $D/^{18}O$ analysis would indicate that aquifer temperatures for the high bicarbonate springs have never been greater than 80°C. The radiocarbon ground water ages reported in Table VI-7 indicate long residence times for these waters.

Thermal Waters of the Maple Grove Area

The Maple Grove area lies in a highly faulted and fractured zone near the convergence of the East and West Gem Valley fault system. This area also marks the convergence of the Portneuf and Bear River Ranges. The thermal springs included in this group as by the discriminant analysis are

S-8, S-10, S-11 and S-12. These springs are all located along a six kilometer reach of the Bear River. An initial attempt to include springs at sites B-28, B-30, S-7, B-17 and S-9 on the basis of proximity and/or appreciable sodium chloride content was not allowed by the discriminant analysis.

The thermal springs of the Maple Grove area vary in temperature from 40°C at Treasureton Warm Spring (S-10) to 75°C at Maple Grove Hot Springs (S-11). These springs all have sodium chloride type waters, but also have appreciable concentrations of the other major ions. The Cleveland Hot Springs (S-8 and S-9) have considerably more calcium, bicarbonate, and sulfate than the Maple Grove Hot Springs (S-11 and S-12). In this respect they are intermediate between the calcium bicarbonate type spring at S-7 and the predominantly sodium chloride spring at Maple Grove. The Maple Grove Hot Springs are quite similar in their major ion composition to the thermal springs of the Basin and Range Province which are discussed in the next section, although they have a somewhat higher proportion of calcium, bicarbonate, magnesium, and sulfate.

The WATEQF analysis of saturation indicates that the Maple Grove group of thermal waters varies from somewhat oversaturated to somewhat undersaturated with respect to aragonite, calcite, and dolomite. The exception to this is site S-12 which is highly undersaturated with respect to all of the above minerals. Chalcedony geothermometry indicates aquifer temperatures of 76°C at Treasureton Warm Spring up to 86°C at Maple Grove Hot Spring. Radiocarbon ground water ages are 36,000 years B.P. at S-10 and 26,000 years B.P. at S-11.

<u>Thermal Waters of the Basin and Range Province</u>

The Basin and Range Province accounts for the entire portion of the study area west of the Portneuf Range. This physiographic province is characterized by generally north-south trending normal faults of large displacement. Many of these faults have experienced movement in recent times (Witkind, 1975) and as such are thought to provide excellent conduits for the flow of thermal waters. Ryback (1981) describes this area as a thin-crusted region of high heat flow caused by the intrusion of mafic magmas. He characterizes the geothermal systems as "hot spring discharges in fault/fracture zones, especially where these encounter topographic lows". All of the thermal springs considered by this study are located near normal faults or emerge from the alluvium of adjacent grabens.

The prevalent type of thermal water in the Basin and Range Province is dominated by sodium and chloride and depleted in all other ions. Total dissolved solids (TDS) range from less than 500 mg/l in some of the Cache Valley wells (U-7 and B-32) up to 43,500 mg/l at Crystal Hot Springs (U-1). Temperatures vary from barely thermal in the above mentioned wells to 82°C at Squaw Hot Spring well (S-14). The results of the discriminant analysis place all of the thermal waters having greater than 1,200 mg/l TDS in a single group. Those thermal springs and wells with less than 1,200 mg/l were placed in a separate group which lumped them with other low TDS waters. These low TDS waters of the Basin and Range come from two distinct environments: 1) Basin and Range valleys tributary to the Snake River and 2) from wells in the portion of the Basin and Range which is tributary to the Great Salt Lake.

Typically the thermal waters of the Basin and Range Province are saturated or supersaturated with respect to aragonite, calcite, dolomite, talc and tremolite. This applies to both high and low TDS springs. The only important exceptions are the springs of the Malad Valley which are slightly supersaturated to unsaturated with respect to calcite, aragonite, and dolomite and unsaturated with respect to talc and tremolite. A few other thermal wells (S-13, I-15, U-7 and U-8) are also undersaturated with respect to talc and tremolite.

A major consideration for the springs and wells of the Basin and Range Province is the source of the high concentrations of sodium and chloride. These constituents might be concentrated in ground waters as a result of: 1) their presence in the sedimentary sequence, 2) their presence in the valley alluvium, or 3) gradual accumulation due to leaching of marine sedimentary rocks over the course of a long flow system or long residence times. All of these mechanisms for salt accumulation will result in molar ratios of chloride to sodium close to unity.

It has been previously noted that thermal waters from wells in the Great Salt Lake-tributary valleys are lower in sodium chloride than the thermal springs in the same region. The deepest well (U-8) of those considered in the Cache Valley has a TDS of less than 500 mg/l and is also cooler than the thermal springs of the Cache Valley. Murphy and Gwynn (1979) present a model which accounts for the large variations in salinity by mixing. Their model suggests that saline thermal waters flowing up along fault zones bounding the lower Malad River Valley (Utah) mix with low TDS cooler water from the saturated alluvium of the valley. This model would be consistent with the lower temperatures and lower, but still equi-molar, concentrations of sodium and chloride found in the thermal wells.

Feth (1965) presents a map which shows saline ground water at depths of less than 150 m in the Great Salt Lake-tributary valleys of southern Idaho and northern Utah. This would suggest the presence of salts in the alluvium as a result of evaporation. Such conditions might account for the high equi-molar concentrations of sodium and chloride in the thermal waters of the Cache, Lower Bear River, Malad, and Curlew valleys.

The Basin and Range thermal waters from the Snake River tributary valleys are variable in their chemical makeup. They are often dominated by sodium and chloride but always in low concentrations. The sodium to chloride ratios are highly variable, probably indicating that halite is not the source of these constituents. The low calcium and bicarbonate concentrations are consistent with the low partial pressures of CO_2 (PCO_2) calculated by WATEQF and perhaps with the lesser availability of carbonate rocks in this portion of the Basin and Range. The Raft River geothermal wells (R-1) do not have the above described chemistry; they resemble the Salt Lake-tributary thermal waters.

CHAPTER VII

GEOTHERMAL ANALYSIS FROM REGIONAL DEEP DRILLING

Objectives and Method of Study

The general objective of this portion of the study is to utilize data from deep drilling to help define the controls for geothermal systems in southeastern Idaho. This study is based upon the hypothesis that thrust associated structural features and regional stratigraphy form the major controls for geothermal systems in southeastern Idaho.

The specific objectives are listed below:

1. utilize drilling data from oil and gas exploration wells to delineate thrust associated structural features,
2. obtain and evaluate temperature data from deep drilling, and
3. utilize these data to describe controls for geothermal systems in southeastern Idaho.

This study was conducted by identifying and contacting sources of deep drilling data. Geologic and temperature data from oil and gas exploration wells were then compiled and analyzed to determine controls on geothermal systems in southeastern Idaho.

Deep Drilling Data

Introduction

Wildcat exploration for oil and gas has been conducted in the Idaho segment of the overthrust belt since 1926. A total of 42 deep exploration wells have been drilled to date in this portion of the state. Locations of these wells are shown on Figure VII-1. Data available on these sites range greatly in quantity and quality. Little data are available on most of the wells drilled before 1950. Wells drilled in the last 30 years are generally deeper and better data are usually available.

A listing of oil and gas wells drilled in southeastern Idaho is presented on Table VII-1. General data such as location, operator, date, elevation and total depth are given. The availability of geologic or temperature data for these wells is also shown.

Geologic Data

Geologic data are available on 13 of the wells inventoried. Geologic data obtained from exploration wells consist of a list of depths at which various formations were penetrated. This information is generally referred to as the "formation tops". To obtain most of the data, it was necessary to purchase top cards from Petroleum Information Corportion, a service dealing with drilling data. Geologic

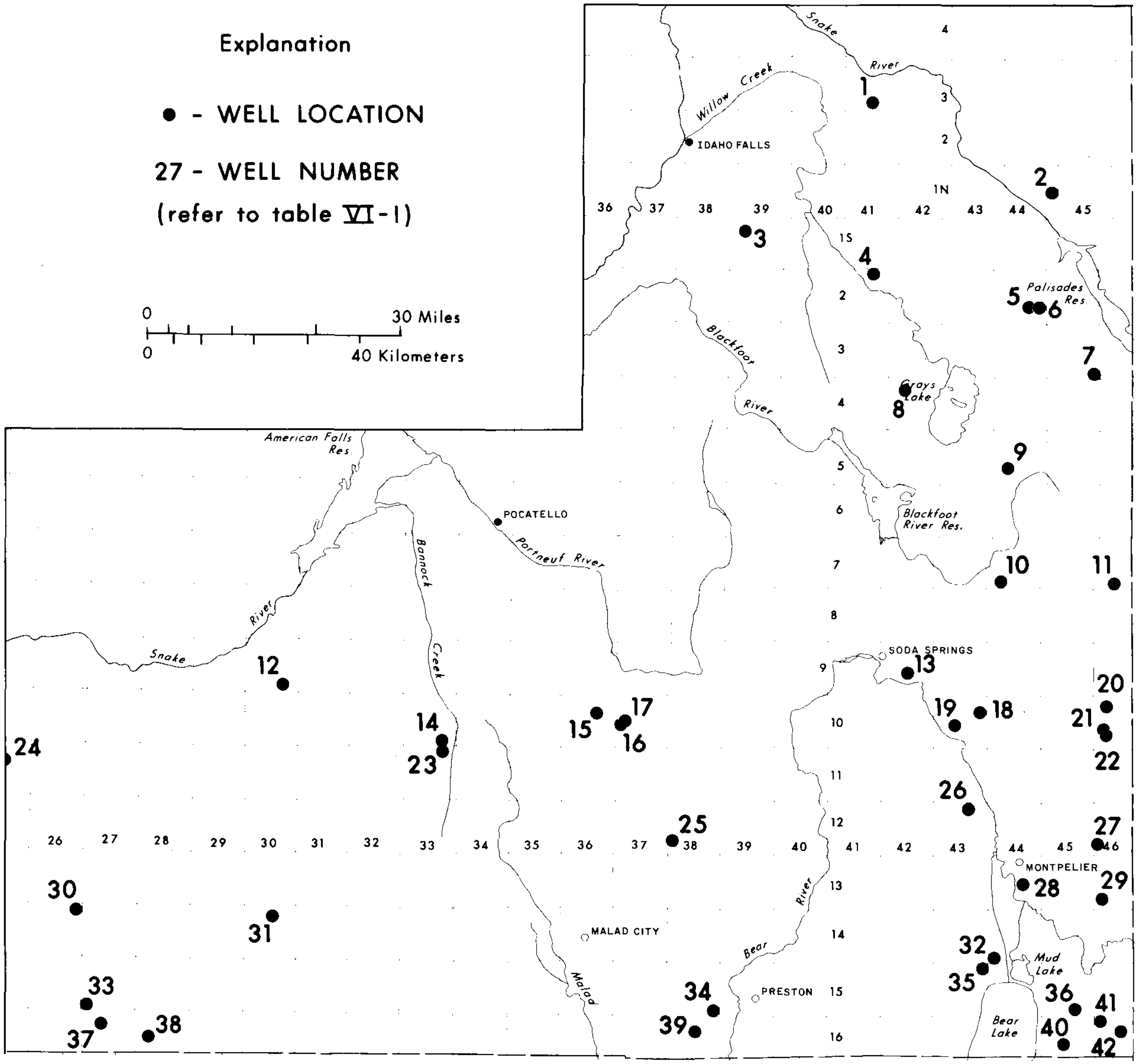

Figure VII-1. Location of oil and gas wells in southeastern Idaho.

Table VII-1. Inventory of oil and gas wells drilled in southeastern Idaho.

Number	Location	County	Well Name	Operator	Completion Date	Elevation (meters)	Total Depth (meters)	Available Data Geology	Available Data Temp.
1	3N 41E 33cc	Bonneville	Sorenson No. 1	California Company	1930	1783	1150	c	
2	1N 44E 24bc	Bonneville	Government No. 1	Edwin Allday	1966	1695	1756		
3	1S 39E 8cca	Bingham	Hoff 1-8 M	Union Oil of California	1979	1737	2625		
4	2S 41E 2aca	Bingham	King No. 2-1	American Quasar	1978	2012	4132	c	d
5	2S 44E 23db	Bonneville	Big Elk Mountain No. 1	Sun-Sinclair	1950	2473	1710	c	d
6	2S 44E 24bcc	Bonneville	T. J. Weber No. 1-A	Pan American	1964	2433	2962	c	
7	3S 45E 36cc	Bonneville	Black Mountain Federal No. 1	American Quasar	1977	2693	4368	c	d
8	4S 42E 9aac	Bonneville	Gentile Valley No. 1	Continental Oil	1978	2080	3021	c	d
9	5S 44E 2cac	Caribou	Stoor "A" No. 1	Phillips Petroleum	1980[a]	2059	246		
10	7S 44E 32aab	Caribou	Dry Valley	Standard Oil of California	1952	2060	2337	c	
11	7S 46E 34ccd	Caribou	Tygee No. 1	Great Western Oil	1926	1890	746		
12	9S 30E 35bb	Power	No. 1	Rockland Valley Oil	1926	1432[b]	472		
13	9S 42E 27dad	Caribou	Ira Ellis No. 1	James Fraizer	1956	1753[b]	1079		
14	10S 33E 35dc	Power	Porter No. 1	States Oil	1969	1575	1176		
15	10S 36E 14db	Bannock	Ashlette No. 1	Cache Oil and Gas	1958	1701[b]	915		
16	10S 37E 19cb	Bannock	Arimo Valley No. 2	Norton Oil and Gas	1928	1463	823		
17	10S 37E 19cc	Bannock	Arimo Valley No. 1	Norton Oil and Gas	1927	1448	412		
18	10S 43E 13dcd	Bear Lake	Big Canyon Federal No. 1-13	Union Texas Petroleum	1979	2070	3577	c	d
19	10S 43E 21ada	Bear Lake	State No. 1	Eastern Idaho Development Co.	1956	1865	1195		
20	10S 46E 8bda	Caribou	Federal No. 1-8	May Petroleum	1978	2337	5104	c	d
21	10S 46E 20dd	Caribou	Federal Elk Valley No. 1	May Petroleum	1976	2294	1194	c	d
22	10S 46E 28bdd	Caribou	Amerada T1-W1	Amerada Petroleum	1963	2285	1254	c	d
23	11S 33E 2ba	Power	Arbon Valley No. 1	Gem State Petroleum	1926	1596	1175		
24	12S 25E 17bb	Cassia		Marsh Basin Oil and Gas	1926	1402[b]	183		
25	12S 38E 8dca	Bannock	Bannock 1-A8	NuDay Exploration	1978	1743	561		
26	12S 43E 3cd	Bear Lake	Bennington No. 3-24	Ladd Petroleum	1979	1963	3590		
27	12S 46E 30bc	Bear Lake	Bear Lake Federal No. 1	Rocky Mountain Oil	1954	2195[b]	1528		
28	13S 44E 22ccd	Bear Lake	Jensen No. 21-1	American Quasar	1978	1806	3360		d
29	13S 46E 29dca	Bear Lake	Rigby Williams No. 1	Cities Service Co.	1979	1879	2513		

Table VII-1. Continued.

Number	Location	County	Well Name	Operator	Completion Date	Elevation (meters)	Total Depth (meters)	Available Data Geology	Available Data Temp.
30	14S 26E 1bd	Cassia	Griffith-White No. 1	Al Griffith and Simplot	1973	1417[b]	2134-2438		
31	14S 30E 10cc	Oneida	Juniper No. 1	Phillips Petroleum and Utah Southern	1951	1610	2129		
32	14S 44E 31ccb	Bear Lake	99 x 101	J. Holme Dunford	1977	1808	247		
33	15S 27E 31cd	Cassia	No. 1	Al Griffith and Simplot	1974	1478[b]	1219		
34	15S 38E 36ba	Franklin	Idaho Willet No. 1	Willet Flying Service	1966	1402	1362		
35	15S 43E 1dd	Bear Lake	99 x 104	J. Holme Dunford	1977	1808	247		
36	15S 45E 34aa	Bear Lake	Government Sheep Creek No. 1	Standard of California	1954	2137	2063		
37	16S 27E 9cd	Cassia	No. 1	Al Griffith and Simplot	1974	1521	1250		
38	16S 28E 20bd	Cassia	Nielson No. 1	Al Griffith and Simplot	1973	1610	2129		
39	16S 38E 15ab	Franklin	August Jensen No. 1	Utah-Idaho Development	1956	1402[b]	1595		
40	16S 45E 21bbc	Bear Lake	North Eden Federal No. 22-11	American Quasar	1980	2103	2862	c	d
41	16S 46E 6bba	Bear Lake	North Rabbit Creek Federal No. 6-21	American Quasar	1980	2055	3539		d
42	16S 46E 10bc	Bear Lake	Grace Federal No. 10-1	American Quasar	1978	2323	3615	c	d

[a] Well not completed.

[b] Estimated from topographic map.

[c] Data on formations penetrated obtained.

[d] Data from bottom-hole temperature, high resolution temperature log or drill stem test obtained.

data from deep drilling, such as formation tops, can be used to interpret the subsurface structure in the area.

Analysis of deep drilling data indicates that several wells drilled in southeastern Idaho penetrated thrust zones. Many of the structural features are identified by the oil companies using sophisticated geophysical prospecting. Identification of thrusts or thrust zones in drill holes is partially based upon evidence of an altered stratigraphic sequence. Wells may penetrate a repeat of section or intersect a stratigraphically older formation above a younger formation. The zones between altered stratigraphic sequences are interpreted by oil companies to be thrusts or thrust zones.

Examples of this interpretation can be seen on four geologic logs presented on Table VII-2. The Union Texas Petroleum well, Big Canyon Federal No. 1-13, penetrated the Pennsylvanian Wells Formation and the Mississippian Madison Formation. Drilling then encountered the younger Jurassic Twin Creek Formation. Interpretation of this well by Union Texas Petroleum places the Meade thrust between the Madison Formation and the Twin Creek Formation.

An example of a repeat of section is shown in the geologic log of well Federal No. 1-8 drilled by May Petroleum (Table VII-2). This well penetrated a normal sequence of strata from the Upper Jurassic Pruess Formation through lower Triassic Dinwoody Formation. The well then

Table VII-2. Examples of geologic logs from four wells drilled in southeastern Idaho showing faults penetrated.

Well Name and Location	Formation Age	Formation Name	Depth Penetrated (meters)
Big Canyon Federal No. 1-13	Pennsylvanian	Wells	0-638
10S 43E 13dcd	Mississippian	Madison	638-841
		-fault-	
	Middle Jurassic	Twin Creek	841-1176
	Lower Jurassic	Nugget	1176-1442
	Upper Triassic	Ankareh	1142-1561
	Lower Triassic	Thaynes	1561-3186
	Lower Triassic	Woodside	3186-3307
	Lower Triassic	Dinwoody	3307-3557
			total depth 3557
Federal No. 1-8	Upper Jurassic	Pruess	0-495
10S 46E 8bda	Middle Jurassic	Twin Creek	495-2332
	Lower Jurassic	Nugget	2332-2635
	Upper Triassic	Ankareh	2635-2996
	Lower Triassic	Thaynes	2996-3545
	Lower Triassic	Woodside	3545-3606
	Lower Triassic	Dinwoody	3606-3971
		-fault-	
	Lower Triassic	Woodside	3971-4606
	Lower Triassic	Dinwoody	4606-5105
			total depth 5105
Grace Federal No. 10-1	Upper Jurassic	Pruess	0-503
16S 46E 10bc	Middle Jurassic	Twin Creek	503-1353
	Lower Jurassic	Nugget	1353-1650
	Upper Triassic	Ankareh	1650-1687
		-fault-	
	Lower Jurassic	Nugget	1687-2122
	Upper Triassic	Ankareh	2122-2518
	Lower Triassic	Thaynes	2518-3057
	Lower Triassic	Woodside	3057-3245
	Lower Triassic	Dinwoody	3245-3439
	Permian	Phosphoria	3439-3524
	Pennsylvanian	Wells	3524-3615
			total depth 3615
King No. 2-1	Cretaceous (?)	Unnamed	0-218
2S 41E 2aca	Lower Cretaceous	Gannett	218-802
	Lower Cretaceous	Ephraim	802-976
	Upper Jurassic	Stump	976-1160
	Upper Jurassic	Pruess	1160-1556
		-fault-	
	Upper Jurassic	Stump	1556-1584
	Upper Jurassic	Pruess	1584-1829
	Middle Jurassic	Twin Creek	1829-2608
	Lower Jurassic	Nugget	2608-2960
	Upper Triassic	Ankareh	2960-3347
	Lower Triassic	Woodside	3347-3447
	Lower Triassic	Dinwoody	3447-4022
	Pennsylvanian	Wells	4022-4132
			total depth 4132

intersected the lower Triassic Woodside and Dinwoody formations for a second time. Interpretation indicates a thrust fault is between the repeat of section (Wagner, written communication, 1980). Other repeats of section are shown on the geologic logs of wells Grace Federal No. 10-1 and King No. 2-1 drilled by American Quasar.

The Big Canyon Federal No. 1-13 drilled by Union Texas Petroleum penetrated the Meade thrust at 843 m below the surface. Water reportedly flooded the hole at a depth of 750 m. It is not known whether this increased flow of water into the hole was associated with the thrust feature.

None of the data from deep drilling indicated that the thrust zones had either significantly higher or lower hydraulic conductivity than the adjacent units. It is probable that the most important hydrologic impact of the thrust zones at depth is the disruption of the normal stratigraphic sequence of formations.

Temperature Data from Deep Drilling

Temperature data were obtained on 13 of the deep wells drilled in southeastern Idaho (Table VII-3). Data for each well varies in quantity and quality. Three forms of temperature data are available from oil and gas exploration wells: 1) high resolution temperature log (HRT), 2) bottom hole temperature (BHT), and 3) drill stem test temperature

Table VII-3. Temperature data obtained on wells drilled in southeastern Idaho.

Well Name and Location	Type of Temperature Measurement	Measurement Depth or Interval (meters)	Maximum Recorded Temperature (°C)
King No. 2-1 2S 41E 2aca	HRT	0-3810	210*
Big Elk Mountain No. 1 2S 44E 23db	DST	1538-1545	103*
Black Mountain Federal No. 1 3S 45E 36cc	BHT	2040	50
	BHT	2709	73
	BHT	3673	92
	BHT	4158	100*
Gentile Valley No. 1 4S 42E 9acc	BHT	1175	160
	BHT	2913	158
	BHT	3010	150
	HRT	0-1149	68
	HRT	0-2915	166
	HRT	0-3008	160*
Big Canyon Federal No. 1-13 10S 43E 13dcd	DST	837- 845	110
	DST	1595-1615	104
	DST	3015-3053	143
	DST	3301-3360	159
	DST	3524-3551	161*
Federal No. 1-8 10S 46E 8bda	BHT	963	33
	BHT	2740	83
	BHT	3014	79
	BHT	4826	138
	BHT	4914	151
	BHT	5105	188*
Federal Elk Valley No. 1 10S 46E 20dd	BHT	1194	40*
Amerada T1-W1 10S 46E 28bdd	BHT	610	29
	BHT	1219	49*
Jensen 21-11 13S 44E 22ccd	BHT	3500	74*
North Eden Federal No. 22-11 16S 45E 21bbc	DST	2473-2551	81
	DST	2557-2618	92*
North Rabbit Creek Federal No. 6-21 16S 46E 6bba	BHT	3537	80*
Grace Federal No. 10-1 16S 46E 10bc	BHT	3615	83*
Stoor A #1 5S 44E 29	HRT	0-2485	138
	HRT	0-4103	154
	HRT	0-4483	190

* indicates temperatures used to calculate gradient.

(DST). The applicability of these data to a geothermal investigation is limited because the data were collected to aid oil and gas exploration and not for the assessment of geothermal systems. Temperature data are also limited by the accuracy of the instruments and the procedure used.

HRT logs are made with a resistance thermometer, an element whose electrical resistance changes with temperature (Lynch, 1962). HRT logs are generally run by the petroleum industry to check the placement of the cement grouts. Drying cement generates heat, thus, the location of the cement can be determined by running an HRT log. Given the limitations, the HRT log can also be used to profile the temperature in the borehole. Summaries of HRT logs for eight wells are presented in Figures VII-2 to VII-9. The difficulty in interpreting HRT logs is demonstrated by the differences between the multiple logs for Gentile Valley #1-9 (Figure VII-3a,b,c) and Stoor A #1 (Figure VII-4a,b,c).

Temperatures at the bottom of a well are recorded when using most electric and radioactive logging techniques. A maximum recording resistance thermometer is used to record the maximum temperature at the bottom of a well. The BHT is used as a temperature correction to calibrate electrical and radioactive logs. The circulation of drilling fluids in the well greatly affects the temperature equilibrium. Generally, suites of electrical and radioactive logs are run after drilling has stopped and the fluid in the hole has

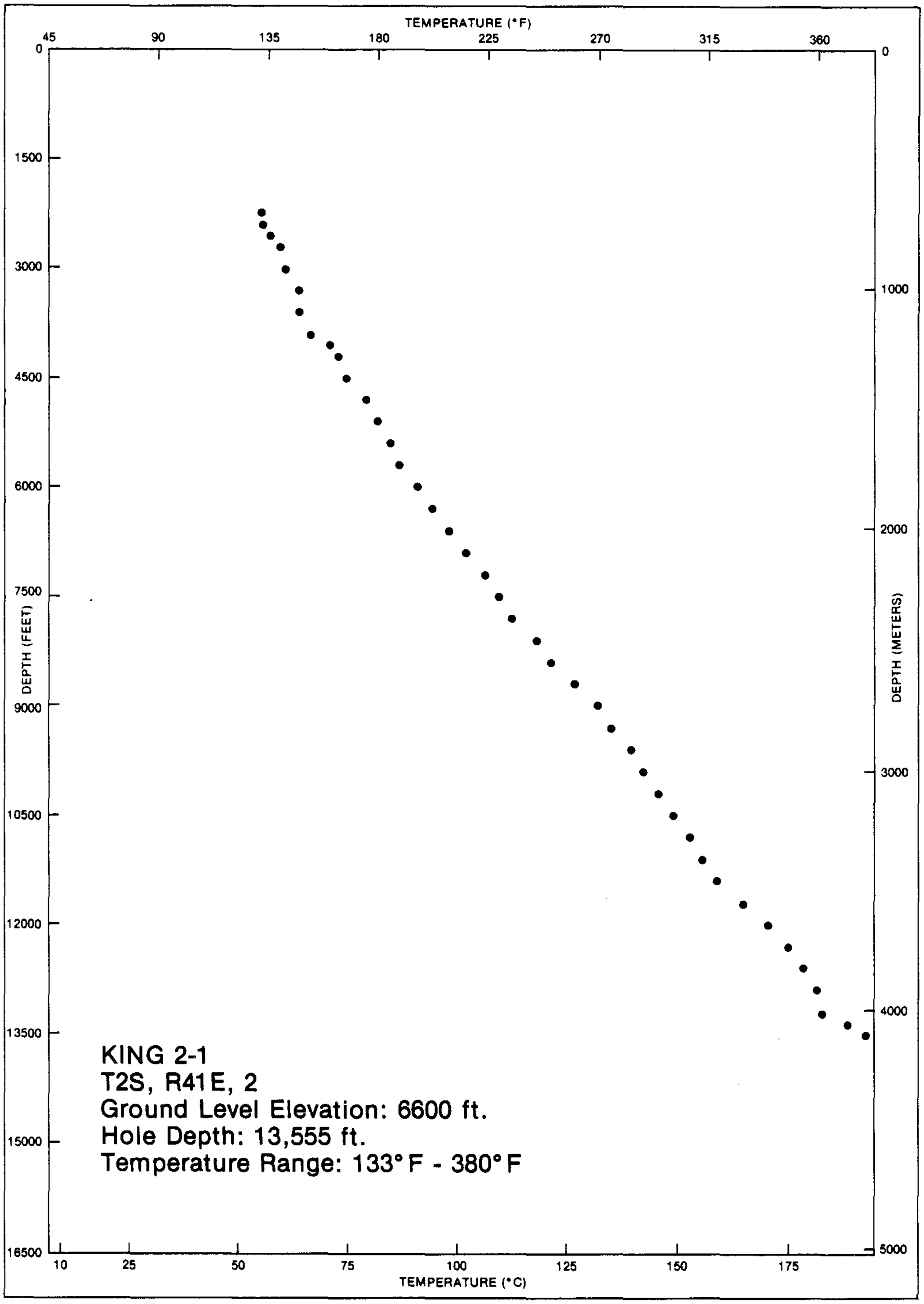

Figure VII-2. High resolution temperature log for King 2-1

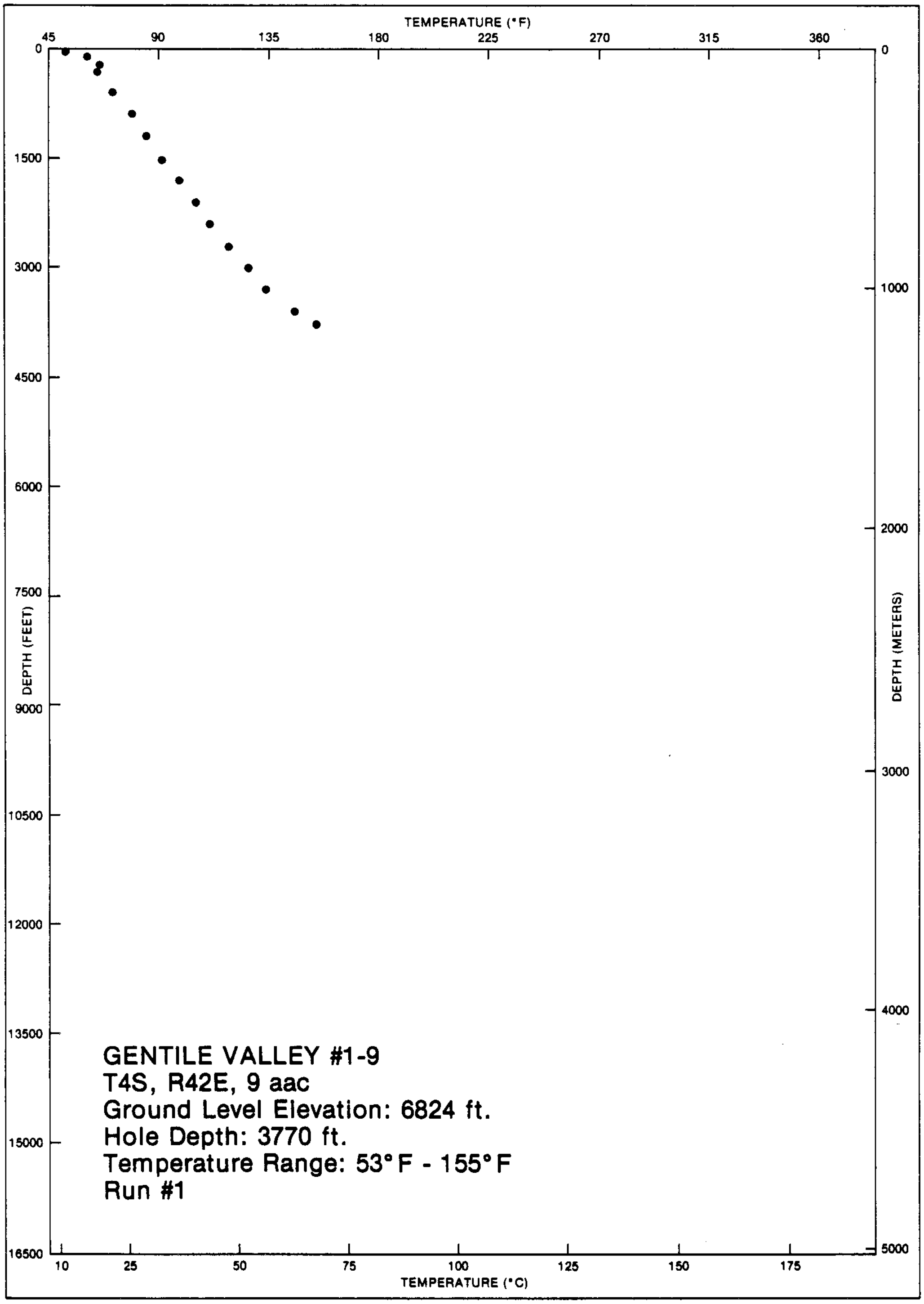

Figure VII-3a. High resolution temperature log for Gentile Valley #1-9: Run #1

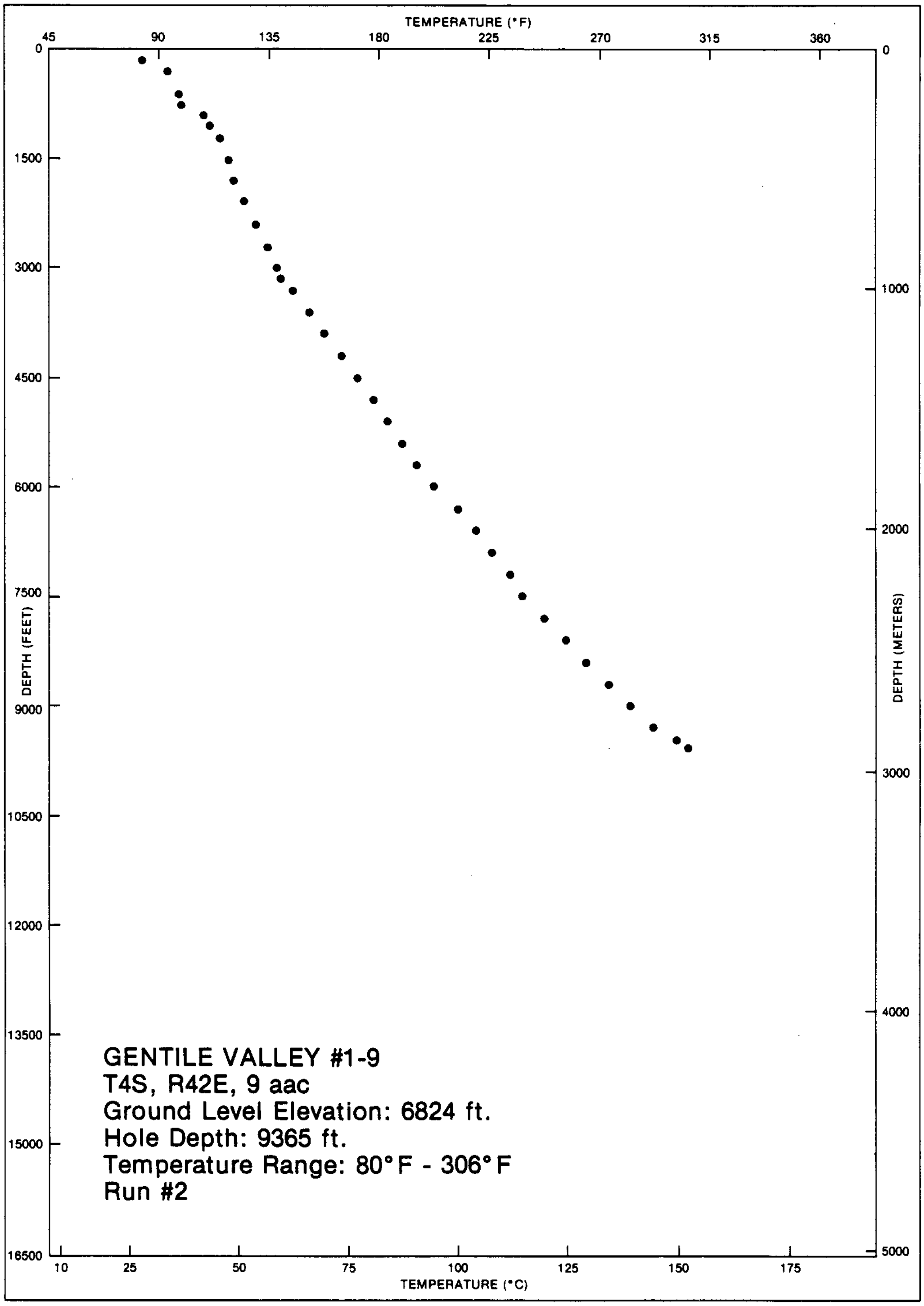

Figure VII-3b. High resolution temperature log for Gentile Valley #1-9: Run #2

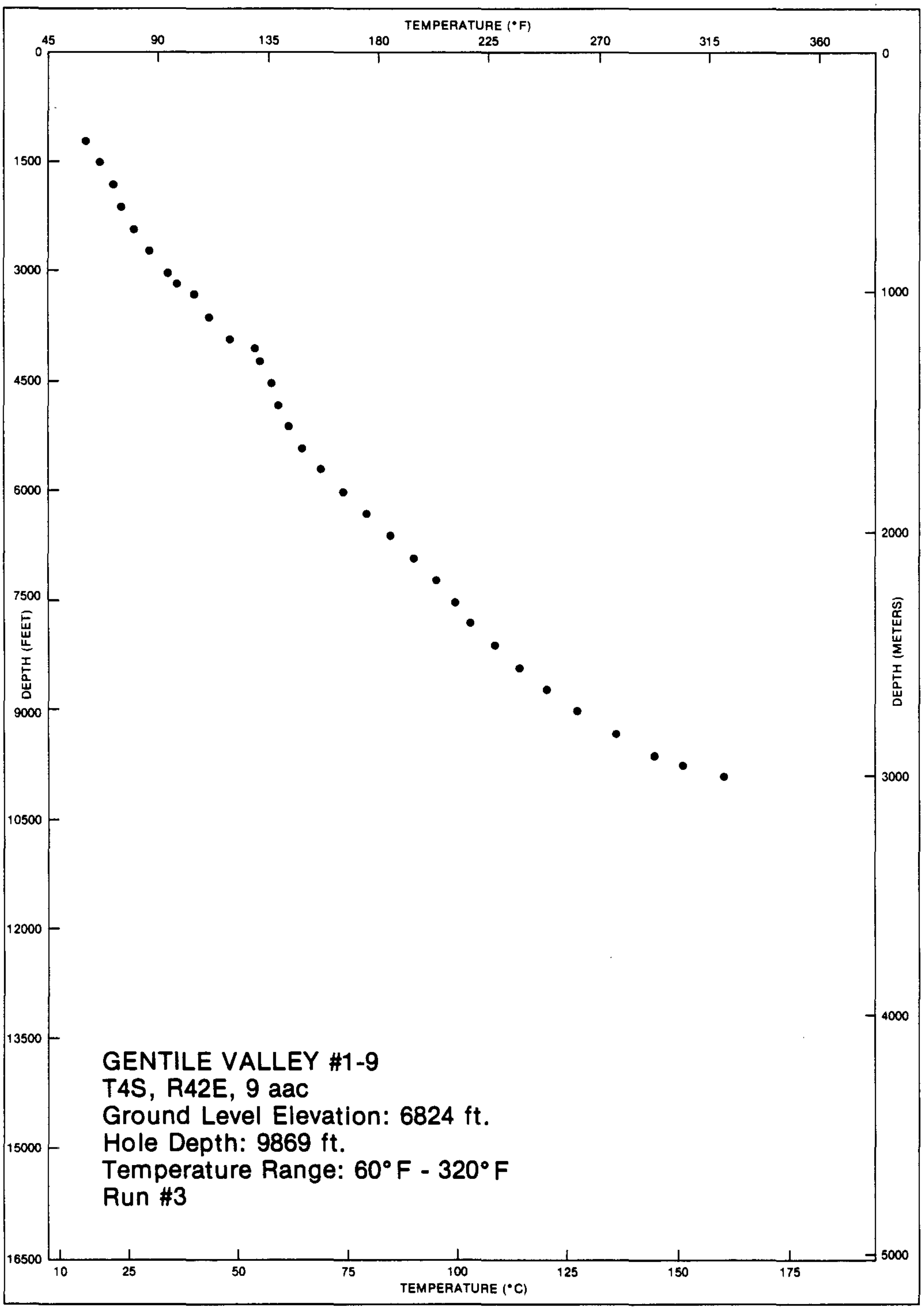

Figure VII-3c. High Resolution temperature log for Gentile Valley #1-9: Run #3

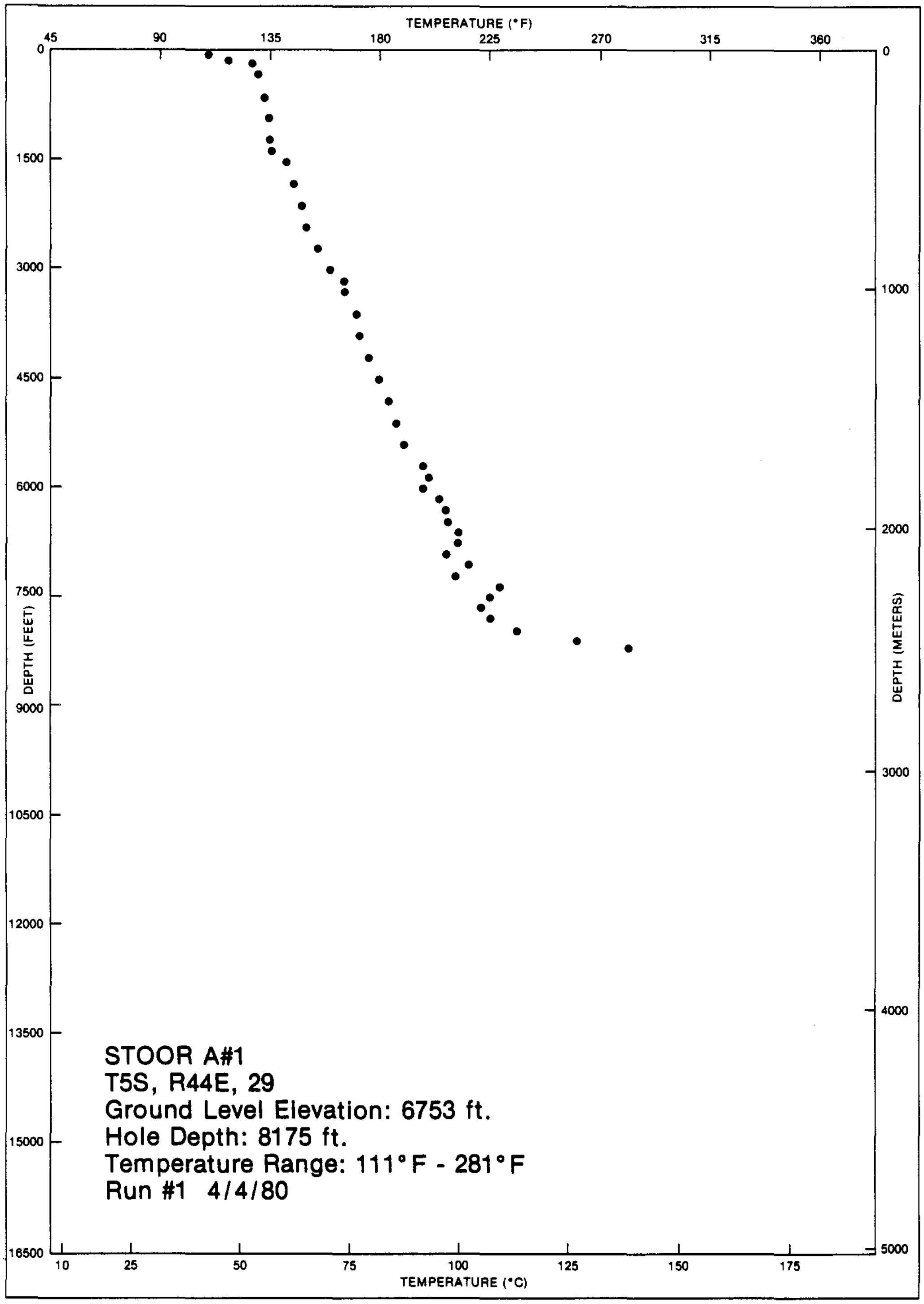

Figure VII-4a. High resolution temperature log for Stoor A#1: Run #1

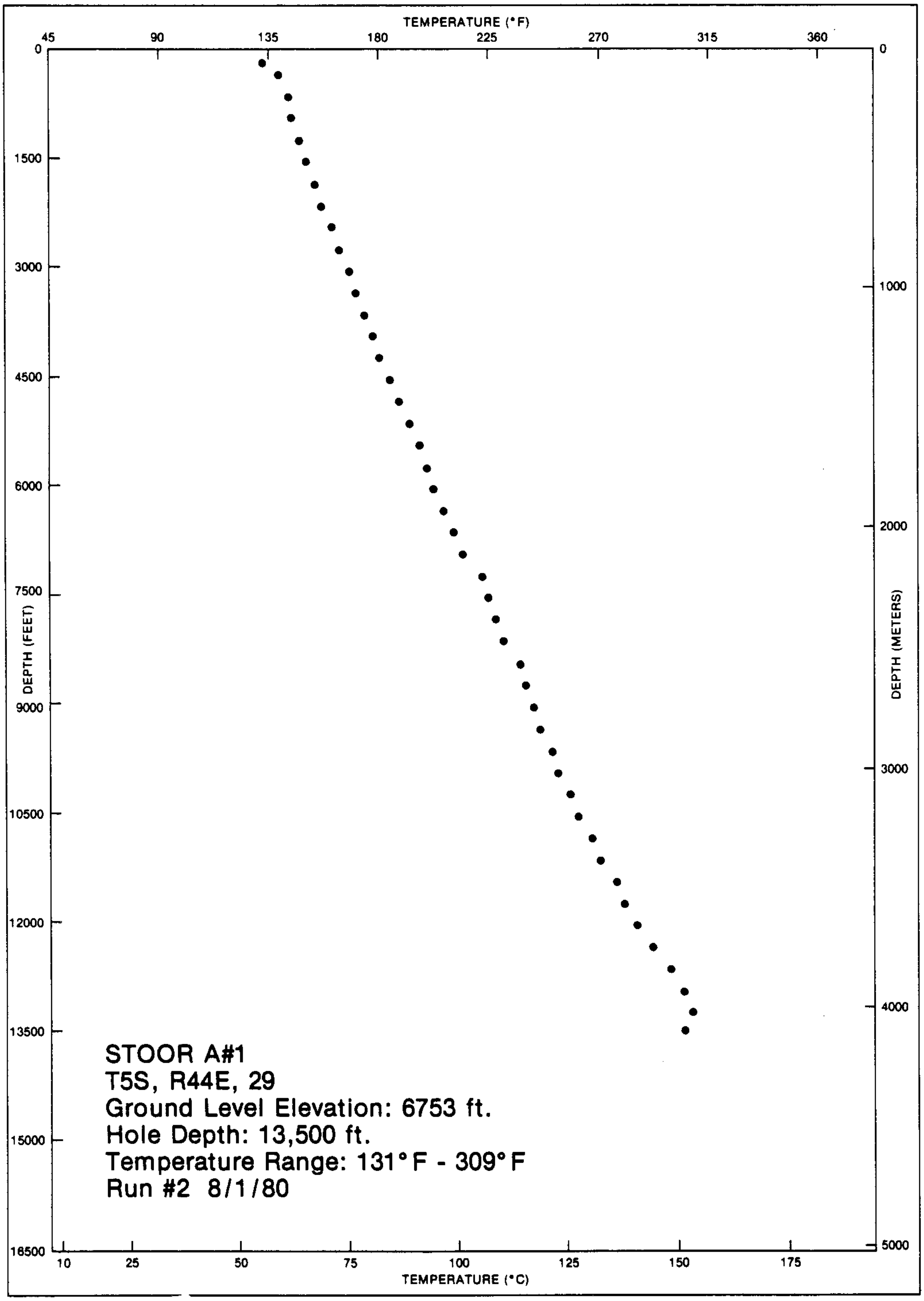

Figure VII-4b. High resolution temperature log for Stoor A#1: Run #2

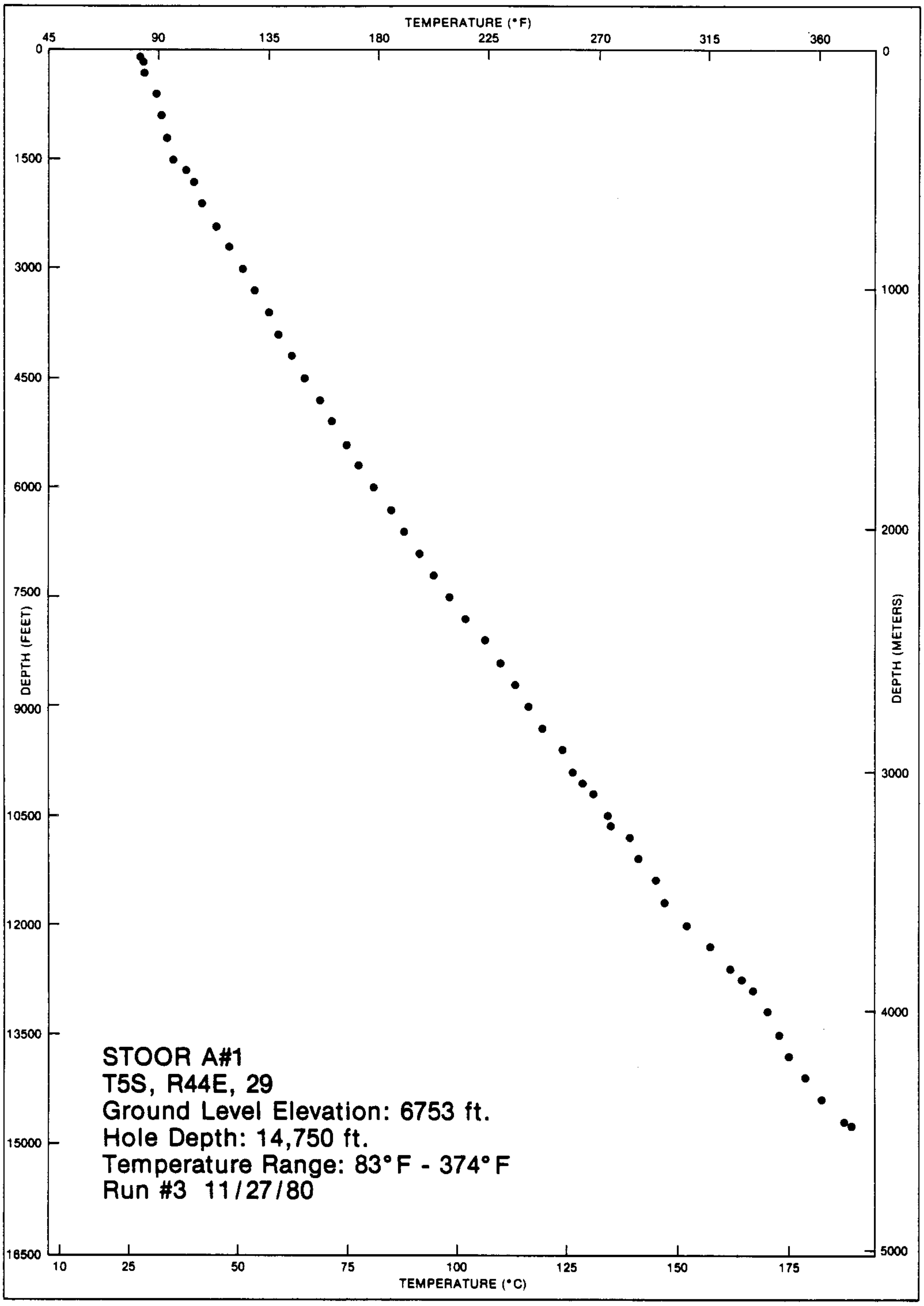

Figure VII-4c. High resolution temperature log for Stoor A#1: Run #3

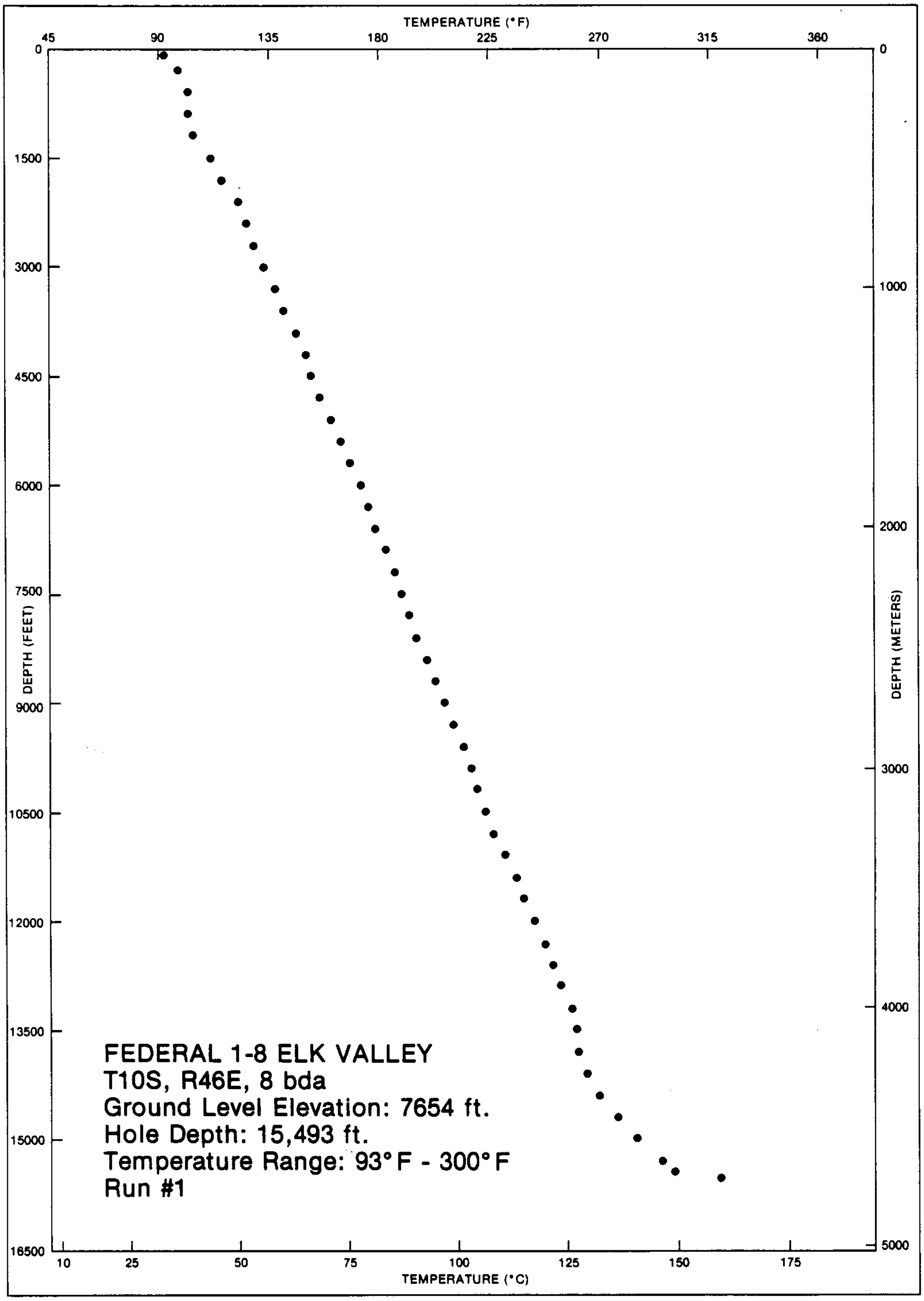

Figure VII-5. High resolution temperature log for Federal 1-8 Elk Valley

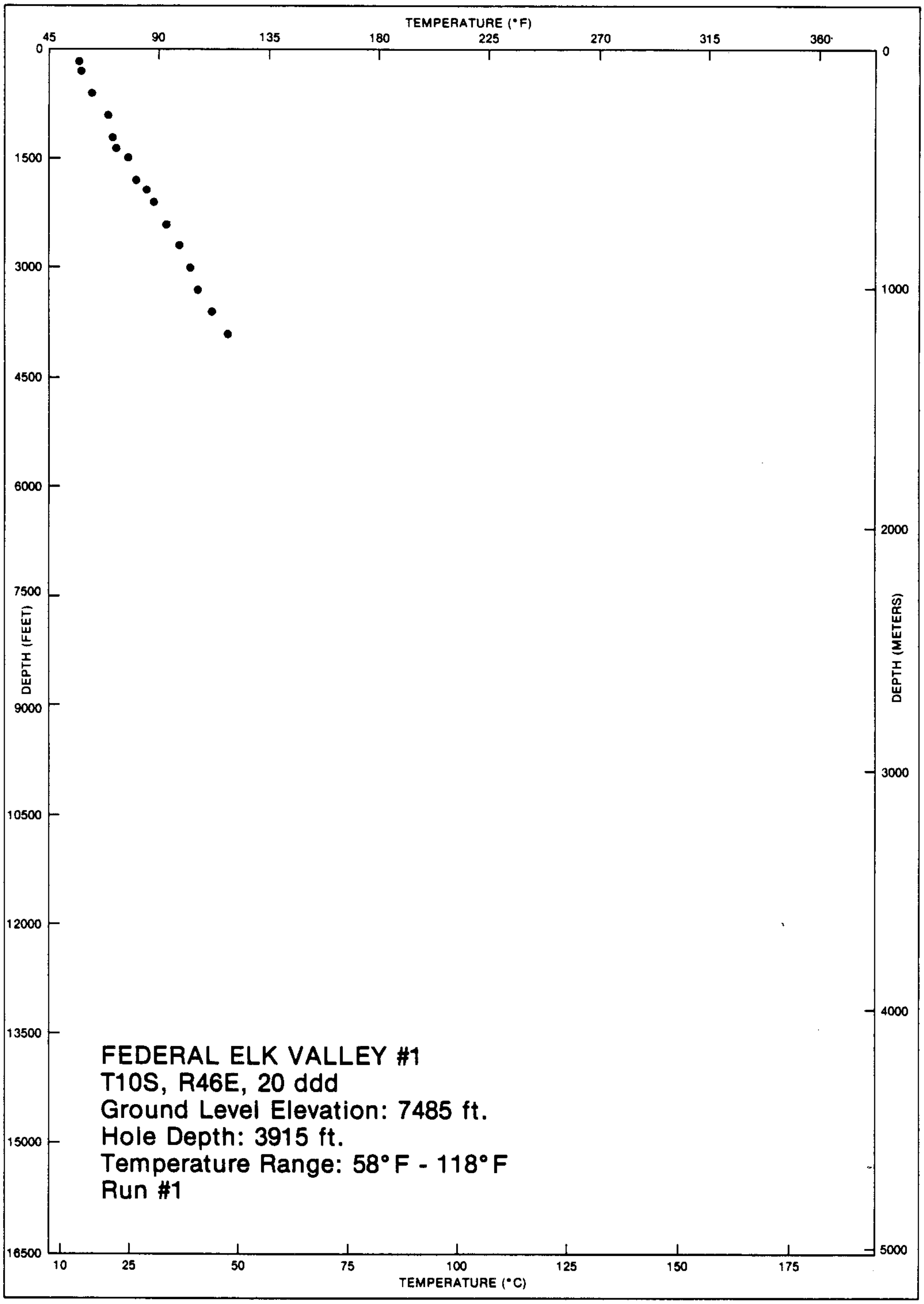

Figure VII-6. High resolution temperature log for Federal Elk Valley #1

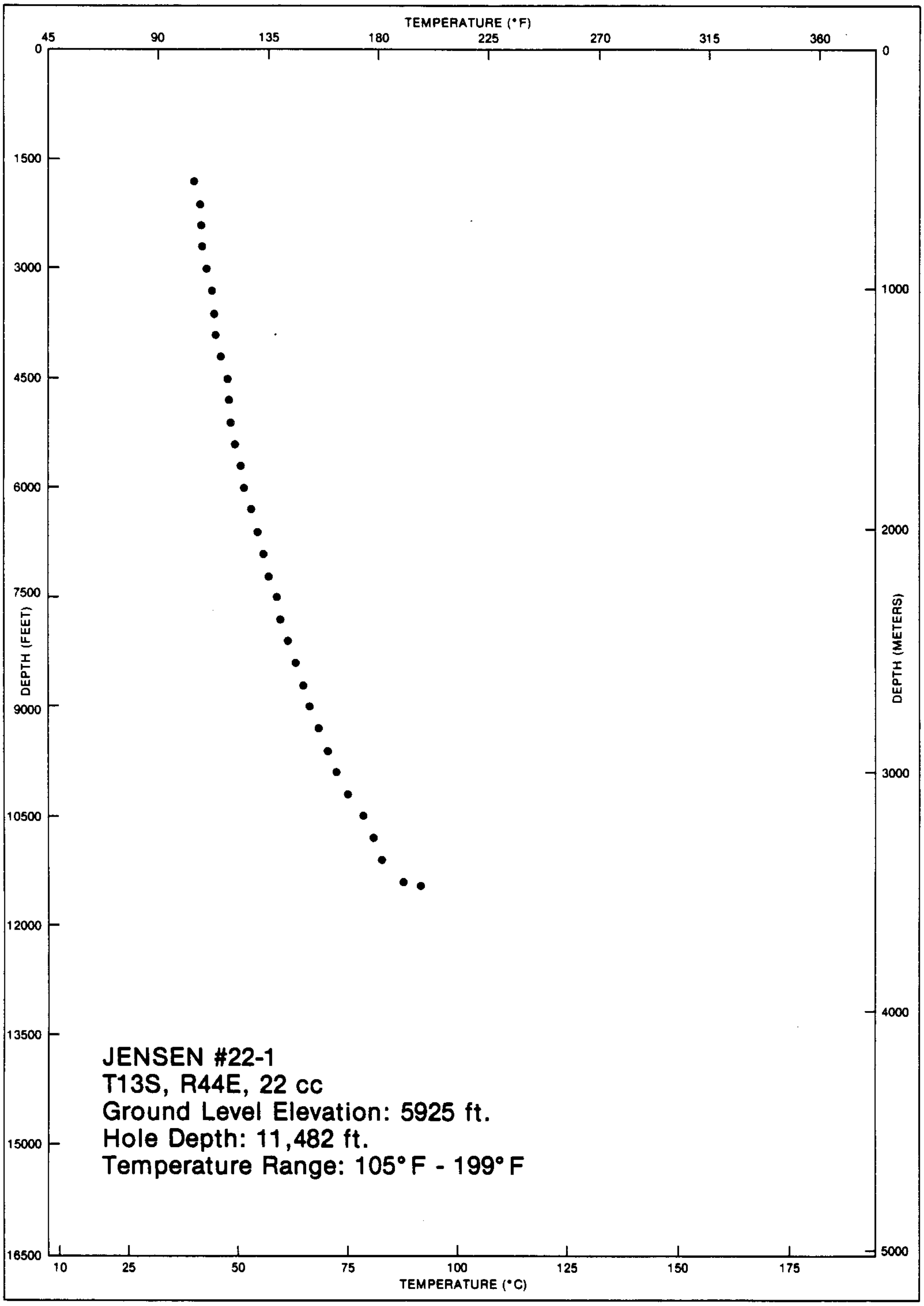

Figure VII-7 High resolution temperature log for Jensen #22-1

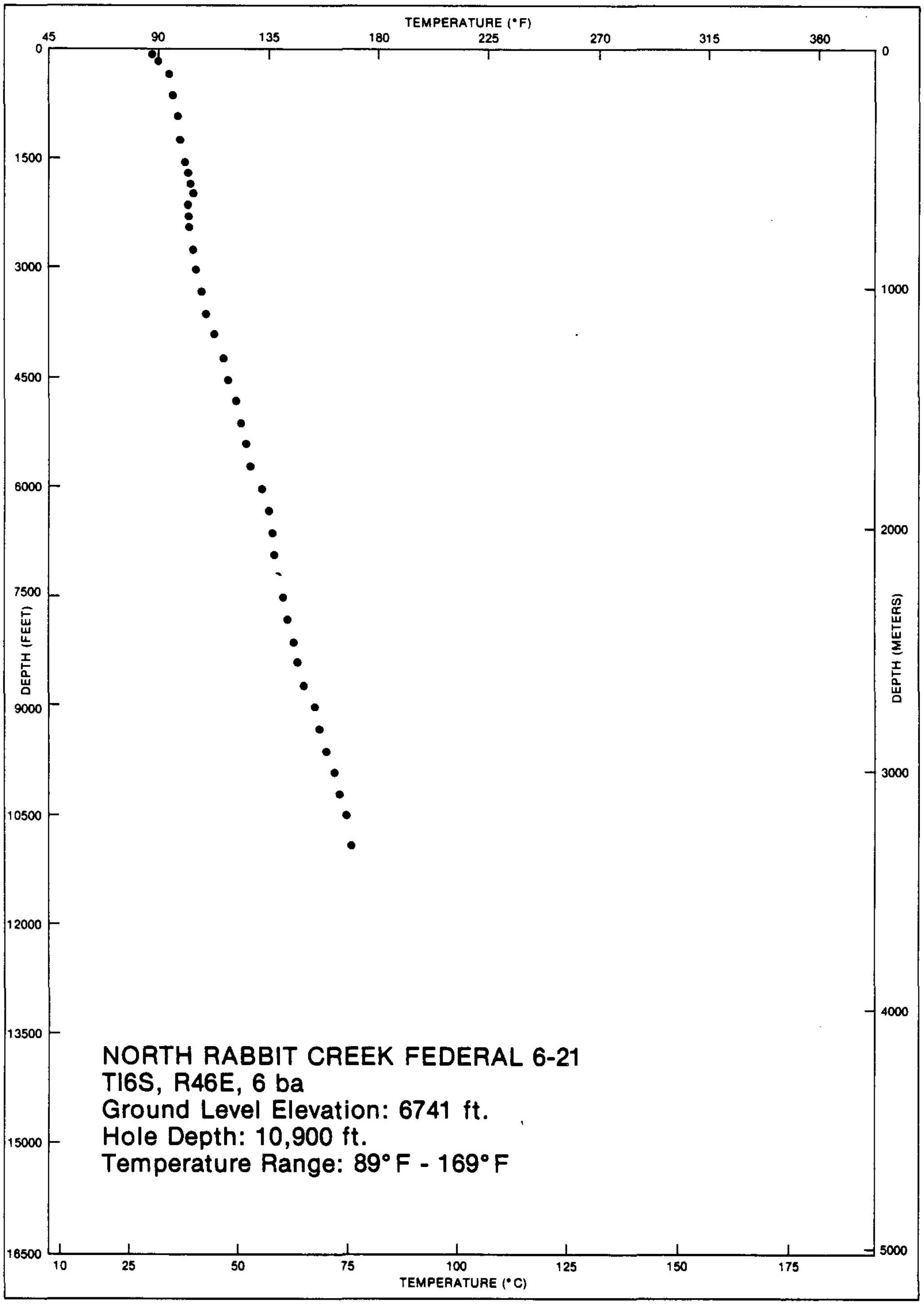

Figure VII-8. High resolution temperature log for North Rabbit Creek Federal 6-21

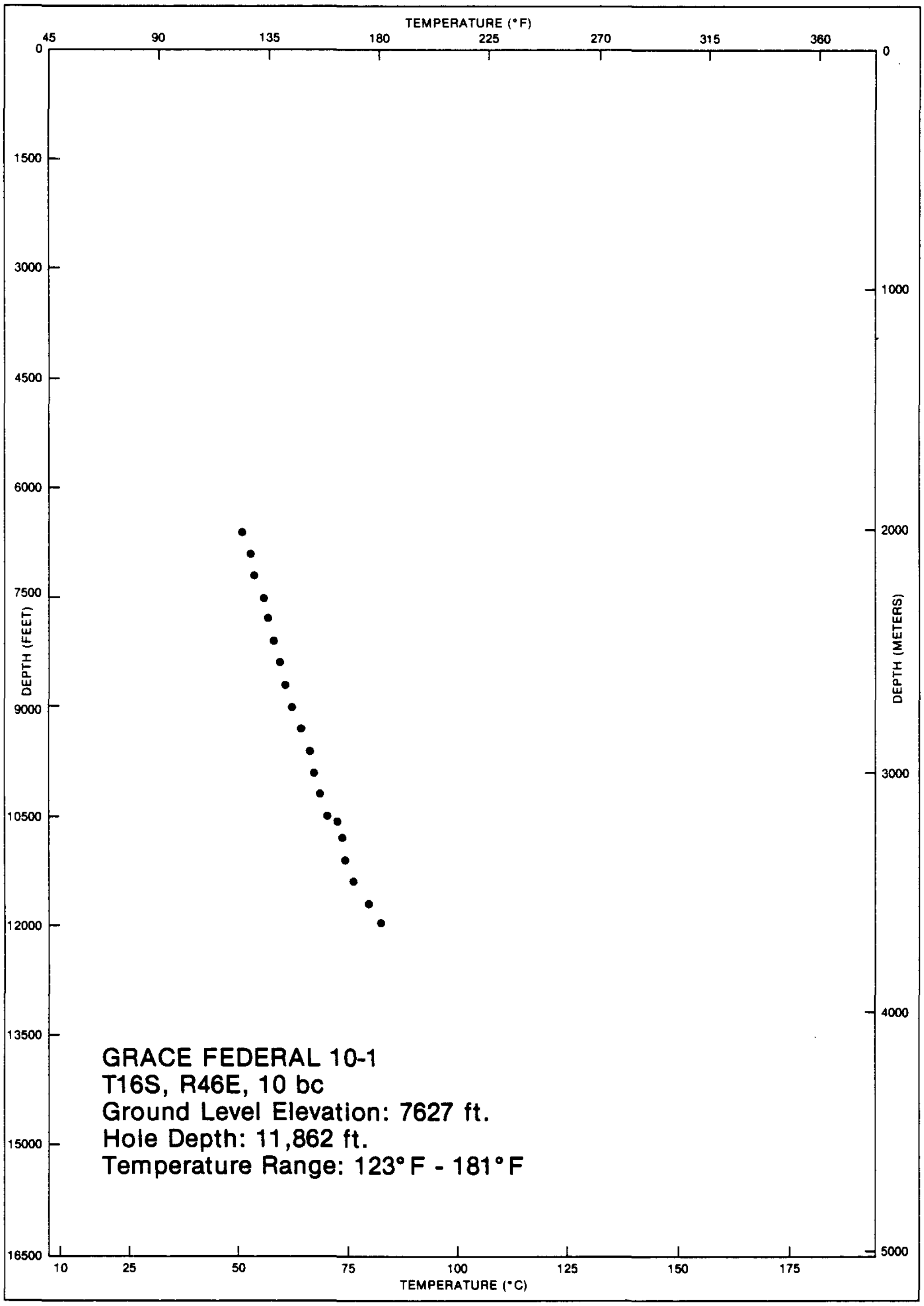

Figure VII-9. High resolution temperature log for Grace Federal 10-1 reached approximate equilibrium. For the purpose of this study, BHT readings are considered to represent the actual temperature at the given depth.

A drill stem test is the temporary completion of a well during drilling or after setting casing to measure formation pressures and to obtain samples of formation fluids or gases for evaluation (Jenner, 1973, p. 127). Drill stem tests are made by lowering a valve, a packer and a length of perforated pipe on the end of the drill pipe to the level of the formation to be tested. The packer is set to seal off the interval from the mud column above. Then the valve is opened allowing the formation fluid to flow into the hole and be produced through the drill pipe (Lynch, 1962). The temperature of the formation fluid is recorded during the drill stem test. This DST temperature is considered to be representative temperature of the fluid in the formation (Prestwitch, verbal communication, 1980).

Geothermal Gradient

The earliest estimate of a geothermal gradient for the area is 4.0°C/100 m (Mansfield, 1927, p. 320). Mitchell (1976b) estimated an identical gradient for the Blackfoot Reservoir area. Based upon heat flow, studies of the Snake River Plain region, Brott and others (1976) estimated the gradient near Rexburg, Idaho, to be in the range of

1.6-11.8°C/100 m. The average geothermal gradient for the earth's crust as a whole is approximately 2.6°/100 m (Decker, 1976).

Temperature data from deep drilling are used in this study to determine if any areas have a high geothermal gradient. The maximum recorded temperature (BHT, HRT, or DST) at the bottom of a well minus the mean annual air temperature 9°C (Mansfield, 1927) gives the actual temperature increase at depth. This value divided by the depth yields the temperature gradient at that site. The location of 12 wells in southeastern Idaho and the calculated gradient for each are shown on Figure VII-10. Figure VII-11 shows the geothermal gradients for deep holes in southeastern Idaho in comparison with Mansfield's (1927) estimate and the world-wide estimate.

The geothermal gradients presented in Figures VII-10 and VII-11 range from 1.9°C/100 m to 6.1°C/100 m. Three well sites in the northern portion of the area have relatively high gradient values compared to the gradients discussed earlier. These well locations and their calculated gradients are:

King No. 2-1, T2S, R41E, 2aca, 5.3°C/100 m;

Big Elk Mountain No. 1, T2S, R44E, 23db, 6.1°C/100 m

Gentile Valley No. 1-9, T4S, R42E, 9aac, 5.0°C/100 m.

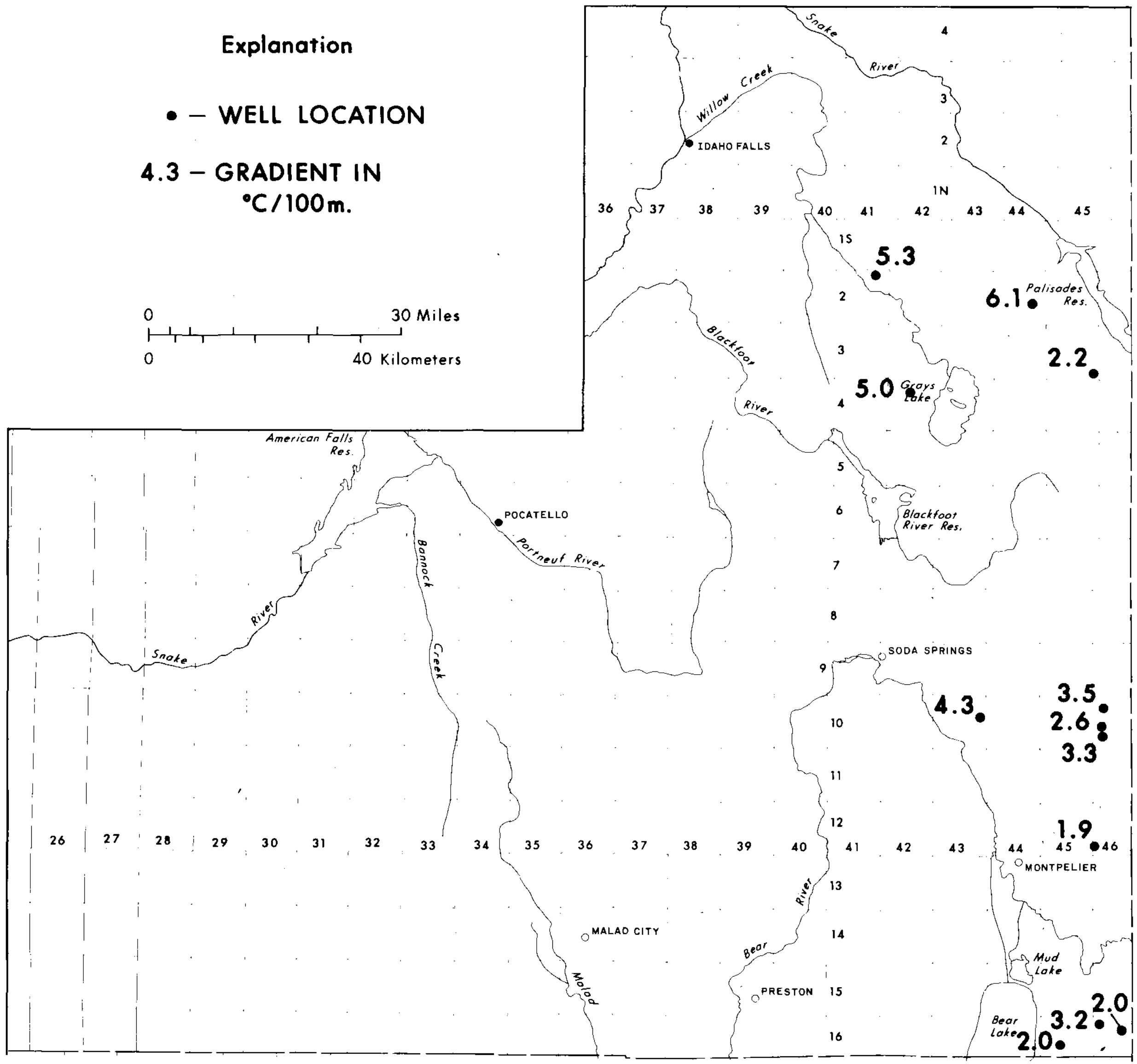

Figure VII-10. Calculated geothermal gradient of selected oil and gas wells in southeastern Idaho.

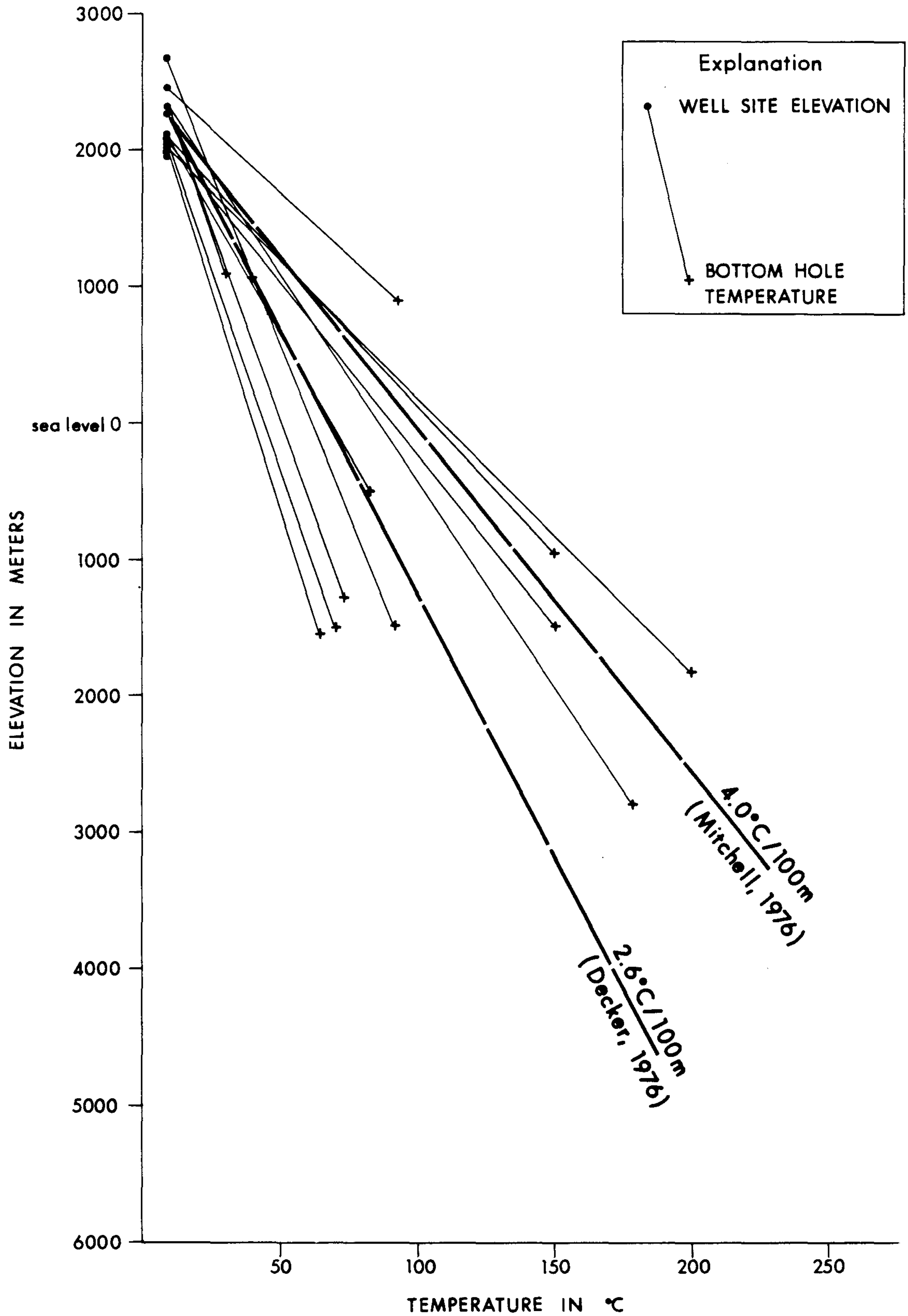

Figure VII-11. Bottom hole temperatures versus total depth and surface elevation in comparison to suggested geothermal gradients. (Assume mean annual air temperature of 9°C.)

Further evaluation is needed to determine if these wells penetrate a major geothermal system.

A geologic log and a HRT log for an individual well are presented to show the difficulty involved in determining if a thrust zone in the study area has any influence on the geothermal gradient. The geologic log and HRT log of well King No. 2-1, drilled by American Quasar, is presented in Figure VII-12. The geologic log indicates a thrust fault at 1556 m. The HRT log does not deviate in any distinct manner near the fault. In this example, it appears that the thermal gradient does not significantly vary near the fault zone. This implies that the thrust zone is not a direct control for the geothermal system.

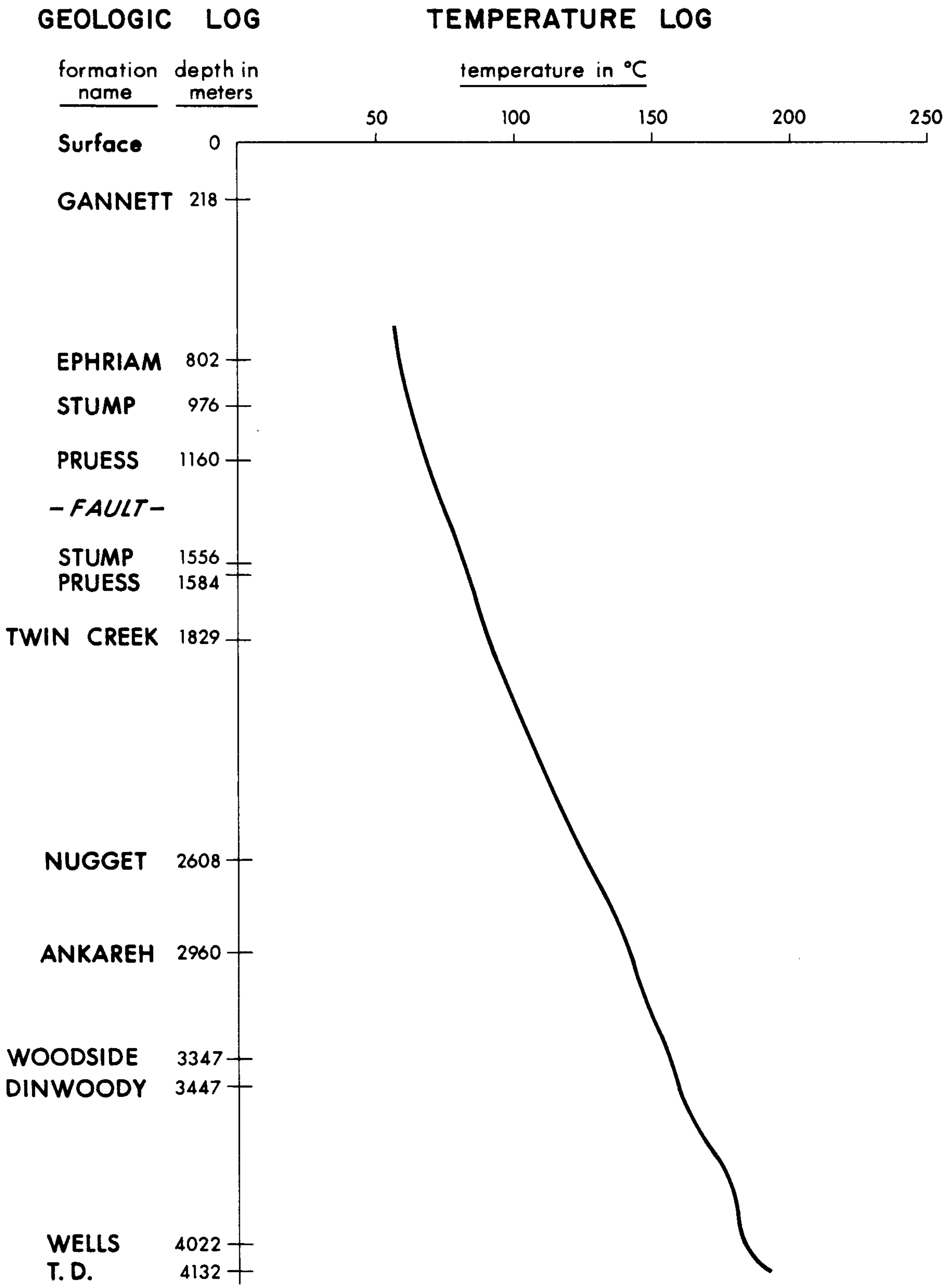

Figure VII-12. Geologic log and temperature log of well King 2-1

CHAPTER VIII

CONCLUSIONS

Conclusions from the Analysis of Hydrogeology

1. Most thermal and non-thermal discharges are controlled by structural features with secondary control by stratigraphy.
2. Graben bounding faults are most important in controlling thermal flow systems.
3. Thrust faults do not appear to be primary controlling features for thermal flow systems. Thermal springs are not located along surface traces of thrust faults; HRT logs from oil and gas test wells do not show thermal anomalies where thrust faults are intercepted at depth.

Conclusions from a Consideration of the Tabular Physical and Chemici Data

1. The total discharge of thermal waters within the study area is quite small. Discharges of 30°C or more amount to approximately 500 l/s.
2. Thermal springs with temperatures greater than 40°C discharge from regional topographic lows.
3. Thermal springs with temperatures greater than 50°C are very depleted in calcium and bicarbonate.

4. Thermal springs with temperatures greater than 50°C are associated with faults on which recent movement has occurred.

5. TDS values of greater than 40,000 mg/l found in oil well analyses probably represent zones of essentially stagnant water.

Conclusions from the Grouping Analyses

1. Graphic and statistical analyses of the major-ion data enabled the delineation of several statistical distinct water types which are associated with geographically distinct areas. These are:
   - (a) Sodium chloride waters of the Swan Valley to Star Valley graben.
   - (b) Calcium bicarbonate waters of the Meade Peak thrust block and adjacent areas.
   - (c) Sodium chloride waters of the Maple Grove area.
   - (d) High sodium chloride waters of the Basin and Range province.
   - (e) Low TDS waters from various locales throughout the study area.

2. Deuterium and oxygen-18 results indicate that, with the exception of sites S-13 and S-14, aquifer temperatures are not significantly above 80°C in the study area; also, that differences in recharge elevation are not apparent.

3. Carbon isotope analyses indicate that the thermal waters of the study area which were analyzed for ^{14}C have undergone contact times in excess of 25,000 years B.P. for those springs whose temperatures are greater than 25°C. The extremely low concentrations of modern carbon in the thermal waters above 25°C indicate that essentially no mixing of waters younger than several thousand years has occurred.

Conclusions from the Analysis of Geochemical Environments of Thermal Ground Water

1. The thermal springs that discharge along the west side of the Swan Valley to Star Valley graben are characterized by water older than 25,000 years B.P. These flow systems appear to be recharged in the Caribou Range. The saline nature of the water may be a result of contact with the salt beds in the Pruess or Gypsum Springs formations.
2. The thermal springs and wells of the Meade Peak thrust block and adjacent areas are characterized by calcium bicarbonate waters with aquifer temperatures of less than 80°C and surface temperatures of less than 45°C. Ground water ages in this area range from 12,000 to greater than 25,000 years B.P. These waters discharge along graben bounding faults to the west of the Meade Peak block.

Large amounts of CO_2 are evolved by some of these springs.

3. The sodium chloride thermal springs of the Maple Grove area are old ground waters which discharge near the southern end of the Gem Valley near the intersection of two graben-bounding fault systems. Maximum aquifer temperature for these springs appears to be about 80°C.
4. The thermal springs of the Basin and Range valleys tributary to the Great Salt Lake are highly saline and their chemistry is dominated by sodium chloride. $D/^{18}O$ results indicate that the water from two thermal occurrences in the northern Cache Valley have been heated above 80°C. All of these springs are associated with recent extensional faulting.
5. The thermal waters of the Basin and Range valleys tributary to the Snake River have much lower TDS values than the other Basin and Range waters. This may be indicative of shorter contact times. These springs are also associated with recent extensional faulting.
6. With very few exceptions the Basin and Range thermal occurrences are saturated or supersaturated with respect to talc and tremolite, probably indicating the higher silica concentrations and higher aquifer temperatures of these flow systems.

REFERENCES

Allmendinger, R. W., 1981, Structural Geometry of Meade Thrust Plate in Northern Blackfoot Mountains, Southeastern Idaho: Am. Assoc. Pet. Geol. Bull., v. 65, n. 3, p. 509-535.

Armstrong, F. C., 1969, Geologic Map of the Soda Springs Quadrangle, Southeastern Idaho: U.S. Geol. Survey Misc. Geol. Inv. Map I-557.

Armstrong, F. C., and Cressman, E. R., 1963, The Bannock Thrust Zone, Southeastern Idaho: U.S. Geol. Survey Prof. Paper 374-J, 22 p.

Armstrong, F. C., Leeman, W. P., and Malde, H. E., 1975, K-Ar Dating, Quaternary and Niogenevolcanic Rocks of the Snake River Plain, Idaho: Am. Jour. Soc., v. 275, p..225-250.

Armstrong, F. C., and Oriel, S. S., 1965, Tectonic Development of Idaho-Wyoming Thrust Belt; Am. Assoc. Pet. Geol. Bull., v. 49, n. 11.

Arrigo, J. L., 1982, Hydrostratigraphy of Selected Formations in Southeastern Idaho: M.S. Thesis, Univ. of Idaho, Moscow, 111 p.

Back, W., 1963, Preliminary Results of a Study of Calcium Carbonate Saturation of Ground Water in Central Florida: Inter. Assoc. Sci. Hydrology Bull., v. 8, n. 3, p. 43-51.

Back, W., and Hanshaw, B. B., 1970, Comparison of Chemical Hydrogeology of the Carbonate Peninsulas of Florida and Yucatan: Jour. of Hydro., v. 10, p. 330-368.

Back, W., and Hanshaw, B. B., 1971, Rates of Physical and Chemical Processes in a Carbonate Aquifer, _in_ Advances in Hydrosciences Series 106: Am. Chem. Soc., p. 77-93.

Baglio, J. V., 1983, Analysis of Geothermal Ground Water Flow Systems in and around Bear River Range, Southeastern Idaho: M.S. Thesis, Univ. of Idaho, Moscow, 83 p.

Blackstone, D. L., Jr., 1977, The Overthrust Belt Salient of the Cordilleran Fold Belt Western Wyoming - Southeastern Idaho - Northeastern Utah, _in_ Joint Wyoming-Montana-Utah Geological Associations Guidebook Rocky Mountain Thrust Belt Geology and Resources: Wyoming Geol. Assoc., p. 367-384.

Breckenridge, R. M., and Hinckley, B. S., 1978, Thermal Springs of Wyoming: Geological Survey of Wyoming, Bull. 60.

Bright, R. C., 1960, Geology of the Cleveland Area, Southeastern Idaho: M.S. Thesis, University of Utah, Salt Lake City, 220 p.

Brott, C. A., Blackwell, D. D., and Mitchell, J. C., 1976, Geothermal Investigations in Idaho, Part 8, Heat Flow in the Snake River Plain Region, Southern Idaho; Idaho Dept. of Water Res., Water Info. Bull., n. 30, 195 p.

Chebotarev, I. I., 1955, Metamorphism of Natural Waters in the Crust of Weathering; Geochim. Cosmochim, Acta, v. 8, pp. 22-48, 137-170.

Cloud, P. E., 1968, Atmospheric and Hydrospheric Evolution on the Primitive Earth: Science, v. 160, p. 729-736.

Comrey, A. L., 2973, A First Course in Factor Analysis: Academic Press, New York, 316 p.

Conner, J. L., 1980, Geology of the Sage Valley 7-1/2 Minute Quadrangle, Bear Lake and Caribou Counties, Idaho, and Lincoln County, Wyoming: M.S. Thesis, Brigham Young Univ.

Craig, H., 1961a, Standard for Reporting Concentrations of Deuterium and Oxygen-18 in Natural Waters: Science, v. 133, p. 1833-1834.

Craig, H., 1961b, Isotopic Variations in Meteoric Waters: Science, v. 133, p. 1702-1703.

Craig, H., 1963, The Isotopic Geochemistry of Water and Carbon in Geothermal Areas in Nuclear Geology on Geothermal Areas: Spoleto, Sept. 9-13. Consiglio Nazionale delle Ricerche, Laboratorio di Geologia Nucleare, Pisa, 53 p.

Craig, H., 1966, The Measurement of Oxygen Isotope Paleotemperatures, in Stable Isotopes in Oceanographic Studies and Paleotemperatures: Spoleto, July 26-27, 1965. Consiglio Nazionale delle Ricerche, Laboratoria di Geologia Nucleare, Pisa, p. 1-24.

Cressman, E. R., 1964, Geology of the Georgetown Canyon-Snowdrift Mountain Area, Southeastern Idaho: U.S. Geol. Survey Bull. 1153, 105 p.

Cressman, E. R., and Gulbrandsen, R. A., 1955, Geology of the Dry Valley Quadrangle, Idaho: U.S. Geol. Survey Bull. 1015-I, 18 p.

Decker, E. R., 1976, Geothermal Resources, Present and Future Demand for Power and Legislation in the State of Wyoming: Wyoming Geol. Survey, Public Information Series-1, 21 p.

deVries, H., 1958, Variation in Concentration of Radiocarbon with Time and Location on Earth: Proc. Koninkl. Ned. Akad. Wetenschap., v. B51, p. 94-102.

Dion, N. P., 1969, Hydrologic Reconnaissance of the Bear River Basin in Southeastern Idaho: Idaho Dept. of Water Reclam., Water Info. Bull., n. 13, 66 p.

Dion, N. P., 1974, An Estimate of Leakage from Blackfoot Reservoir to Bear River Basin, Southeastern Idaho: Idaho Dept. Water Admin., Water Info. Bull., n. 34, 24 p.

Domenico, P. A., 1972, Concepts and Models in Groundwater Hydrology: McGraw-Hill, New York, 405 p.

Drake, J. J., and Harmon, R. S., 1973, Hydrochemical Environments of Carbonate Terrains: Water Res. Res., v. 9, n. 4, p. 949-957.

Eardley, A. J., 1967, Idaho-Wyoming Fold and Thrust Belt: Its Division and an Analysis of Its Origin in Anatomy of the Western Phosphate Field: Intermountain Assoc. of Geologist, L. A. Hale, Ed., Salt Lake City, Utah, p. 35-44.

Everett, B., 1974, Cluster Analysis: John Wiley and Sons, New York, 122 p.

Faure, G., 1977, Principles of Isotope Geology: John Wiley and Sons, New York, 464 p.

Feth, J. H., and others, 965, Preliminary Map of the Conterminous United States Showing Depth to and Quality of the Shallowest Ground Water Containing More Than 1000 ppm Dissolved Solids: U.S. Geol. Survey Hydrologic Investigations Atlas HA-199.

Freeze, R. A., and Cherry, J. A., 1979, Groundwater: Prentice-Hall, Inc., Englewood Cliffs, New Jersey, 604. p.

Freeze, R. A., and Witherspoon, P. A., 1966, Theoretical Analysis of Regional Groundwater Flow, I: Analytical and Numerical Solutions to the Mathematical Model: Water Res. Res., v. 2, n. 4, p. 641-650.

Freeze, R. A., and Witherspoon, P. A., 1967, Theoretical Analysis of Regional Groundwater Flow, II: Effect of Water Table Configuration and Subsurface Permeability Variations: Water Res. Res., v. 2, n. 4, p. 641-650.

Gardner, L. S., 1961, Preliminary Geologic Map of the Irwin Quadrangle, Caribou and Bonneville Counties, Idaho, and Lincoln and Teton Counties, Wyoming: U.S. Geol. Survey Open-file Map 61-53.

Garrels, R. M., and Christ, C. L., 1965, Solutions, Minerals and Equilibria: Harper and Row, New York, 450 p.

Geyh, M. A., 1970, Carbon-14 Concentration of Lime in Soils and Aspects of the Carbon-14 Dating of Groundwater, in Isotope Hydrology: Vienna, Internat. Atomic Energy Agency, p. 215-224.

Giri, N. C., 1977, Multivariate Statistical Inference: Academic Press, New York, 319 p.

Godwin, H., 1962, Half-life of Radiocarbon: Nature, v. 195, p. 984.

Goodnight, J. H., Barr, A. J., Sall, S. P., and Helwig, J. T., 1976, A User's Guide to SAS 76: SAS Institute, Inc., Raleigh, N. C., 494 p.

Gretener, P. E., 1979, Pore Pressure: Fundamentals, General Ramifications and Implications for Structural Geology: AAPG Course Note No. 4, 131 p.

Gulbrandsen, R. A., McLaughlin, K. P., Honkala, F. S., and Clabaugh, S. E., 1956, Geology of the Johnson Creek Quadrangle, Caribou County, Idaho: U.S. Geol. Survey Bull. 1042-A, 21 p.

Hair, J. F., Jr., Anderson, R. E., Tatham, R. L., and Grablowsky, 1979, Multivariate Data Analysis: Petroleum Publishing Co., Tulsa, Oklahoma, 360 p.

Harmon, R. S., White, W. B., Drake, J. J., and Hess, J. W., 1975, Regional Hydrochemistry of North American Carbonate Terrains: Water Res. Res., v. 11, n. 6, p. 963-967.

Hatch, J. F., 1980, Geology of the Elk Valley Quadrangle, Bear Lake and Caribou Counties, Idaho, and Lincoln County, Wyoming: M.S. Thesis, Brigham Young Univ.

Hayden, F. V., 1873, U.S. Geol. and Geog. Survey Terr. 6th Ann. Rept., p. 269-271.

Hem, J. D., 1970, Study and Interpretation of the Chemical Characteristics of Natural Water: U.S. Geol. Survey Water-Supply Paper 1473, 363 p.

Hinckley, B. S., and Breckenridge, R. M., 1977, Auburn Hot Springs, Lincoln County, Wyoming: Twenty-ninth Annual Field Conference - 1977 Wyoming Geolological Association Guidebook, p. 707-710.

Hostetler, P. B., 1964, The Degree of Saturation of Magnesium and Calcium Carbonate Minerals in Natural Waters: Internat. Assoc. Sci. Hydrology, Pub. 64, p. 34-49.

Hounslow, A., Fitzpatrick, J., Cerrillo, L., and Freeland, M., 1978, Oberburden Mineralogy as Related to Ground-water Chemical Changes in Coal Strip Mining: U.S.E.P.A., EPA-600/7-78-156, 299 p.

Hsu, K. J., 1963, Solubility of Dolomite and Composition of Florida Ground Waters: Jour. of Hydrology, v. 1, p. 288-310.

Hubbell, J. M., 1981, Description of Geothermal Flow Systems in the Vicinity of the Caribou Range, Southeastern Idaho: M.S. Thesis, Univ. of Idaho, 105 p.

Huntsberger, D. V., and Billingsley, P., 1977, Elements of Statistical Inference: Allyn and Bacon, Inc., Boston, Mass., 384 p.

Jacobson, R. L., and Langmuir, D., 1970, The Chemical History of Some Spring Waters in Carbonate Rocks: Groundwater, v. 8, n. 3, p. 5-9.

Jenkins, D. E., 1981, Geology of the Auburn 7-1/2 Minute Quadrangle, Caribou County, Idaho, and Lincoln County, Wyoming: M.S. Thesis, Brigham Young Univ.

Jenner, J. W., 1973, Drilling for Oil in Modern Petroleum Technology: 4th Ed., Haloted Press a Division of John Wiley and Sons, Inc., New York, 36 p.

Keller, A. S., 1963, Structure and Stratigraphy Behind the Bannock Thrust in Parts of the Preston and Montpelier Quadrangles, Idaho: Ph.D. Dissertation, Columbia Univ., 204 p.

Klein, J., Lerman, J. C., Dauwon, D. E., and Liniok, T., 1980, Radiocarbon Concentration in the Atmosphere - 8000 Year Record of Variations in Tree Rings: Radiocarbon, v. 22, n. 3, p. 950-961.

Lang, W. B., 1959, The Origin of Some Natural Carbon Dioxide Gases: Journal of Geophysical Research, v. 64, n. 1, p. 127-131.

Langmuir, D., 1971, The Geochemistry of Some Carbonate Ground Waters in Central Pennsylvania: Geochem. Cosmochem. Acta., v. 35, p. 1023-1045.

Libby, W. L., 1946, Atmospheric Helium Three and Radiocarbon From Cosmic Radiation: Physical Review, v. 69, n. 11-12, p. 671-685.

Lowell, W. R., 1952, Phosphatic Rocks in the Deer Creek-Wells Canyon Area, Idaho: U.S. Geol. Survey, Bull. 982-A, 52 p.

Lynch, E. J., 1962, Formation Evaluation: Harper and Row, New York, 422 p.

Mabey, D. R., 1978, Gravity and Aeromagnetic Anomalies in the Rexburg Area of Eastern Idaho: U.S.G.S. Open-file Report 78-382, 19 p.

Mabey, D. R., and Oriel, S. S., 1970, Gravity and Magnetic Anomalies in the Soda Springs Region, Southeastern Idaho: U.S. Geol. Survey Bull. 713, 150 p.

Mansfield, G. R., 1920, Geography, Geology, and Mineral Resources of Part of Southeastern Idaho, With Description of Carboniferous and Triassic Fossils, by G. H. Girty: U.S. Geol. Survey Prof. Paper 152, 453 p.

Mansfield, G. R., 1952, Geography, Geology and Mineral Resources of the Ammon and Paradise Valley Quadrangles, Idaho: U.S. Geol. Survey Prof. Paper 238, 92 p.

Mayo, A. L., 1982, Ground Water Flow Patterns in the Meade Thrust Allochthon, Idaho-Wyoming Thrust Belt, Southeastern Idaho: Ph.D. Dissertation, Univ. of Idaho, 181 p.

Meisler, H., and Becher, A. E., 1967, Hydrogeologic Significance of Calcium-magnesium Ratios in Groundwater from Carbonate Rocks in the Lancaster Quadrangle, Southeastern Pennsylvania; U.S. Geol. Survey Prof. Paper 575-C, p. C232-C235.

Mitchell, J. C., 1976a, Geothermal Investigations in Idaho, Part 5, Geochemistry and Geologic Setting of Thermal Waters of the northern Cache Valley area, Franklin County, Idaho: Idaho Dept. of Water Res., Water Information Bull. n. 30, 46 p.

Mitchell, J. C., 1976b, Geothermal Investigations in Idaho, Part 6, Geochemistry and Geologic Setting of the Thermal and Mineral Waters of the Blackfoot Reservoir Area, Caribou County, Idaho: Idaho Dept. of Water Res., Water Information Bull. n. 30, 47 p.

Mitchell, J. C., Johnson, L. L., and Anderson, J. E., 1980, Geothermal Investigations in Idaho, Part 9, Potential for Direct Heat Application of Geothermal Resources; Idaho Dept. of Water Res., Water Information Bull. n. 30, 395 p.

Mohammad, O. M. J., 1976, Evaluation of the Present and Potential Impacts of Open Pit Phosphate Mining on Groundwater Resources Systems in Southeastern Idaho Phosphate Field: Ph.D. Dissertation, Univ. of Idaho, 166 p.

Montgomery, K. M., and Cheney, T. M., 1967, Geology of the Stewart Flat Quadrangle, Caribou County, Idaho: U.S. Geol. Survey Bull. 1217, 63 p.

Mook, W. G., 1976, The Dissolution-exchange Model for Dating Groundwater with Carbon-14 _In_ Proceedings of Eighth International Conference on Radiocarbon Dating: Royal Soc. of New Zealand, v. 1, p. 342-352.

Muller, A. B., 1977, Essai D' Application des Variations de Teneur en Radiocarbone Dissous a L'etude des Aquiferes Libres: Le Cas de la Nappe Phreatique au Nord et a L'est du Lac Tchad: Dissertation for Doctor of Engineering; Univ. of Pierre Et Marie Curie (Paris VI), 28 June.

Muller, A. B., 1980, 1981, Written and Oral Communication: Sandia National Laboratories, Albuquerque, New Mexico.

Murphy, P., and Gwynn, J. W., 1979, Geothermal Investigations at Selected Thermal Systems of the Northern Wasatch Front, Weber and Box Elder Counties, Utah: Report of Investigation of the Utah Geol. and Mineral Survey, n. 141, 50 p.

Natrella, M. G., 1963, Experimental Statistics - National Bureau of Standards Handbook 91: U.S. Dept. of Commerce, Washington, D. C.

Olsson, I. V., 974, Some Problems in Connection with the Evaluation of Carbon-14 Dates: Geologiska Forenigens i Stockholm Forhandlingar, v. 96, p. 311-320.

Ott, Lyman, 1977, An Introduction to Statistical Methods and Data Analysis: Belmont, California, Duxbury Press, 730 p.

Peale, A. C., 1872, Report on Minerals, Rocks, Thermal Springs, etc.: U.S. Geol. Survey Terr., Fifth Ann. Rept., p. 165-204.

Pearson, F. J., Jr., and Hanshaw, B. B., 1970, Sources of Dissolved Carbonate Species in Groundwater and Their Effects on Carbon-14 Dating, in Isotope Hydrology: Internat. Atomic Energy Agency, Vienna, p. 271-285.

Piper, A. M., 1944, A Graphic Procedure in the Geochemical Interpretation of Water-analysis: Trans. Am. Geophys. Un., v. 25, p. 914-928.

Prestwitch, S., 1980, Verbal Communication, U.S. Dept. of Energy.

Proskta, H. J., and Embree, G. F., 1978, Geology and Geothermal Resources of the Rexburg Area, Eastern Idaho: U.S.G.S. Open-file Report 78-1009, 14 p.

Ralston, D. R., Arrigo, J. L., Baglio, J. V., Coleman, L. M., Hubbell, J. M., Mayo, A. L., Souder, K., 1981, Geothermal Evaluation of the Thrust Zone in Southeastern Idaho: Research Technical Completion Report, Idaho Water and Energy Res. Inst., 110 p.

Ralston, D. R., Mohammad, O. M. J., Robinette, M. J., Edwards, T. K., 1977, Solutions to Water Resource Problems Associated with Open-pit Mining in the Phosphate Area in Southeastern Idaho: Completion Report for Ground Water Study Contract No. 50-897, U.S. Dept. of Agriculture, Forest Service, 125 p.

Ralston, D. R., Wai, C. M., Brooks, T. D., Cannon, M. R., Corbet, T. F., Singh, H., and Winter, G. V., 1980, Interactions of Mining and Water Resource Systems in the Southeastern Idaho Phosphate Field: Idaho Water Res. Res. Inst., 214 p.

Rauch, H. W., and White, W. B., 1977, Dissolution Kinetics of Carbonate Rocks, Effects of Lithology on Dissolution Rate: Water Res. Res., v. 13, n. 2, p. 381-394.

Renner, J. L., White, D. E., and williams, D. L., 1975, Hydrothermal Convection Systems _in_ Assessment of Geothermal Resources of the United States: U.S.G.S. Circular 726, p. 5-57.

Richards, R. W., and Bridges, J. H., 1911, Sulphur Deposits Near Soda Springs, Idaho: U.S. Geol. Survey Bull. 470, p. 499-503.

Rioux, R. L., Hite, jR. J., Dyni, J. R., and Gere, W. C., 1975, Geologic Map of the Upper Valley Quadrangle, Caribou County, Idaho: U.S. Geol. Survey Map GO-1194, 6 p. and 1 plate.

Royse, F., Jr., Warner, M. A., and Reese, D. C., 1975, Thrust Belt Structural Geometry and Related Stratigraphic Problems Wyoming- Idaho-northern Utah, _in_ Deep Drilling Frontiers of the Central Rock Mountains, D. W. Bolyard, Ed.: Rocky Mountain assoc. of Geol., Denver, Colorado, p. 41-54.

Rubey, W. W., 1955, Early Structural History of the Overthrust Belt of Western Wyoming and Adjacent States: Wyoming Geol. Assoc. Guidebook, 10th Annual Conf. Green River Basins, p. 25-127.

Ryback, L., 1981, Geothermal Systems, Conductive Heat Flow, Geothermal Anomalies in Geothermal Systems _in_ Principals and Case Histories, ed. by Ryback, L., and Muffler, L. J. P., John Wiley and Sons, New York, 359 p.

SAS Institute, Inc., 1979, SAS User's Guide: 1979 Edition, SAS Institute, Raleigh, N.C., 494 p.

Savage, C. N., 1961, Geology and Mineral Resources of Bonneville County, Idaho: Idaho Bureau of Mines and Geology, County Report 5, 108 p.

Seitz, H. R., and Norvitch, R. F., 1979, Groundwater Quality in Bannock, Bear Lake, Caribou and Part of Power Counties, Southeastern Idaho: U.S. Geol. Survey Water Resource Investigations 79-14, Open-file Report, 51 p.

Smith, R. B., and Shar, M. L., 1974, Contemporary Tectonics and Seismicity of the Western United States: Geol. Society of America, v. 85, p. 1205-1218.

Souder, K., 1983, Regional Hydrogeochemistry of Geothermal Systems in the Overthrust Region in Southeastern Idaho: M.S. Thesis, Univ. of Idaho, in progress.

Staatz, M. H., and Albee, H. F., 1966, Geology of the Garns Mountain Quadrangle Bonneville, Madison, and Teton Counties, Idaho: U.S. Geol. Survey Bull. 1205, 122 p.

Stanley, W. D., 1972, Geophsical Study of Unconsolidated Sediments and Basin Structure in Cache Valley, Utah and Idaho: Feol. Soc. America Bull., v. 83, no. 6, p. 1817-1830.

Stearns, N. D., Stearns, H. T., and Waring, G. A., 1937, Thermal Springs in the United States: U.S.G.S. Water-Supply Paper 679-B, p. 59-206.

Stiff, H. A., Jr., 1951, The Interpretation of Chemical Water Analysis by Means of Patterns: Jour. Petrol. Technology, v. 3, n. 10, p. 15-17.

Suess, H. E., 1955, Radiocarbon Concentration in Modern Wood: Science, v. 122, p. 415-417.

Tamers, M. A., 1975, Validity of Radiocarbon Dates on Groundwater: Geophys. Survey, v. 2, p. 217-239.

Toth, J., 1963, A Theoretical Analysis of Groundwater Flow in Small Drainage Basins: Jour. Geophys. Res., v. 68, n. 16, p. 4785-4812.

Truesdell, A. H., and Jones, B. F., 1974, WATEQ, A Computer Program for Calculating Chemical Equilibria of Natural Waters: Jour. Research, U.S. Geol. Survey, v. 2, n. 2, p. 233-248.

Turner, J. M., Muller, A. B., and Long, A., 1980, Annual ..O and D Fluctuation in Rainfall and Runoff in the Tucson Basin and Their Relations to Groundwater Recharge _In_ Proceedings of 6th Annual Midwest Meeting of American Geophysical Union: Am. Geophys. Union, Dekalb, IL, Sept. 18-19, 1980.

U. S. Department of Commerce, 1964, Climate Summary of the United States - Supplement for 1951 Through 1960: Climatography of the United States no. 86-8, 50 p.

U. S. Department of Interior and U. S. Department of Agricultural, 1976, Draft EIS, Development of Phosphate Resources in Southeastern Idaho: 3 volumes.

U. S. Environmental Protection Agency, 1979, Methods for Chemical Analysis of Water and Wastes: Environmental Monitoring ans Support Laoratory, EPA-600/4-79-020, 460 p.

Vogel, J. C., and Ehhalt, D., 1963, The Use of Carbon Isotopes in Groundwater Studies _in_ Radioisotopes in Hydrology: Vienna, Internat. Atomic Energy Agency, p. 383-396.

Wagner, J. P., 1980, Written Communication, U.S. Geol. Survey.

White, D. E., 1957a, Thermal Waters of Volcanic Origin: Geol. Soc. Am. Bull., v. 68, p. 1637-1658.

White, D. E., 1957b, Magmatic, Connate, and Metamorphic Waters: Geol. Soc. Am. Bull., v. 68, p. 1659-1682.

White, D. E., 1960, Summary of Chemical Characteristics of Some Water of Deep Origin _in_ Short Papers in the Geological Sciences: U.S. Geol. Survey Prof. Paper 400-B, p. B452-B454.

White, D. E., Hem, J. D., and Waring, G. A., 1963, Data of Geochemistry, Chapter F., Chemical Composition of Subsurface Waters, 6th Edition: Geol. Survey Prof. Paper 440-F, 67 p.

Wigley, T. M., 1975, Carbon-14 Dating of Groundwater from Closed and Open Systems: Water Res. Res., v. 11, n. 2, p. 324-328.

Wigley, T. M., and Muller, A. B., 1981, Fractionation Corrections in Radiocarbon Dating: Radiocarbon 23, p. 173-190.

Winter, G. V., 1979, Groundwater Flow Systems of the Phosphate Sequence, Caribou County, Idaho: M.S. Thesis, Univ. of Idaho.

Young, H. W., and Mitchell, J. C., 1973, Geothermal Investigations in Idaho, Part 1, Geochemistry and Geologic Setting of Selected Thermal Waters: Idaho Dept. of Water Res., Water Info. Bull, n. 30, 43 p.